Solar Backscatter Ultraviolet Spectral Radiometer Mod 2

NASA

NOAA

SBUV/2

SBUV/2 Final Engineering Report for Flights 2 and 3 (S/Ns 003 and 004)

Doc. No. B6802-102

B6802-102
SBUV/2
FLTS. 2 and 3

SBUV/2 FINAL ENGINEERING REPORT
For Flights 2 and 3
(SNs 003 and 004)

Document No. B6802-102

22 December 1993

Prepared for

NATIONAL AERONAUTICS AND SPACE ADMINISTRATION
Goddard Space Flight Center
Greenbelt, MD 20771

in accordance with
Contract NAS5-29230, Item 37C

BACG Approvals

Prepared by

Phil Mehalko
SBUV/2 Test Engineer

Kathery E. Lopez
SBUV/2 Program Secretary

Faith Seyzon-Rayl
Project Released

Approved by

V. Wayne Nelson
SBUV/2 Project Manager

Charles A. Springer
SBUV/2 Systems Engineer

93-12-22
Date

TABLE OF CONTENTS

ILLUSTRATIONS

ILLUSTRATIONS

ILLUSTRATIONS

TABLES

TABLES

TABLES

Section 1
INTRODUCTION

1.1 SCOPE

This document describes, from a functional and physical standpoint, the design and operation of the Solar Backscatter Ultraviolet Spectral Radiometer Mod. 2 (SBUV/2) and its related Ground Support Equipment (GSE). The design described herein is based on the design accomplished by Ball Aerospace and Communications Group (BACG) in accordance with the requirements specified in GSFC Specification S-480-12.

Section 2 of this document contains a system description of the instrument and a system performance summary. Section 3 contains a description of the major components of the SBUV/2 instrument. Section 4 describes the instrument calibration and component tests. Section 5 contains a description of the related Ground Support Equipment. Section 6 contains a listing of acronyms and other clarifying notes to facilitate the reader. Figure 1-1 shows the major items of hardware that comprise the instrument and its related GSE.

The flight SBUV/2 instruments currently on contract are scheduled to be flown on NOAA-F and subsequent NOAA flights. The instruments are integrated to the Advanced TIROS-N (ATN) satellite which is a modified version of earlier TIROS satellites. The TIROS payloads are launched from Vandenburg Air Force Base, California.

This document is written for the Flight Models 2 and 3 configurations. See Table 1-1 for a list of differences between this and Flight Models 1, 4, 5, and 6.

Contractual authority for this document is Line Item 29C of Contract NAS5-29230. Requests for additional copies or questions regarding this document should be directed to:

Ball Aerospace and Communications Group
P.O. Box 1062
Boulder, Colorado 80306
Attention: SBUV/2 Project Manager

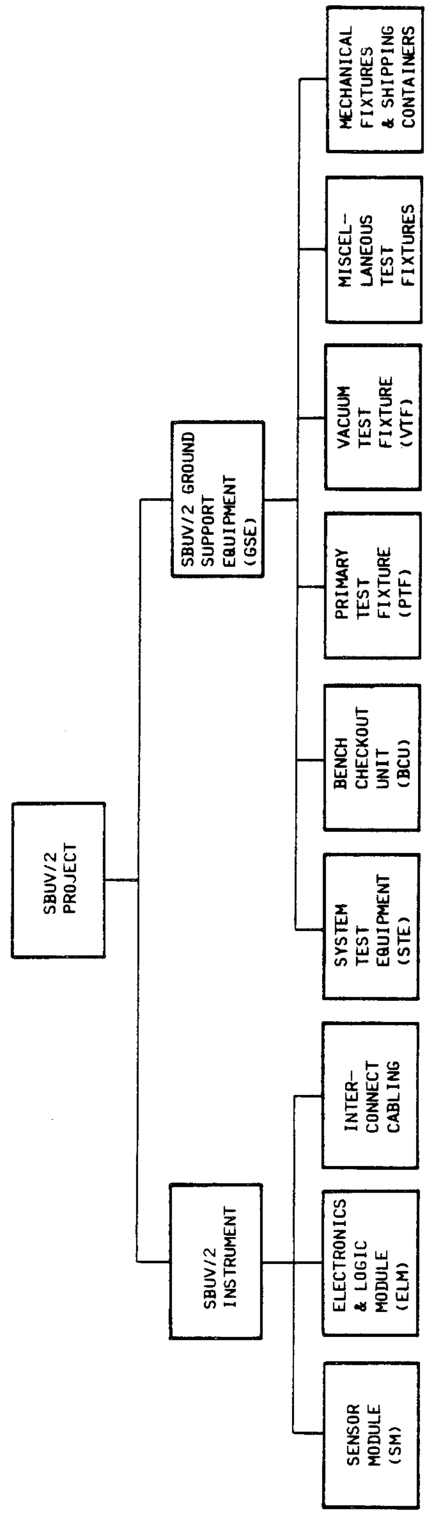

Figure 1-1
Hardware Breakdown of the SBUV/2 Project

1.2 REFERENCED DOCUMENTS

The documents listed in the following subparagraphs are listed for reference. These referenced documents will be revised throughout the course of the program. The SBUV/2 Configuration Manager maintains a current listing of the latest issue in effect as well as copies of all documents.

1.2.1 GSFC DOCUMENTS

- S-480-12: Specification Title, "TIROS Backscatter Ultraviolet Spectral Radiometer Mod 2 (SBUV/2)

1.2.2 MARTIN MARIETTA DOCUMENTS

- IS-2280259: Specification Title, "TIROS -N General Instrument Interface"
- IS-2295548: Specification Title, "TIROS-N Unique Instrument Interface for the SBUV/2 Radiometer"

1.2.3 BACG DOCUMENTS

- 67901 FM2 SBUV/2 Instrument Assembly
- 67901-505 FM3 SBUV/2 Instrument Assembly
- DD66598 Electrical Interface and Functional Logic Diagram

CONFIGURATION COMPARISON FOR SBUV/2 INSTRUMENTS
NOVEMBER 1993

	APPLICATION						
CONFIGURATION ITEM	EMU S/N1	FM1 S/N2	FM2 MOD 3 S/N3	FM3 MOD2 SN/4	FM4 SN/5	FM5 MOD4 S/N6	FM6 S/N7
Hamamatsu Photomultiplier tube, preamp, and bleeder string for 5 dynodes	Y	N	Y	Y	Y	Y	Y
Diffuser drive at 80 Hz stepping frequency & mechanism modifications	N/A	N	Y	Y	Y	Y	Y
Redesigned cal lamp housing & diffuser interlock	N/A	N	Y	Y	Y	Y	Y
Cal lamp polarity switching added, diffuser heater current tlm. deleted.	N/A	N	Y	Y	N	Y	Y
LVPS 25 volt regulator	Y	N	Y	Y	N	Y	Y
Increase cal lamp door comparitor reference current	N	N	Y	N	N	Y	Y
Aluminum foil EMI shield	N/A	N	N	N	Y	N	N
Mesh EMI shield	N/A	N	Y	Y	N	Y	Y
Redesigned grating shaft/housing and encoder finger ring	N	N	N	N	Y	Y	Y
Redesigned grating bearing clamps	N	N	N	Y	N	Y	Y
Alignment mirrors in place of cube	N	N	Y	Y	Y	Y	Y
Cal lamp heater added, baseplate heater deleted	N/A	N	Y	Y	Y	Y	Y
Additional lift fixture attach points	N	N	Y	Y	Y	Y	Y
Blacken Ebert cover	N	N	Y	Y	Y	Y	Y
Enlarge shroud, +Y side	N/A	N	Y	Y	Y	Y	Y
Change Grating memory Prom, from 6611 to 6641	N	N	N	Y	Y	Y	Y
Grating Servo telemetry deleted	N	Y	Y	Y	Y	Y	Y
Anode preamp (Range 2) gain roll-off added	N	N	Y	Y	Y	Y	Y
J-Y Gratings, Max. Efficiency 250nm	Y	N	N	N	N	N	N
J-Y Gratings, Max. Efficiency 180nm	N	Y	Y	Y	Y	Y	Y
"Air" spaced depolarizer (not contacted)	Y	N	N	N	N	Y	Y
Square depolarizer	N	N	N	N	N	Y	Y
"Hammerhead" grating shaft stop	Y	N	N	N	N	N	N
"Short arm" grating shaft stop	N	Y	Y	Y	N	N	N
Motor rotor grating shaft stop	N	N	N	N	Y	Y	Y
Diffuser radiator covered by thermal blanket	N/A	N	Y	Y	Y	Y	Y
CCM oscillation prevention	N	N	Y	N	N	Y	Y
Electrometer Radiation Shield	N	N	Y	Y	N	Y	Y
Grating Servo DAC MOD	N	N	Y	N	N	Y	Y
Diffuser Baffle, +Y and +Z	N/A	N	N	N	N	Y	N

Section 2
INSTRUMENT DESCRIPTION AND OPERATION

2.1 SCOPE

This section describes the SBUV/2 instrument at system-level and its theory of operation. The SBUV/2 consists of two major modules: a Sensor Module, and an Electronics and Logic Module. A summary of the pertinent system performances is also included. Descriptions of the major components of the two modules are contained in Section 3.

2.2 PURPOSE OF INSTRUMENT

The SBUV/2 is an operational remote sensor designed to map, on a global scale, total ozone concentrations and the vertical distribution of ozone in the earth's atmosphere. Knowledge of the temporal and spatial distribution of atmospheric ozone is important since ozone strongly absorbs solar ultraviolet energy and prevents this harmful radiation from reaching the earth's surface. The purpose of the SBUV/2 instrument is to provide data, on an continous operational basis, from which the distribution of ozone can be determined.

To determine the distribution of ozone, two separate measurements are needed. First, the SBUV/2 instrument measures the backscattered spectral radiance of the solar ultraviolet radiation from the earth. Second, a direct solar spectral irradiance is measured. Both measurements are made in the spectral range from 160 to 400 nanometers (nm). From the ratio of the two measurements, the distribution of ozone can be determined. This data will further the understanding of:

- The structure and dynamics of the ozone layer
- Photochemical process in the atmosphere and the influence of trace constituents on the ozone layer

2.3 INSTRUMENT INTERFACES WITH THE SPACECRAFT

The instrument-to-spacecraft interfaces are described in Martin Marietta (formerly GE) Interface Specifications IS-2295548 and IS-2280259. Specification IS-2295548 describes specific electrical, mechanical, optical, operational, and test interfaces unique to the SBUV/2 instrument. Specification IS-2280259 contains general electrical, mechanical, optical, thermal, magnetic, electromagnetic and environmental interface information applicable to FM2 and FM3 TIROS-N instruments. Specification IS-2280259 also contains general information for design and fabrication of ground support equipment.

2.4 SYSTEM DESCRIPTION AND OPERATION

The SBUV/2 instrument (see Figure 2-1) consists of two separate modules: a Sensor Module (SM), and an Electronics and Logic Module (ELM). The SM is mounted to the earth-facing surface of the Advanced TIROS-N (ATN) Equipment Service Module (ESM). The ELM is mounted in a bay within the ESM. The ELM is connected electrically to the Sensor Module via a cable assembly which is provided by the spacecraft contractor. All spacecraft electrical interfaces with the instrument are made through the Electronics and Logic Module (see Figure 2-2).

The Sensor Module contains a spectral scanning double monochromator, a cloud cover radiometer, mechanisms, and electronics. The ELM contains the remainder of the electronics for control of the Sensor Module.

The SBUV/2 instrument measures backscattered solar radiation in a nominal 11.3° x 11.3° field-of-view (FOV). In the Nadir direction, 12 discrete, 1.1nm wide wavelength bands between 252.0 and 339.8nm are used for the ozone measurements.

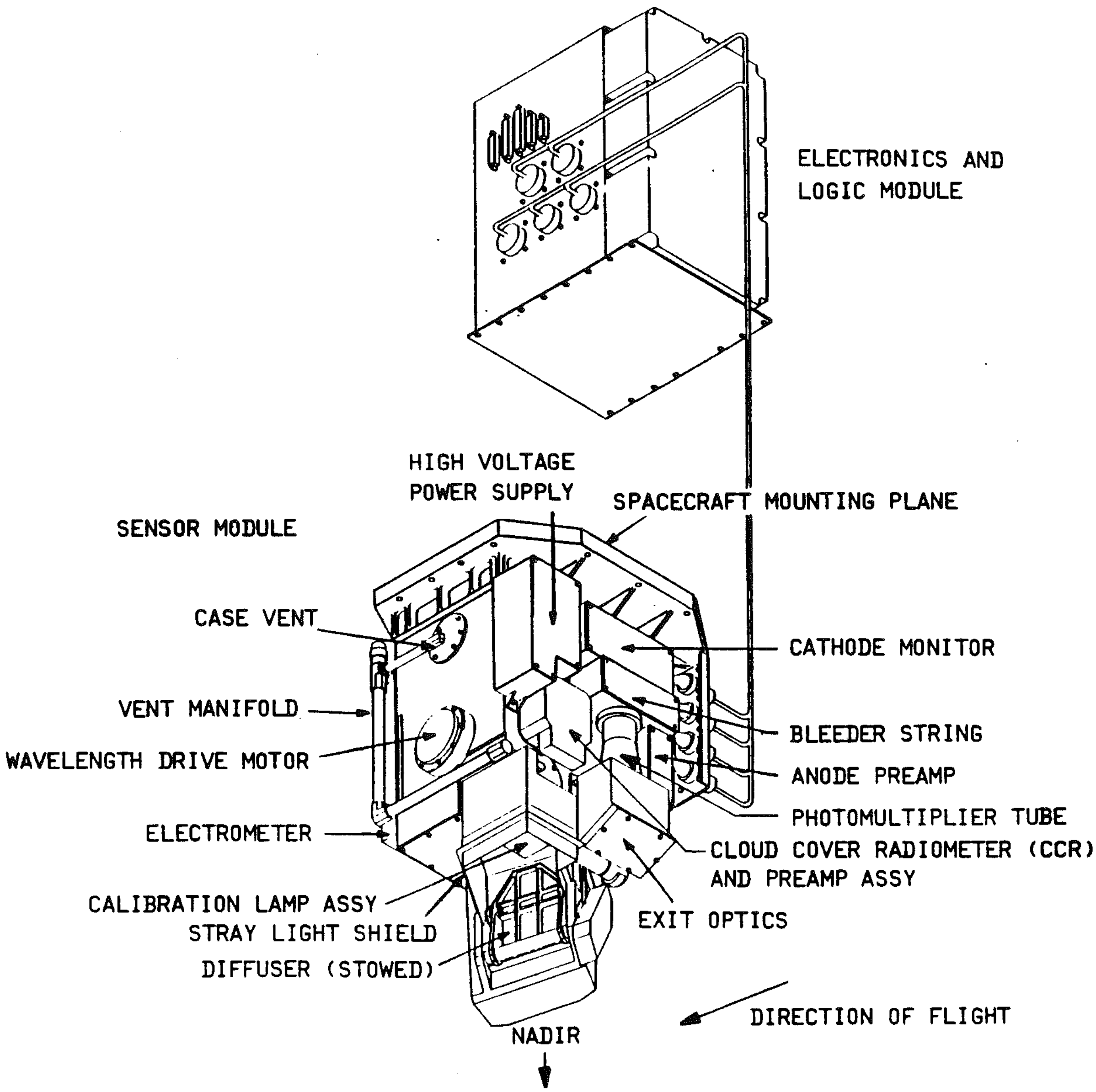

Figure 2-1
SBUV/2 Instrument

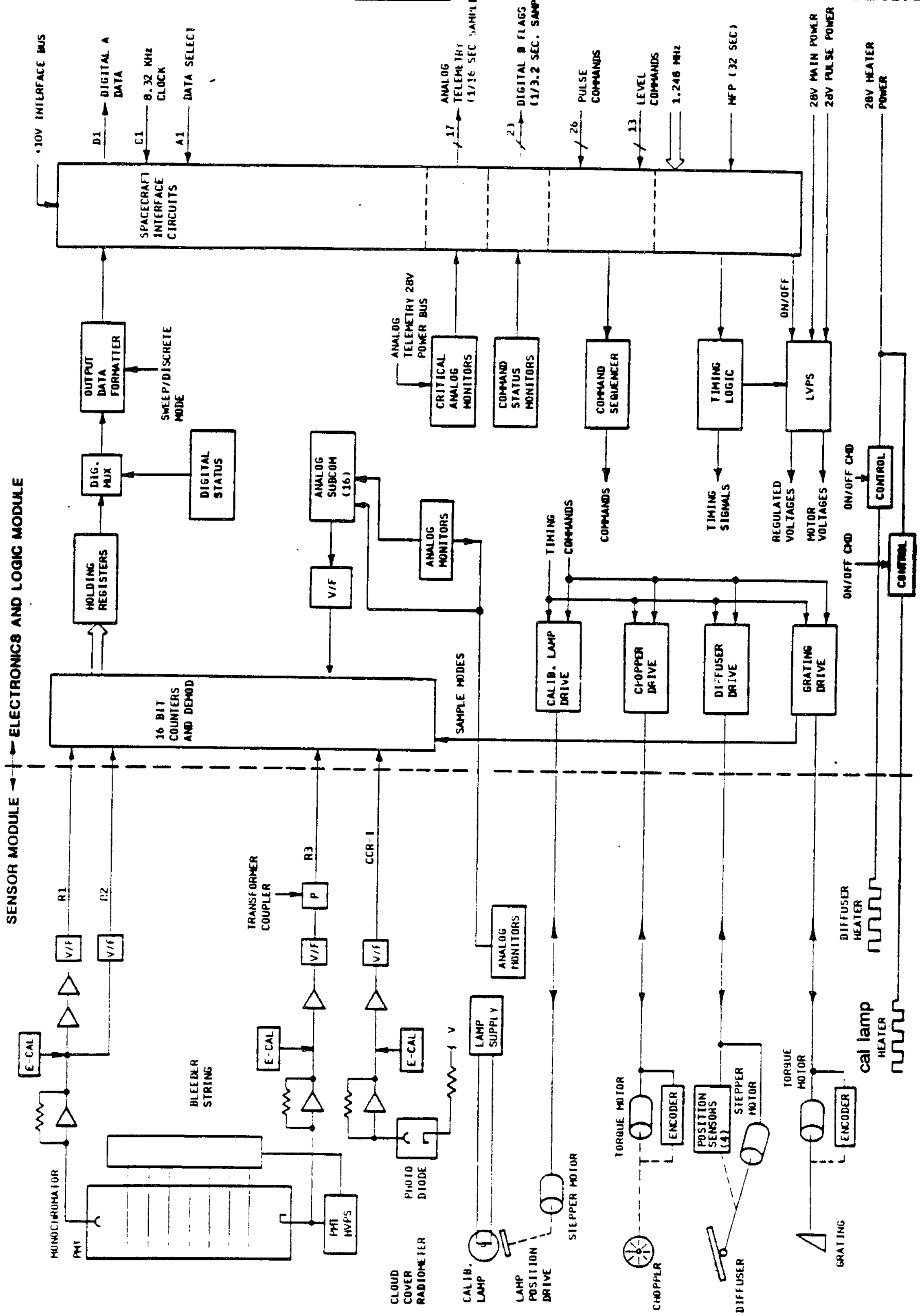

Figure 2-2
Block Diagram of SBUV/2 Electrical System

The solar irradiance is determined at the same 12 wavelength bands by deploying, upon ground command, a diffuser to reflect sunlight into the instrument field-of-view. The atmospheric radiance measurement relative to the solar irradiance measurement is used for determining ozone profiles.

The SBUV/2 instrument can also measure the solar irradiance or the atmospheric radiance with a continuous spectral scan from 160 to 400nm in increments of nominally 0.148nm. These measurements provide data on other photochemical processes in the atmosphere.

A separate narrowband filter photometer channel, called the Cloud Cover Radiometer, (CCR) continuously measures the earth's surface brightness at 379nm, i. e., outside the ozone absorption band. The CCR is located in the same structure as the monochromator. Its field-of-view is nominally the same size (11.3° x 11.3°) as, and is co-aligned with, the monochromator's field-of-view.

The following subparagraphs describe the instrument operating phases and modes; the parameters that are measured; and the component that performs the measurements. Also included is the instrument performance summary.

2.4.1 OPERATIONAL PHASES AND MODES

The SBUV/2 is a non-spatial scanning, spectrally-scanning instrument. It operates in several phases and modes that are selected on command. There are three operational phases, four monochromator modes, four scene modes, and a diffuser decontamination mode. The operational phases are:

- Launch and Orbital Acquisition Phase. The monochromator aperture is covered by a two-position calibration lamp assembly; the diffuser is stowed; and the power is off.

- Mission Phase. This is the normal operating mode. Selected combinations of four monochromator modes and four scene modes are possible.

- Standby Phase. The baseplate heater can be turned on if needed. However, analysis shows that this will not be required.

The four monochromator modes are:

- Discrete Mode. The gratings are stepped through 12 discrete wavelength positions and dwell at each position for 1.25 seconds. This is repeated until another mode is selected.

- Sweep Mode. The gratings are continuously moved to cover the wavelength range of 400 to 160nm in 0.074nm steps. This is repeated until another mode is selected.

- Wavelength Calibration Mode. The gratings are stepped to 12 discrete positions around the 253.7nm line from the on-board mercury calibration source. This is repeated until another mode is selected.

- Position Mode. The gratings are moved to, and stopped at, the position commanded. The gratings will stay in this position until commanded to another position or into another mode. This mode is used primarily for system test and calibration and during the post-launch evaluation. It is not used during normal mission operations.

The four scene modes are:

- Earth View Mode
- Sun View Mode
- Wavelength Calibration Mode
- Diffuser Check Mode.

All data is obtained during the Mission Phase. Figure 2-3 shows the various mode combinations that can be used during the Mission Phase. The primary science data is collected when viewing the earth and the sun. The Cloud Cover Radiometer (CCR) views the same scene as the monochromator, sampling incoming energy at 379nm.

The Launch Phase, Diffuser Check Sequence, Diffuser Decontamination Mode, and four scene modes are chosen by selecting one of four positions for the diffuser, and one of two positions for the wavelength calibration lamp. The wavelength calibration lamp is a mercury lamp housed within the deployable door over the entrance apertures. Figure 2-4 shows the combinations and the monochromator operating modes (grating drive mechanism) that go with them. The positions of the diffuser and calibration lamp and the operation of the grating drive define the operating mode.

In the Launch Phase, the diffuser is stowed in an enclosure, protected from outgassing products, debris and combustion products from the orbit-adjust thrusters. The calibration lamp assembly serves as a contamination cover over the entrance aperture for both the monochromator and the CCR.

In the Earth View Mode, the diffuser remains stowed and the lamp assembly is deployed to the open position. The monochromator operates in either the Discrete or Sweep Mode.

In the Sun View Mode, the diffuser is deployed to 28° below the instrument Y-Z plane. Sunlight is reflected into the entrance aperture during a portion of each orbit.

			MONOCHROMATOR MODES					
	OBSERVED SOURCE	VIEWING MODES	SWEEP MODE*	DISCRETE MODE*	WAVELENGTH CALIBRATION MODE*	MONO-CHROMATOR POSITION MODE	CCR MODES	DIFFUSER DECONTAMINATION MODE
SCENE MODES	EARTH	RADIANCE MODE	✓	✓		✓	✓	INSTRUMENT APERTURE PROTECTED, DIFFUSER HEATER ON
SCENE MODES	SUN	IRRADIANCE MODE	✓	✓		✓	✓	
SCENE MODES	DIRECT VIEW OF Hg LAMP	DIFFUSER CHECK SEQUENCE	✓		✓	✓		
SCENE MODES	DIFFUSER ILLUMINATED BY Hg LAMP	DIFFUSER CHECK SEQUENCE	✓		✓ (OPTIONAL)	✓		
	CYCLE TIME REMARKS		192 SEC	32 SEC	32 SEC	CONT. SAMPLES	CONT. SAMPLES	BY COMMAND

*PORTIONS OF THESE MODES PROVIDE FOR ELECTRONIC CALIBRATION OF THE MONOCHROMATOR ELECTROMETERS

A/N 1968

Figure 2-3
Instrument Operating Modes (Mission Phase)

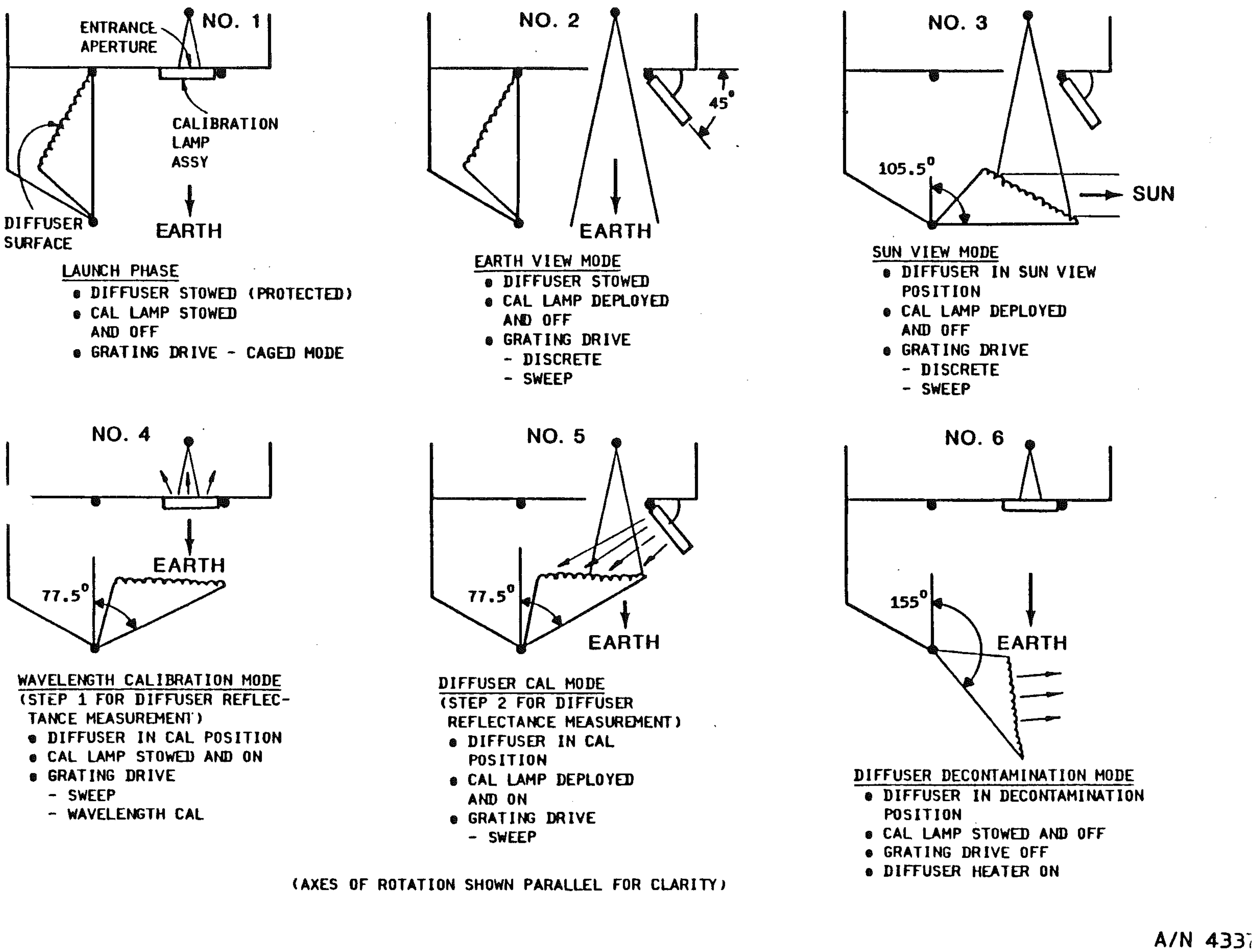

Figure 2-4
Diffuser and Calibration Lamp Positions

The frequency of the allowed sun-viewing opportunities and their durations depend upon the orbit geometry. For the nominal mission, the spacecraft is in a sun-synchronous, near-polar orbit with the ascending node between 1300 and 1800 local mean time. Orbit period is approximately 101 minutes. The spacecraft +X axis is always vertical downward; the spacecraft +Y axis points back along the velocity track; and the +Z axis is along the positive normal to the orbit. The sun lies within 80° of the +Z axis. In spacecraft coordinates, the sun line cones about the +Z axis at an angle γ, once every orbit. Figure 2-5 shows its path in direction space. The diffuser is on the bottom of the spacecraft in a location where parts of the spacecraft shadow it whenever the sun is above the Y-Z plane or to the -Y side of the X-Z plane.

When the sun is less that 62° from the +X axis, the earth shadows the whole spacecraft during part of the orbit. Thus, the diffuser can be sunlit only when the sun is in the shaded region of Figure 2-5.

The diffuser must be tilted so it sees no earthshine, putting its normal within 28° of the -X axis. So, as the sun approaches the limb of the earth (at 62° from the +X axis), the diffuser is illuminated at an extremely large incidence angle.

Providing the solar array is not in a configuration to cast a shadow onto the SBUV, the sun can illuminate the instrument diffuser once per orbit as the gamma angle varies over the range $\sim 10° \leq \gamma \leq \sim 80°$. Solar data is normally collected by use of one of the following automated data sequences: Discrete Sun Enable of Sweep Sun Enable, which have a predetermined solar observation time of 280 seconds and 360 seconds, respectively. A longer solar observation time can be provided if the automated sequences are not used and the diffuser is deployed at the appropriate time. The maximum observation time is determined by the gamma angle and position of the spacecraft in orbit. Figure 2-6 and 2-7 provides a family of curves $\sim 10°$ to $\leq \gamma \leq \sim 80°$. These plots assume only that solar observation begins as the sun crosses the Y-Z plane of the spacecraft.

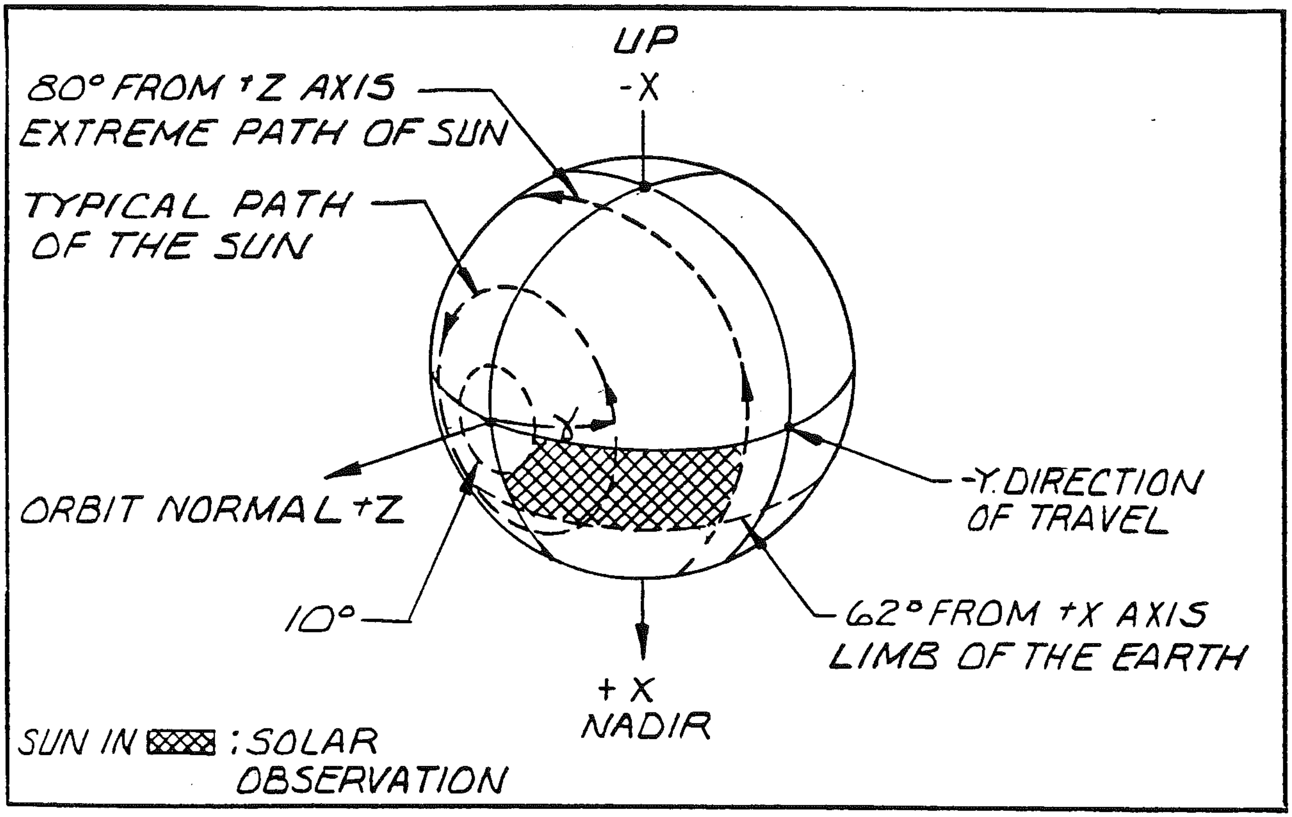

Figure 2-5
Geometry for Solar Irradiance Measurement (In Direction Space)

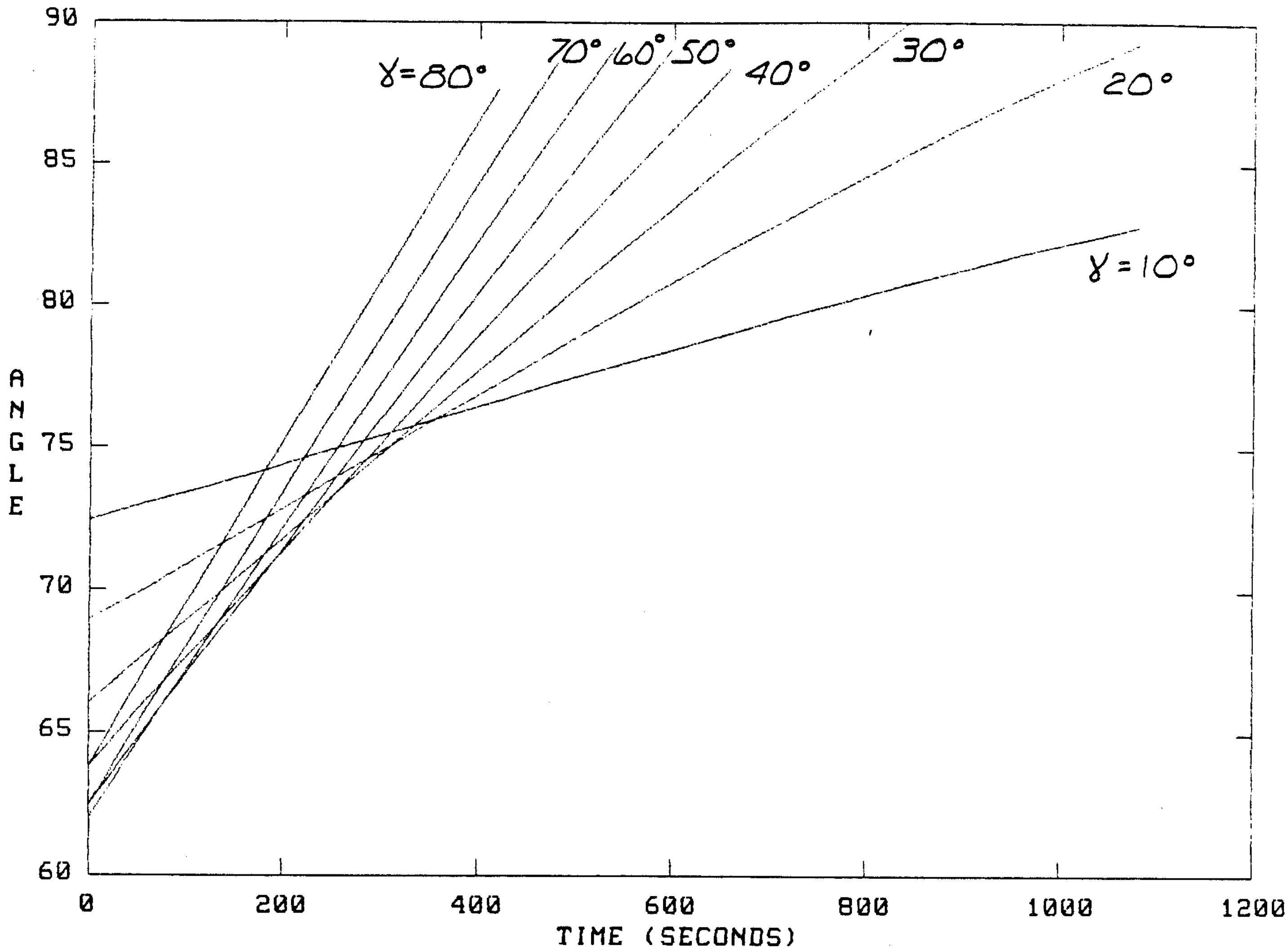

Figure 2-6
Solar Angle of Incidence

IDL

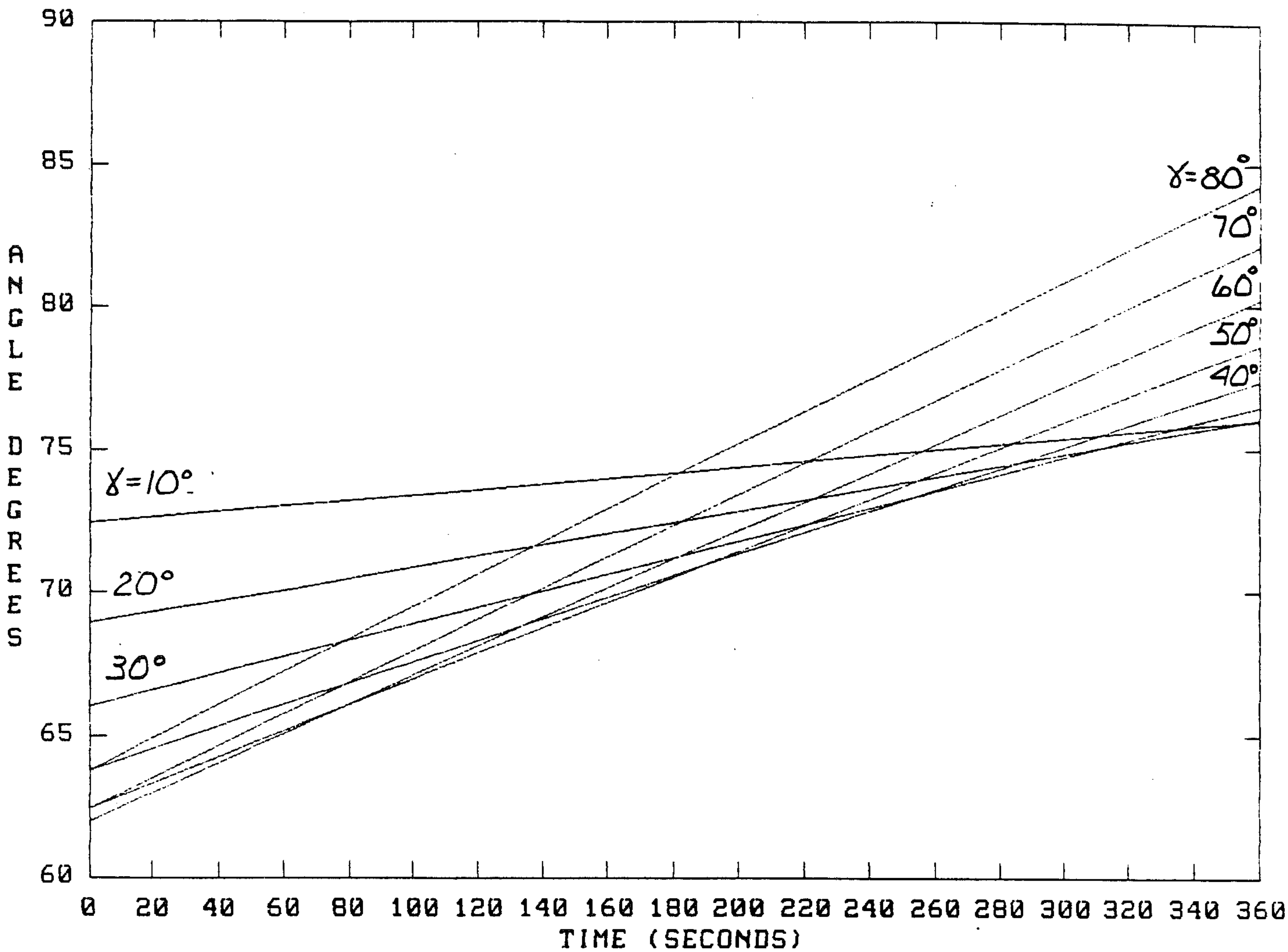

Figure 2-7
Solar Angle of Incidence

During the Wavelength Calibration Mode (see Figure 2-4), the diffuser is directly in front of the instrument aperture and the calibration lamp assembly is closed covering both apertures. In the Sweep Mode, the monochromator scans over the mercury lines at 184.0, 253.7, 302.2, 313.2, 365.0 and 404.7nm. In the Wavelength Calibration Mode, the monochromator can be commanded to sequence through 12 discrete wavelengths around any desired line from the mercury source.

In the Diffuser Check Mode, the monochromator views the diffuser which is illuminated by the wavelength calibration lamp (See Figure 2-4). The monochromator scans the same six lines as in the Wavelength Calibration Mode. The ratios of the two sets of data (the lamp directly and the lamp reflected from the diffuser) provide the check of diffuser relative spectral reflectivity. These two measurements are completed within seven minutes.

In the Diffuser Decontamination Mode, both instrument apertures (the monochromator and the CCR) are covered by the Calibration Lamp Assembly (aperture door). The diffuser is pointed away from the instrument and the 5W heater is turned on, heating the diffuser to approximately 70°C.

The monochromator has four distinct modes as shown in Figure 2-3:

- Discrete Mode
- Sweep Mode
- Wavelength Calibration Mode
- Position Mode.

The sequencing for each monochromator mode is controlled from either a fixed, ground-programmable memory (FIX System) or from a random access memory programmable by command (FLEX System). The desired memory is selected by command.

Each monochromator mode defines a unique wavelength sequence and a data sampling sequence. At the end of each mode sequence (except the Position Mode), the preamplifiers are switched out, and up to five precision voltage levels are inserted into the electronics for calibration of the analog electronics and the voltage-to-frequency converters.

Beginning at the start of the first major frame following a Discrete Mode command, the gratings sequentially move to and dwell at the 12 discrete wavelengths. Figure 2-8 shows the wavelength-versus-time profile. The signal at each wavelength is integrated for 1.25 seconds. An additional 0.75 second is allowed for moving to and settling at the next wavelength. Thus, the 12 discrete wavelengths are covered in 24 seconds. This allows eight seconds for returning to the first discrete wavelength, electronic calibration, and waiting for the start of the next major frame. The12 discrete wavelengths specified in GSFC S-480-12 are stored in the FIX system. Any 12 wavelengths can be commanded into the FLEX system.

Beginning at the start of the first major frame following receipt of a Sweep Mode command, the wavelength range from 407nm to 160nm is scanned in nominally 0.074nm steps. Figure 2-9 shows the wavelength-versus-time profile. The monochromator signal is integrated for 0.1 second resulting in nominally 0.148nm sample increments. Therefore, approximately 1680 spectral measurements are made between 407nm and 160nm. This takes about 168 seconds. The grating drive then retraces to 407nm and waits for the start of the next major frame. Thus, the total cycle time for the Sweep Mode is 192 seconds. Electronic calibration takes place during the time period between 168 seconds and 192 seconds. The starting position (407nm) is stored in the FIX system. Any starting position can be commanded into the FLEX system. During operation, either starting point will be followed by the 1680 spectral measurements. Grating motion is limited by stops placed well outside the normal wavelength range.

The Wavelength Calibration Mode is functionally very similar to the Discrete Mode. Beginning at the start of a major frame, it moves to and dwells at 12 separate wavelengths, each separated by nominally 0.296nm, (four steps) around any single desired line source. At each wavelength, data is integrated for 1.25 seconds. Figure 2-10 shows the timing for this mode and an example of the resulting data. The FIX system stores the starting wavelength for the 253.7nm mercury line and the remaining 11 wavelengths are achieved through logic. The FLEX system can be programmed to start sequencing at any wavelength.

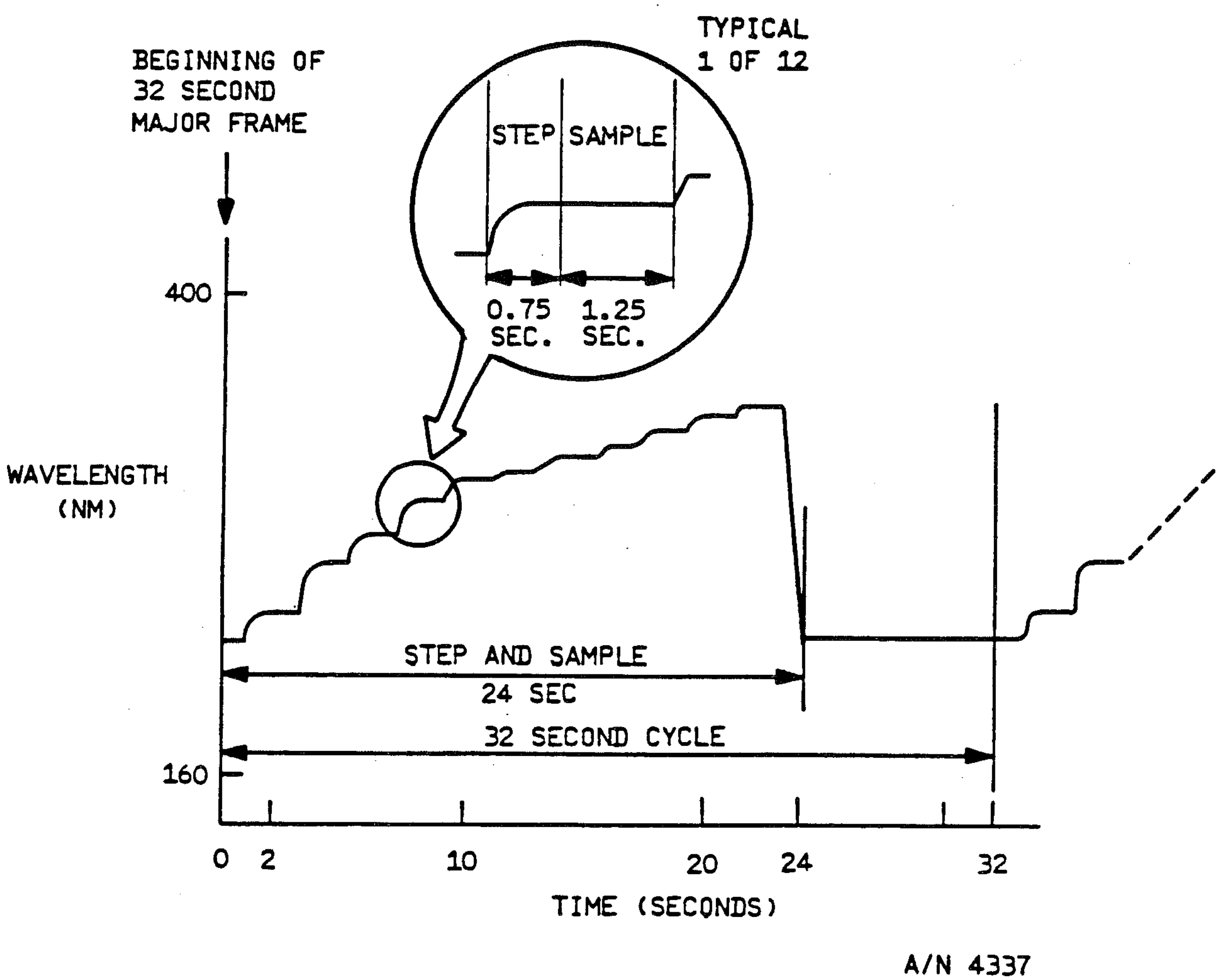

Figure 2-8
Discrete Mode Timing

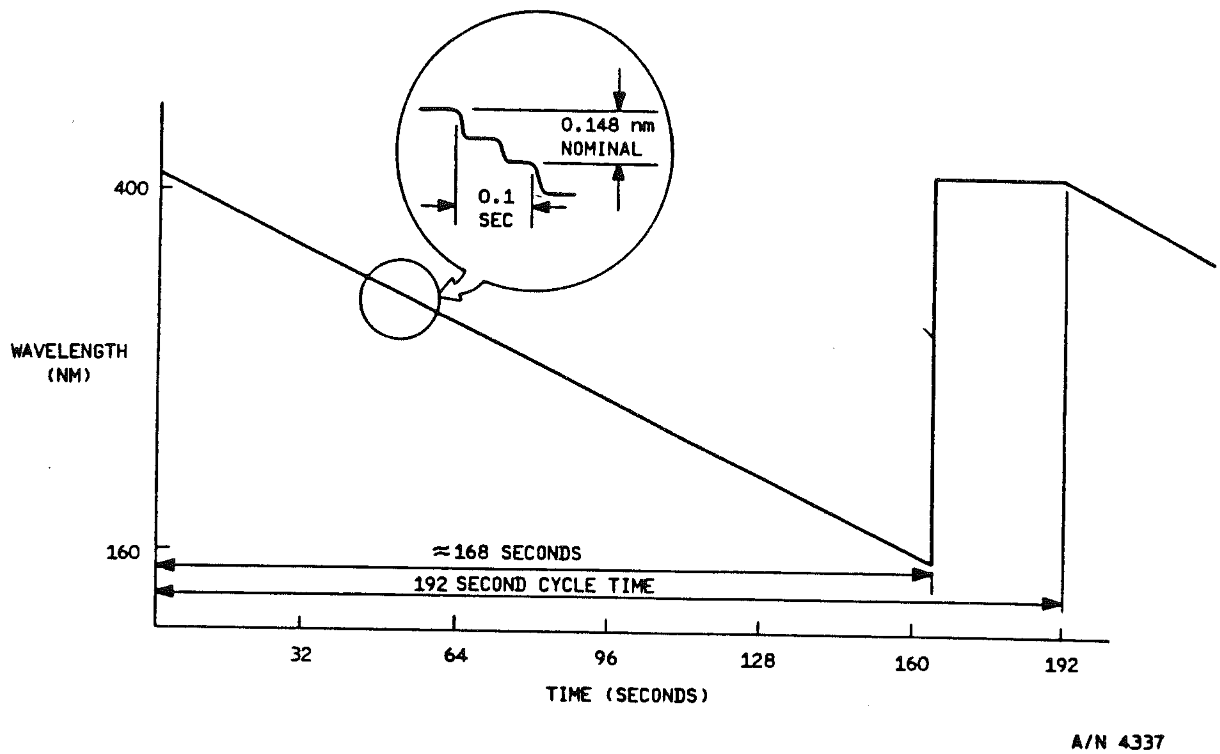

Figure 2-9
Sweep Mode Timing

Upon receipt of a Position Mode command and at the start of the next major frame, the grating goes to the grating shaft position at the position location in memory. The FIX system contains the 280nm position. However, any position can be commanded into the FLEX system. The grating will remain at this position until a new position is loaded into the FLEX system or until receipt of a new mode command. In the Position Mode, data is integrated for 1.25 seconds during every two second period as in the Discrete Mode. There is no E-CAL during the Position Mode.

2.4.2 RADIOMETRIC INPUT

Both the monochromator and the cloud cover radiometer are designed to view sources or targets that are larger than their 11.3° x 11.3° fields-of-view (such as the earth), and to measure the average radiant power within the field-of-view. When viewing the sun, which is smaller than the instrument's field-of-view, the on-board instrument diffuser takes the rays from the one-half degree sun and provides a diffuse source that overfills the instrument field-of-view.

The range of radiant power (that the monochromator and the cloud cover radiometer measure) is illustrated in Figure 2-11. Solar irradiance values have been converted to radiance levels at the on-board diffuser by using an average diffuser transfer factor or efficiency of 0.22 mW/m^2-sr-A per mW/m^2-A.

The efficiency or throughput of the monochromator is strongly dependent upon the wavelength, especially below 180nm where the transmissions of the depolarizer and photomultiplier tube faceplate substantially drop off. Figure 2-12 shows the range of photomultiplier anode currents for the monochromator. The maximum radiance values are typically encountered in the equatorial regions and the minimum radiances over the polar regions. Figure 2-12 also shows the range of cathode currents for the cloud cover radiometer. More discussion on the parameters effecting the system throughput are covered in Section 2.5.

In addition to accommodating a wide range of radiance levels, the depolarizer makes the SBUV/2 instrument relatively insensitive to different levels of polarization. The instrument also contains a precise wavelength drive system.

2.4.3 SENSOR MODULE DESCRIPTION

Figure 2-13 highlights the optical elements to aid in following the light paths through the Sensor Module. Figure 2-14 is a functional block diagram of the Sensor Module.

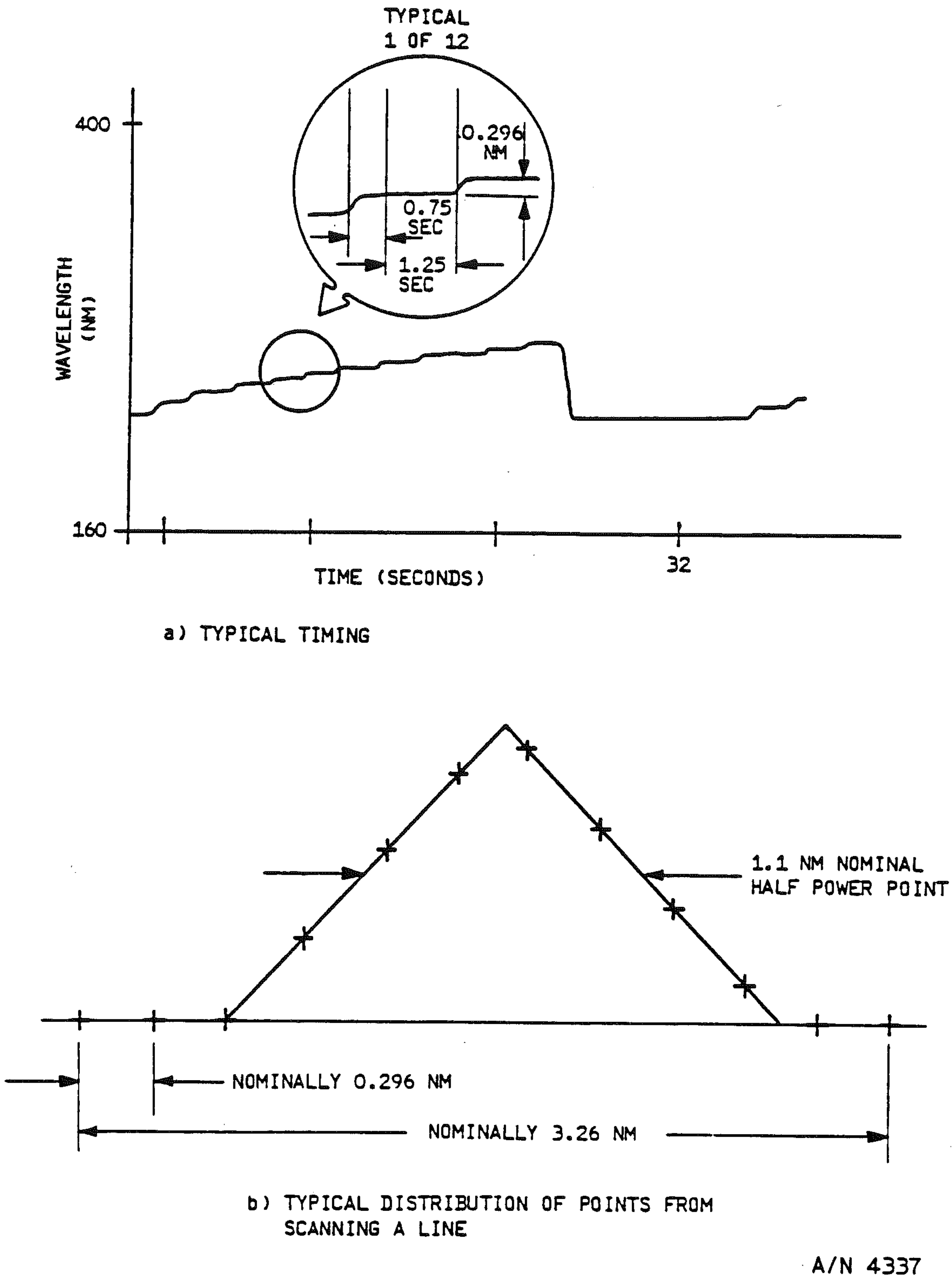

Figure 2-10
Wavelength Calibration Mode Timing

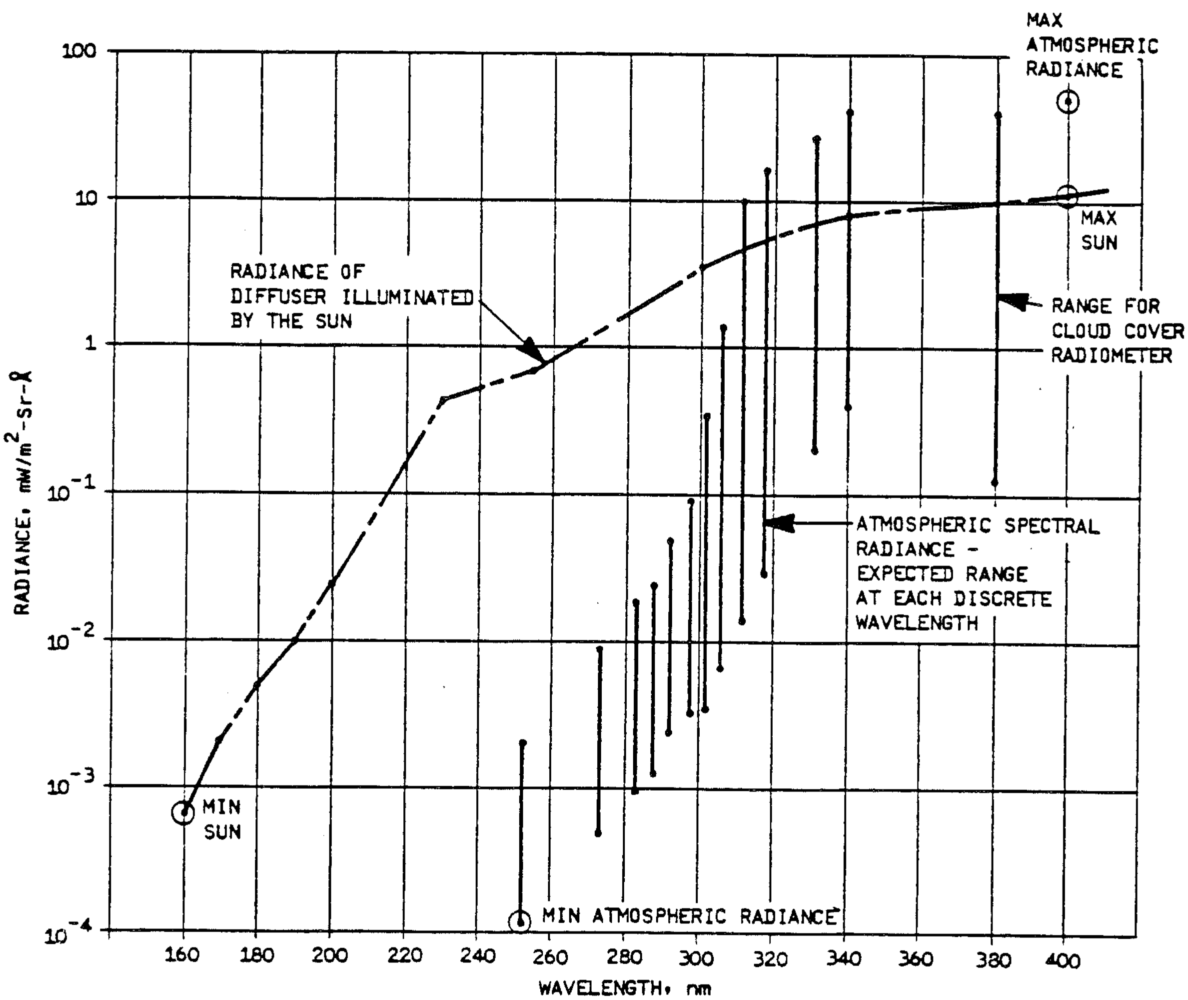

Figure 2-11
Range of Radiance to be Measured

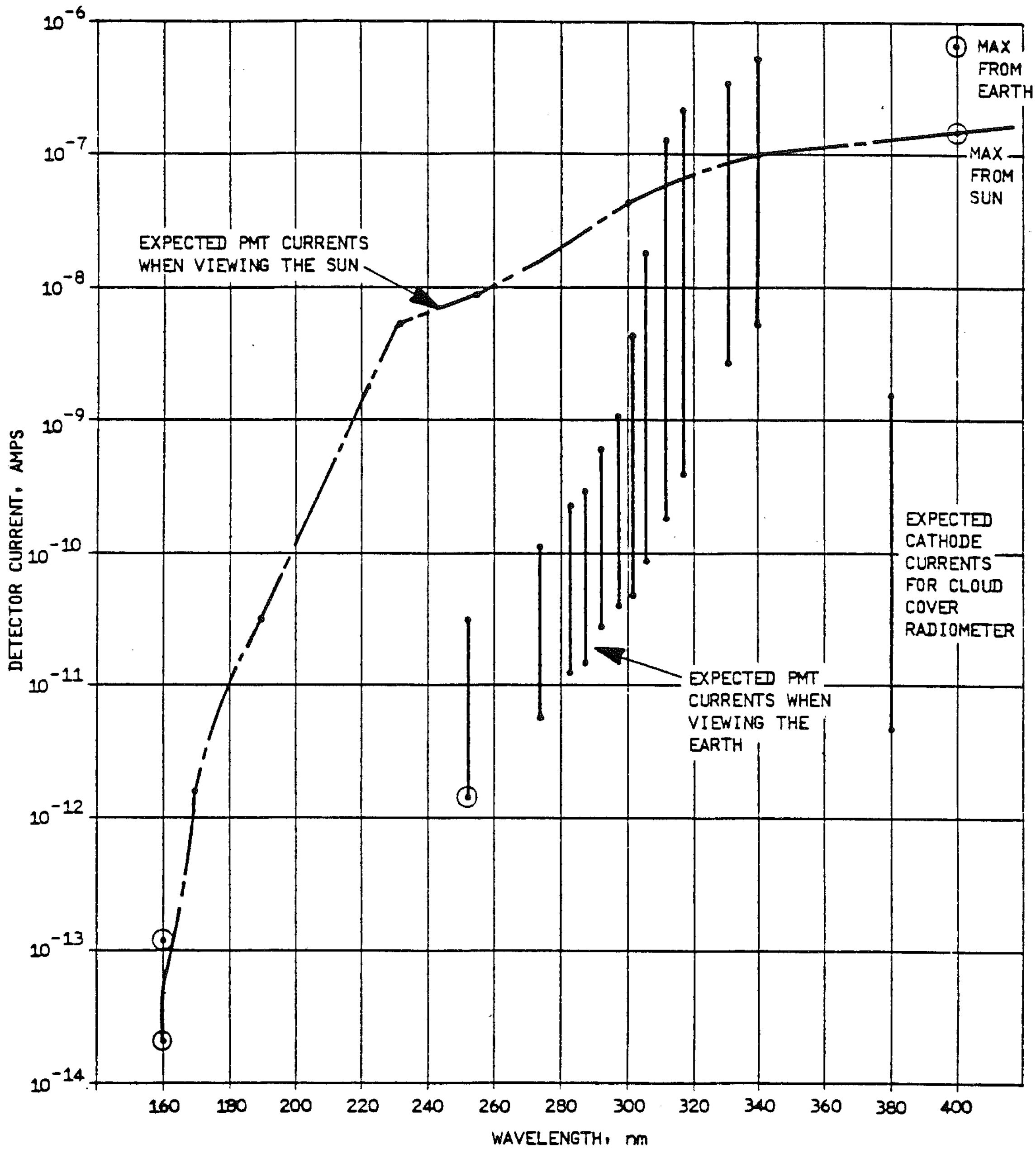

Figure 2-12
Range of Detector Currents

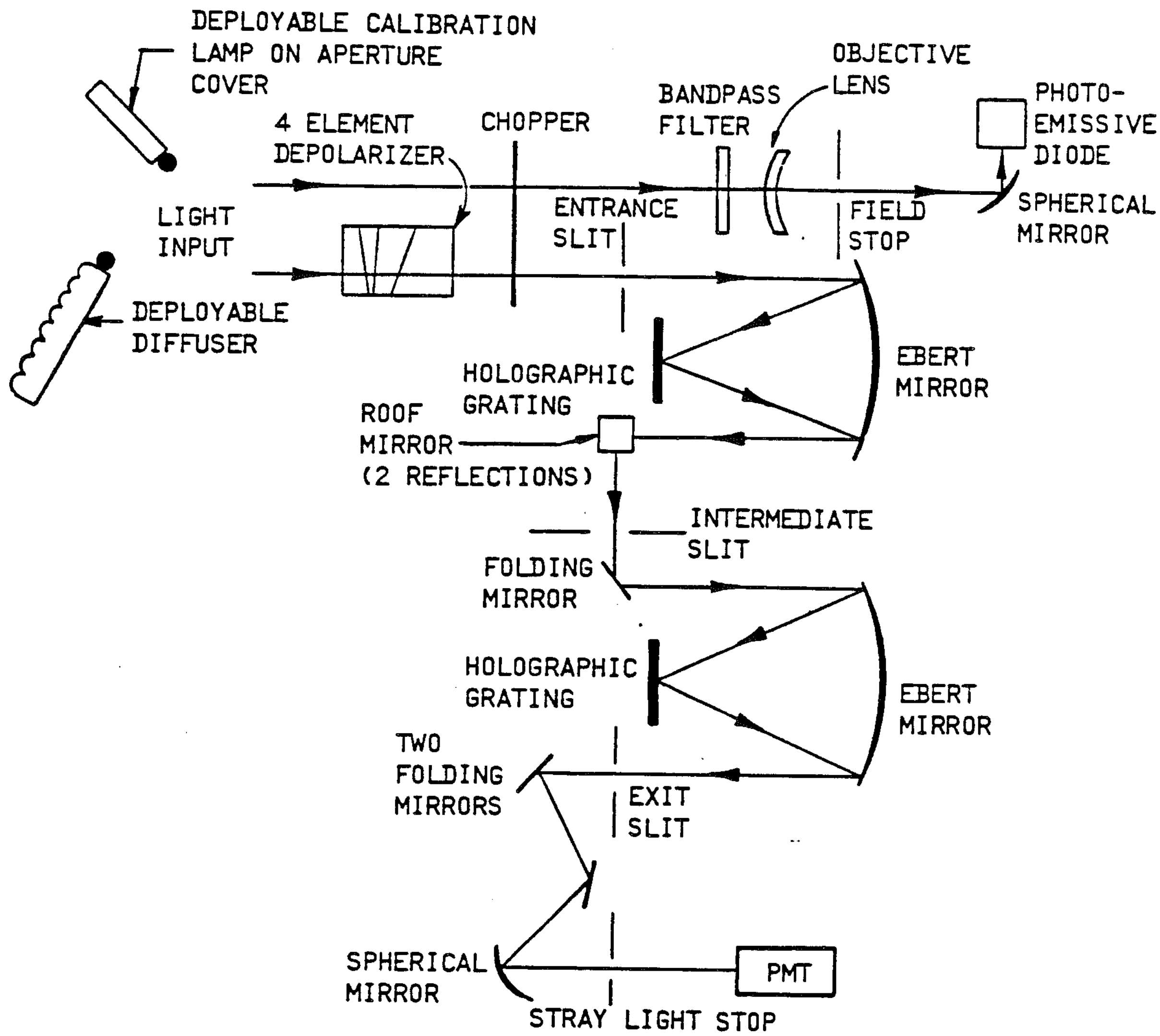

Figure 2-13
Simplified Optical Path

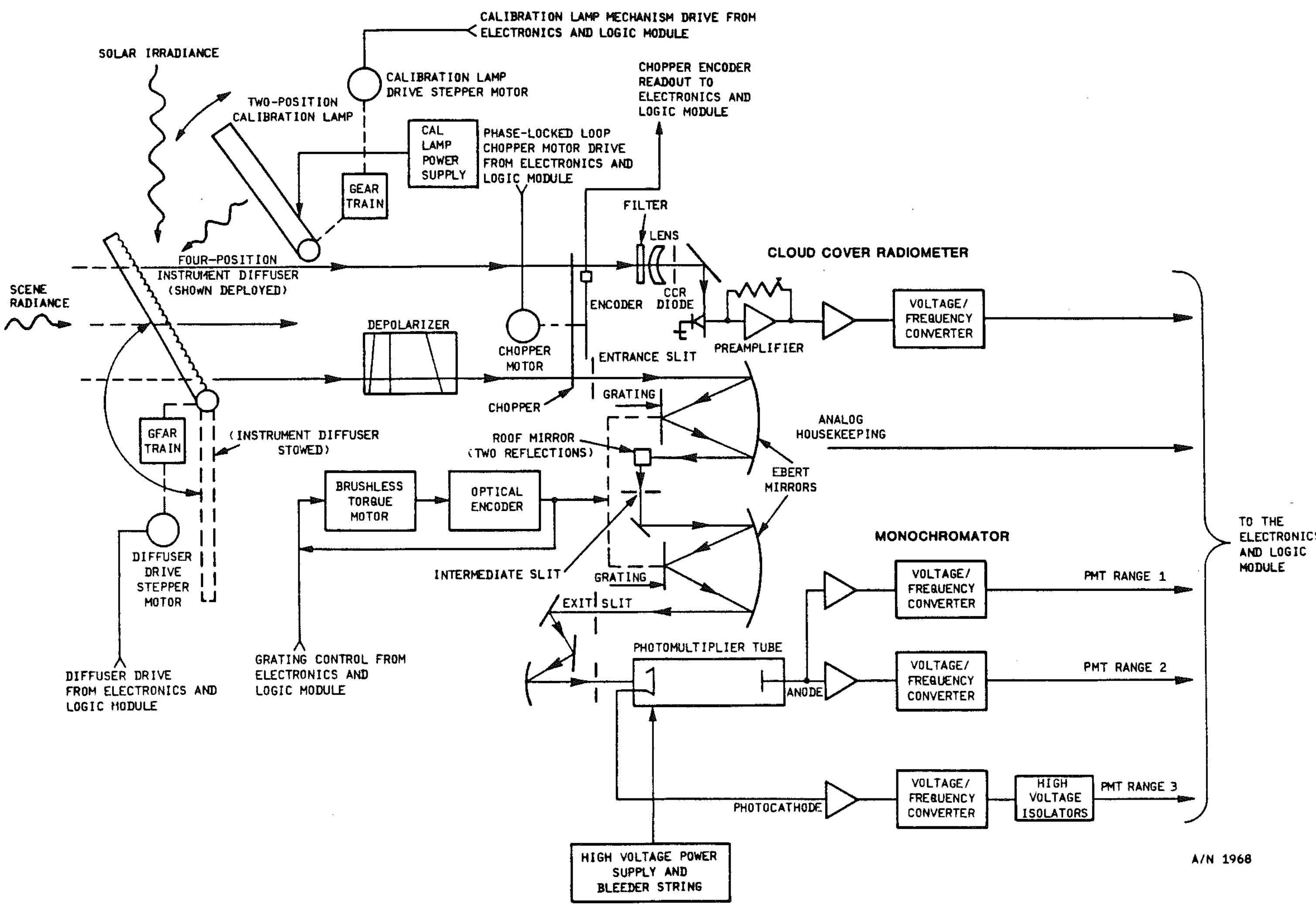

Figure 2-14
Functional Diagram of the Sensor Module

Photons reach the entrance aperture from several possible sources. First, with the diffuser stowed and the aperture cover open, earth radiation directly enters the aperture. Second, with the diffuser deployed to the sun view position, solar radiation is reflected into the aperture. Third, for in-flight calibration, light from an on-board mercury lamp, located in the aperture cover, can be directed straight into the aperture or reflected from the diffuser when the diffuser is in the calibration position.

The light passes through a four-element cultured quartz depolarizer and is chopped before reaching the entrance slit of the monochromator. Light for the cloud cover radiometer does not pass through the depolarizer but is chopped immediately. The chopper consists of a five-bladed wheel that is driven in phase-lock at four revolutions per second (20 Hz chopping frequency) by a three-phase brushless DC motor.

Energy at the entrance slit of the monochromator undergoes two reflections from each of the Ebert mirrors, three reflections at the intermediate mirrors, and diffraction at each of the two gratings before leaving the monochromator at the exit slit. After three more reflections in the exit optics, the energy passes through the quartz faceplate of the photomultiplier tube (PMT) and strikes the photocathode where it is converted to current.

In the PMT, the current is amplified by the factor of 500 between the cathode and the anode. The currents at the cathode and the anode are sensed with trans-impedance preamplifiers. To cover the large range of signals, two gain stages are used at the anode (Range 1 and Range 2) and one gain stage at the cathode (Range 3). The analog signals are converted to digital frequencies in the voltage-to-frequency converters. These digital signals are routed to the Electronics and Logic Module where digital synchronous demodulation and integration occurs in up/down counters.

All of the cathode circuitry through the voltage-to-frequency converters floating at the negative high voltage potential of the cathode. Input and output signals pass through high voltage transformer isolators.

In addition to serving as the high signal (low gain) range for the monochromator signals, the cathode current monitor is also used to measure the PMT gain at the anode. This is done on the ground by taking the ratio of the cathode and anode signals where the ranges overlap.

The angular position of the gratings determines the center wavelength of the nominal 1.1nm bandpass of the monochromator. The grating position is controlled in a closed loop servo system using a brushless DC torque motor and an optical encoder. Electronics located in the Electronics and Logic Module provide the grating control and sequencing.

The cloud cover radiometer (CCR) consists of a lens, a 3.0nm-wide filter centered at 379nm, a folding mirror, a photoemissive diode, and a preamplifier. The diode converts the incident photons to a current which is converted to a voltage in the preamplifier. In the electrometer, the preamplifier output is amplified and passed through a voltage-to-frequency converter. In a manner similar to the monochromator channels, the digital signal is then synchronously demodulated and integrated in the Electronics and Logic Module.

2.4.4 ELECTRONICS AND LOGIC MODULE

The Electronics and Logic Module (ELM) consists of 11 printed circuit boards which plug into a mother board plus the Low Voltage Power Supply (LVPS). Figure 2-15 is a functional block diagram of the total Electronics and Logic Module.

The Electronics and Logic Module is a single-point electrical interface between the spacecraft and the Sensor Module. All inputs and outputs to the spacecraft except power (Digital A, Digital B, Commands, Analog, Clocks and Timing) come into the spacecraft interface circuit board. After being preconditioned in this board, the clock, timing and commands are routed to the timing and command boards as applicable. The digital multiplexer and formatter takes digital data from the Sensor Module and digital status data from the ELM. It then formats them and gates them to the interface board which sends them to the TIROS Information Processor (TIP) in the spacecraft. The timing board generates all of the timing and clock signals, such as the chopper drive reference clock, demodulation and integration clocks, and stepper motor rate clocks.

The low voltage power supply accepts input power directly from the spacecraft. It provides analog and digital circuit voltages, motor drive voltages, and preconditioned inputs for the high voltage and calibration lamp power supplies in the Sensor Module. It filters the +28V main bus and the +28V pulse load bus before it is converted. Post regulators are on some outputs.

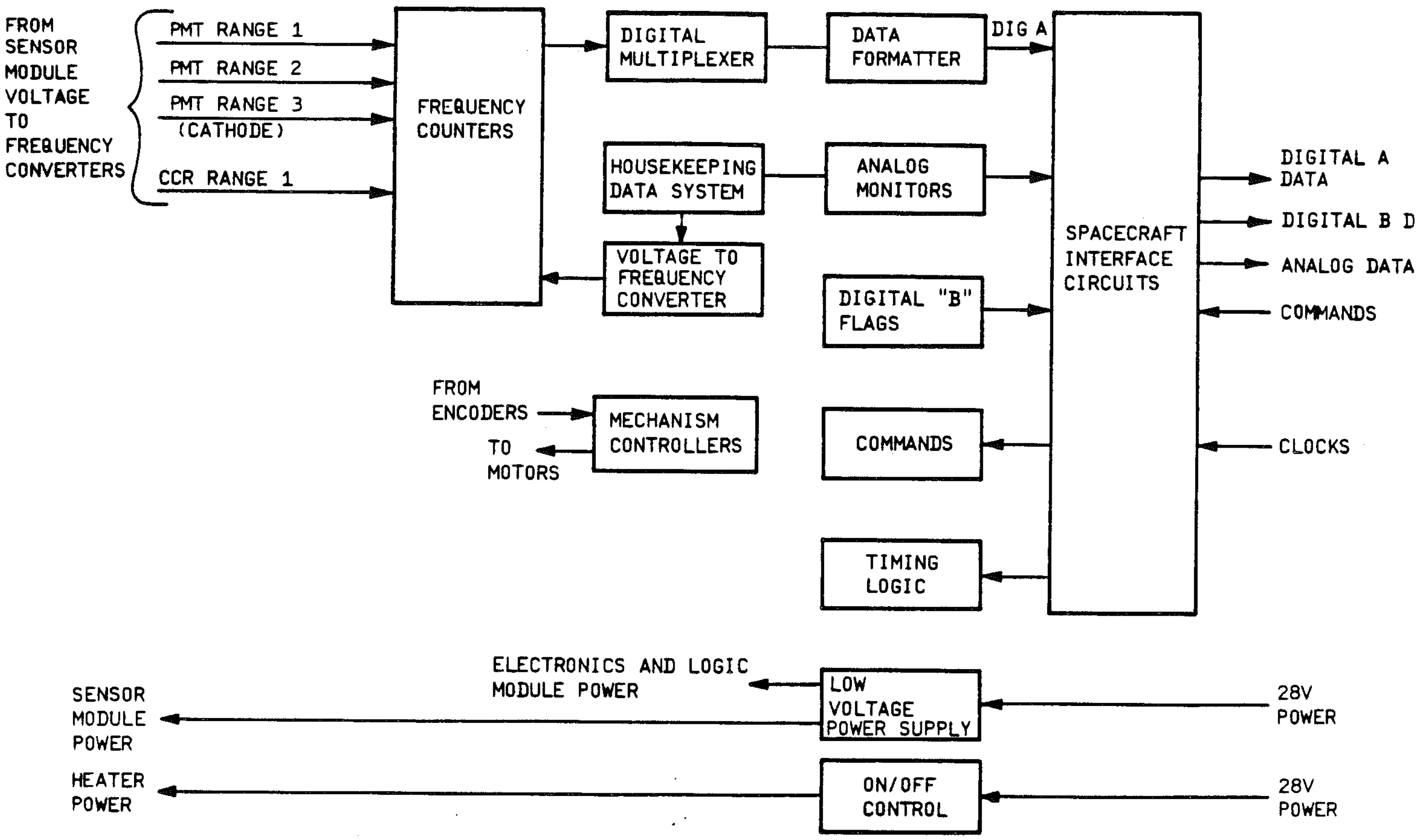

Figure 2-15
Functional Block Diagram, Electronics and Logic Module

2.5 SYSTEM PERFORMANCE SUMMARY

2.5.1 SYSTEM PERFORMANCE PARAMETERS

A summary of all pertinent system performance parameters, some measured and some estimated, is given in Table 2-1. The following describes the data listed in the columns of the table. This data is derived in System Engineering Report (SER) numbers SBUV-NE-81-130 and SBUV-NE-81-182.

Wavelength Column. The wavelengths given are the 12 discrete wavelengths and the five selected short wavelengths and the long wavelength at which the signal-to-noise ratio is specified. The Cloud Cover Radiometer wavelength of 379nm is also included.

Radiance Column. The radiance levels given are the minimum and maximum expected levels over which the instrument is specified to operate. Signal-to-noise ratios are calculated at the minimum levels.

Diffuser Efficiency Column. This is a calculated value of the lambertian diffuser for an incident angle of approximately 70°.

Solid Angle Instantaneous Field-of-View Column. This is the solid angle subtended by the 11.33° square field-of-view of the instrument.

Depolarizer Efficiency Column. This is the estimated efficiency of the double Wellaston prism depolarizer. The material is optical grade cultured crystalline quartz. Note the broad uncertainty below 200nm in the depolarizer efficiency due to the variability in the transmission of cultured quartz from lot to lot.

Chopping Factor Column. The two major factors effecting the chopping factor are the finite rise and fall times of the the chopped scene (2.2 msec) caused by finite width of the aperture, and the absolute phase difference between the chopped waveform and the demolulation signal at the demodulator. This latter factor can be electronically adjusted to close to zero, leaving the 0.432 value shown for the monochromator and 0.45 for the CCR channel.

Aperture Area Column. The areas of the 1.3 x 30mm entrance slit for the monochromator and the 4 x 4mm entrance aperture of the CCR.

Mirror Efficiency Column. Entering light undergoes ten mirror reflections on its pass through the double Ebert-Fastie monochromator. The reflecting surfaces are aluminum overcoated with magnesium flouride (M_gF_2). The mirror efficiency is calculated as the tenth power of the mean value of the expected individual efficiencies, which are indicated in the lower right hand corner of the box. For the CCR, the value shown is the transmission of the lens.

Grating Efficiency Column. The entering light is dispersed by two gratings. The efficiency is computed using the square of the expected efficiency of the grating, which is shown in the lower right hand corner of the box. For the CCR, the value shown is the average transmission of the bandpass filter between the half-power points.

Spectral Bandwidth Column. This is the nominal value of the spectral bandwidth at the half-power points.

PMT Faceplate Efficiency Column. The PMT faceplate is constructed of cultured quartz. The transmission and reflectance losses are listed in this column. For the CCR, the value shown is the reflectance of the mirror.

PMT Responsivity Column. The values given are based on the specified quantum efficiency for the PMT photocathode (no faceplate loss) and for the CCR photodiode (including faceplate).

Average Cathode Current Column. The current waveform is a chopped signal containing system and PMT noise. The values given are the long-term averages at the given input levels. They are calculated as the product of the terms across the table:

- Radiance: $I_k = N_\lambda \Omega \varepsilon_p C_f A \varepsilon_m{}^{10} \varepsilon_g{}^2 \Delta\lambda \varepsilon_f R\lambda$
- Irradiance: $I_k = H_\lambda \upsilon_d \Omega \varepsilon_p C_f A \varepsilon_m{}^{10} \varepsilon_g{}^2 \Delta\lambda \varepsilon_f R\lambda$
- CCR: $I_k = N_\lambda \Omega C_f A \varepsilon_1 \varepsilon_f \varepsilon_m \Delta\lambda R_\lambda$

where the individual factors are a function of wavelength in some cases. For the Cloud Cover Radiometer, "A" refers to the aperture area of the CCR channel: ε_1, ε_m, ε_f refer to the lens, mirror, and filter efficiencies, respectively. For the CCR optics, $\Delta\lambda$ refers to the spectral bandwidth of the CCR filter, and R_λ is the responsivity of the CCR photo-diode. The values shown for the cathode current monitor are merely the largest and smallest shown in the table.

PMT Gain Column. The nominal gain chosen for the PMT is 500.

Preamplifier Gain Column. All preamplifiers are set at the gains shown.

Electronic Gain Column. The Range 1 gain is set to give a full scale input to the voltage-to-frequency converter (8 volts, allowing 2 volts overscale) with 232 x 10^{-12} amperes of peak anode current (this is 100 x 10^{-12} amperes of average anode current). The other gains are calculated to give a 655-count overlap in ranges as seen by the instrument output.

Voltage-to-Frequency Ratio Column. The full scale input to the voltage-to-frequency converter is 10V peak. With 10V peak in, we want 2^{16}-1=65535 counts out over the 1.25-second integration time. With a 0.45 chopping factor, this gives:

$$V_f = \frac{65535 \text{ Counts}}{(1.25 \text{ seconds})\ (10 \text{ Volts})\ (0.432)} = 12136 \text{ Hz/Volt, (11,651 for the CCR)}$$

as the voltage-to-frequency ratio.

Integration Time Column. The monochromator integration time for the sweep mode is 0.1 second and for the discrete mode is 1.25 seconds. For the Cloud Cover Radiometer, the integration time is 1.25 seconds, except when the monochromator is in sweep mode. Then the CCR integration time is 1 second.

Average Counts Out Column. This is calculated as:

- Monochromator Counts Out: $I_k G_p G_a G_e V_f \tau$
- CCR Counts Out: $I_K G_A G_E V_F \tau$
- Cathode Current Monitor Counts Out: $I_k G_A G_E V_F \tau$

Average Anode Current Column. This is the average cathode current, I' multiplied by the PMT gain, G_p. Only the values at the lower incidence levels are needed for calculating SNR. Note that in using these anode currents for calculating SNR, no PMT dark current or offset current (radiation-induced) need be added since such terms are integrated out following the voltage-to-frequency conversion by a counter which will count up during the scene time and down during the blank time, thereby restoring the DC baseline to zero.

All noise equations are derived in SER SBUV-NE-81-130, and are summarized in Tables 2-2 and 2-3.

Shot Noise in Signal Column. This noise is the shot noise on the signal current as amplified and degraded by the PMT. The values given are for the anode signal except for the CCR and cathode current monitor entries.

PMT Dark Noise Current Column. This value is derived from the PMT and photodiode specification and includes such sources as ohmic leakage across and through the tube base, thermionic emission from the photocathode, regenerative effects, ion pulses, nuclear radiation from radioactive isotopes in the glass envelope, secondary corona discharge in the tube.

Feedback Resistor Johnson Noise Column. This noise is caused by thermally excited charge carriers in the large feedback resistor.

Preamplifier Input Noise Column. This is based on use of LH0052 op amps for the preamplifier. These have an equivalent input noise voltage spectral density of $30 \times 10^{-9} V/\sqrt{Hz}$. The noise model contains non-linear functions of Δf so the values reflected as current at the input (the anode) are different for the discrete and sweep modes.

Preamplifier Input Leakage Shot Noise Column. The specified noise current spectral density of the LH0052 is less than 1×10^{-15} amp/√Hz resulting in an output noise as shown.

Quantization Noise Column. The classical expression for quantization noise is:

$$\text{Quantization Noise} = \frac{\text{Full Scale Current}}{\text{Full Scale Counts} \sqrt{12}}$$

This is applicable here where each range has a full scale equivalent average anode current of I_{fs} and 16-bit digitization is used. For range 1, $I_{fs} = 2 \times 10^{-13}$ amps, for range 2, $I_{fs} = 10 \times 10^{-11}$ amps, for range 3, $I_{fs} = 2 \times 10^{-9}$ amps (at the cathode) and for the CCR, $I_{fs} = 2.4 \times 10^{-9}$ amps.

Signal-to-Noise Ratios Column. All the noise currents were derived in terms of the equivalent anode current noise. Since the noise currents are all mutually uncorrelated, the signal-to-noise ratio is given by:

$$SNR = \frac{I_A}{[(N_s^2 + N_b^2 + N_p^2 + N_L^2 + N_2^2)\,\Delta f + N_v(\Delta f)^2 + N_q^2]^{1/2}}$$

These values are calculated for the two modes: discrete, where $\Delta f = 0.4$ Hz, and sweep, where $\Delta f = 5$ Hz. The specified limits of SNR are included for comparison. Note that the preamplifier voltage noise depends non-linearly on Δf so two values are listed. The top value is when $\Delta f = 0.4$, and the bottom value is when $\Delta f = 5$.

Cathode Current Monitor Column. The cathode current monitor is the same as Range 3. In order to monitor the gain of the PMT, the range 3 value must have a signal-to-noise ratio slightly over 200 (then Range 2 with 100 times as much signal will have a signal-to-noise ratio of about 2000, so the RSS of both will be about 200). The values listed in this row are the cathode current required to yield a SNR of 200 and the resulting counts and anode current. This is the useful range of gain measurements: from the value of I_k in the table (1.9×10^{-12}) to the saturation value of I_k (2×10^{-9}). For these values, the cathode Range 3 and anode range 2 overlap so a gain calculation can be performed by:

$$\text{PMT Gain} = \frac{5(\text{Range 2 Counts - Offset})}{\text{Range 3 Counts - Offset}}$$

Summary of Noise Sources

Tables 2-2 and 2-3 summarize the various noise sources and their analytic expressions or values.

2.5.2 LINEARITY

The principle source of non-linearity in the instrument is the photomultiplier tube. It is difficult to maintain a high degree of linearity over the seven orders of magnitude over which the instrument must operate. In order to achieve this dynamic range, three separate ranges are used. Range 1 is taken off the anode of the PMT and extends from 10^{-13} to 10^{-10} amps of anode current. Range 2 is also taken off the anode and covers the range from 10^{-10} to 10^{-8} amps of anode current. Range 3 is taken from the cathode and covers the range from 10^{-9} to 10^{-6} amps of (equivalent) anode current. Note that it overlaps Range 2 to provide PMT gain data. (Actually, each range overlaps the others, but the overlap is not normally used except for Range 2/Range 3.)

By taking the upper range (Range 3) off the cathode, many of the potential non-linearities of the PMT are avoided. It is at higher anode currents that such effects as space charge buildup cause PMT non-linearities. The cathode, on the other hand, is very linear over a much wider dynamic range. Its major source of non-linearity is the resistivity of the cathode material which does not become a factor until fairly large current densities occur. Estimated non-linearities of the system are summarized as follows:

Table 2-2
NOISE SOURCES

Noise Source	Analytic Expression	Value
PMT Anode Current Shot Noise	$\overline{i}_A^2 = 2e\ K\ G\ I_A\ \Delta f$	$2.3 \times 10^{-16}\ I_A\ \Delta f$
PMT Cathode Current Shot Noise	$\overline{i}_k^2 = 2e\ I_K\ \Delta f$	$3.2 \times 10^{-19}\ I_k\ \Delta f$
Photodiode Current Shot Noise	$\overline{i}_k^2 = 2e\ I_K\ \Delta f$	$3.2 \times 10^{-19}\ I_K\ \Delta f$
PMT Dark Current Shot Noise, Anode	$\overline{i}_D^2 = 4 \times 10^{-28} A^2/Hz$	$4 \times 10^{-28}\ \Delta f$
PMT Dark Current Shot Noise, Cathode	$\overline{i}_D^2 = 1.6 \times 10^{-33}\ A^2/Hz$	$1.6 \times 10^{-33}\ \Delta f$
Photodiode Dark Current Shot Noise	$\overline{i}_D^2 = 2.6 \times 10^{-30}\ A^2/Hz$	$2.6 \times 10^{-30}\ \Delta f$
Preamplifier Thermal Noise	$\overline{i}_T^2 = 4\ kT/R_T\ \Delta f$	$3.8 \times 10^{-29}\ \Delta f$
Preamplifier Voltage Noise Generator	$\overline{i}_V^2 = \overline{e}_n^2(w)/R_T^2[f_{cc} \ln f_1/f_o$ $+ (1 + 4\pi f_{ce}\ R_T C_T \Delta f)$ $+ (1+2\pi f_{ce} R_T C_T\ \Delta f)$ $+ (1+2\pi f_{ce} R_T C_T)\ 2\pi\ R_T C_T\ )f_1^2 - f_o^2)$ $+ (4/3)\pi^2 R_T^2 C_T^2 (f_1^3 - f_o^3)]$	$6.8 \times 10^{-31} (\Delta f=0.4)$ $8.4 \times 10^{-30} (\Delta f=5)$
Preamplifier Current Noise Generator	$\overline{i}_c^2 = \overline{i}_n^2(w)\ \Delta f$	$1 \times 10^{-30}\ \Delta f$
Second Stage Noise	$\overline{i}_2^2 = 8 \times 10^{-32}\ A^2/Hz$	$8 \times 10^{-32}\ \Delta f$
Quantization Noise	$\overline{i}_q = I_{FS}^2/(2^{32} \times 12)\ A^2$	$1.94 \times 10^{-11}\ I_{FS}^2$

Table 2-3
LIMITS ON OTHER NOISE SOURCES

Noise Source	Analytic Expression	Value
Chopper Wheel Velocity Perturbations	<0.018 Hz	SNR < 4000
PMT Power Supply Noise and Ripple	<26 m volts rms	negligible
Analog Ground Noise and Power Supply Noise	<1 m volt rms	

where:

e = Electron charge (1.6×10^{-19} coulombs)

k = PMT Noise Factor (1.43)

G = PMT Gain (500)

I_A = PMT average anode current

I_k = PMT or photodiode average cathode current

Δf = Bandwidth (0.4 Hz discrete mode; 5 Hz sweep mode)

f_o = 19.8 Hz discrete mode; 17.5 Hz sweep mode

f_1 = 20.2 Hz discrete mode; 22.5 Hz sweep mode

k = Boltzmann's constant (1.38×10^{-23} joule/°K)

T = Temperature (300°K)

R_T = Total preamplifier circuit resistance (~432×10^6)

C_T = Total preamplifier circuit capacitance (111 pF)

f_{ce} = Preamplifier voltage noise corner frequency (70 Hz)

$\overline{e}_n^2(w)$ = Preamplifier white noise voltage spectral density(30×10^{-9} V/√Hz)

$\overline{i}_n^2(w)$ = Preamplifier white noise current spectral density(1×10^{-15} A/√Hz)

I_{FS} = Full scale preamplifier input current on any particular range.

(Range 1 = 1×10^{-10}, Range 2 = 1×10^{-8}, Range 3 = $2 \times 10^{-9} = I_k$, CCR = 2.4×10^{-9})

Non-linear Factor	Magnitude Over Any Range
Photomultiplier Tube	<0.6%
Bleeder String Current Loading	<0.01%
Electronics (worse case)	<0.06%
Total Nonlinearity	<0.67%

Measurements on SN003 and SN004 instruments showed non-linearities of <1.0% on any range.

2.5.3 WAVELENGTH ACCURACY AND REPEATABILITY

The wavelength accuracy depends on the positioning accuracy of the grating drive mechanism and the accuracy of the assumed functional relationship between the position and the wavelength. The grating drive mechanism depends on mechanical and electrical uncertainties, and the position versus wavelength depend on the wavelength calibration accuracy.

2.5.3.1 Positioning Errors

The sources of positioning errors are identified by the electro-mechanical nature of the grating positioning system. Note that these position uncertainties measure the repeatability of the position. The accuracy of the encoder positioning is determined by these position uncertainties and by mechanical imperfections in the encoder and bearings. Once the encoder is assembled, these are repeatable over long periods of time and thus become part of the calibration of the wavelength. Table 2-4 summarizes these results.

2.5.3.2 Ground Calibration Errors

The calibration of the wavelength versus position function involves scanning the grating drive across a number of isolated spectral line sources. Twelve line sources are used in the wavelength calibration. The wavelengths of these sources are known quite accurately so the major errors will involve two considerations. First, the instrument response as the grating is scanned across a line source is triangular in shape with a full width at half maximum of about 1.13nm. The centroid of this response function is determined first. This centroid will be considered to be the effective angle for the particular wavelength in question. Then function is fitted to the 12 or so centroids spaced across the spectral range of the instrument which gives the wavelength as a function of the encoder angle, $\lambda = f(\theta)$.

Table 2-4
POSITIONING ERROR SOURCES

Error Source	Error Magnitude	Contribution to Position Uncertainty
Encoder Disc		
DC unbalance	±0.63 arc-second	±0.63 arc-second
Amplitude variations	±0.31 arc-second	0
Phase jitter	±0.65 arc-second	±0.41 arc-second
Long term disc error	±1.5 arc-second (over 180°)	±0.15 arc-second
Bearing Friction	3.5 oz-in	±0.07 arc-second
Electronic Offset	20 mV at readout preamplifier	±0.05 arc-second
Electronic Noise	8.5×10^{-8} volt/√Hz	±0.03 arc-second
RSS of above terms		±0.77 arc-second
Average wavelength uncertainty at	0.077 nm/step / 19.78 sec/step	±0.003 nm

2.5.3.2.1 Centroid Calculation Errors

In calculating the centroid, two error sources enter. The first is due to the position uncertainty determined in the last section and the amplitude uncertainty of each readout along the response curve. This gives rise to an uncertainty in the location of the centroid of the data points. The second is due to the fact that the centroid of the data points is in general not precisely equal to the centroid of the (ideally smooth) instrument response.

The centroid is calculated as:

$$\bar{\theta} = \frac{\sum_{i=1}^{n} \theta_i N_i}{\sum_{i=1}^{n} N_i}$$

Each angle θ_i and each amplitude value N_i have uncertainties, σ_{θ_k} and σ_{N_K}, for each of the n measurements. We assume these are mutually uncorrelated so the best estimate of the uncertainty in θ is given by:

$$\sigma_{\bar{\theta}}^2 = \sum_{k=1}^{n} [(\frac{\delta\bar{\theta}}{\delta\theta_k} \cdot \sigma_{\theta_k})^2 + (\frac{\delta\bar{\theta}}{\delta N_k} \cdot \sigma_{N_k})^2]$$

or

$$\sigma_{\bar{\theta}}^2 = \sum_{k=1}^{n} \frac{N_k^2}{(\sum_{i=1}^{n} N_i)^2} \cdot \sigma_{\theta_k}^{\;2} + \frac{\sum_{k=1}^{n} (\sum_{i=1}^{n} (\theta_k - \theta_i) N_i)^2}{(\sum_{i=1}^{n} N_i)^2} \cdot \sigma_{N_k}^{\;2}$$

As can be seen, the absolute magnitude of the Ni's do not matter - normalized values can be used. Also, the magnitude of the θ's do not matter so long as the step size is constant (which it will be) since if the step size is a, then $\theta_k = \theta_o + (k-1)a$, so $\theta_k - \theta_i = (k-1)a$.

Hence we can calculate $\sigma_{\bar{\theta}}^2$ by using the estimated response of the instrument to a line source, using relative values for N_i and using a step size of 31.55 arc second for for θ_i (this is the sweep mode step size). Notice that σ_θ is relatively insensitive to small variations in the shape of the response functions. The dominant factors in estimating σ_θ are the number of data points, n, the position uncertainty, σ_{θ_K}, the amplitude uncertainty, σ_θ, and the step size. For an assumed bound on the signal-to-noise ratio of 50 (so the σ_{N_K}=0.02N_k) we estimate:

$$\sigma_\theta \leq 0.46 \text{ arc second}$$

Over the 18° grating angular range, the wavelength step size for a given angular step size varies from about 0.0688 to 0.0772nm for a 19.775 arc second step. So, a rough estimate on the wavelength uncertainty is:

$$\sigma_\lambda \leq 0.0018\text{nm}$$

To estimate the uncertainty in determining the centroid of the response curve, we make the simplifying assumption of a response curve like an isosceles triangle and compute the difference between two sampling patterns; the first symmetrical about the peak of the triangle, the second shifted by 1/2 of a sample step size. We find that the difference is independent of the amplitude of the triangle and its width. The net result is:

$$\text{Sampling error} = 0.069\ \theta_S$$

Where θ_S is the sampling step size. For the wavelength calibration in a sweep mode, the step size is θ_S = 39.55 arc second. Hence:

Sample error = 2.73 arc second

Worse case wavelength error due to sampling = 0.01nm

Note that this error can be halved by using the position mode of the grating drive to step at the grating drives finest increment of 19.78 arc seconds. The sample error is then 1.36 arc second, or ± 0.005nm.

2.5.3.2.2 Errors in Fitting the Grating Function

The functional relationship between the grating angular setting and the wavelength is the grating function. In an ideal system, that function has the form:

$$\lambda = a_1 \sin (a_2\theta)$$

As mentioned, about 12 spectral features will be used to fit the function, i.e., determine the parameters a_1 and a_2. This will be done by minimizing the chi-squared goodness-of-fit test with respect to a_1 and a_2, or by other acceptable means. The goodness of fit and the value of the residual errors will be computed to assure that the parameters determined yield a function which accurately respresents the real system within the prescribed tolerances (basically ± 0.05nm). If the probable error for an agreed on confidence level exceeds this tolerance, then a plot of the residuals will be used to determine what correction factor must be applied, for example adding on a quadratic term, $a_3\theta^2$. The dominant factors determining the non-ideal response function will be the accuracy of the encoder readout which is estimated to be 4.95 arc seconds (or 0.02nm).

An additional uncertainty is due to misalignment of the primary and backup encoder position sensors. This may amount to 1.1 arc-seconds (0.004nm). This is small compared to other inaccuracies so one grating function should suffice for both primary and backup systems. Note that this misalignment is an offset (additive) term in θ so that it is always possible to determine new values of θ for the desired wavelengths for the backup system and program them into one or two of the four redundant fix memory segments for the grating command system (see Section 4). This set of angle data can then be selected simultaneously with selection of the backup encoder sensor in the event of a failure in the primary system.

2.5.3.3 Summary of Wavelength Accuracy and Precision

The factors determining wavelength precision or repeatability are exclusively the positioning errors. The errors in determining the centroid are strictly errors in determining the location of a spectral line. They are used in determining the final goodness of fit for the grating function. This goodness of fit will be determined by adding correction terms to the function until the wavelength accuracy is better than 0.05nm. So we may summarize:

Wavelength Precision	$\leq \pm$ 0.003nm
Centroid Accuracy of a Spectral Line	$\leq \pm$ 0.01nm
Wavelength Accuracy	$\leq \pm$ 0.05nm

2.5.4 IN-FLIGHT WAVELENGTH CALIBRATION

The in-flight wavelength calibration scans across the mercury 253nm spectral line in 12 steps spaced 79.2 arc seconds (about 0.3nm) apart. The measurement precision is just that found in Section 2.5.3.1, ±0.003nm. The accuracy is the accuracy in determining the centroid of the profile, as found in Section 2.5.3.2.1 with $\theta_s = 79.2$. This value is 5.46 arc seconds or 0.02nm. This is compared to a previous value of the centroid, determined on the ground during calibration. Many such ground determinations can be made to improve the accuracy, however, even a single ground determination compared with a single in-flight determination will yield an accuracy of $\pm$0.028nm = $\pm\sqrt{2(0.02)^2}$

In-flight wavelength calibration precision	±0.003nm
In-flight wavelength calibration accuracy	±0.028nm

2.5.5 RADIATION INDUCED NOISE

In order to reduce in-orbit signal contamination due to high energy particle induced radiation noise to less than 1% in the South Atlantic Anomaly, it has been determined that the unchopped radiation induced noise must be less than 8.9×10^{-14} amps of cathode current. (This is noise current in a 5 Hz bandwidth at 20 Hz.) To achieve this, 11nm of aluminum shielding is used to virtually eliminate the election flux. This is followed by 1nm of lead shielding to eliminate Bremsstrahlung radiation produced by the election energy loss. Table 2-5 is a summary of the calculated radiation induced noise.

Table 2-5
RADIATION INDUCED NOISE SUMMARY

Radiation Species/Effects	Induced Noise Current (Cathode)
Electrons <4 MeV	negligible
Protons >300 MeV	$\leq 5.1 \times 10^{-14}$
Protons <300 MeV	$\leq 1.3 \times 10^{-14}$
Bremsstrahlung	$\leq 5 \times 10^{-15}$
Total Radiation Induced Noise (RSS)	$\leq 5.3 \times 10^{-15}$ amps

Section 3
SUBSYSTEM AND COMPONENT DESCRIPTION AND OPERATION

3.1 SCOPE

This section contains a description of the major subsystems and components of the Sensor Module (SM) and the Electronics and Logic Module (ELM). These modules and an interconnecting electrical cable assembly comprise the SBUV/2 instrument (see Figure 2-1, Section 2).

3.2 SENSOR MODULE (SM) DESCRIPTION

A subassembly breakdown of the Sensor Module and its major subassemblies are shown in Figures 3-1 through 3-3. Figure 3-4 is a dimensional view showing relative locations of major components with respect to the structure. Figure 3-5 is a layout of the Sensor Module. The structure of the Sensor Module is a welded aluminum housing which provides the optical bench for the monochromator as well as mounting interfaces for all of the other Sensor Module subsystems.

3.2.1 SENSOR MODULE INTERFACES

3.2.1.1 Envelope, Center of Gravity, and Weight

The Sensor Module space envelope and center of gravity (CG) locations are shown in Figure 3-6a and 3-6b. The weight of the Sensor Module is 59.5 pounds for FM2 and 58.47 for FM3.

3.2.1.2 Mechanical

Figure 3-7a and 3-7b shows the interface hole pattern specified in the Unique Instrument Interface Specification IS-2295548 for mounting the Sensor Module to the spacecraft. Structural analysis showed that two of the attach points were taking very little load. Consequently, to save weight, the structure was modified to eliminate these attach points. The non-used attach points are shown in Figure 3-7a.

The Sensor Module is attached using 1/4-28 fasteners. The pad size at each fastener is limited to 0.28 in^2 area to limit the instantaneous heat flow between the Sensor Module and the spacecraft to 5W with a spacecraft temperature range between zero and 30°C. The instrument mounting feet have a coplanarity of 0.005-inch and the mounting hole pattern is aligned within 0.1° of the instrument Y and X axis.

3.2.1.3 Electrical

The interface between the Sensor Module and the Electronics and Logic Module is described in Section 3.3.1.

3.2.1.4 Optical

Two alignment mirrors are provided on the Sensor Module located as shown on Figure 3-4. One mirror is arranged to be perpendicular to X axis of the instrument (or parallel to the plane of the mounting feet). The second is aligned to be perpendicular to the spacecraft Y axis.

3.2.2 MONOCHROMATOR ASSEMBLY

3.2.2.1 Optical Systems

The monochromator assembly is a double monochromator consisting of two complete monochromators, optically arranged one after the other. This arrangement rejects stray light, both spatial and spectral, much more efficiently than either individual monochromators would if used alone.

The first of the single monochromators is sketched in Figure 3-8. Light passes through the entrance slit, diverges to the Ebert mirror, and is collimated on reflection. The collimated beam is diffracted at the grating. Diffracted light of one wavelength (depending on grating angle) is focused by the Ebert mirror at the exit slit. The exit slit would be placed as shown if there were only a single monochromator.

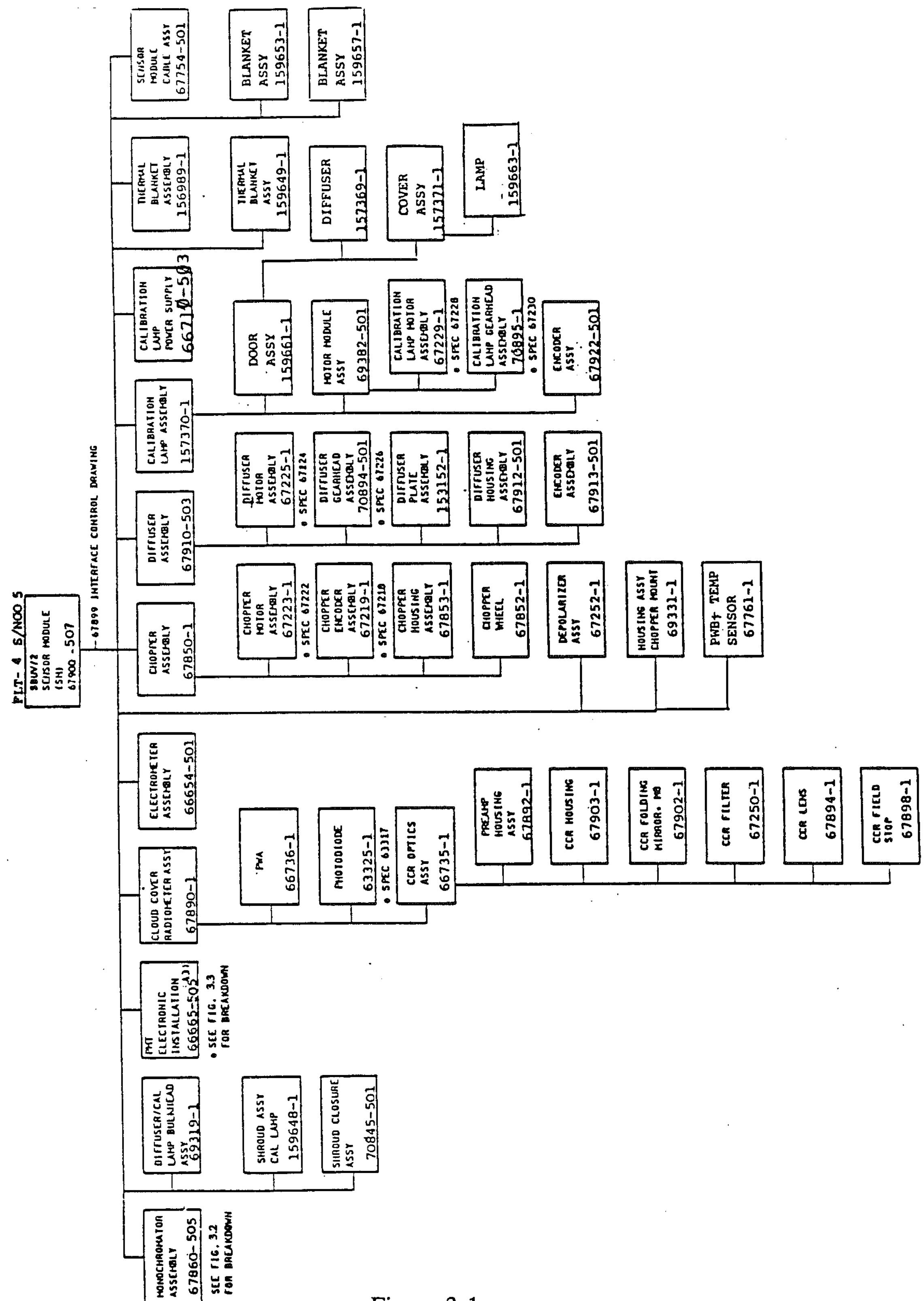

Figure 3-1

Sensor Module Assembly Breakdown

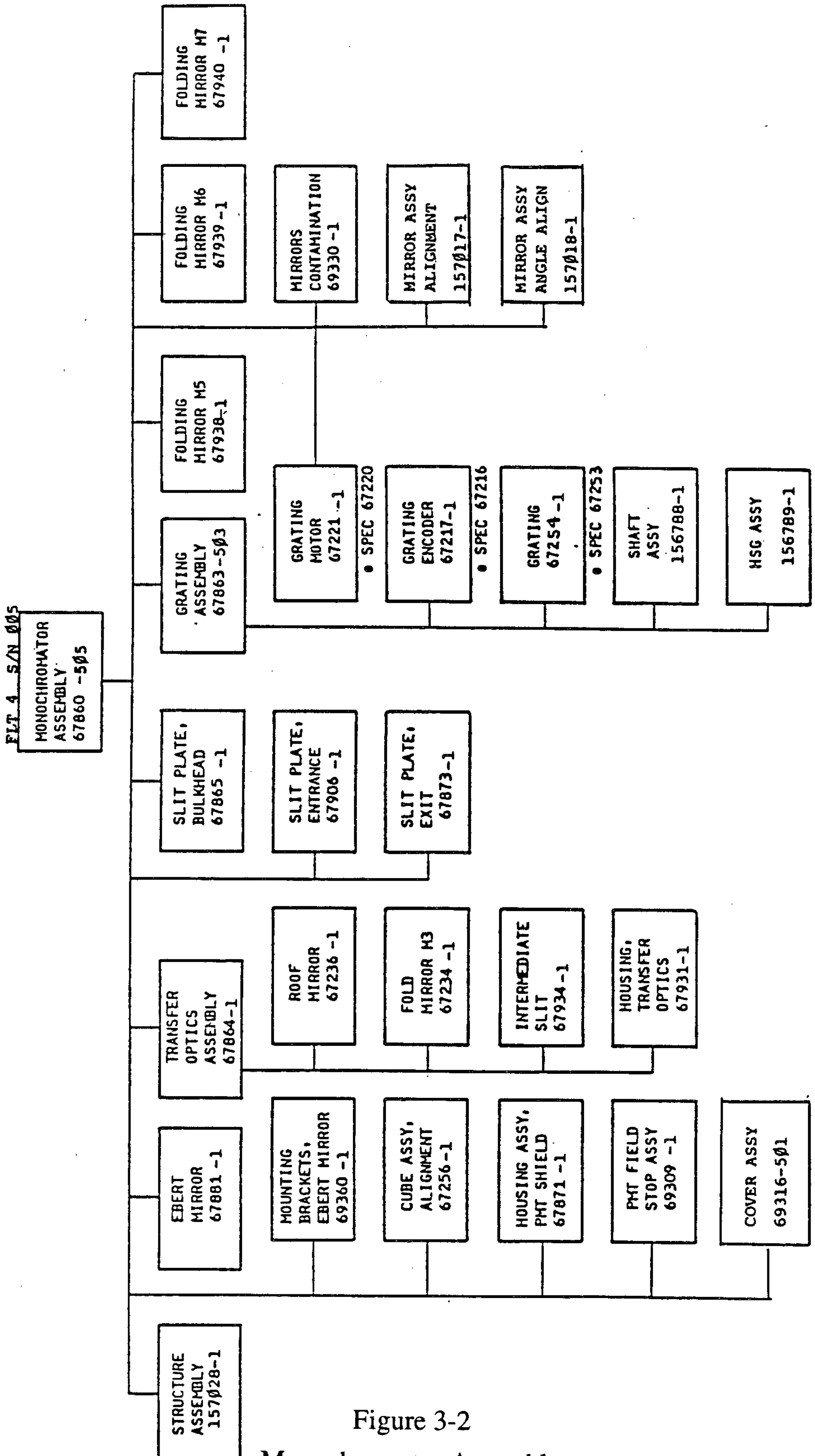

Figure 3-2
Monochromator Assembly

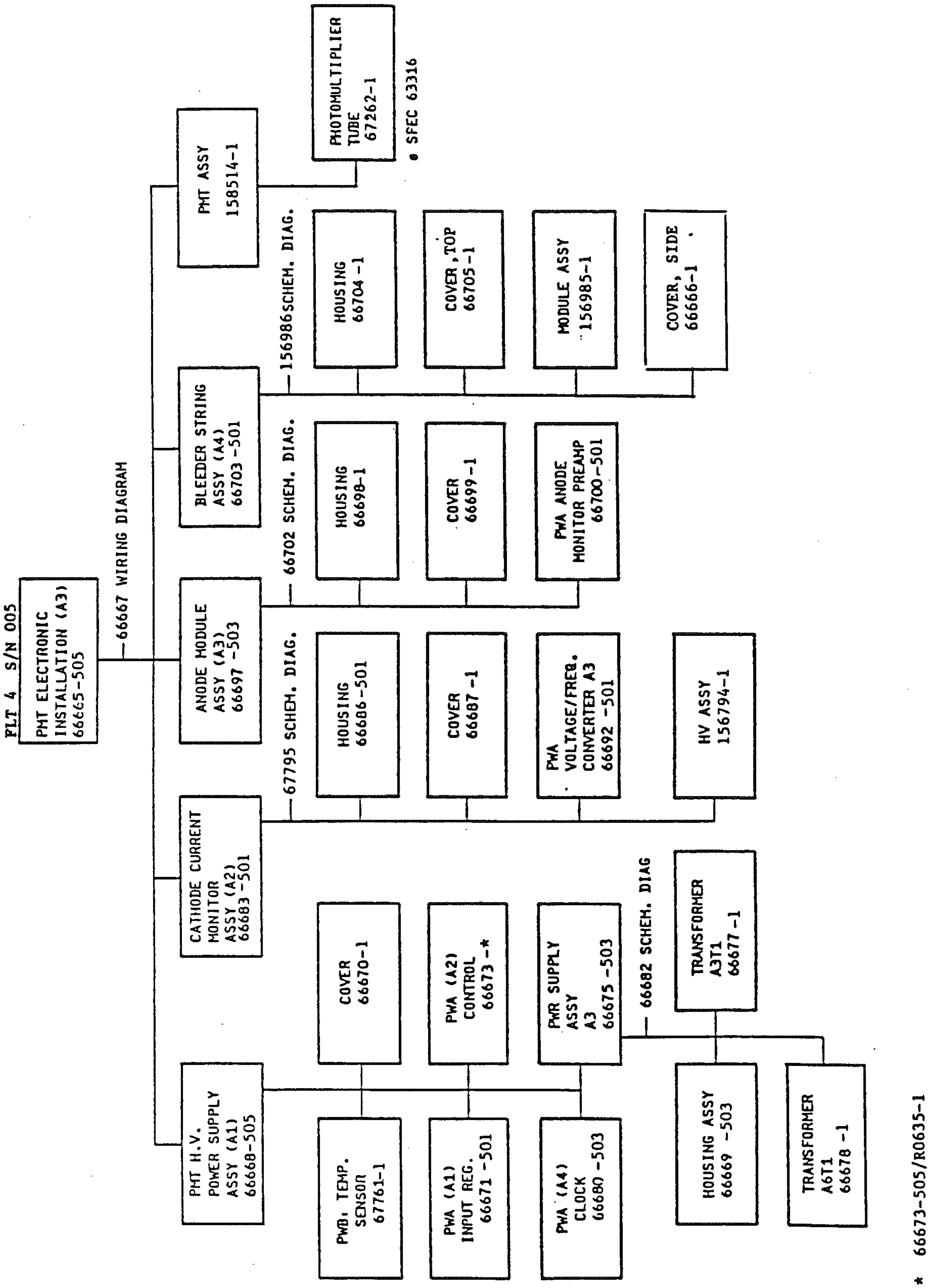

Figure 3-3
PMT Electronic Assembly

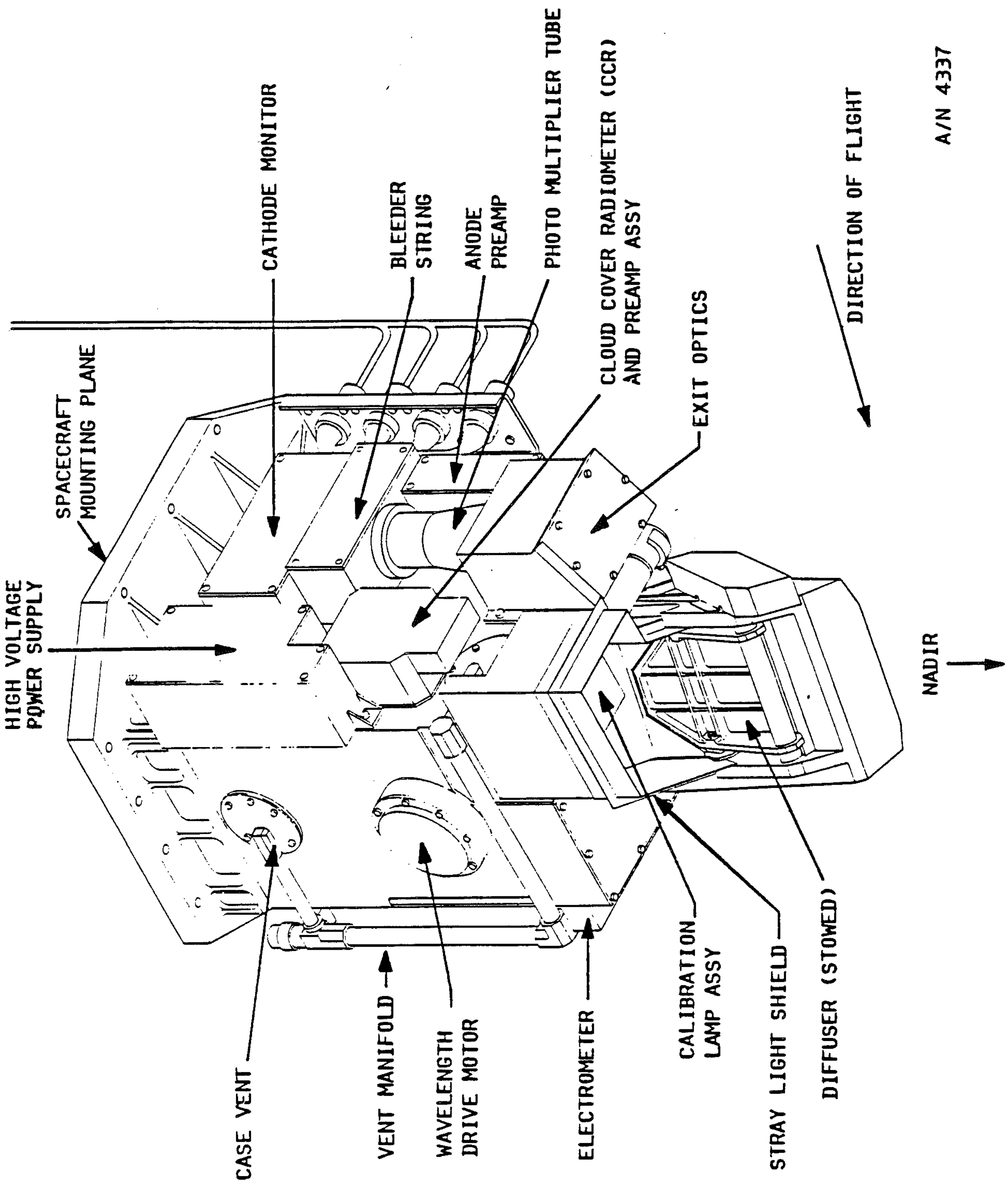

Figure 3-4
Sensor Module

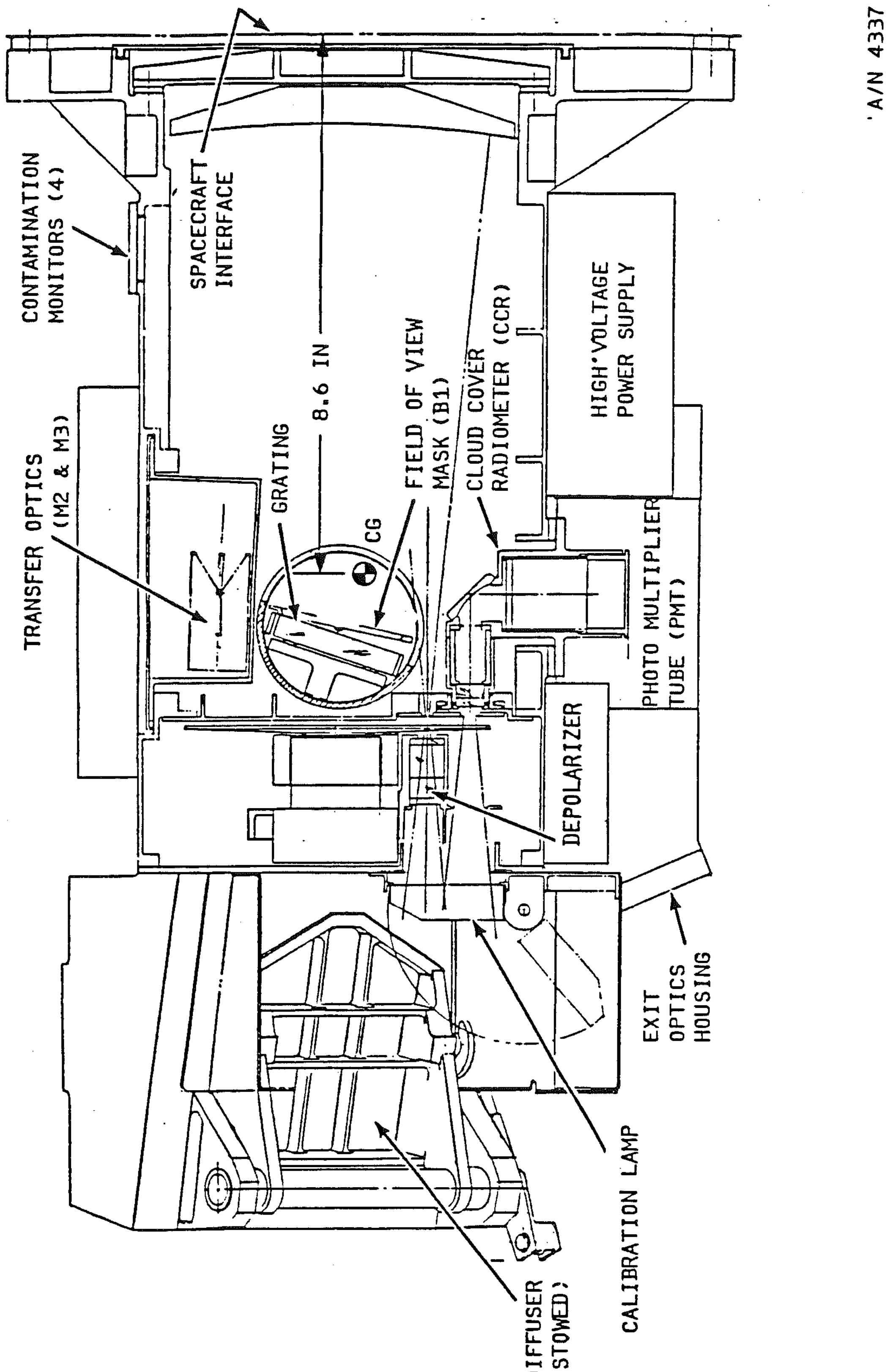

Figure 3-5

Layout of Sensor Module (Sheet 1 of 2)

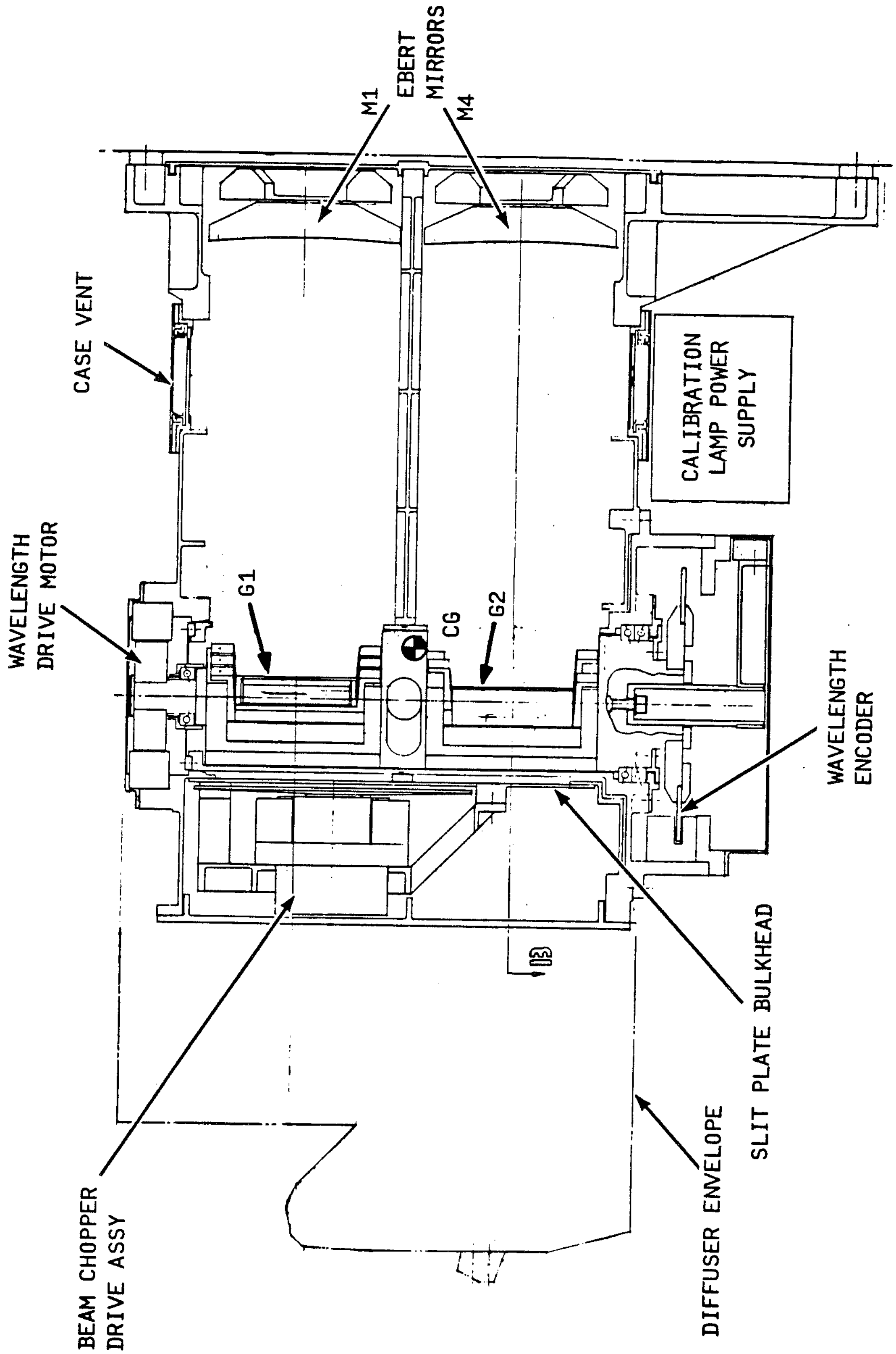

Figure 3-5 (Continued)
(Sheet 2 of 2)

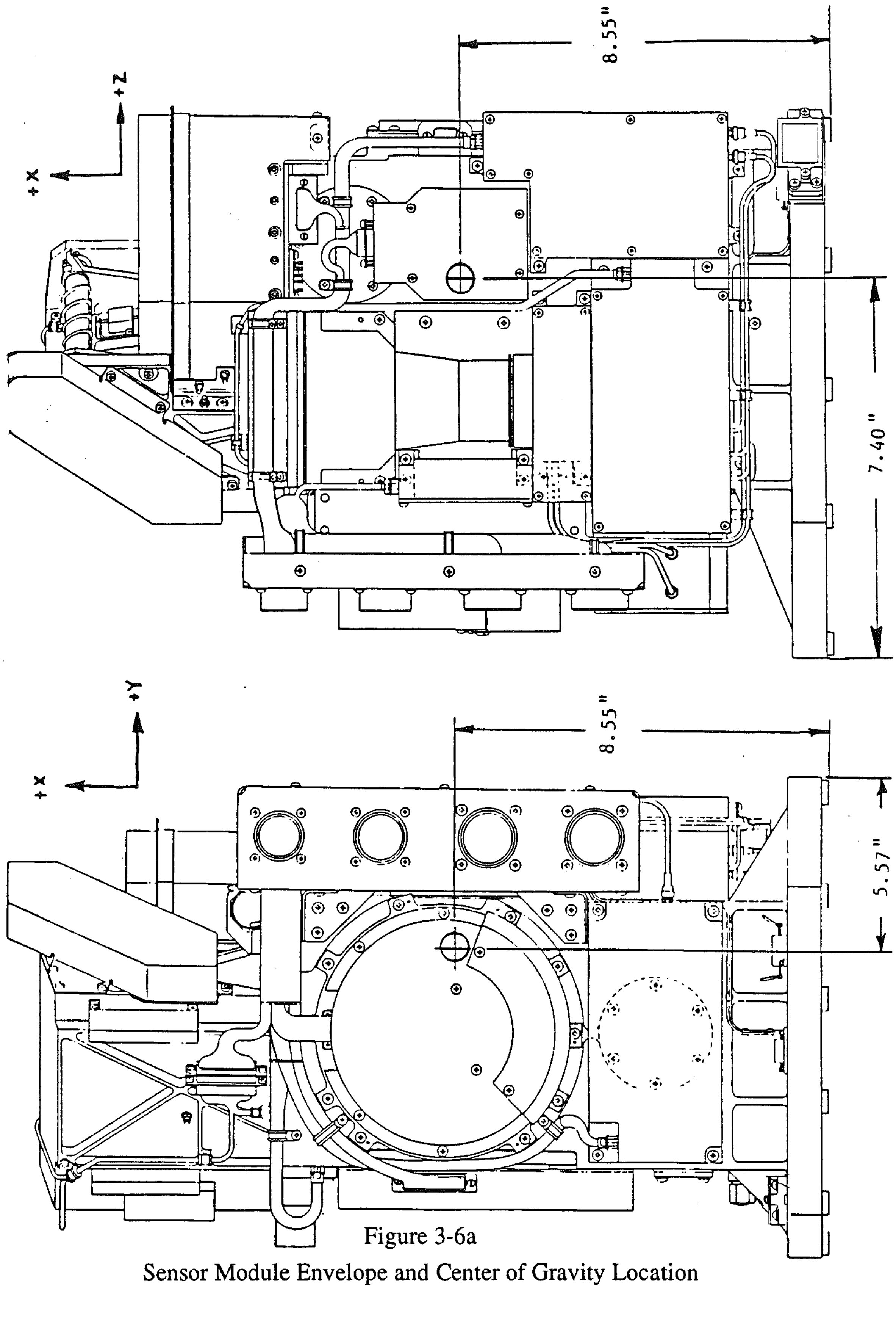

Figure 3-6a
Sensor Module Envelope and Center of Gravity Location

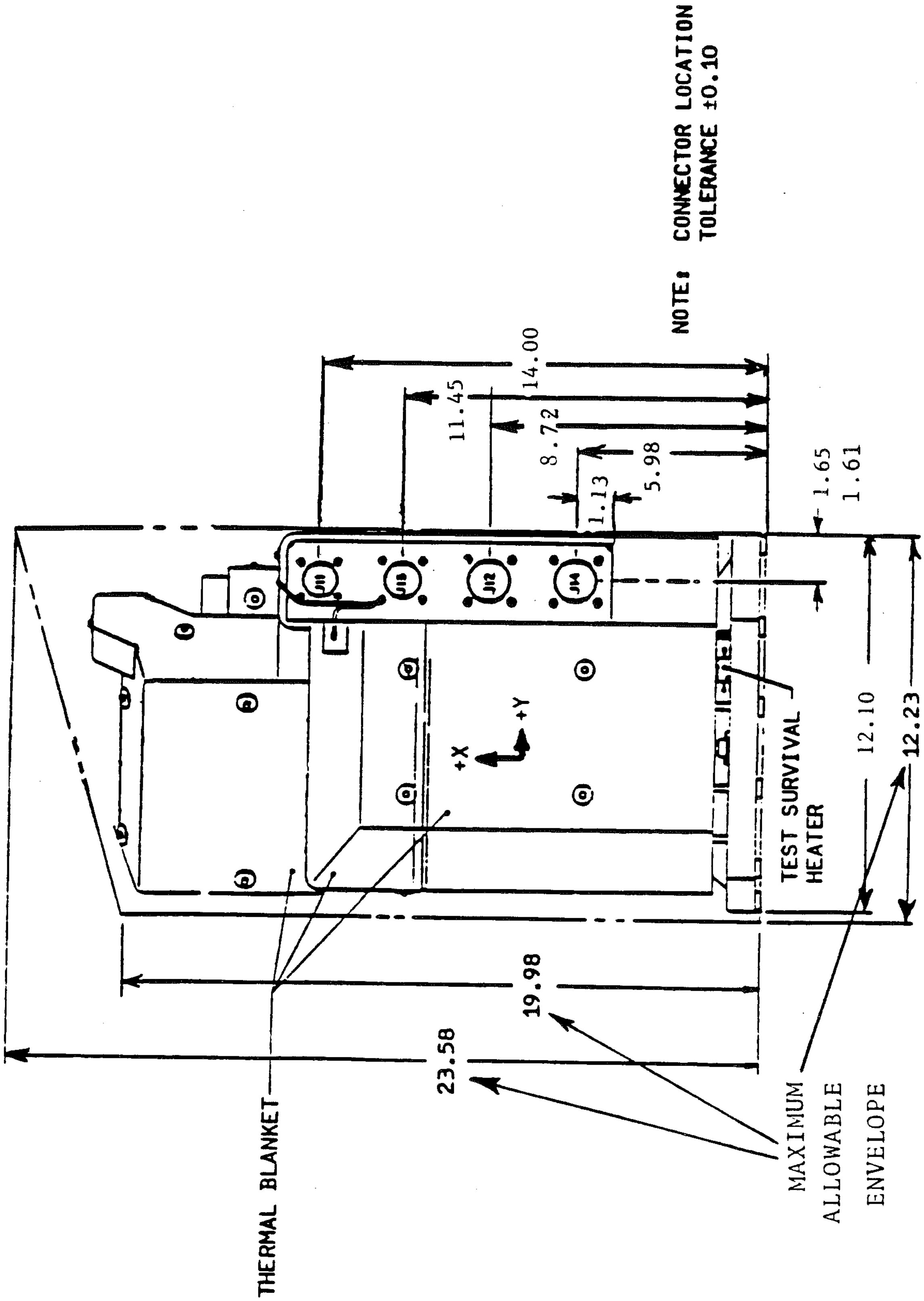

Figure 3-6b
Sensor Module Envelope

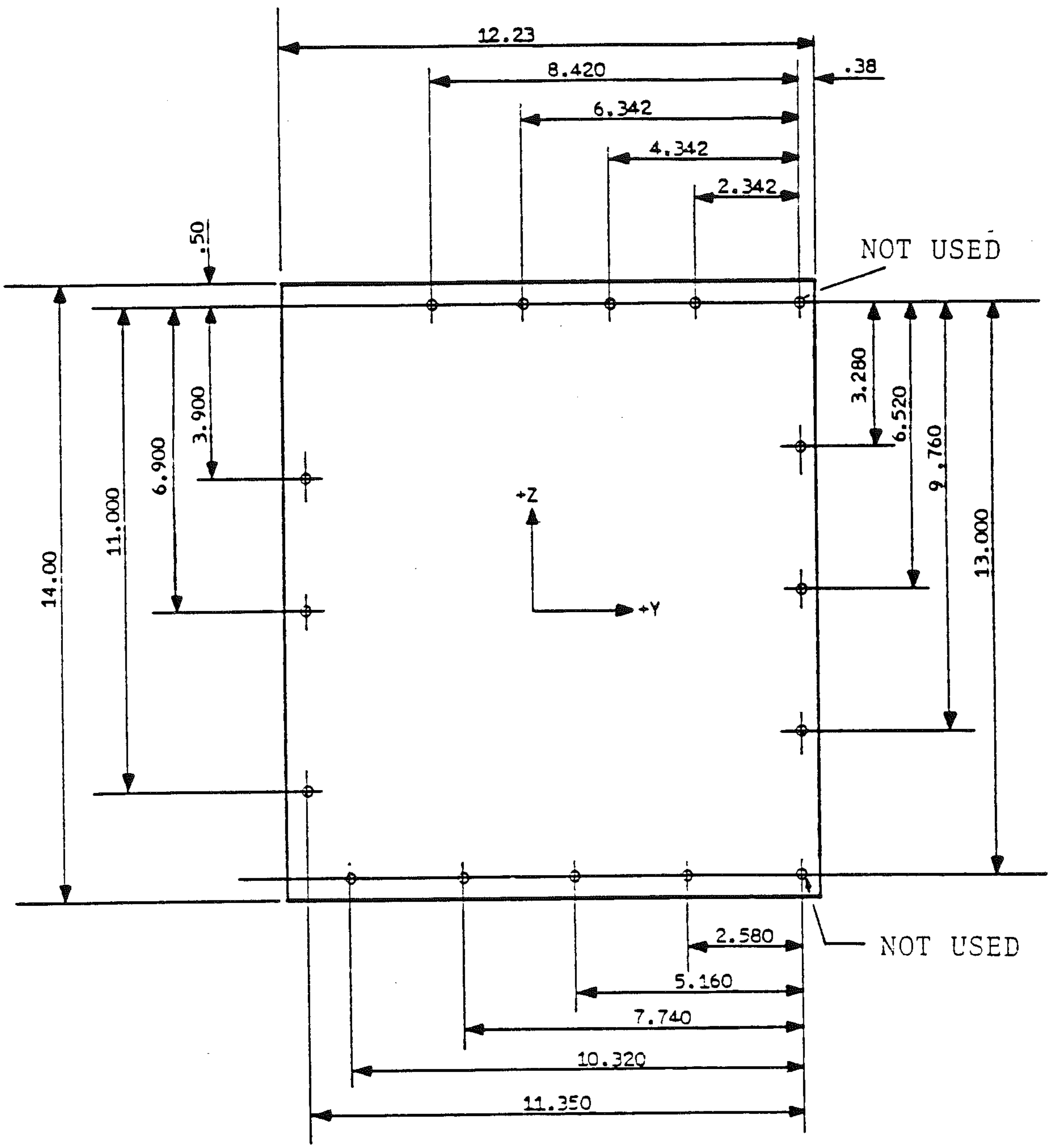

VIEW LOOKING TOWARD SPACECRAFT FROM SENSOR MODULE

Figure 3-7a
Sensor Module to Spacecraft Mounting Interface

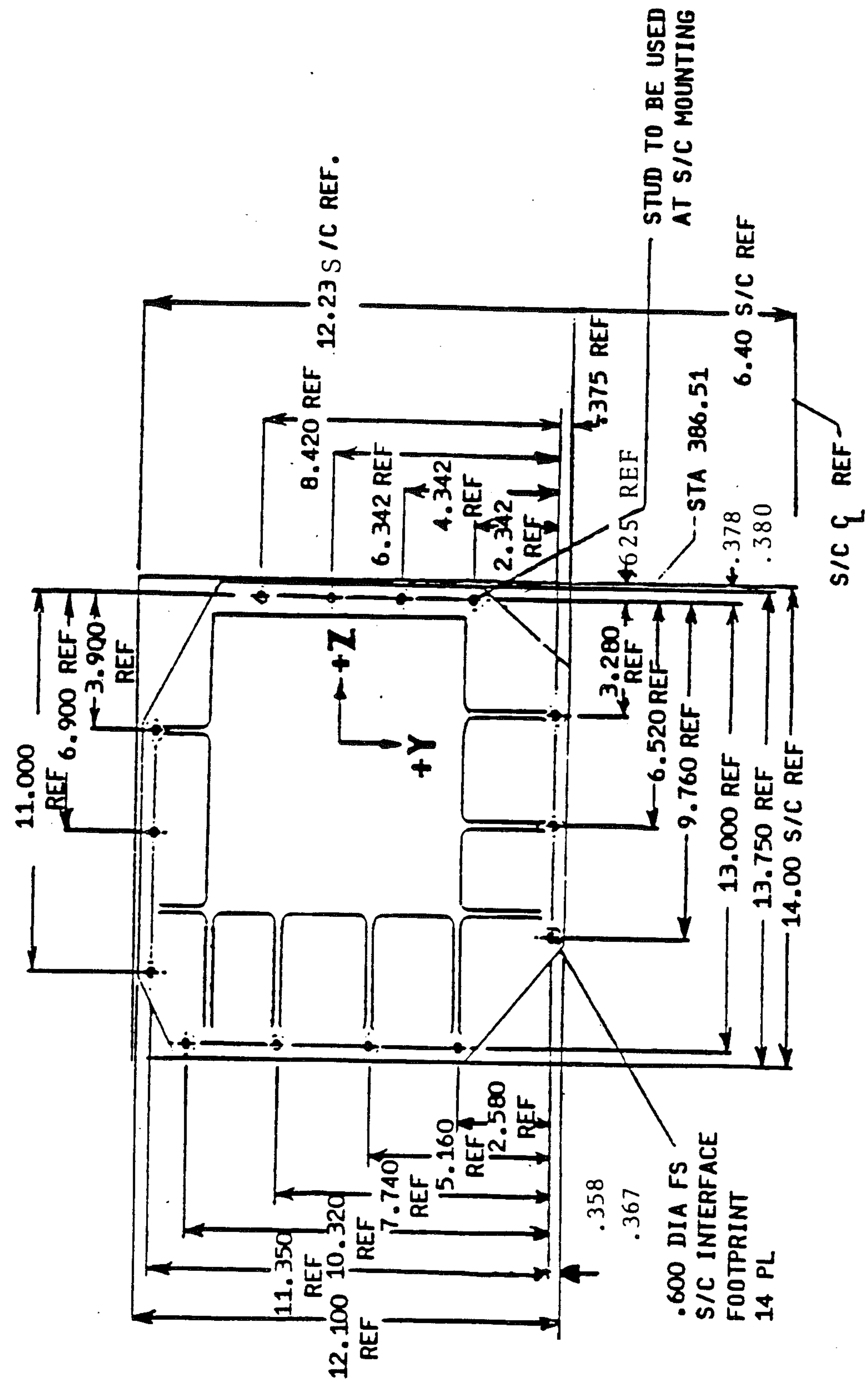

Figure 3-7b
Sensor Module Interface Footprint

There are actually two monochromators in series with each other, so that the exit slit of the first monochromator is the entrance slit of the second. The double monochromator is shown in Figure 3-9. The intermediate slit, which is common to both monochromators, is located in the wall between them. The transfer optics (shown above and below the slit in Figure 3-9) are required to fold the beams. This packaging permits the two gratings to be mounted on the same shaft, which helps guarantee wavelength synchronism between monochromators. The first half of the double monochrometer is shown in Figure 3-10.

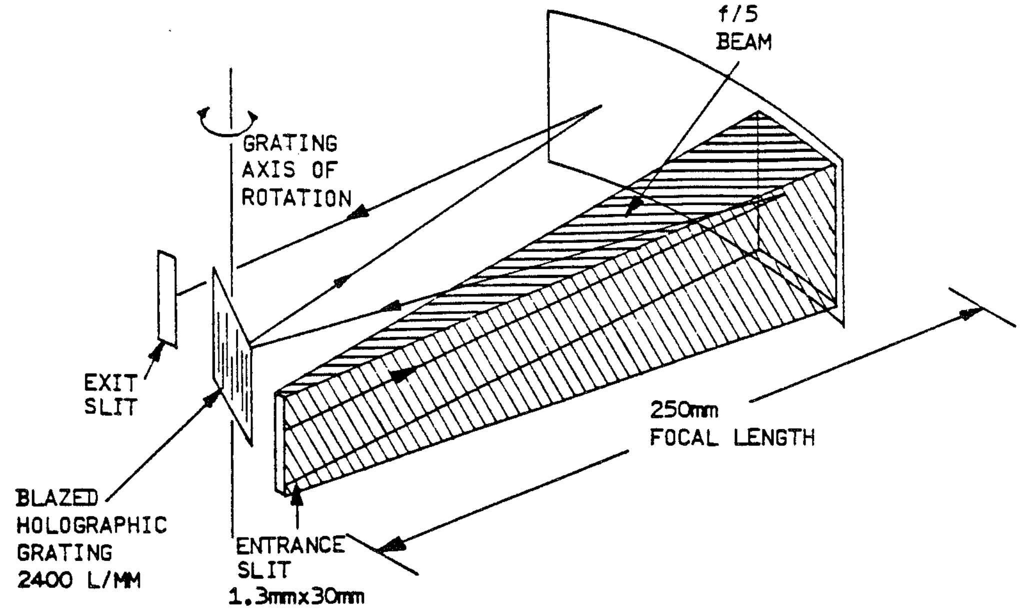

Figure 3-8
One of the Ebert-Fastie Monochromators

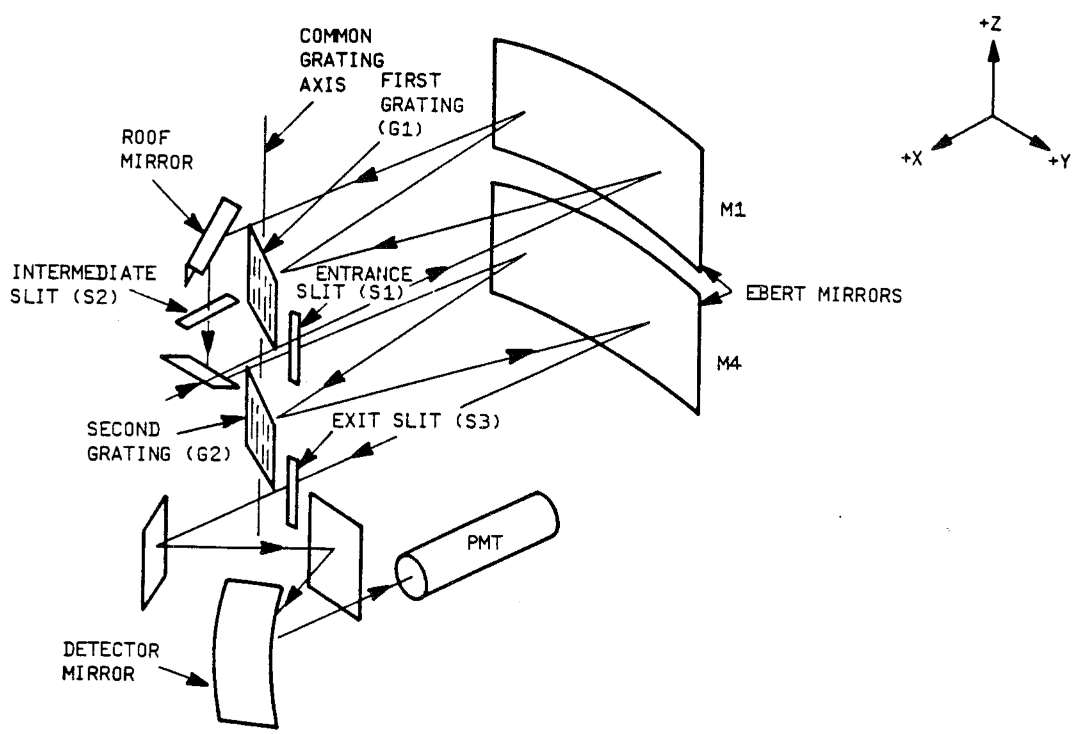

Figure 3-9
SBUV/2 Double Monochromator

The upper transfer element is a "roof" mirror, using two plane mirrors at a 90° angle. This reverses the image at the intermediate slit so that the dispersion (spectral spread) of the second monochromator adds to that of the first. (If both transfer elements, before and after the slit, were simple mirrors, the dispersion of the second monochromator would cancel that of the first.) This double dispersion permits twice the slit width for the same spectral bandpass, as compared with a zero dispersion configuration. The doubled slit width doubles the energy throughput.

The field-of-view is set by a mask at the first grating (G1, Figure 3-9). As shown in Figure 3-5, this mask (B1) is tilted relative to the grating face. The mask is perpendicular to the incoming light when the monochromator is set at about 230nm. This arrangement lessens the change of field-of-view size with grating angle compared with having the mask at the same angle as the grating face. The axis of rotation of the grating shaft is at the center of the mask, so rotation of the shaft causes no lateral motion of the mask; thus the field-of-view pointing direction of the monochromator is constant regardless of wavelengths.

Figure 3-10 shows the main optical dimension of the first half of the double monochromator as it is actually folded. Figure 3-11 shows the arrangement as it would be if it were unfolded, as though the optics were refractive rather than reflective.

Table 3-1 shows the chief optical characteristics of the monochromator components.

The mask at G1 is the field stop of the monochromator. Images of the mask at G1 are found at G2 (the second grating) and at a stray-light mask in the exit optics. The field stop and the entrance slit S1 jointly determine the pointing direction of the field-of-view. Thus, the field stop and S1 are coupled as closely as possible. This way, the pointing direction will be less likely to change with vibration and temperature.

Both G2 and the exit optics mask are larger than the corresponding G1 mask images to ease positioning and imaging tolerances without introducing vignetting. The second (lower, in Figure 3-9) transfer element is slightly concave, so that the image of G1 is smaller and is better focused at G2, minimizing the necessary size of G2. Gratings G1 and G2 are identical, for lowest cost.

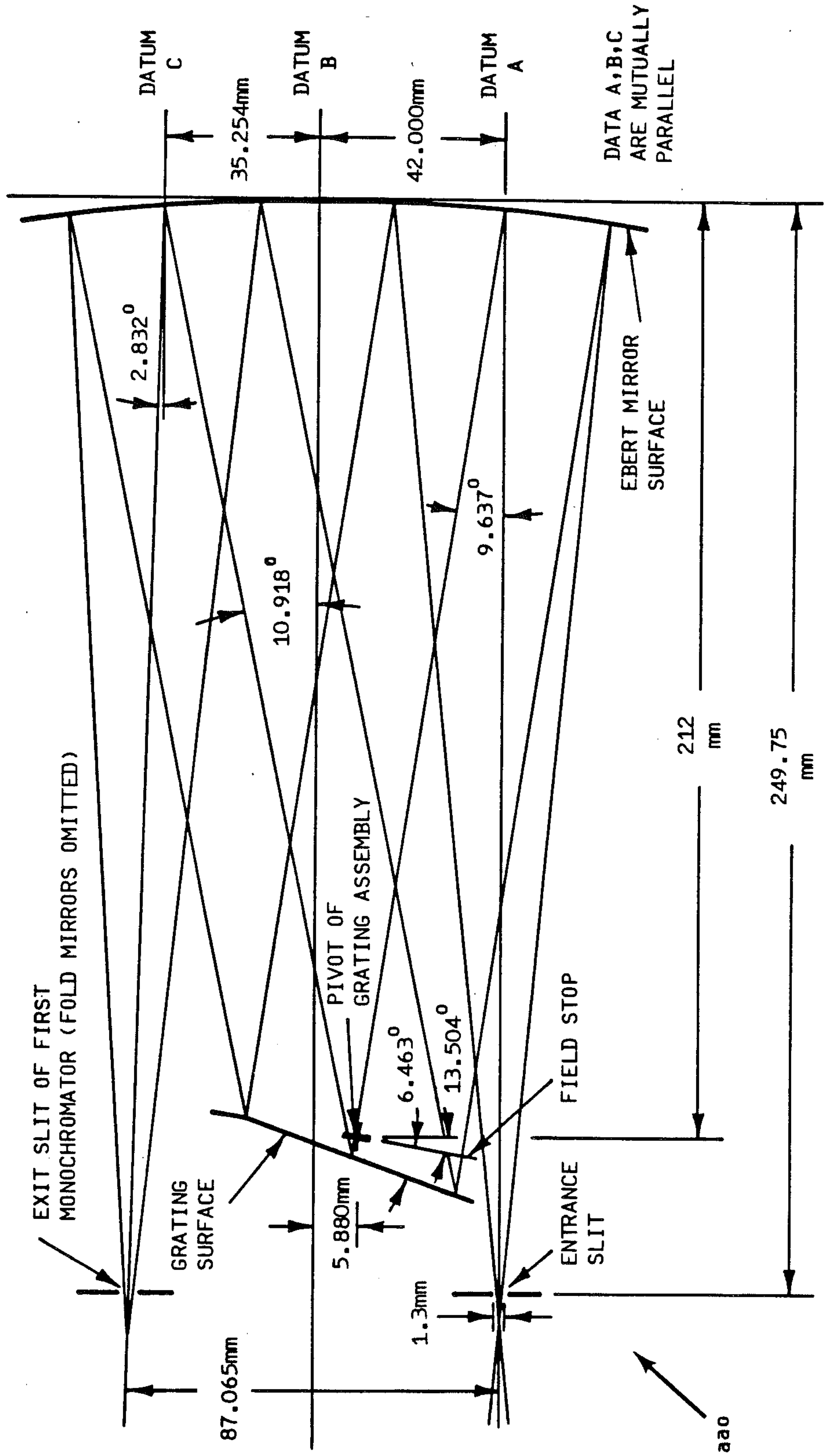

Table 3-10
Optical Diagram of First Half of Double Monochromator

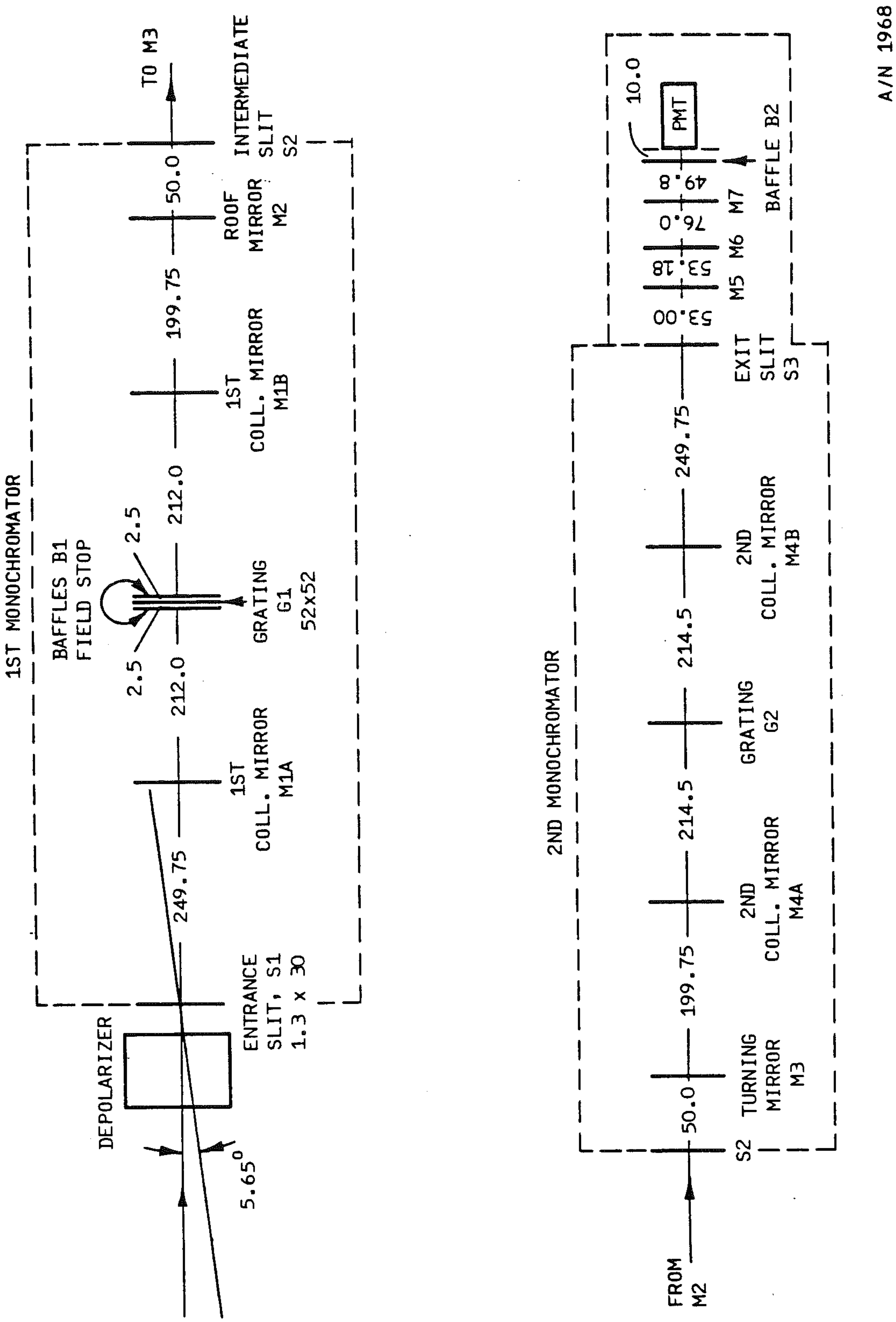

Figure 3-11
Unfolded Layout, Double Monochromator

Table 3-1
SBUV/2 Optical Components

COMPONENT	REFERENCE CALLOUT	NOMINAL VERTEX LOCATION (1)			COMMENTS	FIGURE QUALITY	CLEAR APERTURE (2)	INITIAL POSITION TOLERANCE (3)
		X	Y	Z				
DEPOLARIZER	DP	0	-8	-50	Quadruple Wedge, Crystal Quartz	TBS	45.1 x 10.2	0.5, 0.5, 1.0 20, 20, 20
MONOCHROMATOR:								
• ENTRANCE SLIT	S1	0	0	0	Flat	±0.1mm	30x1.3 Rectangular	
• EBERT MIRROR	M1	0	42	250	Concave, R = 500mm	1λ (633nm)	83x138 Rectangular	
• FIELD STOP	B1	0	35.7	38.0	Flat	±0.1mm		
• GRATING	G1	0	36.1	35.3	Flat	1λ/INCH (633nm)	52x52	
• ROOF MIRROR	M2	0	87.06	50.24	Two Flats form 90° Internal Roof	5λ (633nm)		
• INTERMEDIATE SLIT	S2	50	87.06	50.24	Flat	±0.1mm	34x2.5 Curved Strip, R = 292	
• FOLD MIRROR	M3	100	87.06	50.24	Concave, R = 2400mm	1λ (633nm)		
• EBERT MIRROR	M4	100	42	250	Concave, R = 500mm	1λ (633nm)	83x138 Rectangular	
• GRATING	G2	100	36.1	35.3	Flat	1λ/INCH (633nm)	52x52	
• EXIT SLIT	S3	100	0	0	Flat	±0.1mm	32x1.34 Curved Strip, R = 198	
• FOLD MIRROR	M5	100	0	-53.0	Flat	3λ (633nm)	51x19	
• FOLD MIRROR	M6	100	-31.0	-9.8	Flat	3λ (633nm)	57x36	
• DETECTOR MIRROR	M7	100	-84.5	-63.7	Concave, R = 94mm	3λ (633nm)	76x49	
• SCATTER STOP	B2	100	-83.7	-13.9	Flat	±0.1mm	x , trapezoidal	0.3, 0.3, 0.3, 20, 20, 20
• DETECTOR	PMT	100	-83.5	-3.4	Flat Surface Photomultiplier	±0.1mm	TBS	1, 1, 1, -, -,
CLOUD COVER RADIOMETER:								
• FILTER	F	0	-15.0	2.8	λ = 379nm			
• LENS	L	0	-15.0	6.5	Singlet, Fused Silica			
• FIELD STOP	B3	0	-15.0	17.7	Flat			
• DETECTOR MIRROR	M8	0	-15.0	22.0	Concave, R = 27mm	10λ (633nm)		
• DETECTOR	VPD	0	-22.0	22.0	Vacuum Photodiode		13mm diameter	

(1) X, Y, Z mm, Optical Coordinates (Origin at entrance slit center)

(2) X x Y mm

(3) X, Y, Z mm α, β, γ mrad

In the packaging, the position of the entrance slit S1 is fixed. The final exit slit S3 is fixed in focus, but some adjustment is allowed laterally. This slit arrangement eliminates the need of alignment adjustments which would interact with the chopper position or complicate the exit optics. In this double dispersion monochromator configuration, a properly sized (slightly oversized) intermediate slit (S2) does not effect spectral bandpass shape, which is set only by S1 and S3.

Table 3-2 shows the breakdown of the total optical efficiency for the 12 discrete mode wavelengths. The system has ten total reflections from aluminum and MgF_2 coated mirrors as follows: four at collimating mirrors, five at folding mirrors, and one at the final concave exit mirror. The remaining losses occur in transmission through the depolarizer and the reflections from the two gratings. Accordingly, the expression for optical efficiency is:

$$E_\lambda = R_R^4 \, R_F^5 \, R_G^2 \, R_E \tau$$

From Table 3-2 it is seen that the total optical efficiency varies between 6.10 and 4.76 percent for the discrete mode wavelengths.

The exit optics (see Figure 3-12) use three mirrors and a field mask to image the exit slit on the PMT and block unwanted light coming from the inside of the monochromator. The first two mirrors are plane folding mirrors to facilitate compact packaging. The third of the mirrors is a concave spheroid.

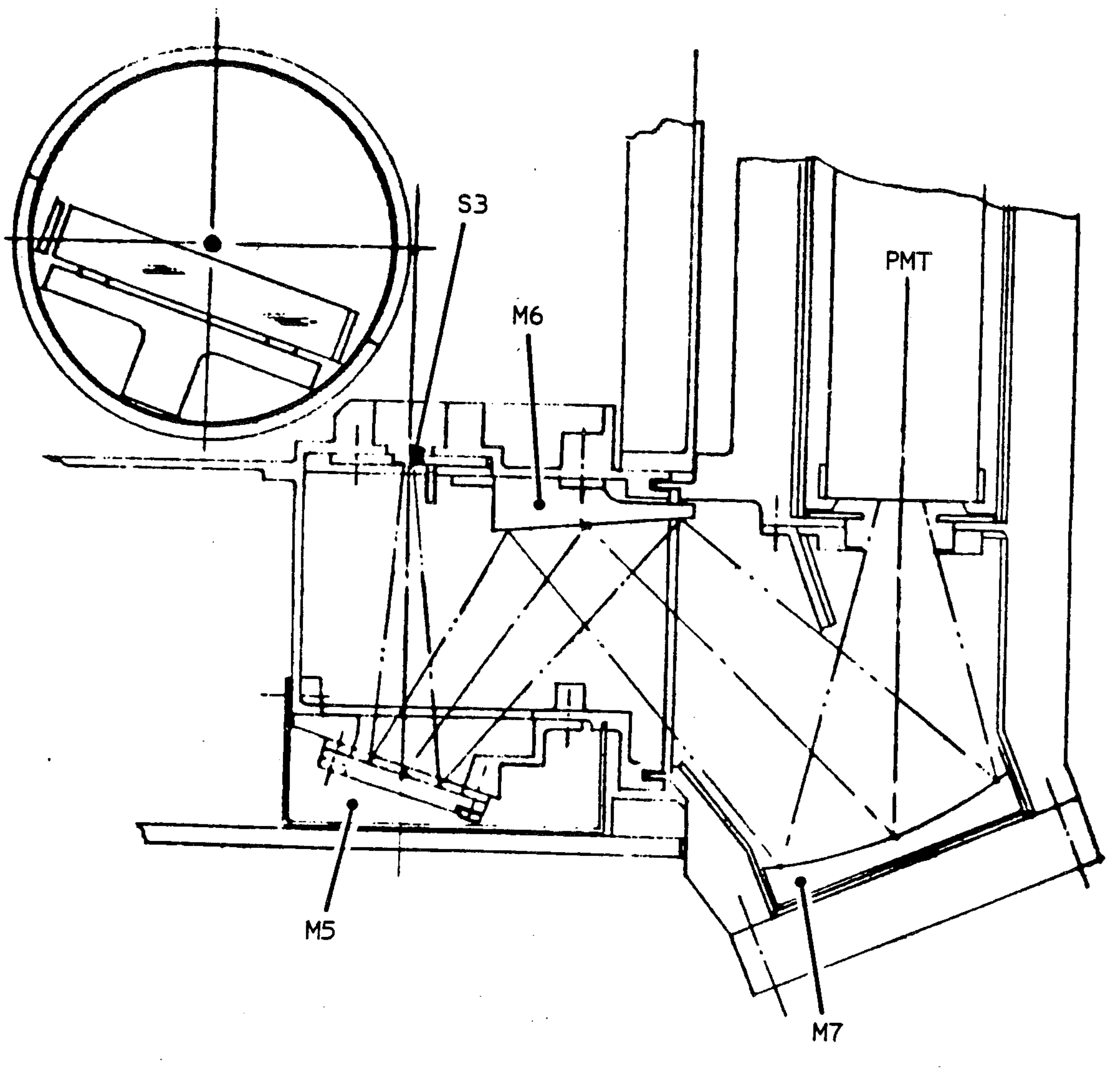

Figure 3-12
Exit Optics

Table 3-2
OPTICAL EFFICIENCY FOR THE 12 DISCRETE MODE WAVELENGTHS
(ESTIMATES)

WAVELENGTH	MIRRORS REFLECTANCE	GRATING EFFICIENCY	DEPOLARIZER TRANSMISSION	TOTAL OPTICAL EFFICIENCY
252.0	0.88	0.502	0.87	0.0610
273.5	0.88	0.472	0.87	0.0539
283.0	0.88	0.458	0.88	0.0514
287.6	0.88	0.454	0.89	0.0510
292.2	0.88	0.448	0.90	0.0503
297.5	0.88	0.442	0.90	0.0489
301.9	0.88	0.440	0.90	0.0513
305.8	0.89	0.437	0.90	0.0535
312.5	0.89	0.431	0.90	0.0571
317.5	0.89	0.427	0.90	0.0511
331.2	0.89	0.417	0.90	0.0487
339.8	0.89	0.412	0.90	0.0476

If the PMT were at a field stop, the scene would be imaged directly on the photocathode, and photocathode response non-uniformity would map directly into non-uniformity of instrument field-of-view response. If the PMT were at an aperture stop (a slit or slit image in SBUV/2), photocathode uniformity would be irrelevant to field-of-view uniformity.

The exit slit is imaged on the photocathode as well as can be done with simple optics. The required photocathode size is 7 x 14 mm. The flux distribution on the photocathode is illustrated in Figure 3-13.

This also gives an image of the instrument field stop (the first grating) just ahead of the PMT face. This is where the field mask is placed to block the PMT from seeing the monochromator walls. This stops what would otherwise be a significant source of stray light.

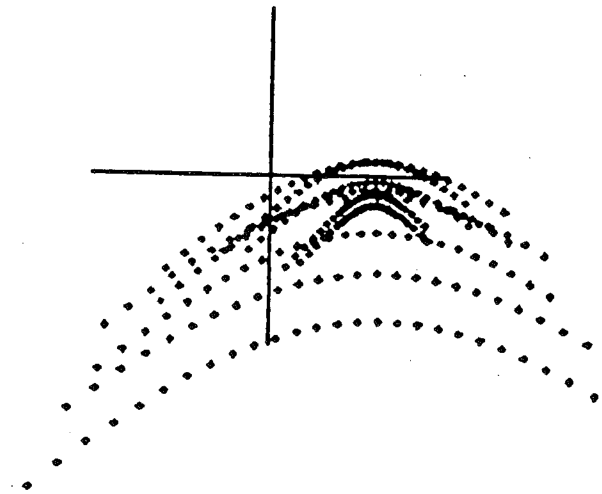

Figure 3-13
Typical Flux Distribution on the PMT Photocathode

3.2.2.2 Monochromator Mechanical System

3.2.2.2.1 Structure

The Sensor Module structure provides the optical bench for support of all the monochromator optical elements, as well as the enclosure for the monochromator. The design requirements for the structure are:

- Strength Margin: 2.0
- Resonance: >100 Hz
- Weight: 13.7 pounds measured, including slitplate bulkhead, diffuser bulkhead, and Ebert mirror cover.

3.2.2.2.2 Optical Elements

The Ebert mirrors are mounted to individual frames. The frames are three-point mounted to the Sensor Module structure and are aligned by shims at the three points. The gratings are mounted in individual frames, spring-loaded against hard front surface registration points. Pads limit mirror travel during launch. The individual frames are mounted to a single base which forms an integral part of the pivot shaft.

The roof mirror of the transfer optics is fixed. The intermediate slit is adjustable in translation in the plane of the slit. The entrance slit is fixed to maintain its position relative to the chopper wheel, and the exit slit is adjustable in translation in the plane of the slit. A single-piece shim, machined to the gap determined at alignment, is used for adjustment of the spherical relay mirror.

Table 3-1 tabulates all the optical element sizes, characteristics, and adjustment requirements. The total weight of all optics and immediate mounting frames and hardware will not exceed 6.5 pounds.

3.2.2.2.3 Grating Drive Mechanism

The grating drive mechanism is a subassembly of the monochromator. Partial disassembly of the motor is required for removal from the monochromator, but the gratings, bearing support system and encoder/readout assembly can be removed as a total subassembly. General characteristics are listed in Table 3-3. The gratings are mounted to a shaft which is bearing-supported at each end. The shaft is driven by a limited angle torque motor directly attached to one end of the grating support shaft for positional control. The grating pivot shaft bearing system consists of a single deep groove bearing adjacent to the motor, and a preloaded duplex bearing pair adjacent to the encoder disc.

The FM2 instrument retains the original design Al shaft and housing while FM3 was reworked to include a Be shaft, Ti housing, and re-designed bearing clamps and encoder finger ring.

FM2 is identical to the EMU and FM1. FM3 is closer to the FM4 instrument; the difference being the bearing and bearing clamps.

The change from Al to Be and Ti was made to move resonances to high frequencies thereby simplifying servo work. The finger ring redesign provides thermal stability to the encoder.

Motor. The motor is a limited angle torque motor with ±15° drive capability. Refer to BASG specification 67220 for the motor description.

Encoder. The optical encoder consists of a 2^{14} disc with four primary read stations and four redundant stations. Coupled with the encoder electronics, the encoder provides 2^{16} resolution with 2^{19} repeatability.

Refer to BASG Specification 67216 for a detailed description of the encoder and its requirements.

Table 3-3
GRATING DRIVE CHARACTERISTICS

Temperature:	
• Operating	0°C to +30°C
• Non-Operating	-10°C to +40°C
Angular Momentum:	0.0014 nms (maximum instantaneous)
Bearing Quality:	ABEC-7
Weight	5.65 pounds measured including gratings and frames
Cycle Time:	
• Sweep Mode	192 seconds
• Discrete Mode	32 seconds
Grating Step:	19.78 arc seconds
Step-to-Step Accuracy:	±4.95 arc seconds
Grating Step Repeatability:	±1.5 arc seconds
Maximum Jitter At Each Step	±0.5 arc second
Shaft Angle Readout Resolution:	19.78 arc seconds

3.2.3 PHOTOMULTIPLIER TUBE (PMT) ASSEMBLY

The Photomultiplier Tube Assembly (see Figure 3-14) consists of a spherical focusing mirror, aperture mask (scatter stop), PMT, shielding, preamplifiers, high voltage power supply, and appropriate electronics and housings.

3.2.3.1 Optics

The spherical mirror images the exit slit onto the PMT. The characteristics of the focusing mirror and scatter stop are included in Table 3-1.

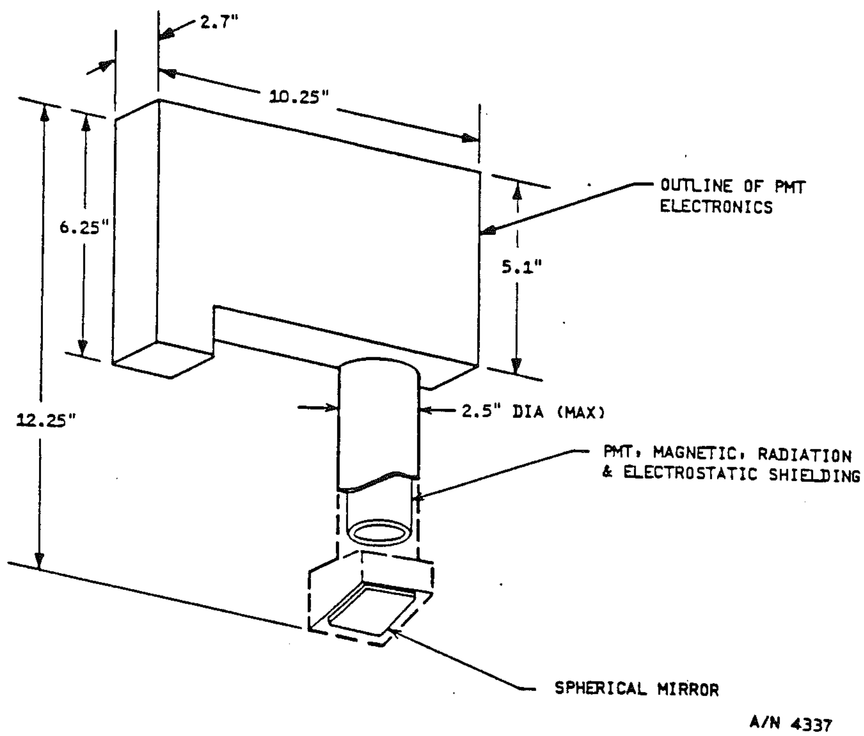

Figure 3-14
PMT Assembly

3.2.3.2 Photomultiplier Tube

The PMT photocathode is a high quantum efficiency bi-alkali on a cultured quartz faceplate to provide a high signal over the 160 to 400nm range. The five dynodes provide a gain of 500. The weight of the PMT is approximately 0.4 pounds. Detailed characteristics of the PMT are contained in BASG Specification 67261. The Flight Model 4 instrument was the first equipped with PMT which did not contain Cs . The result was significant improvement in time response and long-term stability. FM2 and FM3 also utilize the five dynode non-cesiated PMT.

3.2.3.3 Shielding

For protection from charged particle radiation, the shielding around the PMT consists of the PMT aluminum housing and a thin layer of lead. The thicknesses of these materials are:

Aluminum:	11 mm
Lead:	1 mm

3.2.3.4 PMT Electronics

The PMT electronics consists of four electronics boxes containing all of the circuits directly interfacing with the PMT:

- Anode preamplifier
- Bleeder String
- Cathode current monitor preamplifier and electrometer circuitry through the voltage-to-frequency converter
- High voltage power supply including the floating low voltage supplies for the cathode current monitor

These circuits are illustrated in Figure 3-15. The PMT electronics are located directly next to and at the rear of the PMT. Its characteristics are:

- Dimensions: shown in Figure 3-14
- Weight: 6.8 pounds, measured
- Power Dissipation: 2.0 watts nominal orbital average
- Temperature Range: -10°C to +40°C

Characteristics for the circuits are as follows:

Anode Preamplifier:

- Direct-coupled, transimpedance, FET-input preamplifier
- 10V full scale output
- 4.32 x 10^8 ohm feedback resistor
- ≥300 Hz bandwidth
- Nonlinearity 0.1% max full scale
- Double-shielded with inner shield at signal ground and outer shield at chassis

Bleeder String:

- Passive bleeder string for all dynodes
- 100 μA bleeder string current

Cathode Monitor:

- Direct-coupled transimpedance FET-input preamplifier

  (a) 10V full scale output
  (b) 4.32 x 10^8 ohm feedback resistor
  (c) ≥300 Hz bandwidth

- 10 volt full scale output at 2×10^{-9} amp input
- Analog nonlinearity ≤0.1% of full scale
- Analog gain stability better than 1% per 5°C
- Four-level electronic calibration
- VFC peak output frequency 122 KHz at 10 volt DC input
- VFC nonlinearity ≤ 0.1% of full scale
- Double-shielded cathode circuitry with inner shield at -HV and the outer shield at chassis

* For FM2 a capacitor was installed across the feedback resistor to increase closed loop bandwidth which helps prevent oscillations caused by stray capacitance.

- High voltage isolators to couple signals in and out of cathode circuitry
- Response Time -300 KHz per msec minimum.

<u>High Voltage Power Supply:</u>

- Input Voltage: 25V ±0.5V
- Input Regulation: ±2%
- Synchronization Frequency: 52 KHz (free run in absence of synchronization)
- Output Voltage: Is adjustable during test between 500 to 1,400 volts
- Output Current Limit: 150 µamps

- Turn-On: The initial high voltage turn-on is at the low output voltage limit and rises monotonically to settle at the operating voltage

- Turn-Off: The output will decay without overshooting transients

- Output Ripple and Noise ≤ 25 mV peak-to-peak

- High Voltage Bleed-Down Time: <10 seconds

- Output Voltage Stability: ≤ ± 0.08%/24 hours/2°C

- Output Long-Term Drift: ≤ ± 1%

- Output Temperature Stability: ≤ ± 1% over zero to 30°C temperature range

- Input Power: 1.5W at 100 μA output current, measured, including the floating ± 15V output loads

- High Voltage Monitor: Provides a zero to +5V monitor

Floating Low Voltage Supplies: There is one isolated ±15V supply, located in the high voltage power supply, to power the cathode circuitry.

- Voltage: +15V and -15V, ±0.5V
- Regulation: ± 0.5%
- Current: 14 to 20 mA
- Ripple: 5 mV peak-to-peak, maximum
- Isolation: ≥ 500 Megohm
- Maximum Dynode Potential: 1,400 volts

3.2.4 CLOUD COVER RADIOMETER (CCR)

The Cloud Cover Radiometer (CCR) is built as a separate module to simplify fabrication and alignment. This separable assembly consists of a photoemissive diode, field stop, lens, interference bandpass filter, folding mirror, and preamplifier. See Figure 3-16.

Light from the scene goes through the chopper before it gets to the CCR. At the CCR, the light goes through a bandpass filter, a singlet objective lens, and a field stop. A spherical folding mirror then turns the beam 90° and images the light on the detector, which is a vacuum photodiode.

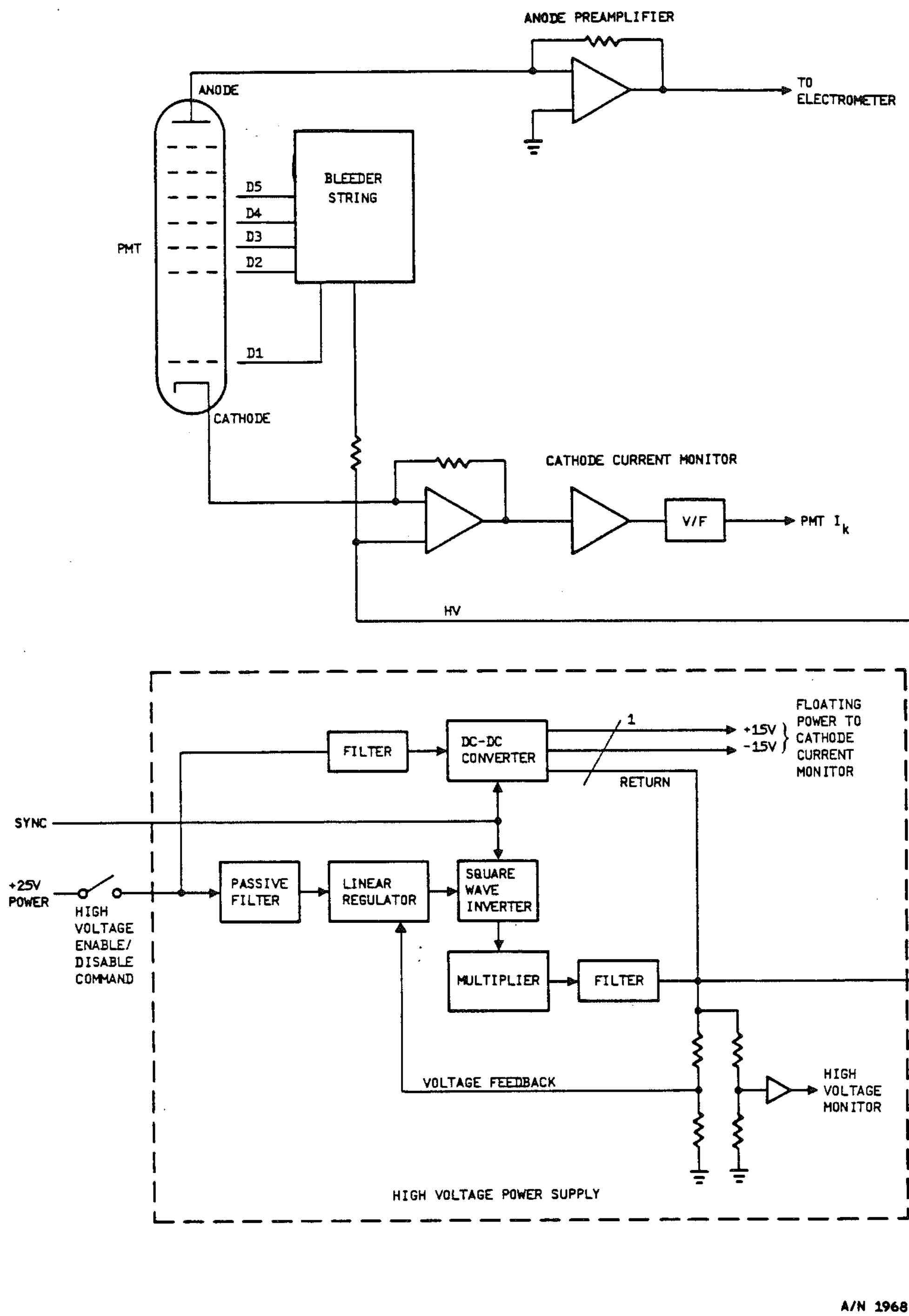

Figure 3-15
Block Diagram of the PMT Electronics

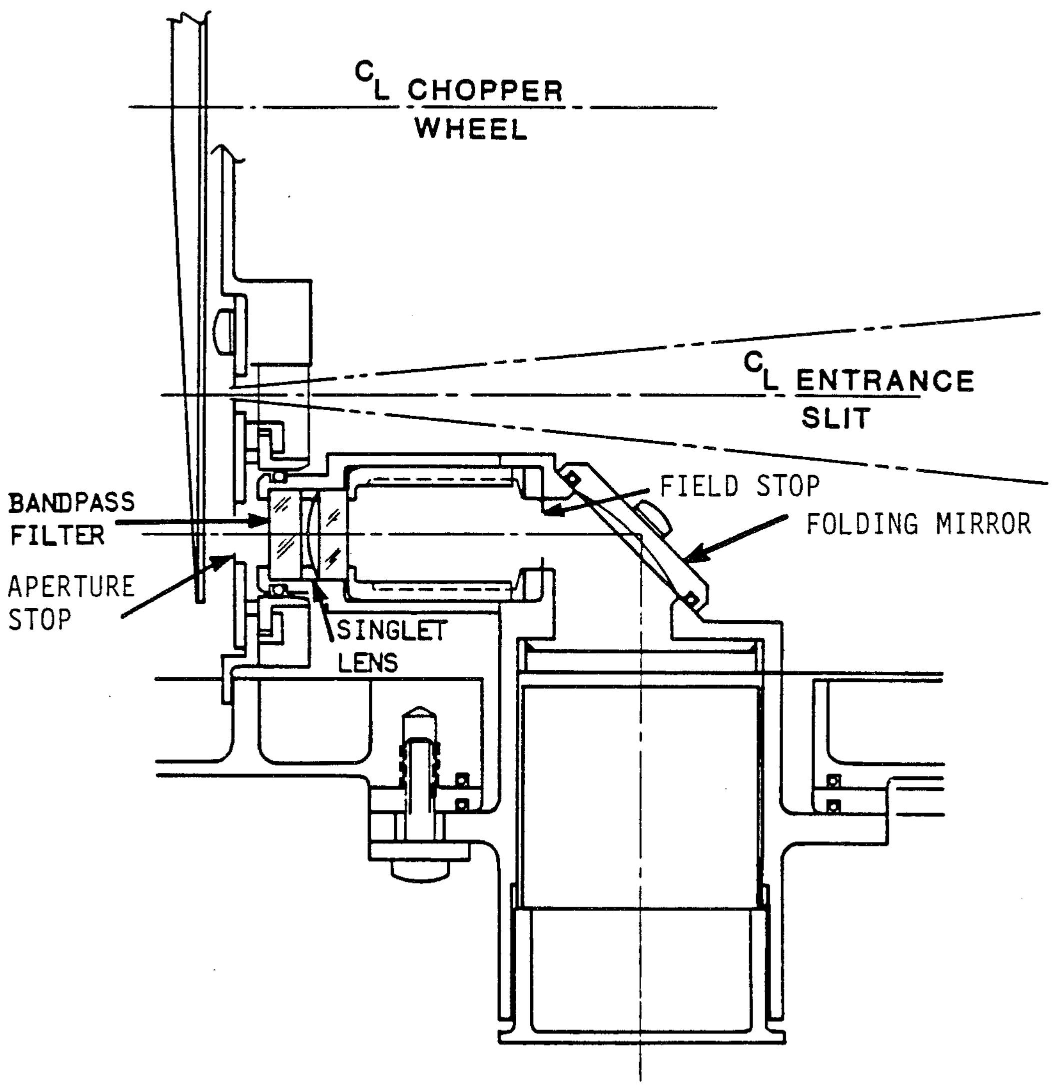

Figure 3-16
Cloud Cover Radiometer

The field stop sets the size of the CCR field-of-view. The folding mirror images the aperture stop (which is at the chopper) on the detector, permitting a smaller detector size and minimizing the field-sensitivity variations that could be caused by a non-uniform detector.

The entire CCR is mounted in a block at the side of the entrance slit of the monochromator so both the CCR and the monochromator can use the same chopper wheel. Co-pointing is set by a machined shim at the mounting boss of the CCR block.

The weight of the assembly is 0.3 pound. It is designed to operate in a thermal environment of -15 to +35°C.

3.2.4.1 Photodiode

The photo-emissive diode is similar to the ITT Diode F4096. The diode has a semi-transparent bi-alkali photocathode of about 13 mm diameter. This diode operates at low voltage (<10V) and easily meets the dynamic range of 320:1. The signal-to-noise ratio at minimum signal is about a factor of two higher than the required 100:1.

Detailed characteristics of the photodiode are contained in BASG Specification 63317.

3.2.4.2. CCR Preamplifier

The anode current passes through a transimpedance preamplifier similar to the PMT preamplifiers but located at the rear of the detector in a shielded enclosure. The output then goes to the electrometer to a single fixed range voltage-to-frequency converter. Preamplifier characteristics are:

- Direct Coupled, Transimpedance FET Input Preamplifier
- Full Scale Current: 2.4×10^9 amp
- 4.32×10^8 ohm Feedback Resistor-
- ≥ 300 Hz Bandwidth
- Double-Shielded with Inner Shield at Signal Ground and Outer Shield at Chassis Ground

3.2.4.3 Optical System

Table 3-1 (Section 3.2.2) describes the sizes and characteristics of the CCR optical elements.

3.2.5 ELECTROMETER ASSEMBLY

This assembly consists of post-amplifiers and voltage-to-frequency converters for two PMT anode ranges and for the cloud cover radiometer range. A temperature sensor is routed to the Electronics and Logic Module for digital conversion.

Figure 3-17 shows the functional block diagram for the Electrometer which includes an electrical calibration generator (E-Cal) housekeeping monitors, and power distribution. Each electrometer signal is amplified and then converted to a frequency that is proportional to its amplitude. The frequency is then routed to the ELM for digital processing. The full scale ranges are:

Monochromator Range 1:	0 to 10^{-10} Amp average anode current
Monochromator Range 2:	10^{-10} to 10^{-8} Amp average anode current
CCR Range 1:	2.4 nA (average) full scale

A summary of the electrometer characteristics is listed in Table 3-4.

The electrical calibration system provides automatic monitoring of both PMT and CCR electrometer channel gains. The system operates by switching in five precision E-Cal voltage levels, chopped at 20 Hz, immediately after the preamplifiers, as shown in Figure 3-17. All detector background is eliminated from the calibration. Calibration is performed during retrace of the grating. The E-Cal levels are designed to provide calibration points on each electrometer range.

Table 3-4
ELECTROMETER CHARACTERISTICS

Package Size:	1.06 x 7.50 x 8.25 inches
Package Weight:	2.50 pounds (measured)
Power:	0.6 watt nominal orbital average
Analog Gain Error:	1% per 5°C
Analog Nonlinearity:	0.1% of full scale; zero to 30°C
Short Circuit Protection:	All outputs
Channel Crosstalk:	<1/2 bit
A/D (V/F) Nonlinearity:	0.1% of full scale
A/D (V/F) Accuracy:	0.04% of full scale at 25°C;
	0.1% of full scale zero to 70°C
E-Cal Levels:	5-Automatic

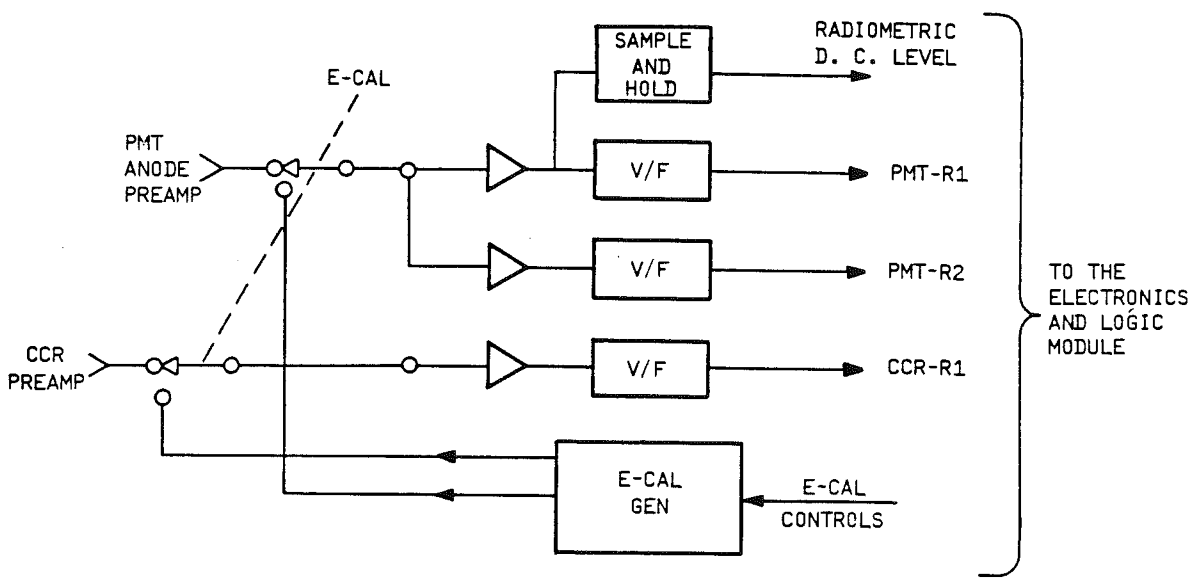

Figure 3-17 1968 A/N
Block Diagram of the Electrometer Assembly

3.2.6 CHOPPER ASSEMBLY

The chopper assembly is an independent subassembly spider-mounted to the slit bulkhead. This assembly chops the incoming radiation to both the monochromator slit and the cloud cover radiometer. It consists of a brushless, three-phase, DC torque motor, a five-aperture chopper and an encoder. The encoder has both a velocity track and a phase track for the phase-locked loop control, and it has three tracks for motor commutation.

The chopping rate is 20 Hz and is accomplished by five apertures in a wheel rotating at 240 rpm. The chopping edges of the apertures are held within a 0.005-inch tolerance band. The wheel diameter (limited by interference with the exit optics housing) is 5.067 inches maximum. Figure 3-18 shows exposed slit areas versus time for one chopping cycle of the monochromator slit.

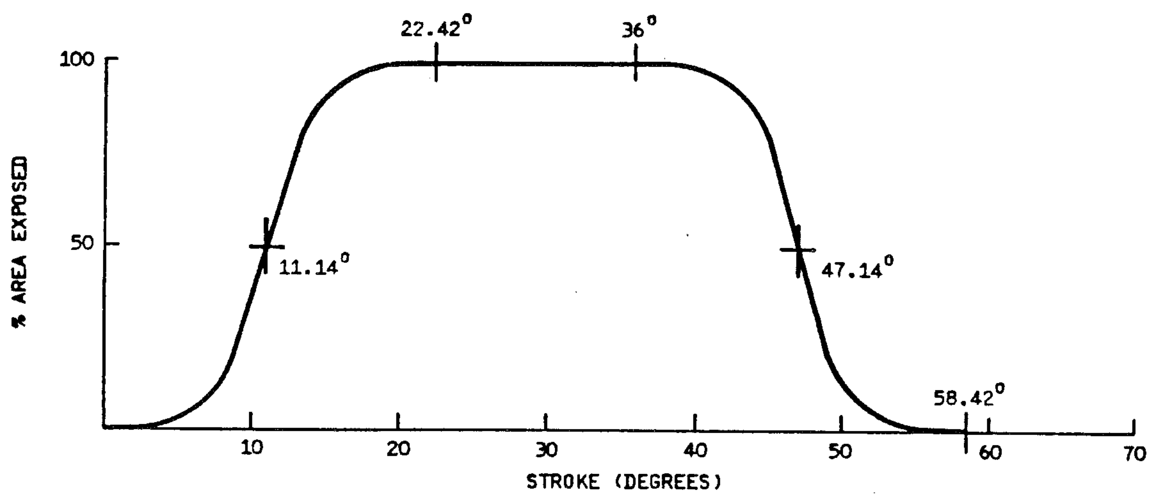

Figure 3-18
Chopper Waveform Characteristics

The wheel is driven by a three-phase brushless DC torque motor, with velocity control and commutation provided by an optical encoder. The encoder provides the phase reference pulse, and the chopper wheel is adjusted with respect to it. Redundant pick-ups are provided. Figure 3-19 shows the cross-section and dimensional extremes of the subassembly. Table 3-6 lists the characteristics of the chopper assembly. Refer to BASG Specification 67222 and 67218, respectively, for characteristics of the torque motor and encoder.

Table 3-6
CHOPPER ASSEMBLY CHARACTERISTICS

Velocity:	240 rpm
Life:	Two years continuous operation
Uncompensated Angular Momentum	0.0045 N-m-s
Weight:	1.5 pounds (measured)
Torque Margin:	3X friction
Bearing Quality:	ABEC-7
Temperature:	
(a) Operating	-10°C to +40°C
(b) Non-Operating	-10°C to +40°C

3.2.7 DIFFUSER ASSEMBLY

To measure the solar irradiance, a ground aluminum diffuser plate overcoated with vacuum deposited aluminum is deployed beneath the instrument so that the instrument views sunlight rather than earth radiation.

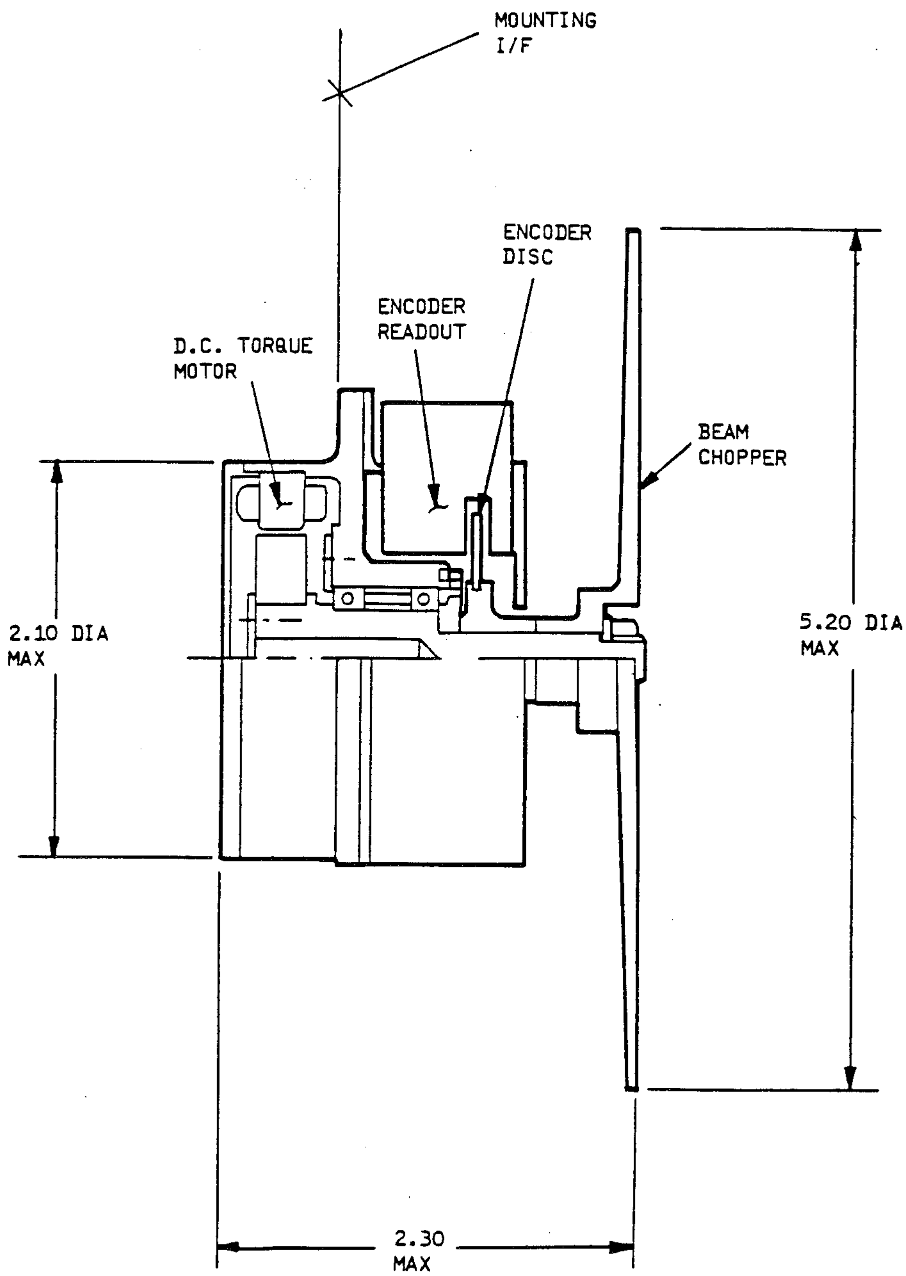

Figure 3-19
Cross-Section of Chopper Assembly

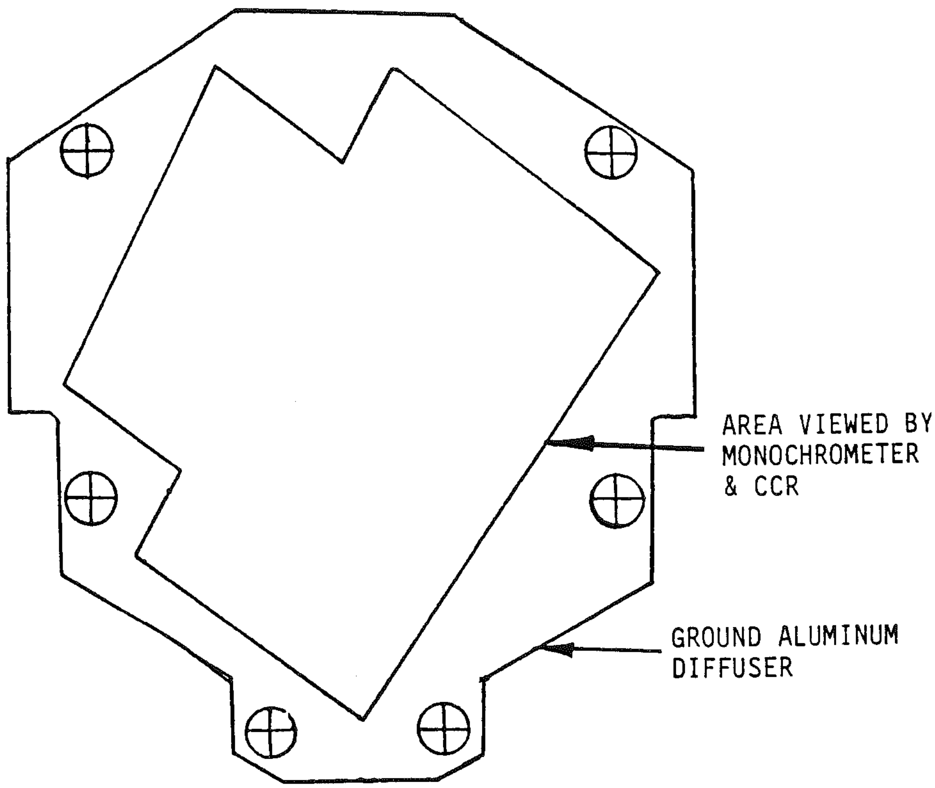

Figure 3-20
Diffuser Plate

In the solar irradiance measurement, the diffuser is deployed so the plate normal 28° from the Zenith-Nadir line (i.e., the plate is tilted 28° from the spacecraft Y-Z plane). The plane of the diffuser is thus tangent to earth's limb, eliminating earthshine from the sun measurements.

Because the brightness of the diffuser plate (see Figure 3-20) varies as the cosine of the angle of incidence of the sunlight, the goniometric response of each instrument is carefully calibrated.

The diffuser is mounted on a single-axis tilt mechanism with four discrete positions: Stow, Monitor, Sun Viewing, and Decontamination. A simple stepper motor deployment mechanism moves the diffuser to each of the four positions. In Stow, the plate is tucked against a shallow enclosure, where the diffuser surface is protected during launch and ordinary (earth-looking) instrument operation. Also, in Stow the working surface of the diffuser is protected from contaminant condensation and solar ultraviolet, which could polymerize any contaminants already present. In Monitor position, the plate is perpendicular to the Zenith-Nadir axis, illuminated by the in-flight reference source, and viewed by the radiometer. In Sun Viewing, the plate normal makes an angle of 28° with the radiometer axis and the sun measurements are made. The diffuser is further extended to a fourth position for decontamination. The diffuser is heated to 300°K minimum, 373°K maximum, to drive off contaminants.

The diffuser is mechanically positioned in any one of the four positions by rotation about a hinge axis. Each position is sensed by optical readout using four LED's and four photo-transistors. The four positions are tabulated in Table 3-7.

Table 3-7
DIFFUSER POSITIONS

Position	Angle to Spacecraft X-axis	Accuracy	Repeatability
Stow	12°	N/A	N/A
Monitor Check	90°		± 4 arc min**
Solar Irradiance	118°	± 0.4°	± 4 arc min*
Decontamination	167.5°	N/A	N/A

*From STOW, PRI and BKUP
**From STOW, PRI or BKUP, but may be on step different (13.5 arc min) PRI to BKUP

The hinge line is parallel to the spacecraft Y-Z plane, and the normal to the hinge line in the Y-Z plane makes an angle of 34° with the +Z axis. The drive motor is a 45° permanent magnet stepper motor. Refer to BASG Specification 67224 for the stepper motor characteristics and Specification 67226 for the gearhead characteristics.

The total mechanism is fully operational in any attitude in a 1g field, positively latched for launch and has the following characteristics:

- Angular Momentum: 0.0022 N-m-s maximum, instantaneous
- Weight: 4.4 pounds measured
- Life: 8,000 cycles
- Temperature:
  - (a) Operating: -10°C to +40°C
  - (b) Non-Operating: -20°C to +60°C

In the Decontamination Mode, the heater power requirements is 4.8 watts.

3.2.8 CALIBRATION LAMP ASSEMBLY

The calibration lamp assembly is used to provide an in-flight reference source for wavelength calibration of the instrument. It also provides the closure for the instrument aperture during storage and launch. As the reference source, it uses a mercury discharge Pen-Ray lamp in an aluminum housing (see Figure 3-21). The lamp is mounted in a reflective housing which is designed to provide a diffuse uniform illumination at the output face of the housing where a ground fused-silica diffuser is located.

The lamp puts out several discrete spectral lines (from 184.9nm to 404.7nm) within the spectral range of the instrument.

The calibration lamp assembly is used in two positions; in the open position the source illuminates the diffuser, and in the closed position the source covers the input apertures and can illuminate them directly. In this position, the lamp diffuser fills the entire field-of-view of the monochromator.

Comparison of the two measurements, made in the sweep mode, permits in-flight evaluation of the diffuser efficiency so that a correction factor can be applied to the data on the ground if appropriate.

A heater attached to the lamp housing is used to keep the partial pressure of the Hg at a level which prevents cold lamp start failure.

The heater is turned on via a calibration lamp heater on command. The calibration lamp power supply is equipped with polarity switching relays which are provided power from the heater supply. Thus, it is necessary to energize the calibration lamp heater for polarity switching to occur. This should be done soon after launch as it is desirable to have the heater on throughout the mission. Should the calibration lamp heater be turned off, the polarity switching circuit will not operate. The lamp will then be subjected to cold starts and the polarity of applied voltage will not change upon each firing as desired.

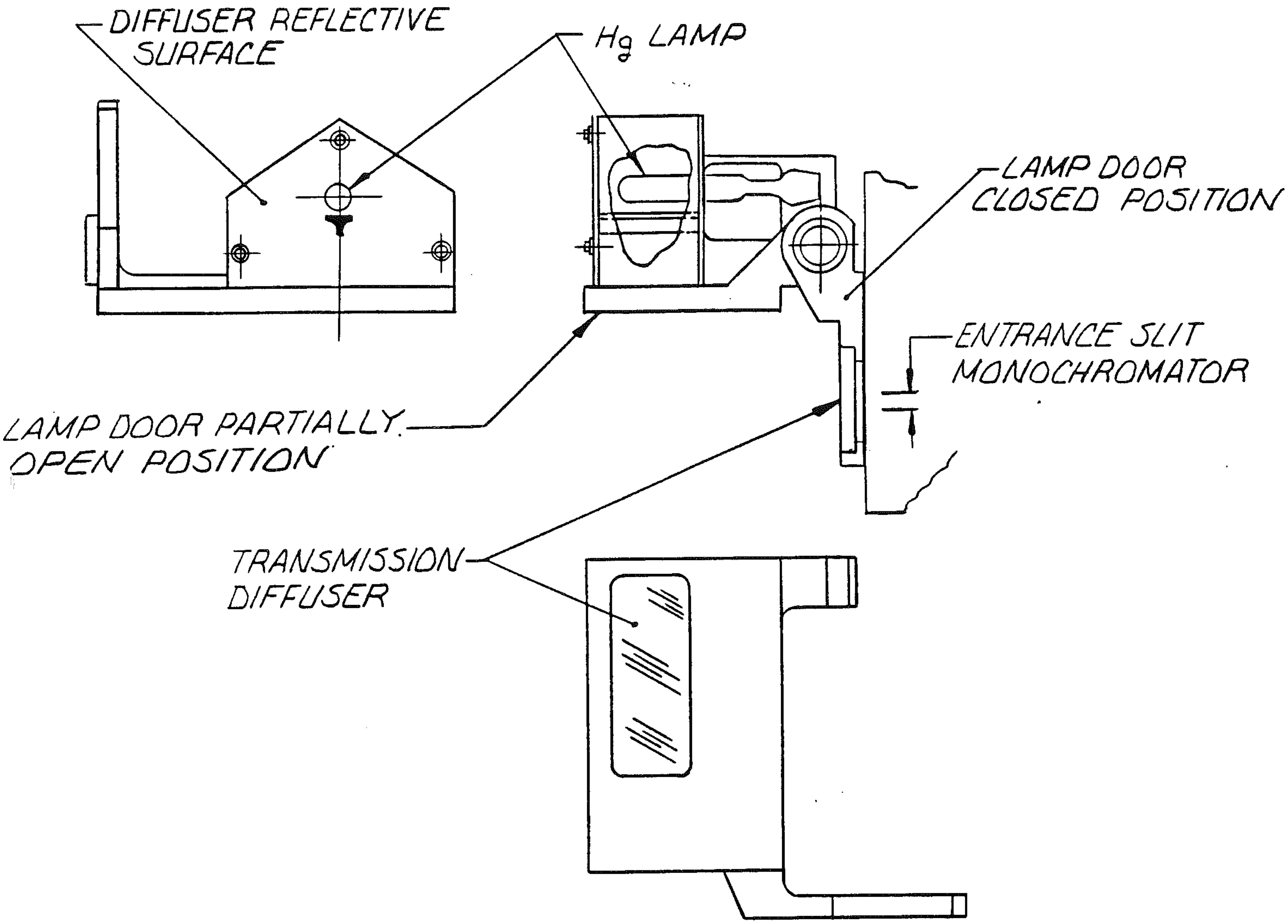

Figure 3-21
Calibration Lamp Assembly

The lamp is operated at a controlled current of 1.0 mA

Mechanically, the assembly is a single-axis rotation, two position device driven directly by a 90° stepper motor through a reduction gearhead. An optical read-out provides position information. Characteristics of the stepper motor and gearhead are contained in BASG Specification 67228 and 67230, respectively.

The total mechanism is fully operational in any attitude in a 1g field, retained in the closed position for launch and has the following characteristics:

• Angular Momentum:	0.0007 N-m-s maximum instantaneous
• Weight:	1.85 pounds (estimated)
• Life:	10,000 cycles
• Stroke: 125° minimum	
• Positional Accuracy:	±1°
• Position Repeatability:	Spring loaded against both open and closed stops
• Temperature:	
(a) Operating:	-10°C to +40°C
(b) Non-Operating:	-20°C to ±45°C

3.2.9 CALIBRATION LAMP POWER SUPPLY

The mercury lamp requires a high starting voltage and a well-regulated operating current. A pulse width modulated converter with current feedback is used to meet these requirements. A block diagram of the power supply is shown in Figure 3-23. Characteristics of the power supply are listed in Table 3-8. The FM2 and FM3 instruments are equipped with a polarity switching circuit which reverses the lamp voltage polarity upon each firing thereby prolonging the stable lifetime of the lamp.

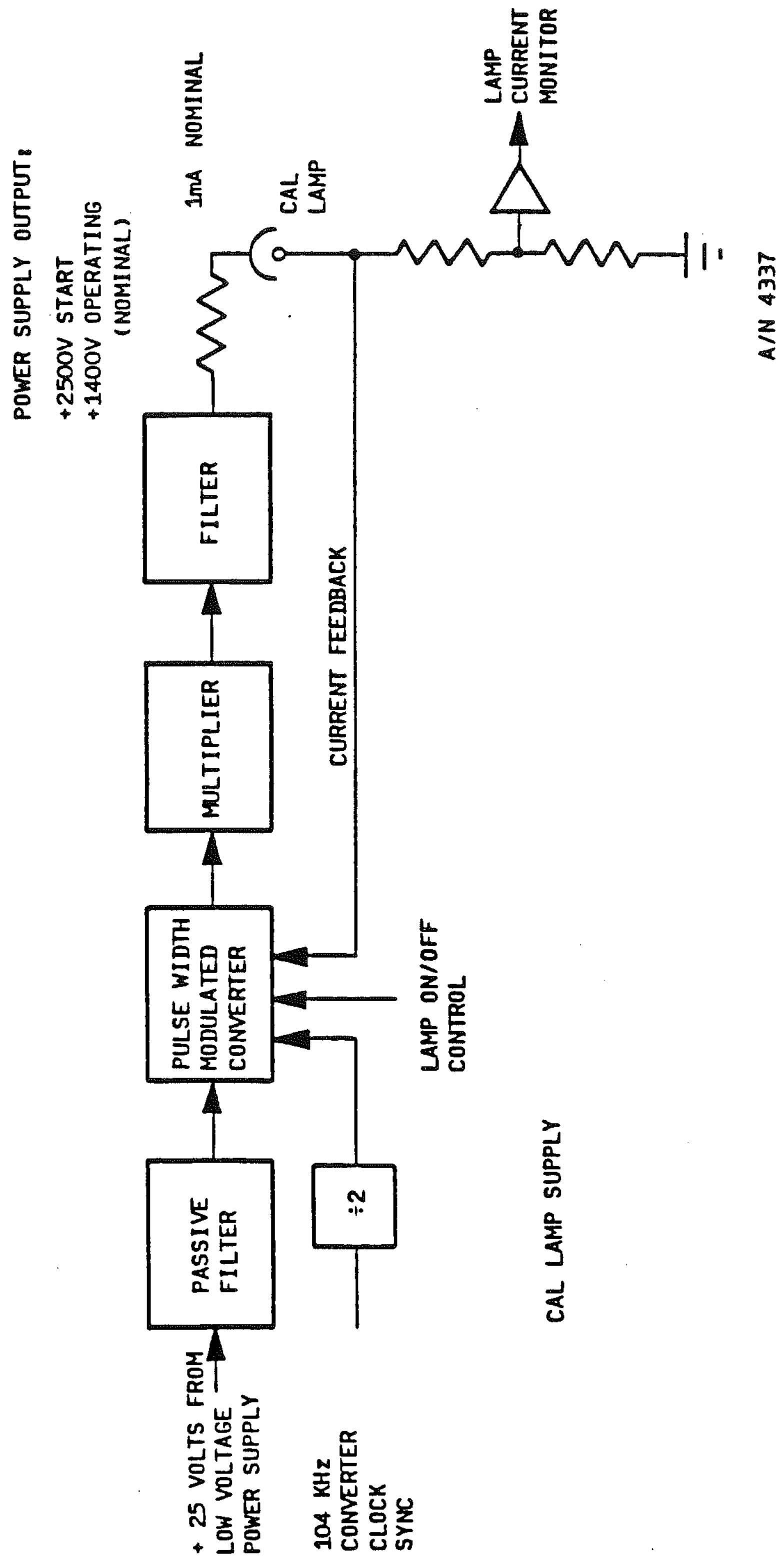

Figure 3-23
Block Diagram of the Calibration Lamp Power Supply

Table 3-8
CALIBRATION LAMP POWER SUPPLY CHARACTERISTICS

A.	PHYSICAL		
	•	Size:	2.0 x 3.375 x 5.20 inches
	•	Weight:	2.2 pounds measured
B.	FUNCTIONAL:		
	•	Input Voltage:	+25 ± 2 VDC
	•	Input Power:	≤ 7W at 10 mA load current
	•	Output Voltage (to start Lamp):	2,500 volts, minimum
	•	Operating Voltage:	1200V to 1500V
	•	Lamp Operating Current:	1.0 mA regulated
	•	Operating Current Regulation:	0.1%
	•	Synchronization Frequency:	52 kHz; free run in absence of synchronization
	•	Housekeeping Monitors:	Lamp current, +5V full scale for 3.25 mA

3.2.10 THERMAL BLANKET ASSEMBLY

The Sensor Module is completely covered with multilayer insulation except for the area around the entrance aperture and a radiator on the diffuser housing. These blankets are constructed of alternate layers of double aluminized 1/4-mil Mylar and Dacron netting, all enclosed in a "pillow case" of single aluminized 3-mil Kapton, with the Kapton side out. The blankets are 0.25 inch thick.

3.2.11 SENSOR MODULE CABLING

The Sensor Module cabling performs the required interconnections between the electrometer and the various subsystems. Each of the subassemblies is provided with individual connectors for easy removal. The cabling schematic is shown in Figure 3-24.

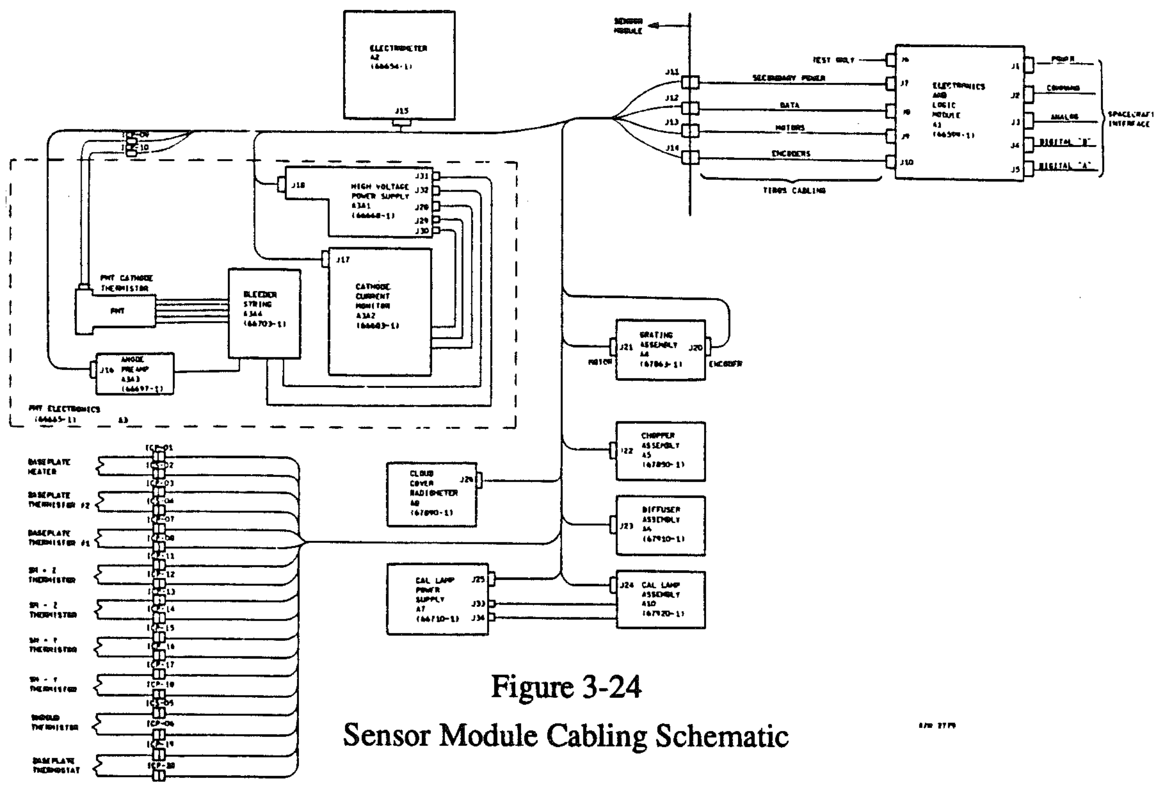

Figure 3-24
Sensor Module Cabling Schematic

3.2.12 MISCELLANEOUS ASSEMBLIES

3.2.12.1 Case Vent Assemblies

Three case vents are provided to allow for pressure differentials between ambient and the internal volume of the monochromator. The vents are passive light tight units providing both molecular and particulate protection for the monochromator. The vents are made of 75 micron corrosion-resistant steel porous mesh. The system prevents pressure differential build-up continuously in either direction without introducing contamination into the monochromator. The three case vents are connected by an aluminum manifold (see Figure 3-4). The open end of the manifold provides a fitting for attaching an auxiliary charcoal filter. This filter is used during spacecraft vacuum test as well as air transportation.

Figure 3-25 shows the vent physical configuration. The performance characteristics are:

- Maximum Ambient Pressure Change: 1.27 psia/sec
- Maximum Differential Pressure (at maximum rate of change): 0.25 psi

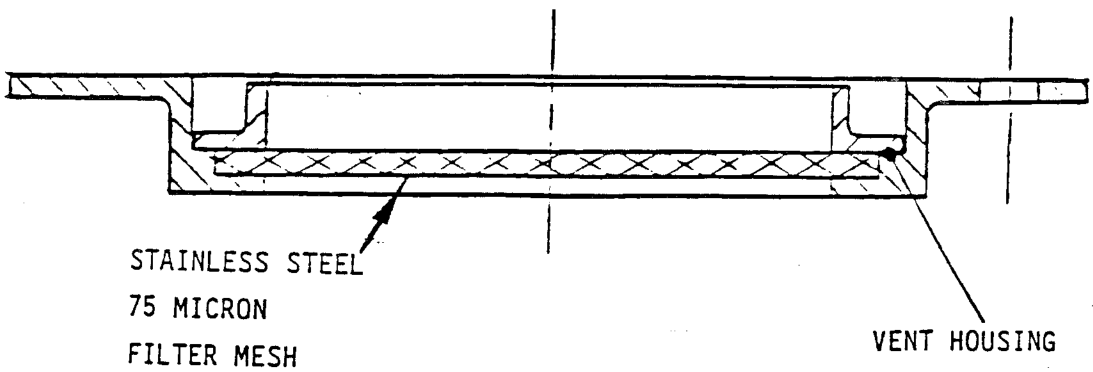

Figure 3-25
Case Vent Assembly

3.2.12.2 Purge System

A purge line is provided to carry dry nitrogen directly into the sensor module. The purge gas enters the monochromator cavities through two fittings in the structure well, one by each Ebert mirror. These fittings are connected by an aluminum pipe to a filter assembly and inlet fitting mounted on the sensor module connector bracket. The filter is a 75 micron stainless steel mesh. The sensor module is shipped with a cap over the purge inlet, and is flown with the cap in place, so that the instrument "breathes" through the vent assemblies.

3.2.12.3 Depolarizer

With its many reflections and two grating diffractions, the monochromator treats input light very non-uniformly, discriminating on the basis of wavelength and polarization state. The depolarizer, which is in the beam immediately before the chopper and entrance slit of the monochromator, scrambles the polarization state of the incoming light so that the monochromator is equally responsive to light of any initial polarization state.

The depolarization (Figure 3-26) uses two Wollaston prisms, each of which includes two quartz wedges with crossed axis. It scrambles by twisting the instantaneous polarization state around the direction in which the ray is going. The twist depends on the location and direction of the ray as it enters the scrambler. The depolarizer is made of optical grade cultured crystalline quartz. This material gives high transmittance and will not degrade measurements by fluorescing. The four optical wedges of the depolarizer are optically contacted to each other (no cement is used, and no internal air or vacuum interfaces exist) for maximum transmission.

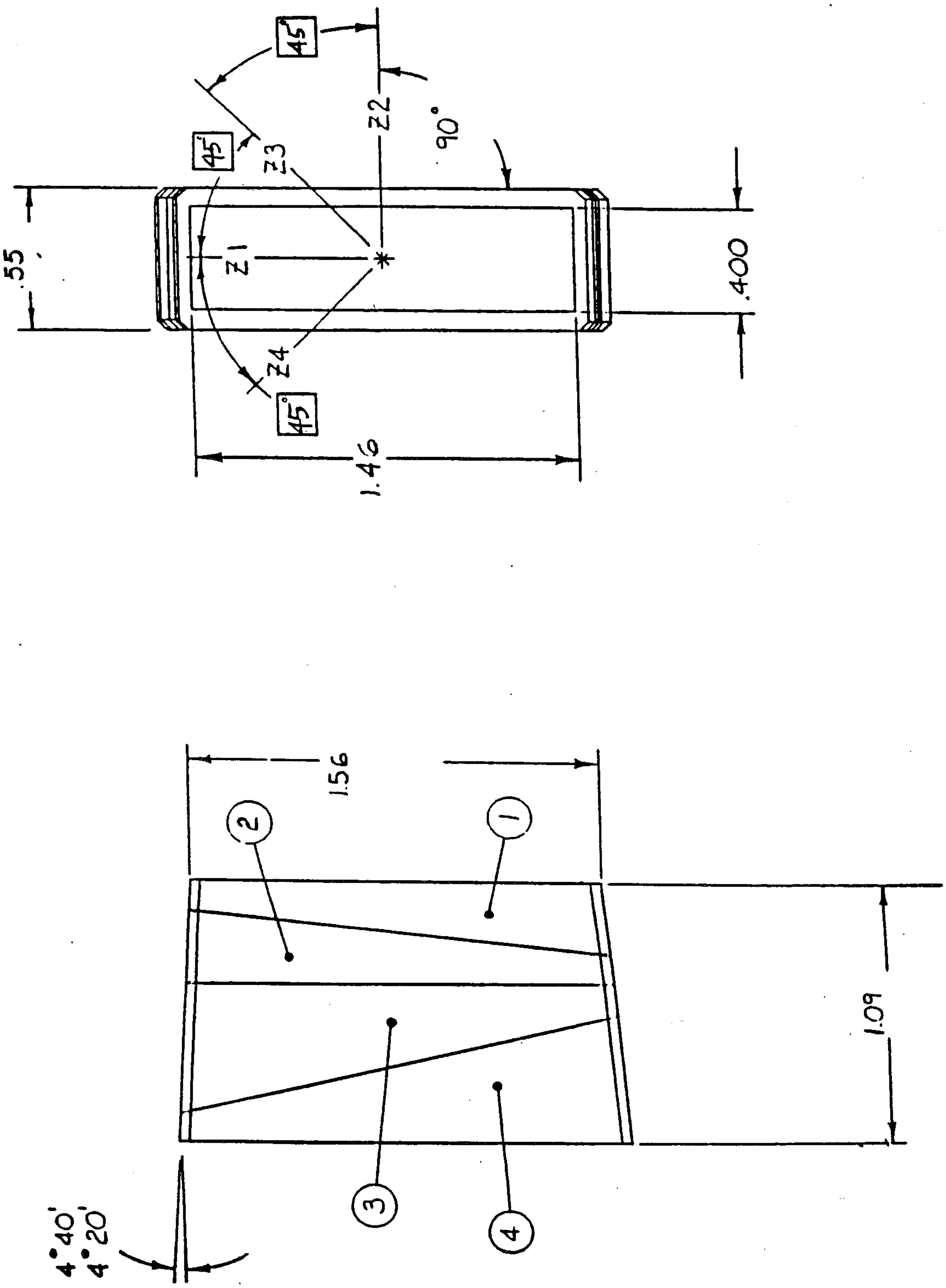

Figure 3-26
Depolarizer

3.3 ELECTRONICS AND LOGIC MODULE DESCRIPTION

The SBUV/2 Electronics and Logic Module (ELM) is located inside the Spacecraft Equipment Service Module and contains the following: low voltage power supply, TIP interface circuits, clock generators, command interface circuitry, data multiplexer and formatter, accumulation counters for the voltage-to-frequency converters, a housekeeping data processor, and drivers for the grating motor, the chopper motor, the diffuser drive motor, and the calibration lamp position motor. The remainder of the electronics are contained in the Sensor Module. Figure 3-27 shows a breakdown of the ELM subsystems. The ELM block diagram is shown in Figure 3-29.

3.3.1 ELM INTERFACES

3.3.1.1 Envelope, Center of Gravity, and Weight

The ELM envelope and center of gravity (CG) location are shown in Figure 3-30. The weight of the ELM, as measured on Flights 2 and 3 and are 25.32 and 25.34 pounds respectively.

3.3.1.2 Mechanical

The ELM is mounted on the inside of the ESM. The mechanical interfaces are specified in the Interface Documents IS-2295548 and IS-2280259. An ELM drill fixture (BASG Drawing No. 67768) fabricated by BASG provides precise location for attaching hardware. The power dissipated by the circuit boards of the ELM is transferred to the ELM case by spring clips riveted to the case. The heat is then conducted to the ESM interior. The ELM temperature will run a few degrees warmer than the ESM (which is specified to be between 0°C and +30°C).

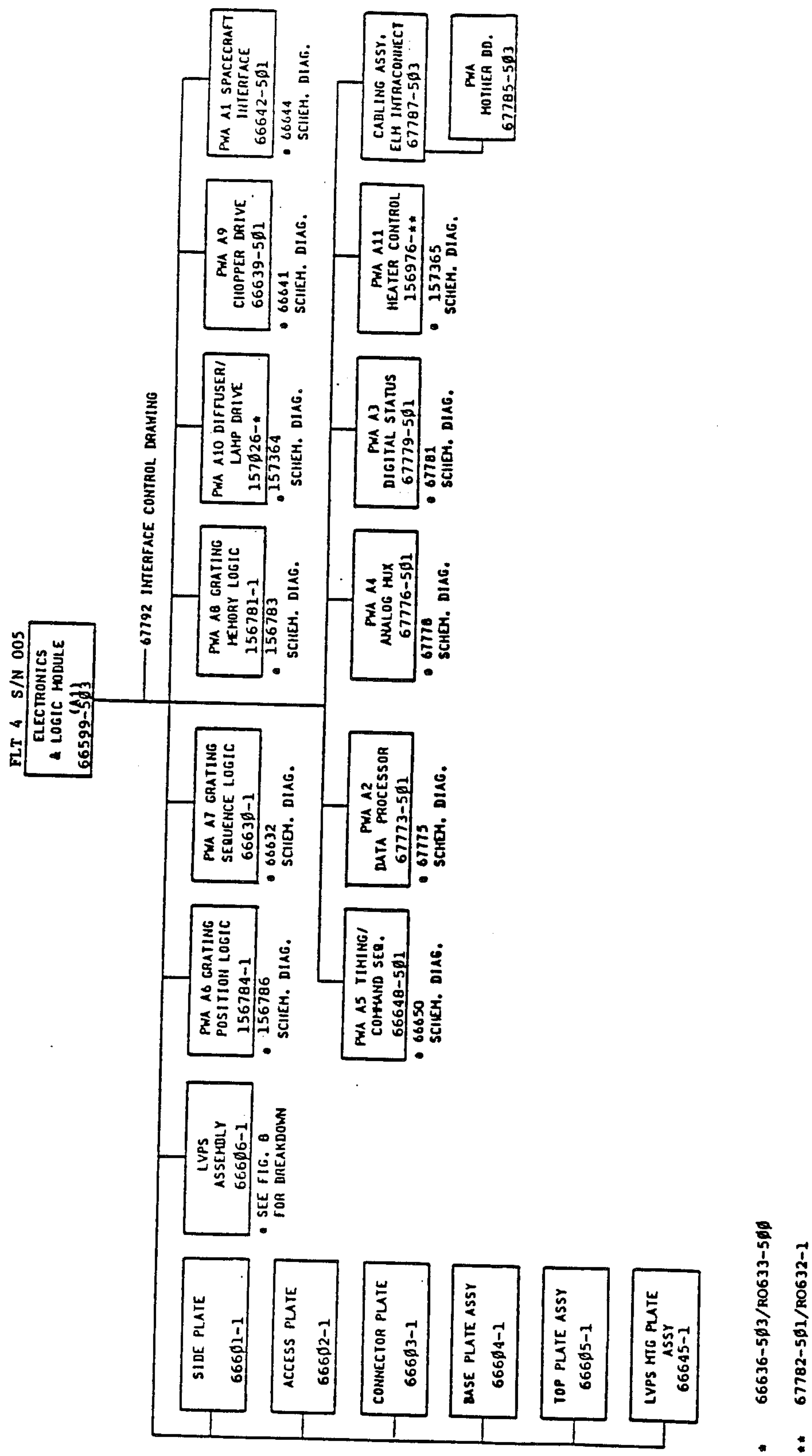

Figure 3-27
ELM Subsystem Breakdown

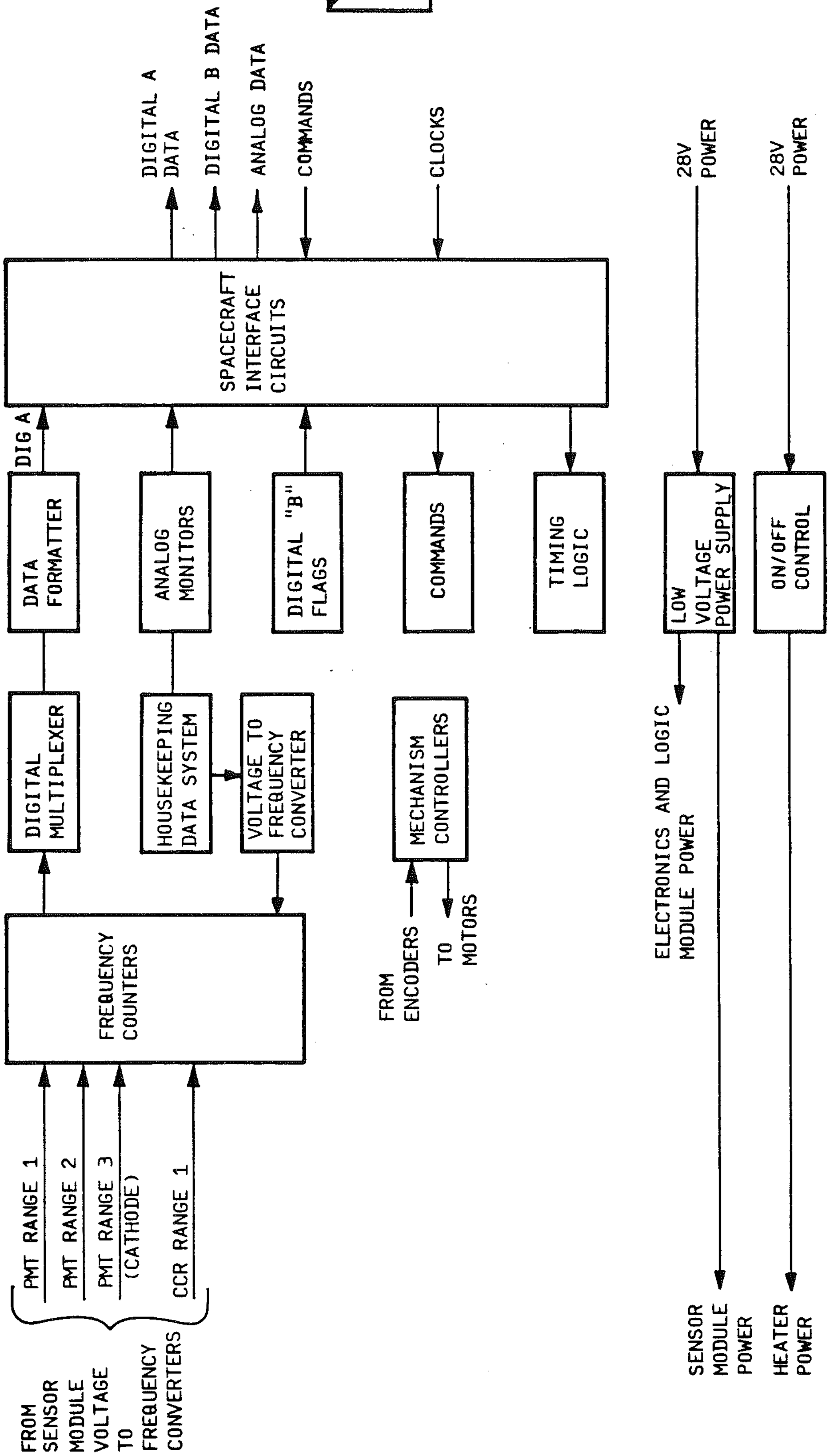

Figure 3-29
ELM Functional Block Diagram

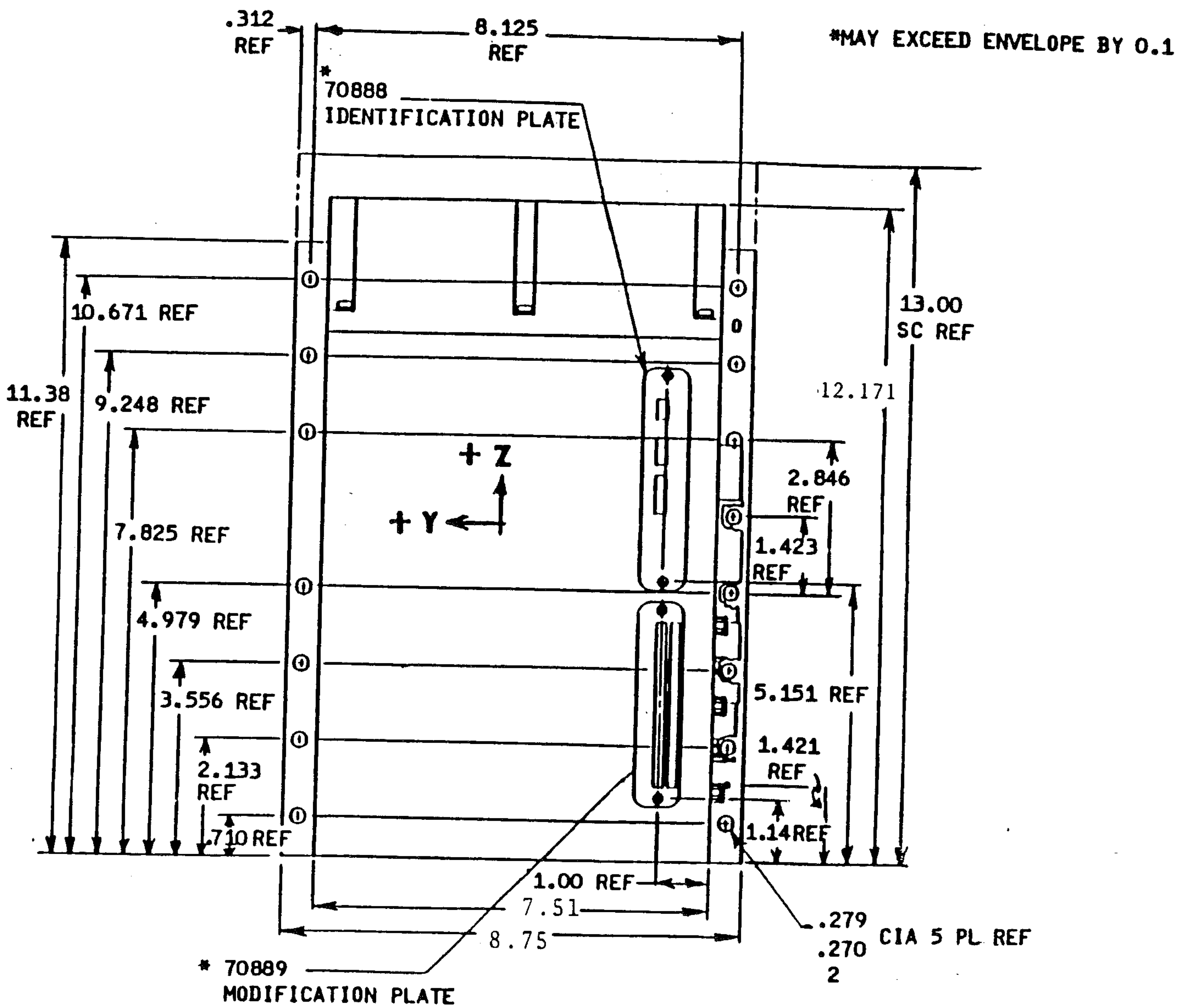

Figure 3-30
ELM Envelope and Center of Gravity Location (1 of 3)

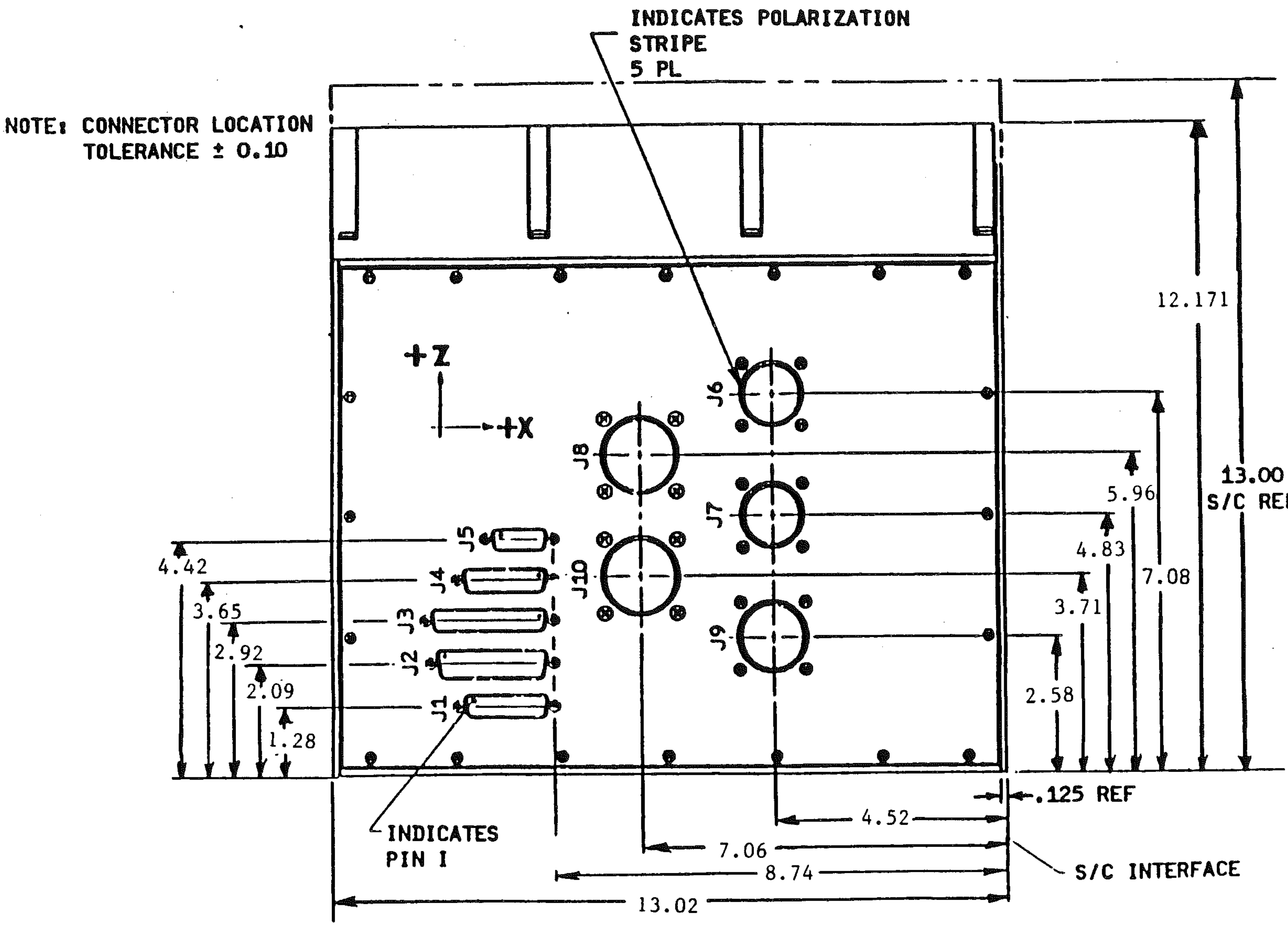

Figure 3-30
ELM Envelope and Center of Gravity Location (2 of 3)

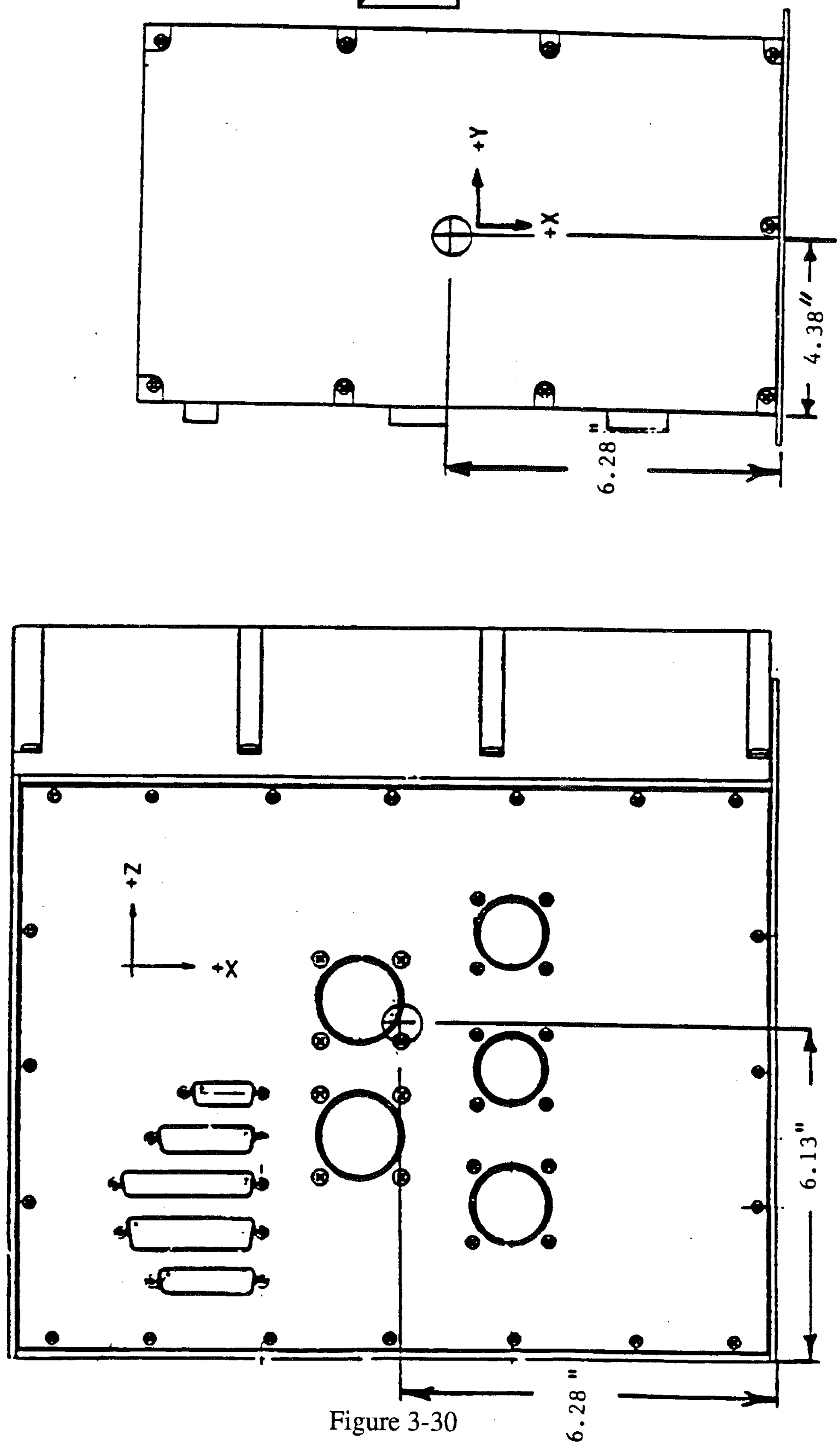

Figure 3-30
ELM Envelope and Center of Gravity Location (3 of 3)

3.3.1.3 Electrical

The ELM uses the TIROS-N standard interface circuits specified in Interface Control Document IS-2295548 for all signals interfacing with the spacecraft. These signals are listed in Table 3-9 along with their intended use and circuit type. The ELM interfaces electrically to the spacecraft and to the Sensor Module. The connectors and cabling requirements are also specified in Document IS-2295548.

Table 3-9
TIROS-N STANDARD INTERFACE CIRCUITS

1.248 MHz clock:	High speed I/F circuit, timing
32-Second Major Frame Pulse:	Slow I/F circuit, used for discrete mode
Digital A Data Enable (A_1)	Fast I/F circuit, data sampling
8320 Hz Clock (C_1):	Fast I/F circuit, data shifting
Digital A Data (D_1):	Fast I/F circuit, data output
Discrete Commands (39);	Slow I/F circuit
+10V I/F Bus:	Use input filter
Digital B Flags (23):	0 V true, 5V false, command verify
Analog Telemetry (17):	0 to 5.12 Volts
Main Power Bus:	Quiet loads, 28V
Pulse Power Bus:	Motor loads, 28V, Heater Loads
Grounds:	See Paragraph 3.2.11

3.3.1.3.1 Interface Circuits

All of the interface circuits are on common printed wiring boards (PWBs) within the ELM. These PWBs can be modified to adapt the instrument to a different spacecraft interface without impacting the remainder of the electronics. All interface circuits, as listed in Table 3-9, use power from the +10V interface bus which has been filtered and current-limited in accordance with the requirements of IS-2295548. Current drawn from the 10V I/F bus is no greater than 10 mA.

3.3.1.3.2 Grounding

The ELM grounding conforms to the grounding requirements of IS-2295548. This includes isolation of the main bus and pulse bus returns from signal return and from chassis. Interface power (+10V) and analog telemetry also have separate returns. Shields are connected to chassis ground except for the detector preamplifiers which require shields common to signal ground.

3.3.2 TIMING SYSTEM

The timing signals are derived from the stable (0.005 ppm) 1.248 MHz TIROS clock and synchronization pulses. This arrangement synchronizes the wavelength drive and data sampling to the TIROS telemetry format.

The timing shown in Figure 3-31 includes frequencies for the power supply synchronization, wavelength drive, signal chopping, data rates, the 32-second discrete sampling period, and the 192-second wavelength sweep period. These last two are locked in phase with the 32-second TIROS synchronizing pulses.

3.3.3 COMMAND SYSTEM

The ELM is operated with 39 commands as listed in Table 3-10. The status of each command is verified with lines to Digital B telemetry as discussed in subsequent sections.

The Master Power On command applies power to the instrument, initializes all control logic, resets the high voltage and lamp power relay to OFF, and returns the grating drive to its home position. The grating mode commands are designed not to depend on any previous mode command (there are no toggling sequences). The last mode command sent takes effect after completion of the current sequence. A typical instrument start-up sequence consists of five pulse commands:

- Master Power On
- Motor Power On
- High Voltage Enable
- High Voltage On
- Grating Mode (1 of 4)

This assumes that the diffuser is in the proper position. The 39 available commands consist of 26 pulse and 13 level commands. The pulse commands are used for power control and quick reaction mode changes. The command system block diagram is shown Figure 3-32. Three pulse commands (No. 37, 38 and 29) are used to initiate automatic command sequences.

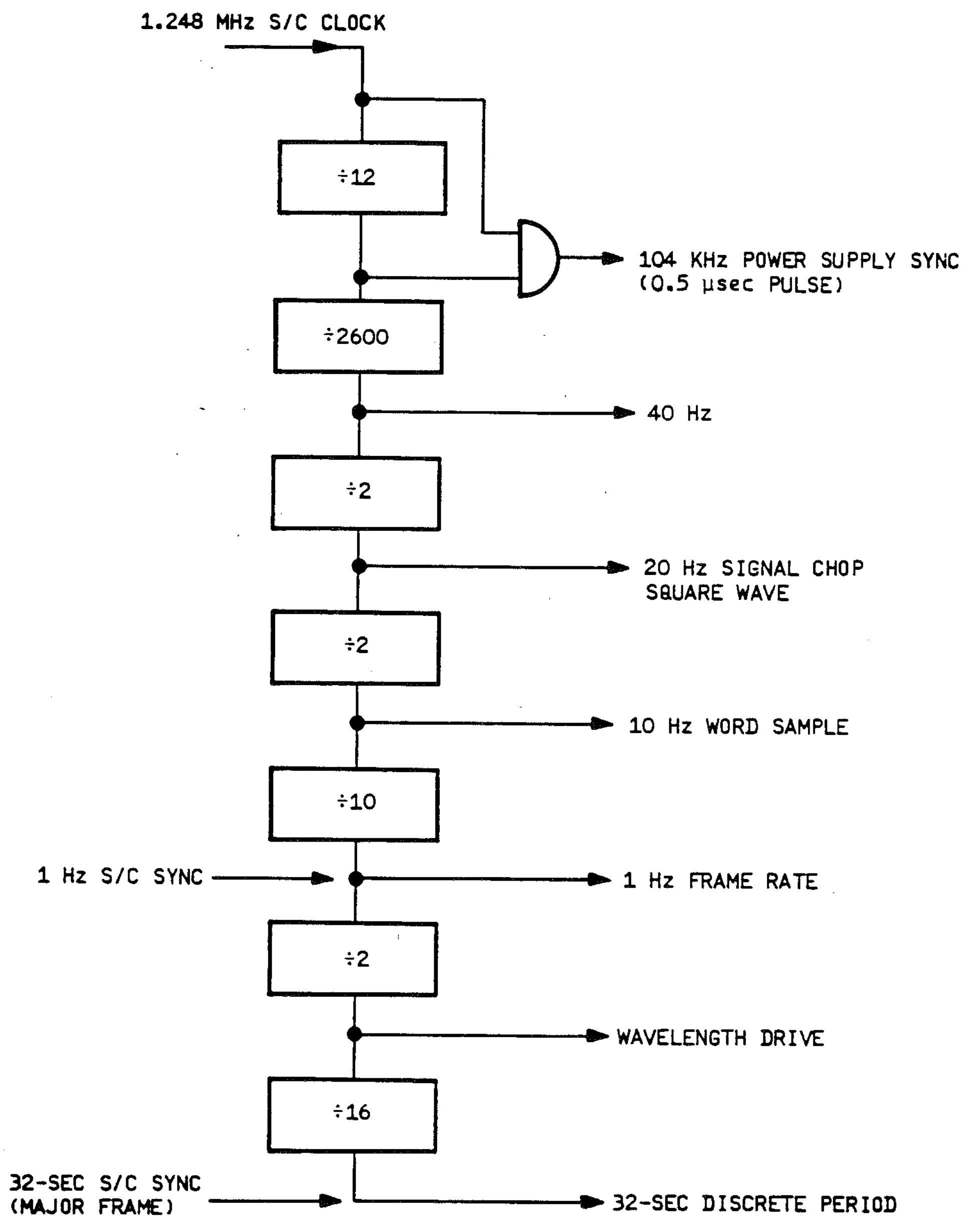

Figure 3-31
Block Diagram of Timing System

Table 3-10
LIST OF COMMANDS

COMMAND DESIGNATION		TYPE OF COMMAND	DIG. B ECHO	DIG. A STATUS
1.	Master Power On/Lamp Off/HV Off	Pulse	On/Off	On/Off
2.	Master Power Off	Pulse		
3.	Grating Mode 1 (Discrete)	Pulse	Yes/No	On/Off
4.	Grating Mode 2 (Sweep)	Pulse	Yes/No	On/Off
5.	Grating Mode 3 (l Cal)	Pulse	Yes/No	On/Off
6.	Grating Mode 4 (Position)	Pulse	Yes/No	On/Off
7.	High Voltage On	Pulse	On/Off	
8.	Motor Power On	Pulse	On/Off	
9.	Motor Power Off	Pulse		
10.	Lamp Enable and On	Pulse	On/Off	
11.	Lamp Disable	Pulse	Disabled/Enabled	
12.	Lamp Assy Open	Pulse	Open/Close	Open/Close
13.	Lamp Assy Close	Pulse		
14.	High Voltage Enable	Pulse	Enabled/Disabled	
15.	Diffuser Position 1 (Stow)	Pulse	Yes/No	Yes/No
16.	Diffuser Position 2 (Monitor)	Pulse	Yes/No	Yes/No
17.	Diffuser Position 3 (Sun)	Pulse	Yes/No	Yes/No
18.	Diffuser Position 4 (Decontaminate)	Pulse	Yes/No	Yes/No
19.	Chop Encoder Sensor, PRI/BAK	Level	PRI/BAK	
20.	Grating Encoder Sensor, PRI/BAK	Level	PRI/BAK	
21.	Diffuser Position Sensor, PRI/BAK	Level	PRI/BAK	
22.	Lamp Position Sensor, PRI/BAK	Level	PRI/BAK	
23.	Grating Drive Memory, FIX/FLEX	Level	FIX/FLEX	FIX/FLEX
24.	Code Strobe - Note 1	Pulse		
25.	Code Address A	Level		True/False
26.	Code Address B	Level		True/False
27.	Code Data Bit 1	Level		True/False
28.	Code Data Bit 2	Level		True/False
29.	Code Data Bit 3	Level		True/False
30.	Code Data Bit 4	Level		True/False
31.	Code Data Bit 5	Level		True/False
32.	Code Data Bit 6	Level		True/False
33.	Cal Lamp Heater On	Pulse	On/Off	
34.	Decontam Heater On	Pulse	On/Off	
35.	Heaters Off	Pulse		
36.	Spare	Pulse		
37.	Discrete Sun Enable	Pulse		On/Off
38.	Sweep Sun Enable	Pulse		On/Off
39.	λ Cal Enable	Pulse		On/Off

NOTES:

1. Commands 24-32 are used to load grating drive FLEX memory. Commands 24-28 are also used to select the memory segment to be read.

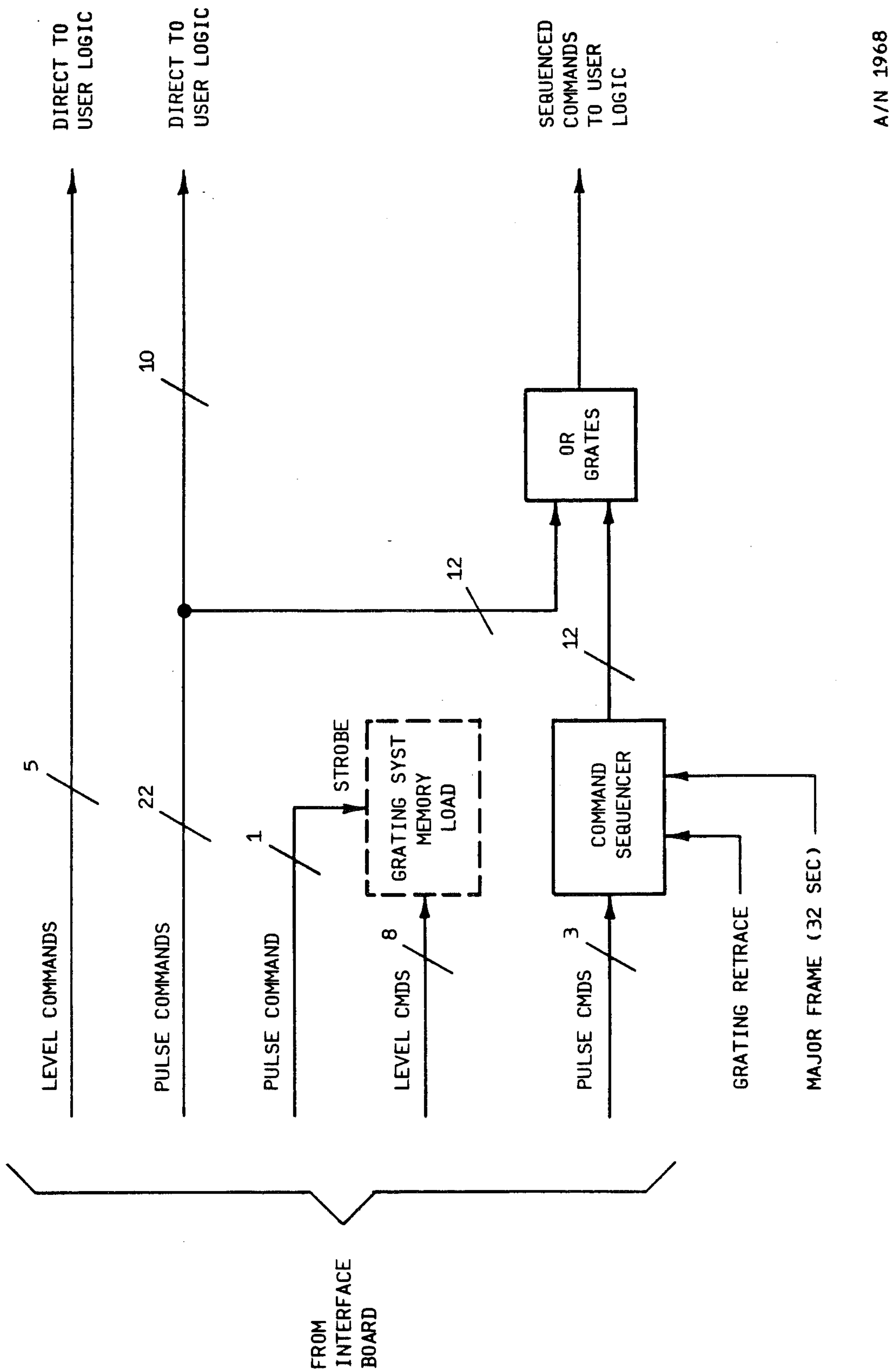

Figure 3-32
Block Diagram of Command System

3.3.4 GRATING DRIVE

The SBUV/2 Grating Drive Electronics points the grating to any one of 3262 positions with a resolution of 19.78 arc-seconds. This corresponds to a nominal spectral resolution of 0.074nm over a range of 240nm (160nm to 400nm) or 17.92 degrees of grating rotation. In addition, the grating can drive to the zero-order position for a total range of 30 degrees for test purposes only. The instrument is shipped with a mechanical stop in place, to prevent the grating from ever reaching the zero order position. Operationally, the pointing is accomplished by loading a target position value - a binary number between -1820 and +3640 (nominal) - into the Position Command Register. The grating servo loop will then position the grating to the desired location as later described.

The four basic operational modes of the grating are DISCRETE, SWEEP and CAL and POSITION.

In the DISCRETE Mode, the Mode Sequence Logic will sequentially read 13-bit Position Command values from a memory and deliver them to the Position Command Register. Twelve values will be read at a rate of one every two seconds. The grating will drive and settle to the new value in less than 0.75 second and hold for the remaining 1.25 seconds while the scene signal is being processed. At the end of the twelfth discrete position, the sequence logic will again fetch the first position. This will cause the grating to drive back to that position (in the opposite direction). At the next telemetry major frame time (every 32 seconds), the sequences will be repeated.

The SWEEP Mode begins by loading the Position Command Register from memory with the value corresponding to 400nm. The grating slews to this location; then, at the next major frame time, the Position Command Register (which is actually a counter) is clocked at a rate of 20 Hz. At this rate, there are two 0.074nm (nominal) steps in the sweep mode integration time of 0.1 second. The nominal spectral bandwidth covered in 0.1 second is then 2 x 0.074 = 0.148nm. When 3360 such 0.074nm steps have been issued, the grating will be at the end of the sweep range. At this time, the starting Position Command is again fetched and loaded into the Position Command Register causing the grating to return to that position. Note that the sweep mode scan actually begins at about 406nm and ends at about 160nm.

The CAL Mode is similar to the DISCRETE Mode. A Position Command is fetched from a memory location; the grating goes to that position, then, the Position Command Counter is advanced four counts once every two seconds for 12 steps beginning after a 32 second major frame sync. This results in 12 calibration steps spaced at 0.296nm (nominal) increments for a total coverage of about 3.256nm. After 12 steps, the starting position is returned and the sequence repeated.

The POSITION Mode is a single position which will drive the grating to a single predetermined target position for a laboratory calibration.

Commands other than the Mode Commands are received by the grating electronics. A FIX Command instructs the Mode Sequence logic to fetch the Position Commands from the programmable read only memory (PROM), while the FLEX Command instructs the logic to fetch from the random access memory (RAM). The Grating Primary/Secondary LED command selects the primary or secondary (redundant) encoder read stations. Coded command data is used to load the FLEX memory and select the desired memory segment as later described.

The grating memory consists of a Programmable Read Only Memory (PROM) implemented with a 512x8 CMOS IC (HM1-6611-8 in FM2 and HMI-6641-8 in CM3) and a Random Access Memory (RAM) implemented with a 256x4 CMOS IC (HS 6551 RH). The PROM is programmed with the Angle Data determined during wavelength calibration. The Angle Data words represent the number of counts (in two's complement binary) clockwise (CW) (positive counts = decreasing wavelength) or counter-clockwise (CCW) (negative counts = increasing wavelength) from the index position on the grating encoder. (Viewed from the encoder end of the grating shaft). The angle data words thus represent the angular position of the grating with respect to the index position. The resolution element of the grating is derived from the sine and cosine track zero crossing, so there are four resolution elements per cycle of the sine track. Since there are 2^{14} cycles of the sine track signal per revolution of the grating, then each resolution element corresponds to 0.005493° or 0.00009587 radians. This about 0.074nm wavelength shift.

The index position is centered nominally at 280nm, or rather, at grating encoder index the wavelength incident on the PMT will be about 280nm. The total operational range of the grating (160 to 400nm) will require about an 18° angular range. For calibration purposes, the grating also drives to zero order which is approximately 12° CW of 160nm or about 20°CW of index. So, the required Angle Data range is about +3640 counts, -1820 counts. This range can be handled with a 13 bit binary word (+4095, -4096 counts). This dictates the memory design.

The FIX (PROM) and FLEX (RAM) memories are identically organized. PROM data is determined in calibration and repeated four times for redundancy. The RAM will allow calibration data to be tested and permit in-orbit correction of angular positioning if some launch induced shift in instrument alignment occurs. The contents of the PROM vary from instrument to instrument principally as a function of the location of the index pulse on the encoder disc with respect to the grating alignment. To pack the required 15 words of 13 bits each in the memory, the format shown in Figure 3-33 is used.

As can be seen, there are four segments identically organized. The memory is designed so that any one of the four segments can be written into be ground command and read out for Angle Data by ground selection.

The selection between the PROM (FIX) or RAM (FLEX) memory is by the FIX/FLEX latched command. When this command is "true", the FIX system will supply the Angle Data beginning at the current grating scan. When the command is "false", the FLEX system (RAM) supplies Angle Data.

The selection of which segment of the selected memory is to be read is accomplished by the CODED DATA group of commands as described in Section 3.3.3.

Whenever power is applied to the instrument (28 volt Main Power), the system initializes to read segment 0, of the fixed memory. If a command is received to change this, then the new segment will be read until it is again changed, or the power is cycled.

	MEMORY ADDRESS DECIMAL	OCTAL	CONTENTS	BIT VALUE Q3	Q2	Q1	Q0	
SEGMENT 0	0	0	DISCRETE	2^3	2^2	2^1	2^0	WORD 0
	1	1		2^7	2^6	2^5	2^4	
	2	2	POSITION 1	2^{11}	2^{10}	2^9	2^8	
	3	3		—	—	—	2^{12}	
	4	4	DISCRETE	2^3	3^2	2^1	2^0	WORD 1
	5	5		2^7	2^6	2^5	2^4	
	6	6	POSITION 2	2^{11}	2^{10}	2^9	2^8	
	7	7		—	—	—	2^{12}	
	8-11	10-13	DISCRETE POS. 3	SAME AS ABOVE				W 2
	12-15	14-17	DISCRETE POS. 4	SAME AS ABOVE				W 3
	16-19	20-23	DISCRETE POS. 5	SAME AS ABOVE				W 4
	20-23	24-27	DISCRETE POS. 6	SAME AS ABOVE				W 5
	24-27	30-33	DISCRETE POS. 7	SAME AS ABOVE				W 6
	28-31	34-37	DISCRETE POS. 8	SAME AS ABOVE				W 7
	32-35	40-43	DISCRETE POS. 9	SAME AS ABOVE				W 8
	36-39	44-47	DISCRETE POS. 10	SAME AS ABOVE				W 9
	40-43	50-53	DISCRETE POS. 11	SAME AS ABOVE				W 10
	44-47	54-57	DISCRETE POS. 12	SAME AS ABOVE				W 11
	48-51	60-63	START OF SWEEP	SAME AS ABOVE				W 12
	52-55	64-67	START OF CAL	SAME AS ABOVE				W 13
	56-59	70-73	POSITION	SAME AS ABOVE				W 14
	60-63	74-77	———	SAME AS ABOVE				W 15
SEG. 1	64-67	100-103	DISCRETE POS. 1	SAME AS ABOVE				W 0
	68-71	104-107	DISCRETE POS. 2	SAME AS ABOVE				↓
	72-127	110-177	DIS. POS. 3-12, START OF SWEEP, START OF CAL., POS., ———	SAME AS ABOVE				W 15
SEG. 2	128-191	200-277	SAME AS ABOVE					W 0 ↓ W 15
SEG. 3	192-255	300-377	SAME AS ABOVE					W 0 ↓ W 15

Figure 3-33
Grating Drive Memory Organization and Command & Data Format

Although the segment selection command can be received at any time, segment selection and memory selection can only change at the end of a scan. In DISCRETE, CAL and POSITION modes, this occurs 24 seconds after the beginning of a Major Frame Sync. In SWEEP mode, this occurs 168 seconds after the Major Frame Sync which begins the sweep mode scan. These times are the beginning of the grating RETRACE. Each scan (DISCRETE, CAL, POSITION or SWEEP) begins at the next major frame sync (32 seconds).

To load the FLEX memory requires specification of an eight bit address and the contents of that address. Since it makes little sense to load anything shorter than a full 13 bit word, this loading can be done by specifying the SEGMENT and WORD to be loaded/changed, then specifying the word contents for each of the four subwords per word. The format is shown in Section 3.3.3.

Note that since the last word in a segment is not used, then, if an entire segment is being written, it would be good practice to end the write sequence with a code "1 0 W_7 W_6 1111" thus setting up a write address to this unused word. Then, if a "00——" CODE DATA word is inadvertently sent, it will be written into the unused word rather than the last active word previously written.

For telemetry purposes, both memories are constantly verified. A 16 bit word in the SBUV/2 Digital A telemetry format at Line 3, word 1, carries a 13 bit word from memory. A two bit segment code and one bit indicating the origin of the word complete the 16 bits. The format is described in Section 3.3.8.

The verify sequence begins at segment 0, Word 0, of the FIX memory and sequences through all 64 words of the FLEX memory and then all 64 words of the FLEX memory, in order. The sequence repeats every 128 seconds, beginning at a MFP (Major Frame Pulse), however, there is no synchronization of the entire 128 second cycle to any other telemetry feature, in other words, the cycle begins at some arbitrary 32 second sync, depending on when power is applied, and repeats every 128 seconds. Location of a specific word in the memory is aided by the FIX/FLEX bit and the segment bits.

The angular location of the grating is determined by the Angle Data in the memory. In the DISCRETE mode each discrete scan angle is fetched from one of the two memories as a two's complement 13 bit binary number. As the grating moves, the pulses from the encoder advance a position counter which is referenced to the index position on the encoder. The difference between the Angle Data and this position counter generates an error signal which moves the motor to reduce the difference. The position mode is similar except there is only one angle. The sweep and cal modes begin at some starting angle dictated by one word of angle data, then that angle is advanced at a fixed rate. The position counter then keeps up with the incrementing angle data by driving the grating.

For those interested in more technical details, the position counter is set, at index, to -1 (a binary 1111 1111 11111). When the grating rotates clockwise, the counter counts down, when counter-clockwise, the counter counts up. This is opposite of the Angle Data. This is necessary because the resulting count and Angle Data are added, thus, it is necessary to track the negative of the position. By setting the counter to -1, the count is then the one's complement. When the angle and position data are added, a 1 is summed with them (carry-in input on the LSB of the adder is used). This is the same as beginning the counter at 0 which would give the two's complement value. By this simple device, the serially shifted output of the position count to the telemetry data is simply inverted to yield the true angular position rather than its negative. This simplifies reading the data.

The position data appears in the telemetry format at Line 6, word 1. The format is given in Section 3.3.8. The diagram summarizes the meaning of the position word.

cw	0000000000001	+1 Decreasing Wavelength
Index	0000000000000	0
ccw	1111111111111	-1 Increasing Wavelength
	↑ SIGN BIT (0=cw, 1=ccw) of Index	

The position data is the actual grating position at the time sampled. Positive numbers represent an angle clockwise of Index viewed from the encoder end of the grating shift. This is in the direction of decreasing wavelength. Negative numbers (2^{12} - 1) represent counter-clockwise of Index.

In the SWEEP mode, a scan begins at the first major frame after completion of the current scan. It takes six frames (192 seconds) to complete a SWEEP mode scan. To indicate which part of the scan the current data is sampled, a sweep mode count is provided. This occurs at Line 0, word 1 (Status 1), telemetry bits 3, 4 and 5 with the formal in Section 3.3.8.

The sweep frame count will continue to sequence 1-6 as long as the grating is in SWEEP mode. When taken out of SWEEP mode, the counter returns at 0 at the major frame occurring at the beginning of the next mode.

Note also that the POSITION data is sampled at the same time as in the DISCRETE mode, however, the position is changing every 0.05 second. So the first position words in frame count 1 will be the start of the sweep position, the second position word (at the next Line 6, word 1 location) will be 19 counts more positive. The next position will be 20 counts more positive, the next 20 counts more, etc. The final count will be 3359 counts more positive than the original starting position.

The remainder of this discussion describes the servo control system for positioning the grating.

The SBUV/2 Grating Drive System uses a closed-loop servo control design that has two modes of operation. The first of these is a coarse-pointing mode that positions the grating within ±10 arc seconds of the desired position. The second mode is a fine-pointing mode that reduces the pointing error to less than ±1.5 arc-seconds, and holds the final position within ±0.5 arc second.

The basic parts of the Drive System consist of the electronic circuitry, a limited rotation brushless DC torque motor, the gratings, and an incremental encoder. The block diagram, Figure 3-34, shows the interconnections of the basic parts and the major subdivisions of the electronic circuitry.

When power is first applied, the Power On Reset simultaneously resets the (13-bit) Position Command Register and initiates the INDEX LOGIC circuit. The INDEX LOGIC circuit "jams" the (13-bit) Encoder Position Counter to a positive or negative number depending on whether the ccw of INDEX is false or true, respectively. A positive number, when added to the "0" in the Position Command Register, results in a positive error which will drive the grating clockwise (CW). A negative will drive the grating CCW.

The INDEX LOGIC circuit maintains these conditions until an Index Pulse is received from the Encoder Conditioning Electronics. The Index Pulse is located at about 10° CW of the end of the travel. Each time it is detected, the Encoder Position counter is zeroed.

The Index Pulse is positioned with respect to the CCW of Index track such that if the index is not detected by the time the track indicates "CW of index", the motor will be reversed. The rotation of the grating will then continue until the Index Logic circuit receives an Index Pulse from the encoder. At that time, the Index Logic circuit is reset, which allows the Encoder Position Counter to start counting and enables the Mode Sequence Logic. Stated another way, the resetting of the Index Logic circuit by the Index Pulse terminates the Power On Reset sequence, and allows the digital portion of the servo electronics to begin operating.

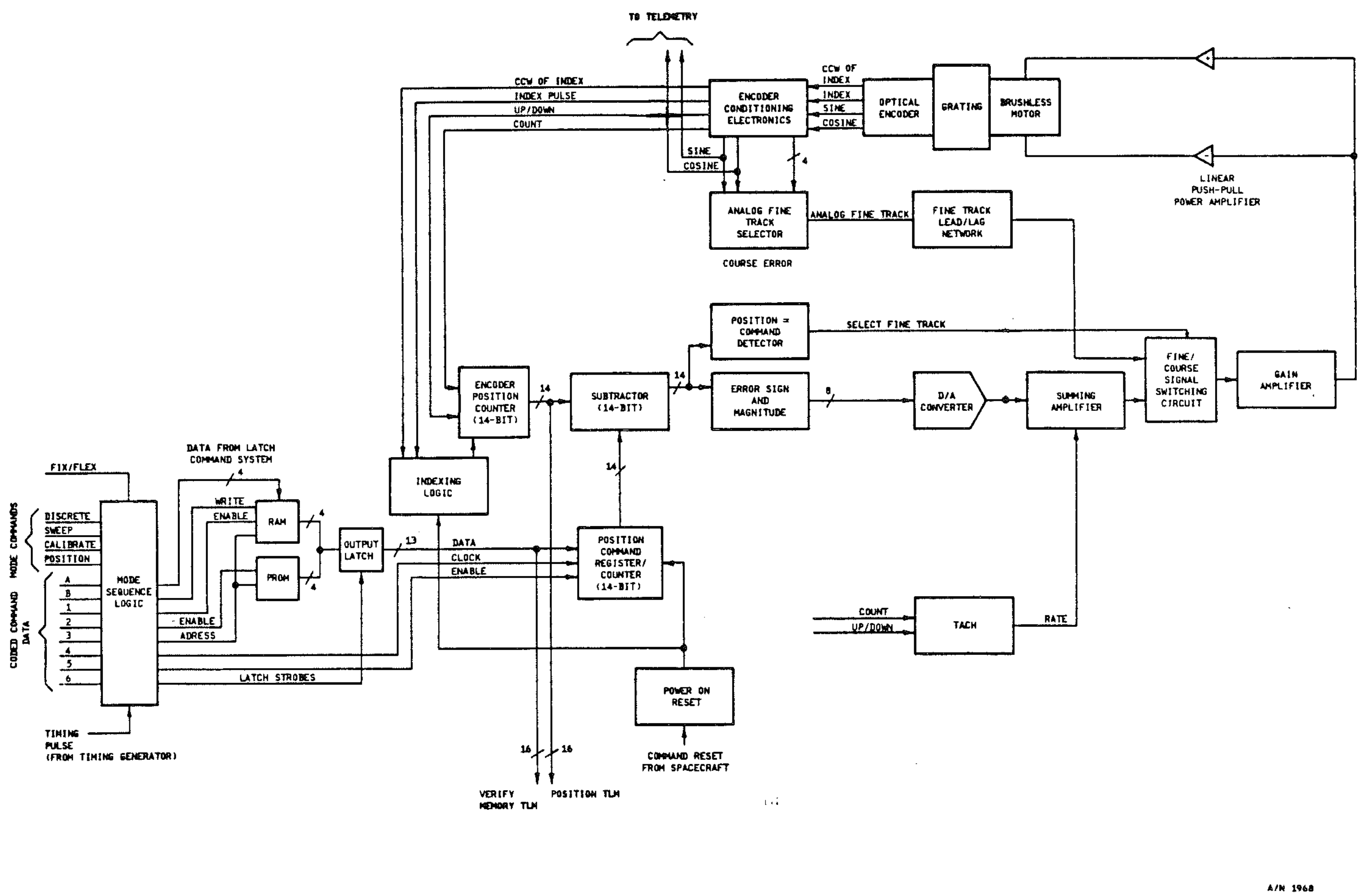

Figure 3-34
Block Diagram of Grating Drive Electronics

The 13-bit Subtractor compares the value that has been loaded in the Position Command Register (PCR) with the number of counts in the Encoder Position Counter (EPC). If the number of counts in the EPC is less than the value in the PCR, the Error Sign and Magnitude circuit puts out a signal whose most significant bit is a logic ONE indicating a counter-clockwise error, and causing the D/A converter to put out a positive voltage which will result in a clockwise movement of the grating. If the number of counts in the EPC is greater than the value in the PCR, the output from the Error Sign and Magnitude circuit will be a logic ZERO, indicating a clockwise error, and resulting in a counter-clockwise movement of the grating. The subtraction is actually accomplished by counting the EPC down for CW grating motion and up for CCW motion. This results in the negative of the true grating position. This is added to the PCR value to obtain the difference, which is called the Digital Error.

If the Error Sign and Magnitude circuit determines that the difference between the EPC and the PCR is greater than 255 counts (in either direction), the output to the D/A converter will have an overscale bit set to a ONE, for a CCW error, or a ZERO for a CW error. Either condition represents maximum error, and the D/A Converter will be either ±10.00 volts or -10.00 volts, respectively. In range errors result in smaller output voltages, at the rate of about 0.6 volts per step of error.

The output of the D/A converter goes into a summing amplifier where it is added to the negative of a Tachometer circuit. The Tachometer circuit is a frequency-to-voltage converter whose analog output is proportional to the signed (CW or CCW) angular velocity of the grating. Its purpose is to limit the angular velocity of the grating thus providing some damping of the grating motion to achieve faster settling times.

The output of the Summing Amplifier goes through a gain stage and then to the Linear Power Amplifier circuit, where the amplitude is converted to a motor drive voltage. This motor drive voltage is applied to a limited rotation DC torque motor causing movement in the clockwise or counter-clockwise direction depending on the polarity. The motor voltage used by the Linear Power Amplifier comes from a ±15-volt supply. Since the amplifier is a push-pull arrangement, the net voltage across the motor can be +30 volts or -30 volts depending on the polarity of the error signal. This is an effective gain of 2.

The encoder is an incremental, optical design with both SINE and COSINE outputs. For accuracy and redundancy, the encoder has four redundant reading stations per SINE or COSINE track (eight stations total), whose individual outputs are summed together. This removes the errors due to shaft and grating ellipsivity and eccentricity. The SINE/ COSINE signals have 16,384 or 2^{14} cycles per revolution. These signals are processed in the Encoder Conditioning Electronics to obtain the signals required for proper operation of the drive system.

For operation in the COARSE Mode, only the Index Pulse, and two digital signals (COUNT and UP/DOWN) are required. These signals are derived by electrically shifting and squaring the 2^{14} analog signals. See Figure 3-35 for more details.

Once the servo system has moved the grating to the point where there is no digital error between the Encoder Position Counter and the Position Command Register, the Position = Command Detector issues a "Select Fine Track" signal to the Fine/Coarse Switching circuit. The appropriate analog signal (COSINE, SINE, -COSINE, or -SINE) is switched into the analog portion of the servo-system. Operation of all the subsequent circuits remains the same, except that the error signal is now derived directly from the encoder and not from the D/A converter, and the servo-system attempts to reduce the analog error signal to zero. A lead/lag compensator in the fine track circuitry reduces the servo "hunting" effect and decreases the settling time as well as the final settling error.

Since there are 65,536 step positions per 360° (of which only 5,315 are used over the 29.2° full scale angular swing), the resolution of the grating is 19.78 arc-seconds. By using the servo-system design, repeatability to any given position can be held to less than ±1.5 arc-seconds.

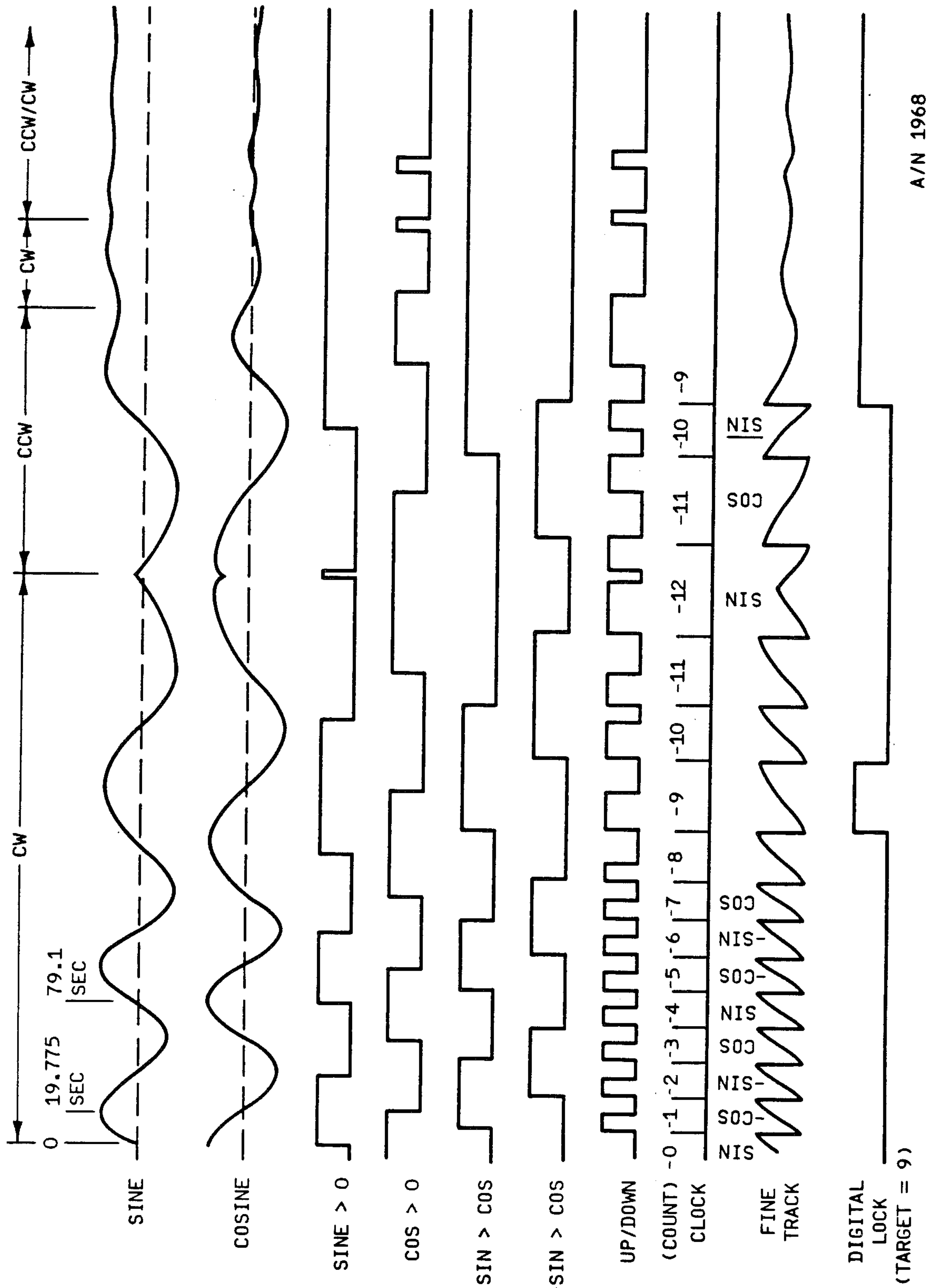

Figure 3-35
Example of Grating Motion

3.3.5 CHOPPER WHEEL DRIVE

The chopper wheel modulates the incoming light at 20 Hz. The modulated signal is synchronously demodulated, filtered, and detected using voltage-to-frequency converters and gated accumulators.

The mechanical characteristics of the chopper are given in Table 3-11. The required chopper phase and velocity accuracy is derived in SER SBUV-NE-80-126. A three-phase, eight-pole brushless DC motor was chosen to drive the chopper. To meet the accuracy requirements, an optical encoder was chosen.

Figure 3-36 is a block diagram of the chopper drive system. A novel approach was decided on due to the high accuracy requirements on phase locking to a low frequency (20 Hz) signal. The basic chopper servo loop is a phase-locked loop locking the 1000 cycle encoder signal to a 4000 Hz reference (the motor, in lock, rotates at four revolutions per second). A phase comparator determines the phase error and drives a linear power amplifier through a one pole, two zero lead-lag network. This loop controls the basic stability of the phase lock. The servo design is such that maximum torque disturbances will not disturb the phase lock by more than 1/2 of the reference/encoder period. This means that if a means can be found to establish the proper 20 Hz phase reference, the chopper will remain in proper 20 Hz phase within the required accuracy (about one 4000 Hz period or one cycle of the 1000 cycle encoder track). The method used to establish this initial phase reference is called digital phase stepping. The details of this will be covered later. It basically involves inverting the 4000 Hz reference which is the same as providing a 180° phase shift of the reference.

The encoder is the heart of the chopper drive. It establishes the basic accuracy of the phase lock. Basically, the encoder generates a very accurate clock where one clock period represents a precise angular rotation of the encoder disc. In this case, there are 1000 clock cycles of the high speed track on the disc. Hence each cycle corresponds to $2\pi/1000 = 6.28\times10^{-3}$ radians. The encoder will be able to maintain an accuracy of $\pm3\times10^{-4}$ radians. The encoder will be able to maintain an accuracy of $\pm3\times10^{-4}$ radians (±1 arc min). In the encoder read head, an LED illuminates a push-pull photo detector through the code disc. As the disc turns, unbalanced currents flow through the push-pull pair. This unbalanced current is detected by an operational amplifier. This amplifier is operated as a current-to-voltage converter. The output of the operational amplifier goes to a comparator

Table 3-11
CHOPPER WHEEL DRIVE REQUIREMENTS & CHARACTERISTICS

<u>MECHANICAL CHARACTERISTICS:</u>

• MOMENT OF INERTIA	2.56 x 102 oz.-in.-sec.^{2}
• STARTING FRICTION	0.1 oz-in.
• NOMINAL RUNNING FRICTION	0.5 oz.-in.
• COLD RUNNING FRICTION	1.0 oz.-in.
• TORQUE DISTURBANCES	0.75 oz.-in. for 0.4 msec.

<u>ENCODER:</u>

• VELOCITY TRACK	1000 CYCLES PER REVOLUTION
• PHASE TRACK	5 CYCLES PER REVOLUTION
• MOTOR COMMUTATION TRACKS	3 TRACKS, 4 CYCLES PER REVOLUTION

<u>MOTOR:</u>

• PHASES	3
• POLES 8	
• TYPE	BRUSHLESS, DC.

<u>VELOCITY:</u>

• MOTOR VELOCITY	4 Hz
• VELOCITY STABILITY	±0.0036 Hz

<u>PHASE:</u>

• CHOPPER PHASING SIGNAL	LOCKED TO 20 Hz DEMOD
• PHASE STABILITY	±0.0057 WHEEL RADIANS

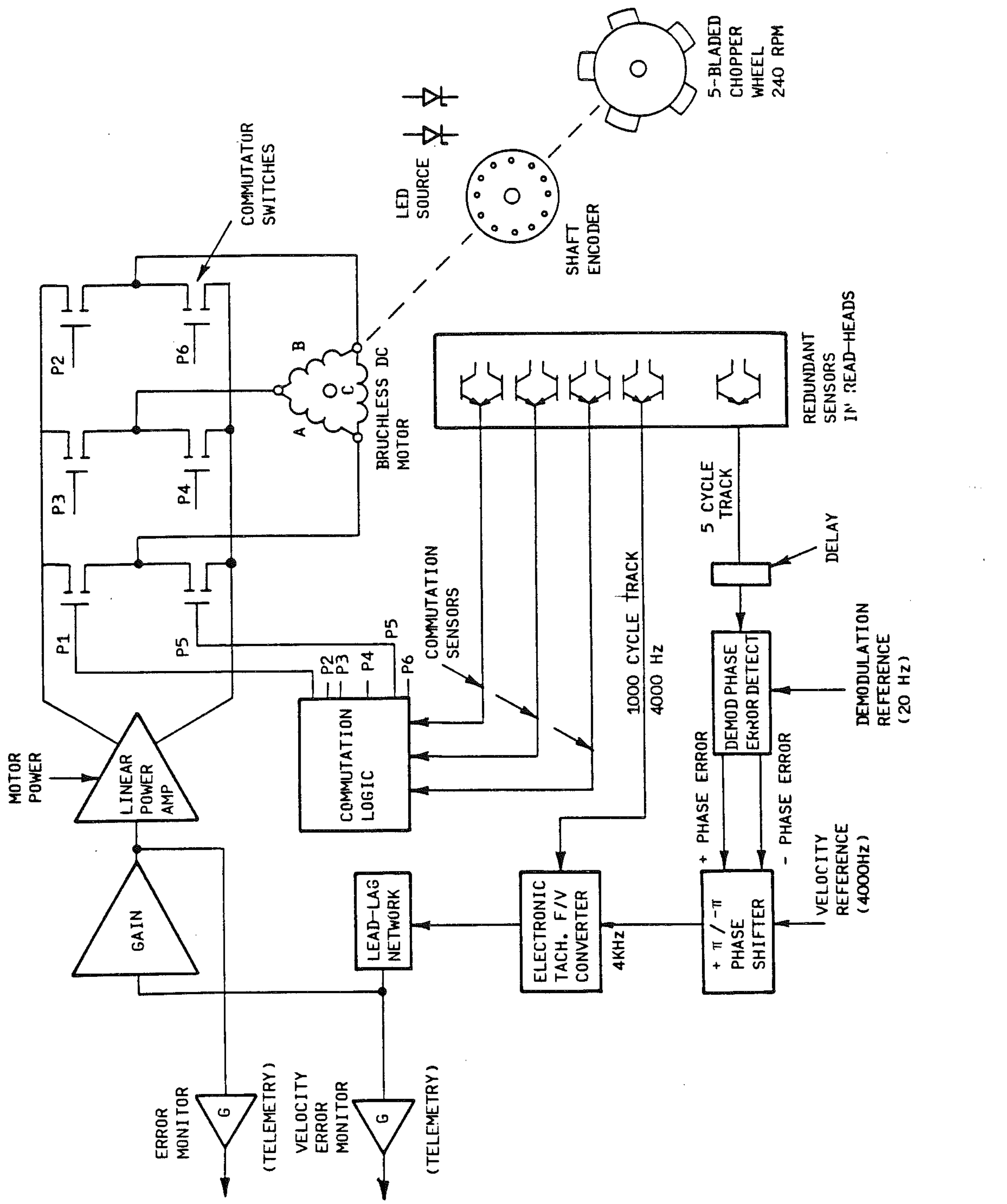

Figure 3-36
Block Diagram of Chopper Drive Electronics

where the waveform is squared up. Notice that the photodetectors are operated from a single +10 volt supply, and the zero reference is established at five volts by a resistor divider. Using this scheme, the interface circuit is slightly simplified since no level conversion to logic levels is required.

The 5-cycle track on the encoder disc is similar in operation. Again a push-pull pair is used. These are accurately matched and view the encoder through a 0.003 inch slit to provide $\pm 4.4 \times 10^{-4}$ radians (1.5 arc min) of accuracy. This corresponds to about 7% of one cycle of the 1000 cycle track.

The three commutation tracks do not require as high an accuracy (±1°) and hence are operated as simple, single ended detectors.

The entire LED/detector system for the encoder is redundant. Two read heads are provided and co-aligned electrically to within ±1 arc min at stations situated 180° apart. Since the 5-cycle track is not divisible by two, this necessitates inverting the 5-cycle signal when the redundant station is used. This is done by the exclusive - OR gate on the 5-cycle detector electronics. The redundant switching is accomplished by VMOS power FET's for the LED current (which is set to 30 ma) and AD7510 analog switches for the photodetectors. All power and grounds are switched so that failure mode short circuits will be isolated by switching to the other system. Fault isolation resistors further prevent power supply loading in case a photodetector (or cable) experiences a ground short circuit fault. This philosophy of fault isolation is used on every path which is determined to not lie in the critical fault path.

The motor used in the chopper drive is a three-phase, eight-hole brushless DC motor. As such, it must be commutated electrically. Three commutation tracks on the encoder will be aligned while the motor is running to achieve minimum peak motor current. The commutation sequence is shown in Figure 3-37 where A, B, and C represent the ideal commutation signals.

The electrical interface to the motor is accomplished by a simple decode network to derive the required six phase signals shown in Figure 3-37. The easiest way to picture the motor operation is by a rotating field vector as schematically produced in Figure 3-37. This rotating field pulls the eight pole rotor around.

The power switching to the motor is provided by 2N6660 VMOS power FETs. These allow direct interfacing to CMOS and have a very low resistance (2 to 3Ω). To turn these devices on, the gate must be more positive than the source. This presents a problem when used in the source follower mode, so a two stage design is necessary (since the CMOS logic levels do not exceed the motor supply voltage: 24 volts). The first stage merely serves as a level converter (also inverting the sense of the signal). To prevent reverse Gate/Source currents, a blocking diode is placed in series with the source. Other diodes from source to drain are placed to prevent damage during power cycling and subsequent field collapse in the motor windings.

A motor current monitor is provided for telemetry.

The design of the phase-lock servo loop is explained in System Engineering Report No. SBUV-FT-81-181. The transfer function is given as:

$$\frac{V_c(s)}{(\theta_{REF} - \theta)(s)} = 56000 \frac{(s+400)(10000)}{(s+4000)(s+10000)}$$

The electrical design uses a CD4046 phase locked loop as the phase detector, to develop $\theta_{Ref} - \theta$, followed by a two-pole one zero filter implemented by an operational amplifier. The additional pole is placed at 10,000 rad/sec to provide a cutoff for ripple produced by the phase comparator. Another pole is provided by the operational amplifier compensation circuitry.

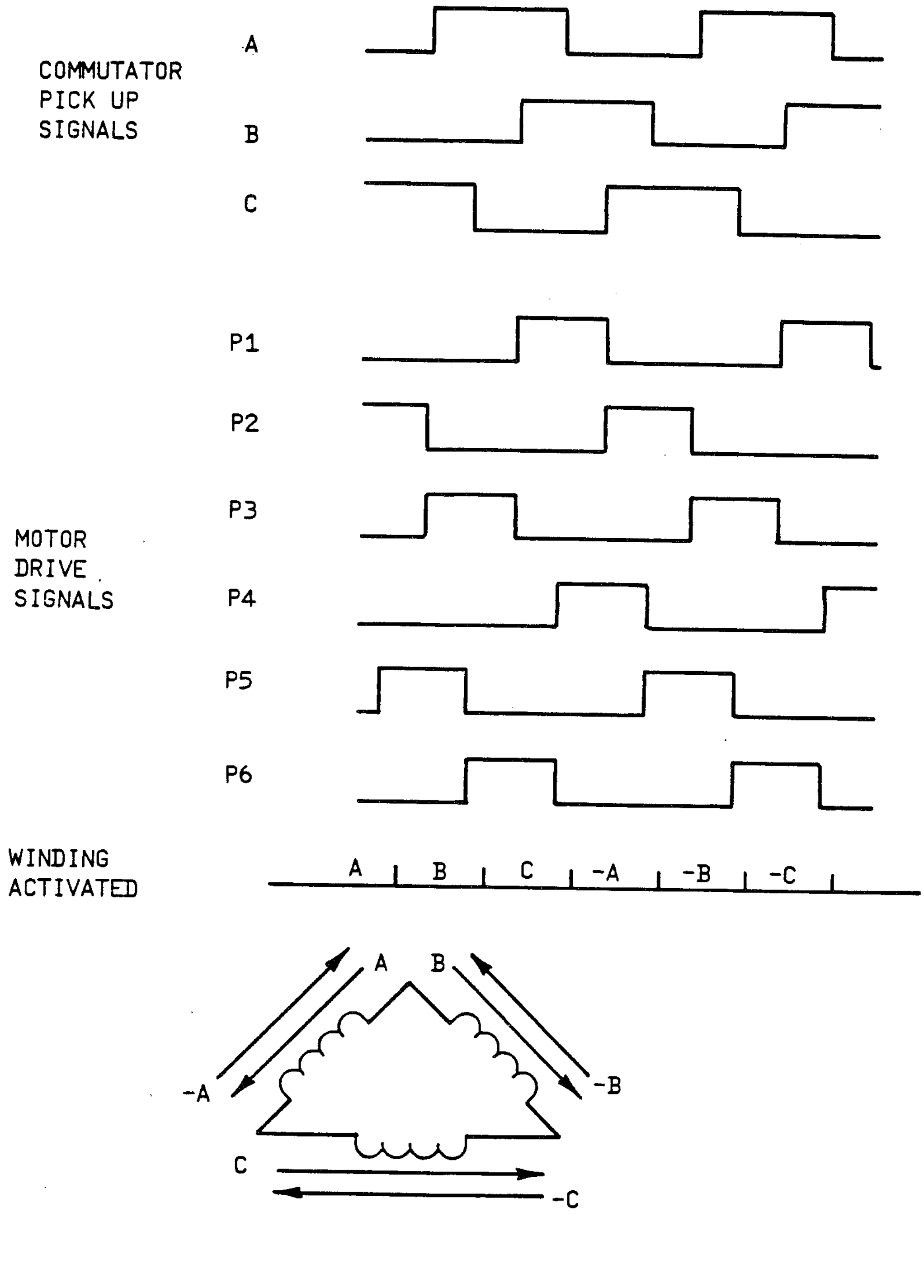

Figure 3-37
Commutator Timing

A model of the 4046 phase detector is discussed in System Engineering Report No. SBUV-NE-81-180. Basically, the 4046 outputs pulses (from its normally high impedance output) whose width is proportional to the phase difference existing on the input pins.

The filter on the output serves to integrate the pulses performing the actual phase error to voltage conversion. This conversion is fairly nonlinear.

The filter on the output of the 4046 is the lead/lag filter determined by the servo analysis. The output of this filter goes to a linear power amplifier.

Note that the linear power amplifier is driven from ground to the +24V motor voltage. This simplifies the commutation switching since the voltage polarity cannot reverse. The actual operating voltage of the motor is set to approximately its mid-range. In this case, the specified motor operates at about nine volts allowing enough voltage range for control.

To achieve phase lock to the 20 Hz demodulation signal being used in the signal processing, a technique of digital phase stepping is used. The 20 Hz demodulation clock is compared to the 5-cycle encoder track. If the leading edges occur within ±1/2 cycle of the 4000 Hz reference, then both are properly phased (i.e., within ± 0.00314 radians). If both are outside of this window, then either a +Phase Error or -Phase Error signal occurs depending upon whether the 5-cycle signal lags or leads the 20 Hz demodulation signal. A +Phase Error will cause the 4000 Hz reference to be inverted at the leading edge of a clock (the clock "skips a beat"). This forces the CD4046 phase detector to output 0 volt pulses for the subsequent phase errors, hence slowing the motor down until the 1000 cycle track is in phase lock with the new reference. This is shown in Figure 3-38, (top). A -Phase Error causes the 4000 Hz reference to be inverted in the middle of a clock pulse (adding a clock), forcing the CD4046 to output +10 volt phase error pulses, speeding the motor up until the 1000 cycle track is in phase lock with the new reference. In either case, the relative phasing is moved either CW or CCW by 1/2 a cycle of the 1000 cycle track, or 0.00314 radians. These phase corrections are made for each cycle of the 5-cycle track, or five times a revolution until the 5-cycle phasing agrees with the 20 Hz demodulation. A maximum of 200 such phase steps are required if the 20 Hz and 5-cycle tracks are 180° out of phase initially. Once in phase, the servo loop gain is such that worse case torque disturbances will not disturb the phase lock by more than about 1/10 of a clock cycle. So once 20 Hz lock is achieved, it should never be broken.

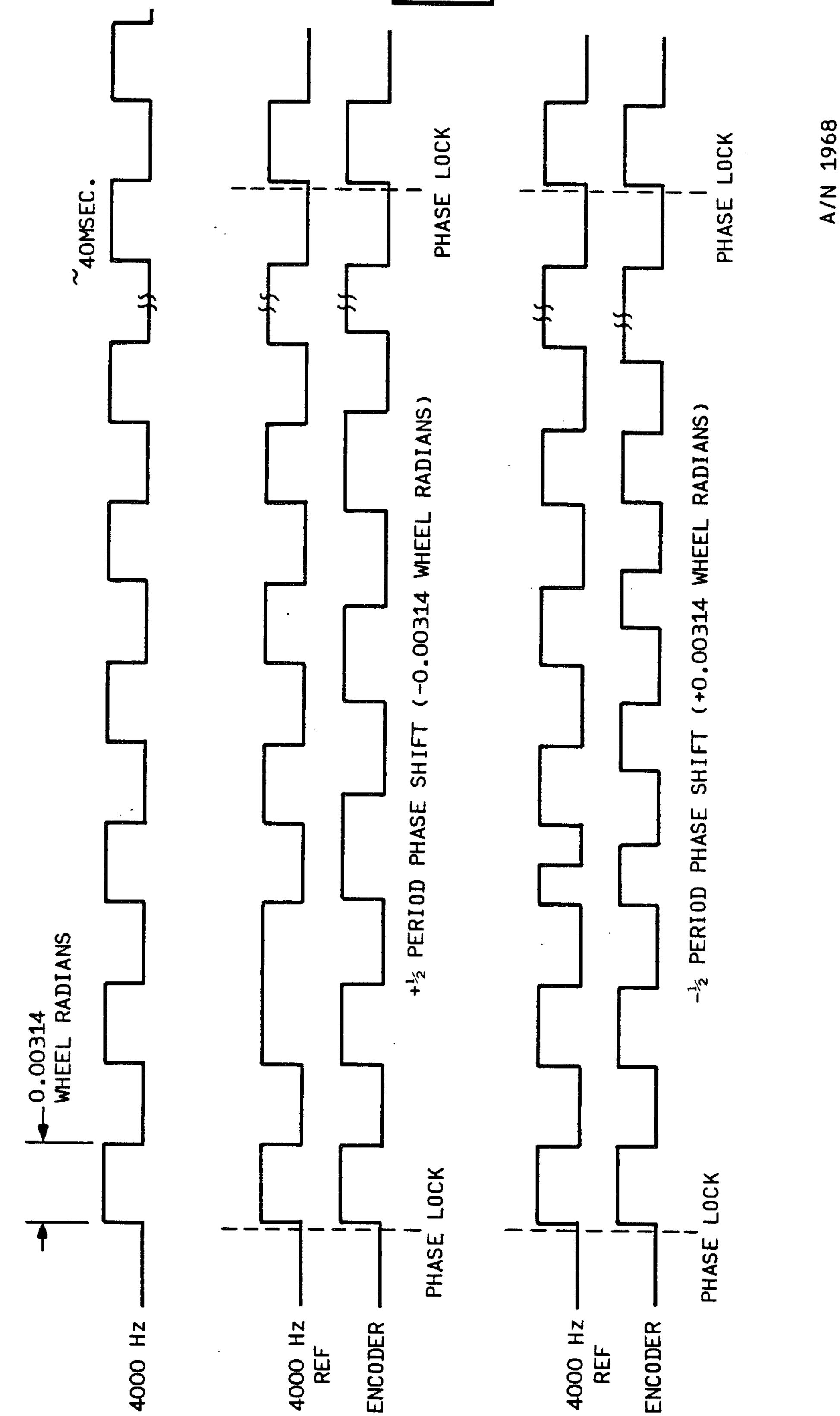

Figure 3-38
Chopper Phase Stepping

Since the apertures in the chopper wheel cannot be mechanically aligned with absolute precision to the 5-cycle encoder track, the alignment must be done electronically. The nominal mechanical alignment is such that the aperture lags the 5-cycle track by 2.5°. This alignment can be done within ± 2°. After assembly of the system and mechanical alignment, the chopped signal waveform is phased with the 20 Hz demodulation waveform by delaying the 5-cycle signal on the Chopper Drive in increments of 0.00314 radians (= 0.18°). This delay is accomplished by programming the four jam inputs on a counter which is clocked by the 4000 Hz signal. This counter begins clocking at the leading edge of the 5-cycle signal. When it reaches a count of 15, the 20 Hz demodulation signal is tested for proper phasing. If the 20 Hz signal rising edge occurs during this count of 15, the phasing is correct. If it occurs before, the +Phase Error sequence occurs. If it occurs after, the -Phase Error sequence occurs. The net result of using the counter, then, is to delay the 5-cycle signal to make up for the mechanical lag of the aperture and resulting time lag of the chopped waveform.

3.3.6 DIFFUSER DRIVE (SEE FIGURE 3-39)

There are four operational positions for the Diffuser Assembly: Stow, Monitor, Sun and Decontamination (see Table 3-12). Movement between these positions is accomplished by a 45° stepper motor drive initiated by ground commands. The position of the diffuser is read out by four LED photo transistor pairs in the gear assembly.

Each position has a single hole corresponding to its position as indicated in Table 3-13, where a "1" indicates a hole.

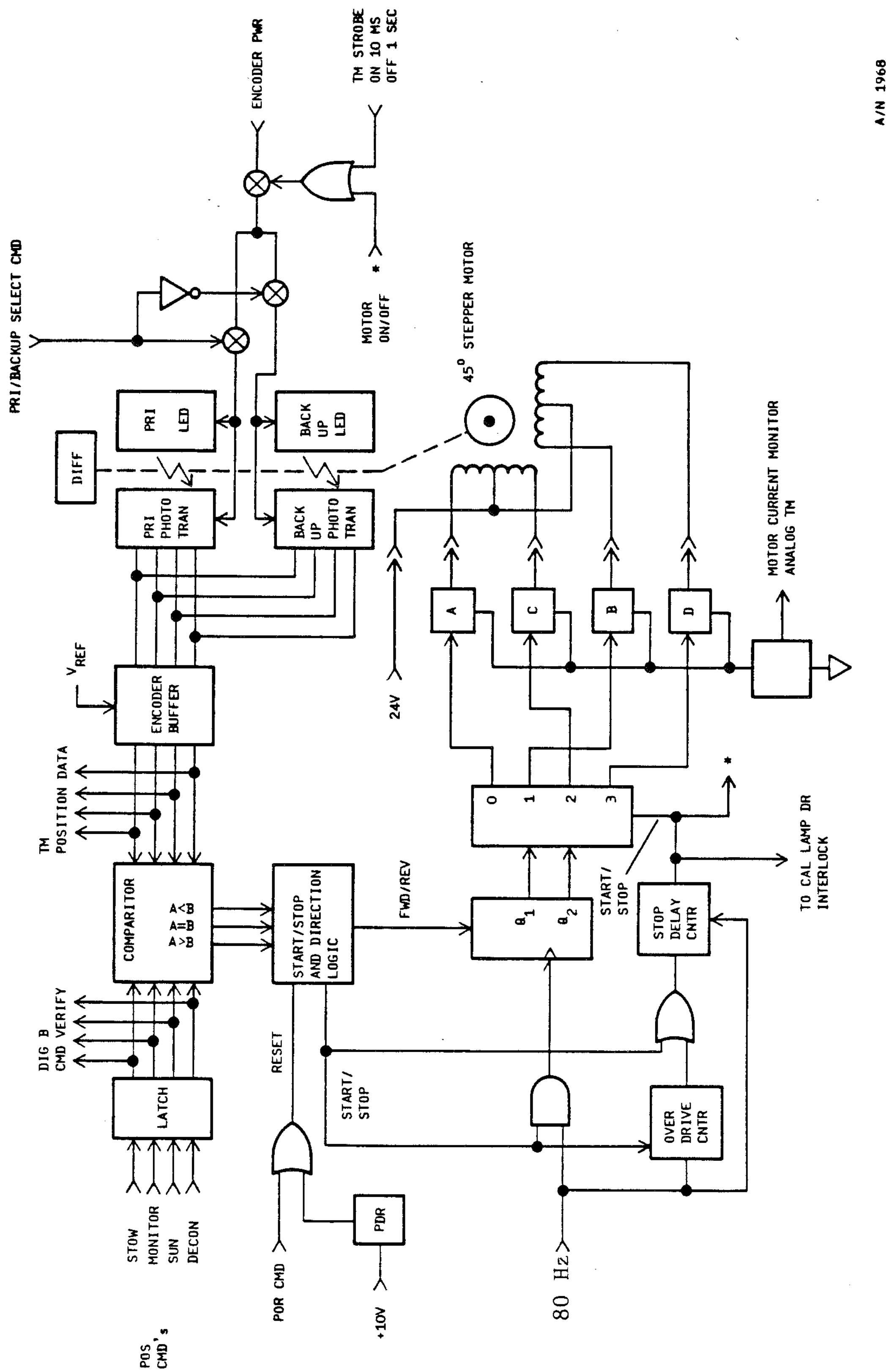

Figure 3-39
Diffuser Drive Logic

Table 3-12
DIFFUSER DRIVE ELECTRONICS CHARACTERISTICS

A. COMMANDS:

- STOW
- MONITOR
- SUN
- DECONTAMINATION
- PWR ON RESET CMD
- ENCODER PWR PRI (1) OR BACKUP (0) (LATCHED)

B. POWER REQUIREMENTS AND DUTY CYCLE:

- Logic +10 VDC, 55mW, Constant
- Motor +24 VDC, 8.8 W, Command Sequence = STOW to MON to SUN to STOW
- LED's +5 VDC, 100mW, Command Sequence = STOW to MON to SUN to STOW

  Telemetry Time = 10 msec every one second

C. DIG A TM

- Position 1 (Stow)
- Position 2 (Mon)
- Position 3 (Sun)
- Position 4 (Decon)
- Over Drive Timer
- Diffuser Position Valid YES/NO

DIG B TM

- Decon Command YES/NO
- Sun Command YES/NO
- Mon Command YES/NO
- Stow Command YES/NO
- LED Primary Backup

D. TIME TO COMPLETE COMMAND (STEP RATE = 80 Hz):

- STOW to MON, MON to STOW = 4.8 sec
- STOW to SUN, SUN to STOW = 6.4 sec
- STOW to DECON, DECON to STOW = 9 sec
- MON to SUN, SUN to MON = 1.4 sec
- MON to DECON, DECON to MON = 4.0 sec
- SUN to DECON, DECON to SUN = 2.5 sec

Table 3-13
DIFFUSER POSITION CODE

	A CMD (MSB) 8 STOW	4 CAL	2 SUN	1 OG	B POSITION (MSB) STOW	CAL	SUN	OG	DIR*	CMP OUTPUT
	0	0	0	0	0	0	0	0	STOP	A = B
NO	0	0	0	0	1	0	0	0	STOP	A < B
CMD	0	0	0	0	0	1	0	0	STOP	A < B
	0	0	0	0	0	0	1	0	STOP	A < B
	0	0	0	0	0	0	0	1		A < B
	1	0	0	0	0	0	0	0	REV	A > B
	1	0	0	0	1	0	0	0	STOP	A = B
STOW	1	0	0	0	0	1	0	0	REV	A > B
CMD	1	0	0	0	0	0	1	0	REV	A > B
	1	0	0	0	0	0	0	1	REV	A > B
	0	1	0	0	0	0	0	0	REV	A > B
CAL	0	1	0	0	1	0	0	0	FWD	A < B
CMD	0	1	0	0	0	1	0	0	STOP	A = B
	0	1	0	0	0	0	1	0	REV	A > B
	0	1	0	0	0	0	0	1	REV	A > B
	0	0	1	0	0	0	0	0	REV	A > B
SUN	0	0	1	0	1	0	0	0	FWD	A < B
CMD	0	0	1	0	0	1	0	0	FWD	A < B
	0	0	1	0	0	0	1	0	STOP	A = B
	0	0	1	0	0	0	0	1	REV	A > B
	0	0	0	1	0	0	0	0	REV	A > B
OG	0	0	0	1	1	0	0	0	FWD	A < B
CMD	0	0	0	1	0	1	0	0	FWD	A < B
	0	0	0	1	0	0	1	0	FWD	A < B
	0	0	0	1	0	0	0	1	STOP	A = B

*
FWD: STOW → DECON
REV: DECON → STOW

Since the Stow position is the most used position, its "1" bit is chosen as the Most Significant Bit (MSB).

When a position command is received, it is latched and compared to the present position of the diffuser. Referring to Table 3-13, the output of the comparator sets the direction of the motor.

The position command also triggers a one shot whose output pulse enables the position sensor power, motor drive logic, 80 Hz clock, and the overdrive counter, and disables the calibration lamp drive (see Figure 3-41).

The motor will drive until the desired position is decoded and compared to the command. If equal, (A=B), the motor stop delay counter is enabled. This delay counter allows the motor to drive a predetermined number of steps before stopping. The delayed stop signal also turns off the sensor power, disables the 80 Hz clock, resets the overdrive counter and enables the Cal Lamp Drive. See timing diagram, Figure 3-41.

The overdrive counter is programmed to stop the motor in the event a position is not reached due to some anomaly. The time set is longer than the longest (Stow-Decon) drive period (approximately 36 sec). If a position is not reached and the overdrive timer times-out and stops the motor, the motor direction will be set to "reverse" since the position code will be all zeros (A>B). A new command is required to correct the situation and will drive the motor in reverse until a position is reached. Now a decision is made by the comparator to stop, go forward or reverse to the command position.

There is a primary (A) and backup (B) set of LED phototransistor pairs for each position of the diffuser. A latched command (1=Pri and O=Backup) selects which is to be used. Power-on-reset will automatically set the primary. The +5V LED power and +10V phototransistor power is turned on when a valid position command is received, and off when the motor stops.

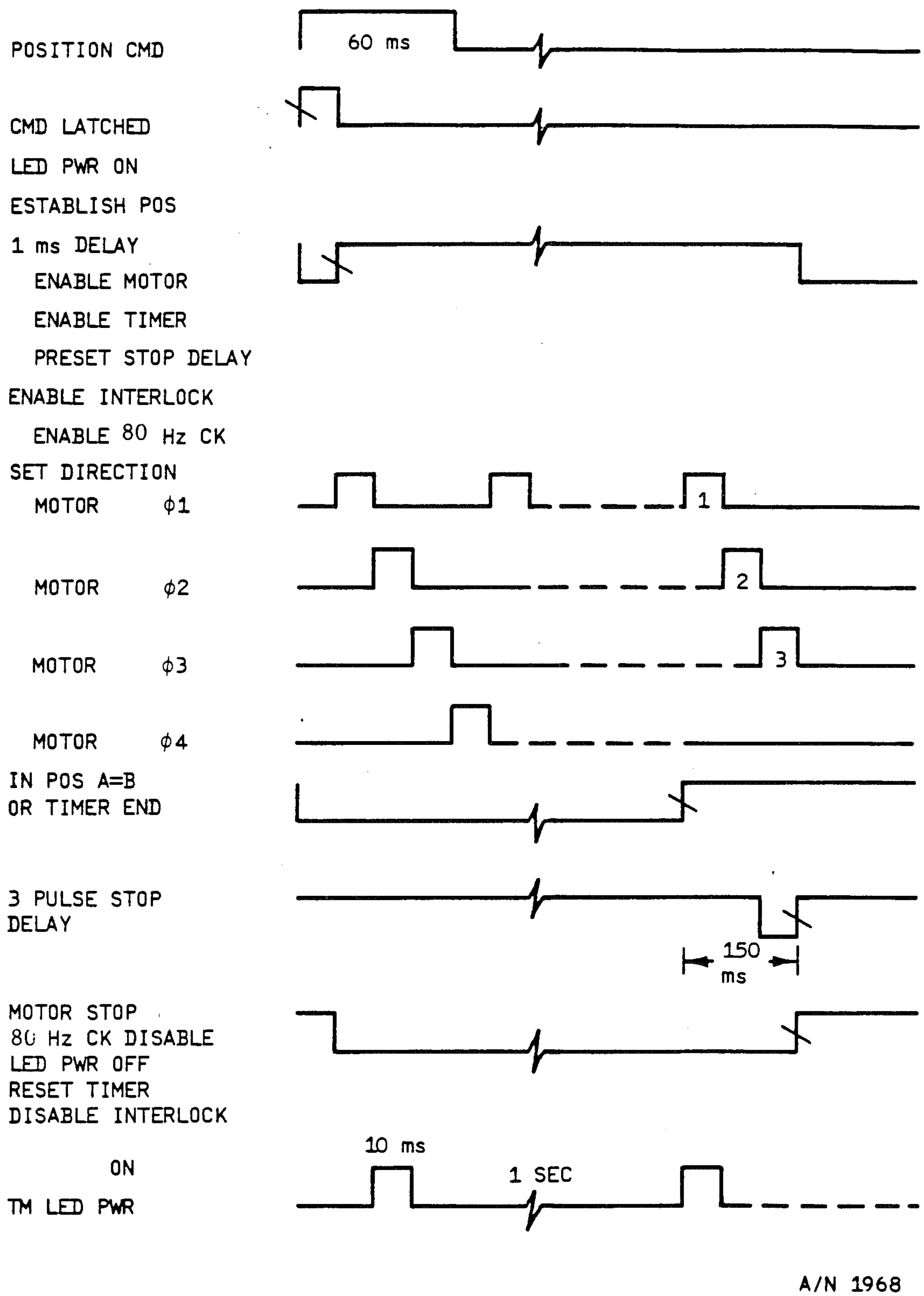

Figure 3-41
Diffuser & Calibration Lamp Drive Timing Diagram

There is also a telemetry strobe that turns power on for 10 ms once per second to read out the present position. The actual motor drive circuitry consists of a two bit counter driving a binary to decimal decoder. The first four lines (0,1,2,3) are used to drive four VMOS power FETs. The power FETs are capable of driving the motor windings at 0.5 amp. See Table 3-14.

Table 3-14
DIFFUSER DRIVE PERFORMANCE

•	Position Accuracy	±0.4° Sun Position, ±1° Others	
•	Position Repeatability	±0.25°	
•	Type of Motor	45° PM Stepper	
		60 Ω per Winding	
		Size 15	
		24 Volt DC	
•	Gear Reduction	188:1	
•	Step Size	0.25°	
•	Step Frequency	80 STEPS PER SECOND	
•	Number of Steps	STOW to CAL	396 steps
		STOW to SUN	513 steps
		STOW to OUTGAS	719 steps
•	Time Required	STOW to CAL	4.8 sec
		STOW to SUN	6.4 sec
		STOW to OUTGAS	9.0 sec

The power-on-reset signal is generated when power is turned on or by the POR command. It will initialize the system by generating a motor stop signal, reset the overdrive counter and motor stop delay counter, set encoder power to primary. There is an interlock system between the diffuser and cal lamp drives to prevent a mechanical interference problem. The cal lamp must be in the open or closed position before the diffuser can operate and, the diffuser must be stopped in a valid position before the cal lamp can operate.

3.3.7 CALIBRATION LAMP POSITION DRIVE

There are two operational positions for the Calibration Lamp Assembly: Closed and Open (see Figure 2-4, Section 2). Movement between these two positions is accomplished by a 90° permanent magnet stepper motor and is initiated by ground command. The drive electronics for the stepper motor is located in the ELM assembly. The cal lamp drive logic is interlocked with the diffuser drive logic to prevent both from operating at the same time. See Figure 3-42 and Table 3-15.

Each position has a single hole corresponding to its position where a "1" indicates a hole.

Since the Open position is the most used position, its "1" bit is chosen as the MSB.

When the Open or Close command is received, it is latched and compared to the present position of the cal lamp. The output of the comparator sets the direction of the motor.

The command also triggers a one shot whose output pulse enables the position sensor power, motor drive logic, 20 Hz clock, and the overdrive counter, and disables the Diffuser Drive (see Figure 3-41).

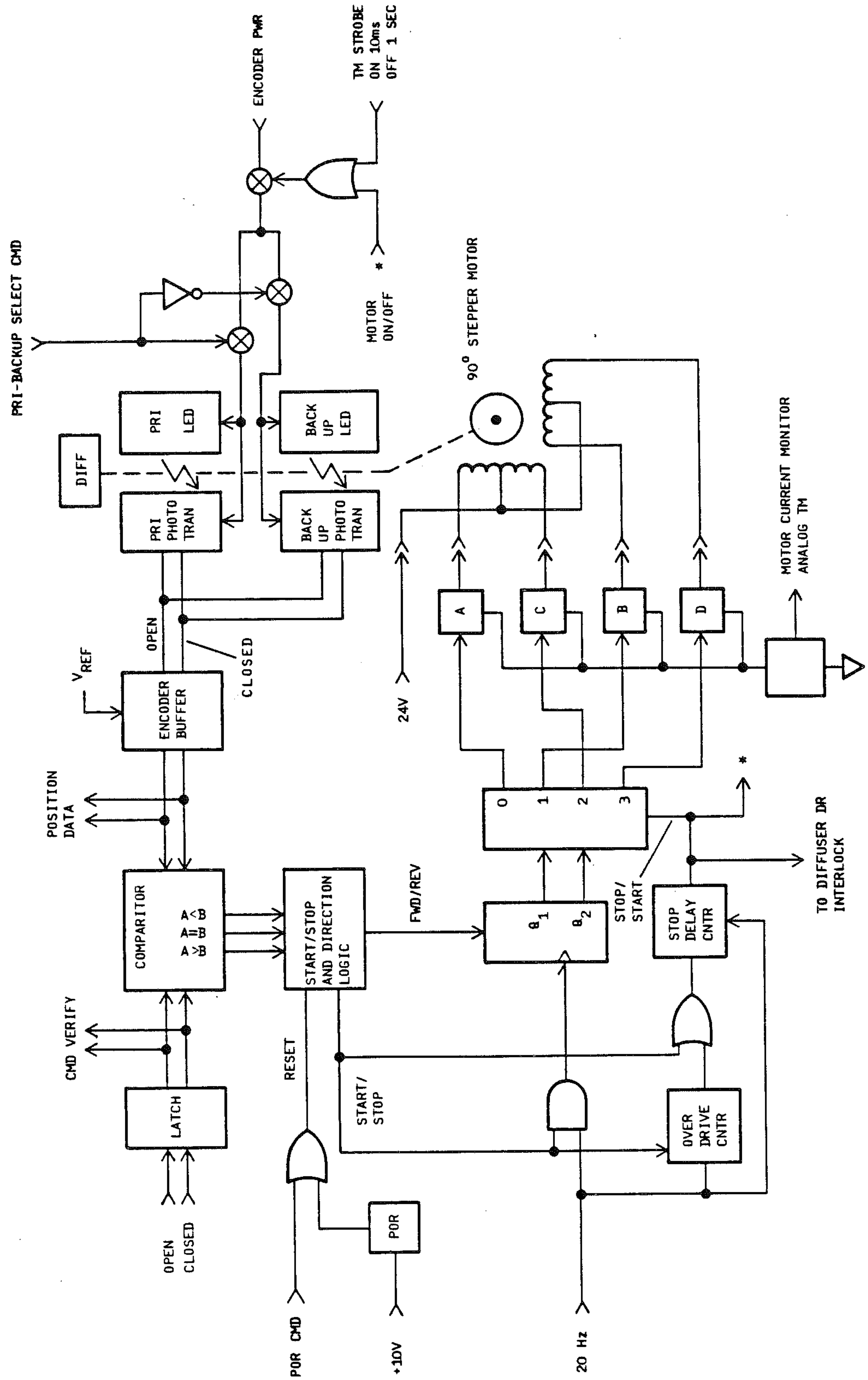

Figure 3-42
Calibration Lamp Drive Logic

Table 3-15

CALIBRATION LAMP POSITION DRIVE ELECTRONICS CHARACTERISTICS

A. COMMANDS:

- Closed
- Open
- Sensor Pwr A or B
- Power on Reset CMD (Latched)

B. POWER REQUIREMENTS AND DUTY CYCLE:

- Logic +10 VDC, 55 mW, Constant
- Motor +24 VDC, 3.6 W, Command Sequence = Open to Close to Open during wavelength calibration cycle
- LED's +5 VDC, 50 mw, Command Sequence = Open to Close to Open during wavelength calibration cycle; Telemetry Time = 10 msec every one second.

C. DIGITAL A TELEMETRY:

- Closed
- Open
- Lamp Position Valid YES/NO
- Overdrive Timer
- Motor Current Monitor

DIGITAL B TELEMETRY:

- Open/Closed Command
- LED Primary/Backup

D. TIME TO COMPLETE COMMAND (STEP RATE = 20 Hz):

- Closed to Open = 4.5 sec
- Open to Closed = 4.5 sec

The motor will drive until the desired position is decoded and compared to the command. If equal, (A=B), the motor stop delay counter is enabled. This delay counter allows the motor to drive a predetermined number of steps before stopping. The delayed stop signal also turns off the sensor power, disables the 20 Hz clock, resets the overdrive counter and enables the Diffuser. See timing diagram, Figure 3-41.

The overdrive counter is programmed to stop the motor in the event a position is not reached due to some anomaly. The time set is longer than the (Open-Closed) drive period (approximately 5 sec.). If a position is not reached, the overdrive timer times-out and stops the motor.

Table 3-15 is a summary of the operating characteristics of the electronics for the Calibration Lamp Position Drive. Table 3-16 contains performance data for the Calibration Lamp Drive.

There is a primary (A) and backup (B) set of LED phototransistor pairs for each position. A latched CMD (1=Pri and O-Backup) selects which is to be used. Power-on-reset will automatically set the primary.

The +5V LED power and +10V phototransistor power is only turned on when a valid position command is received, and off when the motor stops.

There is also a telemetry strobe that turns power on for 10 ms once per second to read out the present position.

The actual motor drive circuitry consists of a bit counter driving a binary to decimal decoder. The first four lines (0,1,2,3) are used to drive four VMOS power FETs. The power FETs are capable of driving the motor windings at 0.18 amp.

The power-on-reset signal is generated when power is turned on or by the POR command. It will initialize the system by generating a motor stop signal, reset the overdrive counter and motor stop delay counter, and set encoder power to primary. There is an interlock system between the diffuser and cal lamp drives to prevent a mechanical interference problem. The cal lamp must be in the open or closed position before the diffuser can operate and, the diffuser must be stopped at a valid position before the cal lamp can operate.

Table 3-16
CALIBRATION LAMP DRIVE PERFORMANCE

• TYPE OF MOTOR	90° PM Stepper 150 Ω Per Winding Size 11 24 Volt DC
• GEAR REDUCTION	60:1
• STEP SIZE	1.5°
• STEP FREQUENCY	20 Steps Per Second
• NUMBER OF STEPS	90 Steps
• TIME REQUIRED	4.5 Seconds

3.3.8 DATA HANDLING

The data handling block diagram is shown in Figure 3-43. Frequency counters are provided for the electrometer and the housekeeping voltage-to-frequency converters. The counters synchronously demodulate and integrate the modulated frequencies by counting up while the chopper aperture is open and counting down while the aperture is closed. In this manner, the background signal is subtracted from the desired signal. The integration time is 1.25 seconds in the discrete wavelength calibrate modes and 0.1 second in the sweep mode.

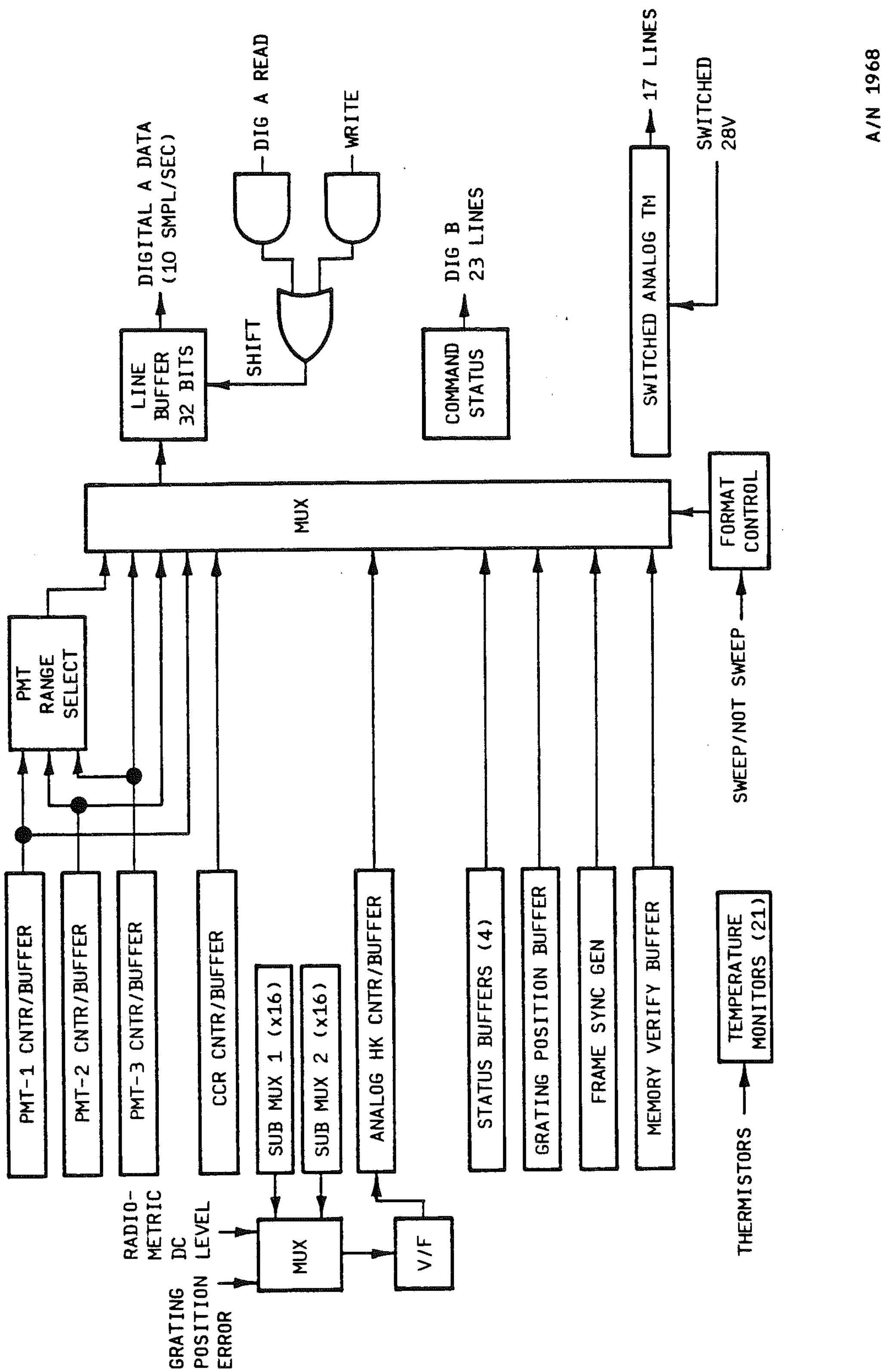

Figure 3-43
Block Diagram of Data Handling System

The contents of each counter are buffered after each integration period and reset for a new integration. The buffered data as well as submultiplexed digital housekeeping data is multiplexed out to the 320-bit output data register where it is read out by the TIP. Logic is provided for proper PMT range selection when in the sweep mode. Analog housekeeping and digital housekeeping are multiplexed into a serial data stream and loaded into the 320-bit register.

Multiplexing is controlled by fixed format logic which utilizes timing and synchronization signals derived from the TIP interface. The output data register is completely loaded one per second at a high clock rate, in between read-out periods. Data is read out by the TIP every 1/20 second in 32-bit groups.

3.3.8.1 Digital A Telemetry Lists and Formats

The SBUV/2 format consists of 20, 16-bit words telemetered every second, for a total data rate of 320 bps. This format is changed only in the sweep mode to accommodate higher monochromator data rates. Only two formats are used as shown in Table 3-17: a discrete mode format and a sweep mode format. Word 1 column contains the CCR data and all housekeeping data, and remains fixed in both discrete and sweep modes. Word 2 is devoted to PMT data, containing the data from all three ranges and the cathode monitor data. This word is switched in the sweep mode to read only the selected PMT Range Data.

The 16 channel analog submultiplexer and the digital status register, both located in the ELM, provide ample capacity for housekeeping and status. Data assignments for the analog submultiplexer are listed in Table 3-18. The analog sub-mux data consists of 8-bit samples which are packed two per 16-bit word. Data assignments for digital status words are listed in Table 3-19.

Table 3-17
DIGITAL A DATA FORMATS

Discrete Modes	Word 1	Word 2
Line 0	Status 1	PMT Range 1 Data
Line 1	Status 2	PMT Range 2 Data
Line 2	Analog Sub Mux	PMT Range 3 Data
Line 3	Memory Verify	Spare
Line 4	Status 3	Spare
Line 5	Status 4	Spare
Line 6	Grating Position	Spare
Line 7	CCR Data	Spare
Line 8	Radiometric DC Level	Spare
Line 9	Frame Sync Code	Spare
Sweep Modes	**Word 1**	**Word 2**
Line 0	Status 1	PMT Selected Range Data
Line 1	Status 2	PMT Selected Range Data
Line 2	Analog Sub Mux	PMT Selected Range Data
Line 3	Memory Verify	PMT Selected Range Data
Line 4	Status 3	PMT Selected Range Data
Line 5	Status 4	PMT Selected Range Data
Line 6	Grating Position	PMT Selected Range Data
Line 7	CCR Data	PMT Selected Range Data
Line 8	Radiometric DC Level	PMT Selected Range Data
Line 9	Frame Sync Code	PMT Selected Range Data

NOTES:

1. All words 16 bits; analog channels are encoded with two, 8-bit samples per 16-bit word
2. Rate is ten lines per second

Table 3-18
DIGITAL A ANALOG SUB-MULTIPLEXER DATA ASSIGNMENTS

Channel No.	Function Name	Channel No.	Function Name
1A	Chopper Motor Current	1B	Spare
2A	Diffuser Motor Current	2B	Diffuser Plate Temp (1)
3A	HVPS Volts	3B	SM Baseplate Temp (2)
4A	Thermistor Bias	4B	25V Power Volts
5A	Cal Lamp Temp (1)	5B	15V Servo Volts
6A	ECAL Ref	6B	-15V Servo Volts
7A	15V Sensors Volts	7B	CCR Diode Temp (3)
8A	-15V Sensors Volts	8B	SM Differential Temp Y-axis (4)
9A	24V Motor Volts	9B	SM Differential Temp Z-axis (4)
10A	5V LED Volts	10B	Diff. Ref. Temp Z-axis
11A	10V Logic Volts	11B	Diff. Ref. Temp Y-axis
12A	Calibration Lamp Current	12B	PMT Cathode Temp (3)
13A	Spare	13B	Spare
14A	Spare	14B	Chopper Phase Error
15A	Spare	15B	Spare
16A	Lamp Motor Current	16B	Spare

NOTES:
(1) 0 to 80°C
(2) -15 to 45°C
(3) -5 to 35°C
(4) ± 5°C

Table 3-19
DIGITAL A STATUS WORDS

Status Word 1

BIT	USE	LOGIC 1 (GND)	STATE 0 (+)
1	Master Power ON/OFF	OFF	ON
2	Discrete Mode/Sweep Mode Format	SWEEP	DISCRETE
3	Sweep Mode Major Frame Word 2^2	True	False
4	Sweep Mode Major Frame Word 2^1	True	False
5	Sweep Mode Major Frame Word 2^0	True	False
6	Retrace	ON	OFF
7	16 Sec (2^2)	True	False
8	8 Sec (2^1)	True	False
9	4 Sec (2^0)	True	False
10	Command Sequence (2^2)	True	False
11	Command Sequence (2^1)	True	False
12	Command Sequence (2^0)	True	False
13	Range ID B-L0	ON	OFF
14	Range ID A-L0	ON	OFF
15	Range ID B-L1	ON	OFF
16	Range ID A-L1	ON	OFF

Status Word 2

BIT	USE	LOGIC 1	STATE 0
1	Range ID B-L2	ON	OFF
2	Range ID A-L2	ON	OFF
3	Range ID B-L3	ON	OFF
4	Range ID A-L3	ON	OFF
5	Range ID B-L4	ON	OFF
6	Range ID A-L4	ON	OFF
7	Range ID B-L5	ON	OFF
8	Range ID A-L5	ON	OFF
9	Range ID B-L6	ON	OFF
10	Range ID A-L6	ON	OFF
11	Range ID B-L7	ON	OFF
12	Range ID A-L7	ON	OFF
13	Range ID B-L8	ON	OFF
14	Range ID A-L8	ON	OFF
15	Range ID B-L9	ON	OFF
16	Range ID A-L9	ON	OFF

Status Word 3

BIT	USE	LOGIC 1	STATE 0
1	R1 Over/Range	O/R	On Scale
2	R2 Oyer/Range	O/R	On Scale
3	R3 Over/Range	O/R	On Scale
4	CCR Over/Range	O/R	On Scale
5	Code Address A	1	0
6	Code Address B	1	0
7	Code Data 1	1	0
8	Code Data 2	1	0
9	Code Data 3	1	0
10	Code Data 4	1	0
11	Code Data 5	1	0
12	Code Data 6	1	0
13	Discrete Sun Enable	ON	OFF
14	Sweep Sun Enable	ON	OFF
15	λ Cal Enable	ON	OFF
16	Spare	Always Off	

Status Word 4

BIT	USE	LOGIC 1	STATE 0
1	Diffuser Stow Pos	Stow	Not Stowed
2	Diffuser Monitor Pos	Monitor	Not Monitor
3	Diffuser Sun Pos	Sun	Not Sun
4	Diffuser Decontam Pos	Decontam	Not Decontam
5	Discrete Mode	ON	OFF
6	Sweep Mode	ON	OFF
7	Diffuser Pos Valid	Valid	Not Valid
8	Diffuser Timer	Time Out	Not Time Out
9	Calib Lamp Open	OPEN	NOT OPEN
10	Calib Lamp Closed	CLOSED	NOT CLOSED
11	Calib Lamp Pos Valid	Valid	Not Valid
12	Calib Lamp Timer	Time Out	Not Time Out
13	Cal Mode	ON	OFF
14	Position Mode	ON	OFF
15	Grating Fix/Flex	FIX	FLEX
16	Grating Index Found	Found	Not Found

3.3.8.2 Analog Telemetry

The telemetry consists of 17 conditioned analog housekeeping monitors wired directly to the TIP. These channels are listed in Table 3-20. These provide back-up monitor channels both while the instrument is on and with the instrument power off. Critical channels are powered with normal instrument power off, for the 28V Analog Telemetry Bus. The peak current drawn from this bus is limited to 10 mA. This bus is regulated in the ELM so measurements are not affected by line voltage changes.

3.3.8.3 Temperature Control and Measurement

Temperature controls consist of ON/OFF commands for the diffuser outgassing heater and the Sensor Module baseplate heater. The passive thermal design controls the temperature of all electronics boxes to within a few degrees of the spacecraft deck (0 to +30°C). Temperature measurements are made with thermistors, which are curve-matched to 0.5%. The circuit consists of a precision resistor divider using resistors with a tolerance of ±0.1%. The ranges covered are listed in Tables 3-18 and 3-20. Temperature monitors are calibrated in counts-versus-temperature in °C. Those read out as analog data are also calibrated in volts versus temperature. Temperature measurements are digitized to eight bits to obtain 0.6°C typical resolution.

3.3.8.4 Digital B Telemetry

The status of each command is verified with 22 lines to Digital B Telemetry as listed in Table 3-21.

3.3.9 LOW VOLTAGE POWER SUPPLY

The Low Voltage Power Supply (LVPS) uses a DC-DC converter with regulators on some outputs as shown in Figure 3-44. This unit provides all of the regulated low voltages for the instrument including the high voltage power supply, the calibration lamp power supply, and the electrometer, all located in the Sensor Module, and all of the electronics in the Electronics and Logic Module.

Additional regulation was added to the LVPS of FM2 and FM3 so that the ± 25 V to the high voltage supply would be better regulated. Ripple on the 25V line coupled into the ± 15 volts supply to the cathode current monitor which is generated in the high voltage supply. The result is a marked improvement in the R3 linearity at low count rates.

Table 3-20
ANALOG TELEMETRY LIST

1. *SM Baseplate Temp #2 (-15 to +45)
2. SM Shroud Temp (-30 to +80)
3. Depolarizer Housing Temp (-15 to +45)
4. HVPS Temp (-15 to +45)
5. *Diffuser Plate Temp #2 (0 to +80)
6. Chopper Motor Temp (-15 to +45)
7. Grating Motor Temp (-15 to +45)
8. Diffuser Motor Temp (-15 to +45)
9. Cal Lamp Motor Temp (-15 to +45)
10. Electrometer Temp (-15 to +45)
11. Cal Lamp Power Supply Temp (-15 to +45)
12. Diffuser Radiator Temp (-15 to +45)
13. ELM Temp (-15 to +45)
14. LVPS Temp (-15 to +45)
15. Diffuser Heater Current
16. Cal Lamp Heater Current
17. **28V Main Power Voltage

*Powered from the 28V switched Telemetry Bus.

**Senses the 28V Main Power Bus prior to the instrument ON/OFF relay.

Table 3-21
DIGITAL B TELEMETRY DATA ASSIGNMENTS

No.	Telemetry Point Name	State* Logic "1"	State* Logic "0"
1.	**Instrument Power On/Off	ON	OFF
2.	**Discrete Cmd Yes/No	Yes	No
3.	**Sweep Cmd Yes/No	Yes	No
4.	**Cal Cmd Yes/No	Yes	No
5.	**Position Cmd Yes/No	Yes	No
6.	HV On/Off	ON	OFF
7.	Motor Power On/Off	ON	OFF
8.	Lamp On/Off	ON	OFF
9.	Lamp Disabled/Enabled	Enable	Disable
10.	**Lamp Assy Open Cm'd/ Close Cm'd	Open Cmd	Close Cmd
11.	HV Enabled/Disabled	Enabled	Disabled
12.	**Diff. Stow Cmd Yes/No	Yes	No
13.	**Diff. Mon. Cmd Yes/No	Yes	No
14.	**Diff. Sun Cmd Yes/No	Yes	No
15.	**Diff. Decontam Cmd Yes/No	Yes	No
16.	Ch Enc Sens Pri/Bkup	Pri	Bkup
17.	Grat Enc Sen Pri/Bkup	Pri	Bkup
18.	Diff Pos'n Sens Pri/Bkup	Pri	Bkup
19.	Lamp Pos'n Sens Pri/Bkup	Pri	Bkup
20.	**Grating Drive Fix/Flex	Fix	Flex
21.	Baseplate Htr On/Off	ON	OFF
22.	Diffuser Htr On/Off	ON	OFF

*Logic "1" is a "True" of "Zero Voltage" state.
**Bit set indicates last command received. Command Action may or may not have been executed.

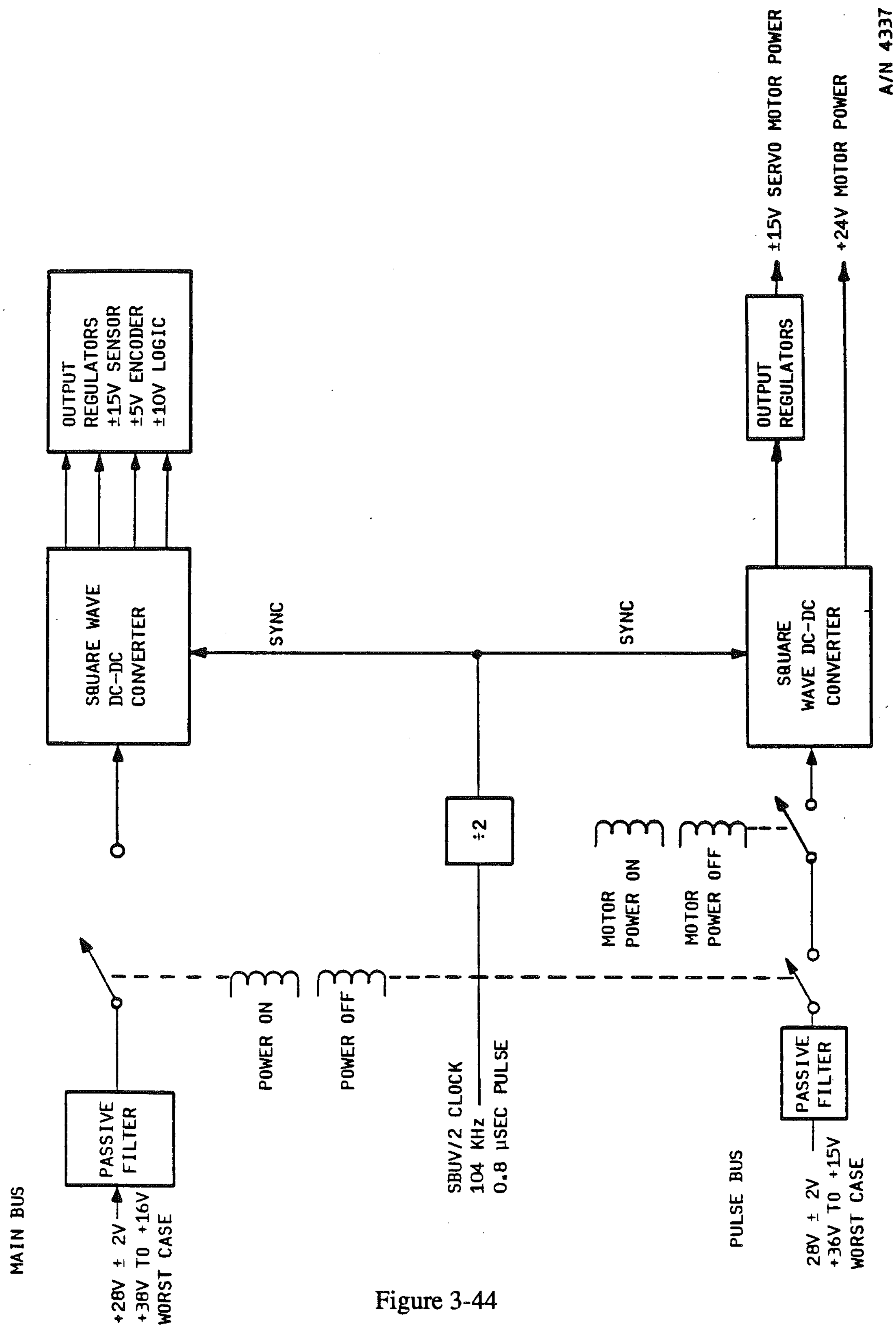

Figure 3-44
Block Diagram of Low Voltage Power Supply

The overall power estimate for the instrument is shown in Table 3-22. See Table 3-24 and 3-25 for actual measurements for actual power measurements and calculations for S/N005. Operating characteristics of the Low Voltage Power Supply are as follows:

1. Regulated Outputs. +5V LED, ± 15V Data, ± 15V Servo, +10V Logic, (see Table 3-23).

Table 3-23
LOW VOLTAGE POWER SUPPLY OUTPUTS

Voltage	Load Current Nominal	Peak	Regulation	Ripple	Tolerance
± 15V Sensor	50 mA	150 mA**	± 1%	25 mV	± 0.25V
± 15V Servo (Pulse Bus)	20 to 200 mA	400 mA*	± 1%	25 mV	± 0.25V
+10V Logic	40 mA	150 mA**	± 2%	50 mV	± 0.50V
+24V Motors (Pulse Bus)	0 to 20 mA	500 mA*	± 10%	50 mV	± 1.0V
+5V Encoders	120 mA	120 mA	± 10%	50 mV	± 0.25V
+25V HVPS and CLPS	200 mA	270 mA	±1%	25 mV	±0.25V

* Worst case is 400 mA at +15V and -15V simultaneously with 500 mA @ +24V
** Worst case is both 75 mA

2. Output Current Limiters. These are provided on all outputs except the 24V motor power. Set at >150% peak load.

3. Input Power Allocation. 12W orbit average, 26W peak (this includes main bus and pulse bus power, but does not include 10V I/F and 28V switched TM bus power).

4. Main Bus Voltage. 28V ± 2.0 VDC; transients are +16V to +38V during which outputs do not exceed ± 10% nominal.

Table 3-22
POWER ESTIMATES

ITEM	PEAK POWER[1] (Watts)		NOMINAL ORBITAL AVERAGE[2] (Watts)		WORST CASE ORBITAL AVERAGE[3] (Watts)	
	BUDGET	ESTIMATE	BUDGET	ESTIMATE	BUDGET	ESTIMATE
CHOPPER MOTOR	1.5	2.9	1.2	0.91	1.5	2.9
TEMPERATURE MONITORS	1.0	0.4	0.8	0.4	0.8	0.4
ELECTROMETER	1.0	0.6	0.8	0.6	0.8	0.6
PMT HIGH VOLTAGE SUPPLY	0.6	0.93	0.6	0.93	0.6	0.93
BLEEDER STRING	1.0	0.12	1.0	0.12	1.0	0.12
CATHODE MONITOR	1.0	0.5	0.8	0.5	0.8	0.5
DATA HANDLING AND TIMING	1.1	0.5	0.9	0.5	0.9	0.5
LOW VOLTAGE POWER SUPPLY LOSSES	5.6	5.6	3.2	3.32	3.2	3.32
GRATING MECHANISM DRIVE	4.2	1.9	1.54	1.25	1.54	1.25
CALIBRATION LAMP	4.0	0.4	0.34	0.12	0.34	0.12
CALIBRATION LAMP SUPPLY LOSS	3.0	0.5	0.26	0.14	0.26	0.14
DIFFUSER MECHANISM DRIVE	10.6[1]	9.5[1]	0.008	0.061	0.008	0.061
CALIBRATION LAMP MECHANISM DRIVE	4.8[1]	4.0[1]	0.006	0.013	0.006	0.013
CONTINGENCY	-8.6	2.15	0.68	3.14	0.25	1.15
TOTAL BUDGET:	26.0	20.6	12.0	12.0	12.0	12.0

1. The peak power was computed assuming that the diffuser mechanism and the calibration lamp mechanism are electrically interlocked and cannot be operated simultaneously.

2. These figures represent a 24 hour orbital average which contains one wavelength calibration cycle followed by operation in the discrete mode for the remainder of the time.

3. The worst case orbital average occurs during a cold orbit and contains a wavelength cal and diffuser monitor auto sequence followed by operation in the discrete mode for the remainder of the orbit.

A/N 4337

5. Pulse Bus Voltage. 28V ± 2.0 VDC; transients are 15V to 36V during which outputs do not exceed ± 15% nominal.

6. Monitors. Voltage monitors are provided on all outputs. These monitors are conditioned to zero to +5.12V.

7. DC/DC Converter Frequency. This will be synchronized to a clock signal of 104 KHz. The converter frequency will free run if the synchronization signal fails.

8. Transient Recovery. The Low Voltage Power Supply will recover from an input voltage transient within three minutes.

9. Reverse Polarity. Input is protected against reverse polarity.

10. Input Current Limit. The input current is not limited in the instrument. The spacecraft fuse provides short circuit protection.

11. Feedback to main Bus. Does not exceed:
    - Two percent (2%) steady state ripple
    - 2.0 mA per microsecond rise fine
    - Peak Current ≤150% of steady state
    - ≤1 amp motor start-up transients

12. Ground Isolation. ≥10 megohms to case and ≥1 megohm between power return and signal ground.

13. Temperature Range. -10°C to 40°C.

14. Commands. Master Power On applies power to the main power and pulse power converters. Master Power Off removes all power from the instrument except heater power. Motor Power On/Off controls the pulse power. Heater Power On/Off controls heater power.

15. Electromagnetic Compatibility and Susceptibility to Interference. EMI filters, beads, and other passive filtering techniques are used to minimize conducted emissions and to reduce susceptibility of the instrument to interference on the spacecraft power and return lines. All switching regulators, DC-DC converters and other noisy circuitry are shielded to minimize radiated emission. The power supply conforms to the EMI requirements of Section 3.4.2 of Specification IS-2295548.

The Flight Models 2 and 3 are located on the TIROS spacecraft in a different position from the Flight Model 1 instrument on NOAA-9. Flight Model 4 was placed next to the 137 MHz dipole antenna which caused severe Range 1 noise problems, FM2 and 3 will be located similarly. To prevent radiation coupling into the SBUV/2 wiring harness and electronic boxes the instruments are provided with an EMI shield of wire mesh sealed all around with conductive velcro. The shield is effective in reducing the noise to acceptable levels.

16. Transient Load Currents.

- Main Bus: Limits current transients to ≤150 percent of steady state for 30 msec maximum, and rate of change to 20 mA per microsecond.

- Pulse Bus: Limits current transients to ≤1 amp for one second and rate of change to 30 mA per microsecond.

Table 3-24
POWER MEASUREMENTS (S/N003 and S/N004)

MODE OR PARAMETER	+28V MAIN BUS		+28 MAIN BUS		+28V TLM BUS		+10V I/F BUS	
	AVE. POWER WATTS	PEAK CURRENT AMP	AVE. POWER WATTS	PEAK CURRENT AMP	AVE. POWER WATTS	PEAK CURRENT AMP	AVE. POWER WATTS	PEAK CURRENT AMP
Requirement (Maximum)	12.0	0.93	*	*	0.092	0.0033	0.080	0.01
Discrete Mode*	6.3	0.235	4.6	0.62	0.092	0.0033	0.080	0.008
Sweep Mode*	6.3	0.235	3.9	0.275	0.092	0.0033	0.080	0.008
Wavelength Cal Mode*	6.3	0.235	4.6	0.62	0.092	0.0033	0.080	0.008
Position Mode	6.3	0.235	3.5	0.14	0.092	0.0033	0.080	0.008
Move-Diffuser	0	0	8.8	0.325	0.092	0.0033	0.080	0.008
Move Cal Lamp	0	0	3.8	0.140	0.092	0.0033	0.080	0.008
Cal Lamp on	3.22	0.115	0	0	0.092	0.0033	0.080	0.008
HVPS ON	1.0	0.035	0	0	0.092	0.0033	0.080	0.008

* Noted Requirement is for Main Bus PLUS Pulse Load Bus.

Section 4
CALIBRATION

4.1 SCOPE

The objective of the calibration program is to achieve a state-of-the-art calibration of the SBUV/2 instrument including response to spectral radiance, response to spectral irradiance, ratio of radiance to irradiance responses, and the temperature dependence of response. Continuity of this calibration is maintained throughout the series of operational instruments.

Figure 4-1 shows the overall calibration flow. The calibration related activities have been lifted out of the overall integration and test plan to clarify the calibration process and delineate the logic flow of the various tests.

4.2 CALIBRATION PROGRAM

The spectral efficiency of each optical component is measured by the suppliers in the course of their acceptance testing. This demonstrates that specifications have been met. Also, it allows prediction of the eventual spectral transmittance of the system. If there is a need, the component efficiency tests can be repeated at BACG. Monitor mirrors accompany the instrument optics throughout the program and are periodically tested for spectral reflectivity.

At the subsystem level of assembly, additional procedures and tests are carried out that support the final calibration. The depolarizer is tested by measuring the residual polarization of initially polarized light after it has passed through the depolarizer. System linearity and dynamic range tests as well as wavelength calibration, bandpass, instrument profile and spectral resolution tests are done before the calibration lamp and diffuser assemblies are installed.

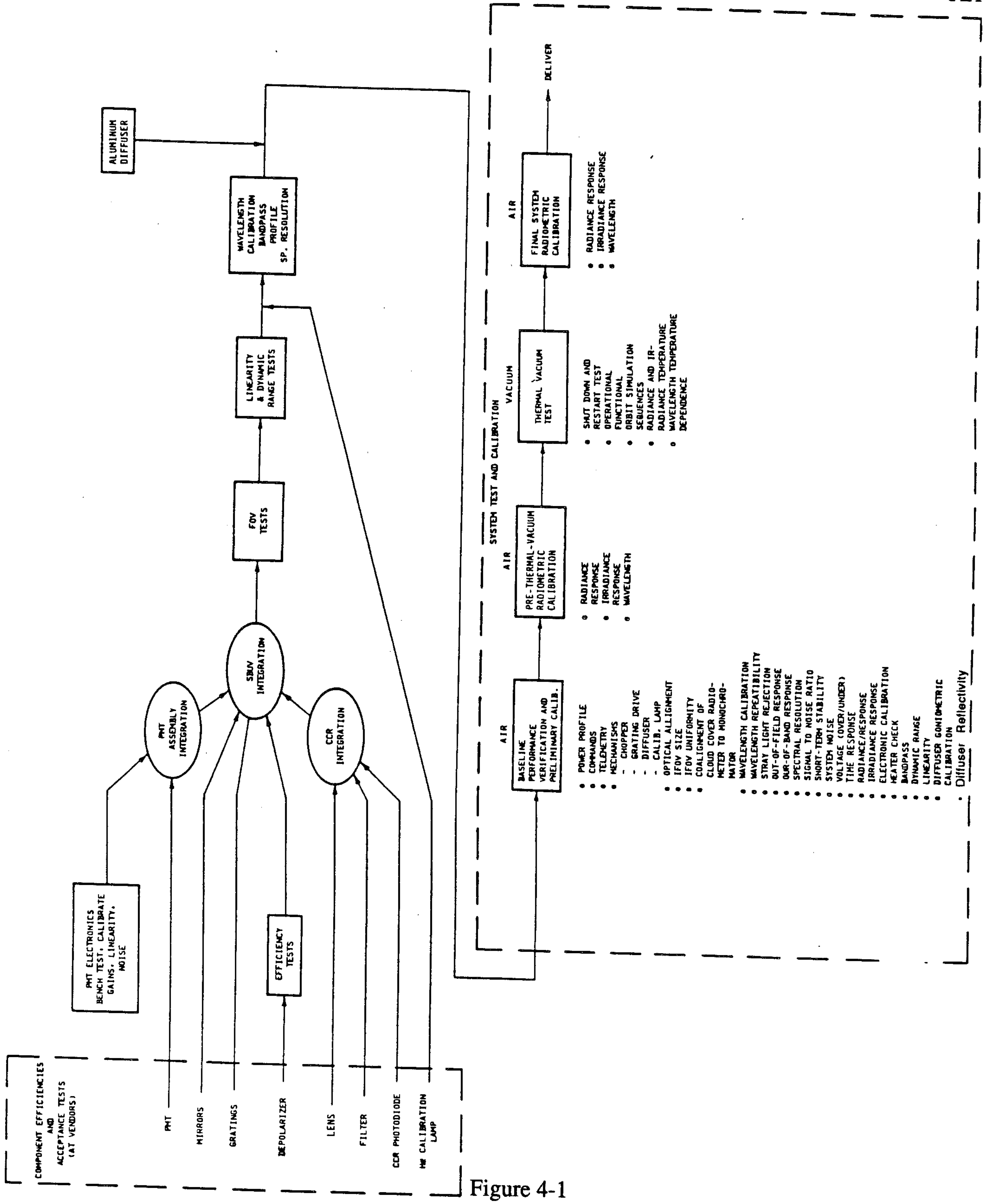

Figure 4-1
SBUV/2 Calibration Plan

After integration of the complete instrument, but before formal verification testing begins, an integration test is run during which final adjustments are made. During this process, the optical alignment is measured and adjusted (if necessary) and all the field-of-view (FOV) related tests are performed, since the same fixture is used for all field-of-view related tests. Field-of-view tests include size, shape, uniformity, and pointing of both the monochromator and CCR fields. Stray light rejection, response time, and power profile tests are also conducted at this stage. Finally, the first radiance/irradiance response tests are run in air, establishing a baseline for all subsequent tests.

A series of diffuser reflectivity tests are run to ensure measurements performed in flight will meet specifications.

Out of band rejection and stray light tests are done in sunlight using the FOV fixture. Parts of the same fixture are used to map the goniometric response of the instrument diffuser. Weight, center of gravity, and dimensional checks are made before the start of environmental testing.

After each vibration test, the radiance/irradiance responses in air are measured and the alignment and field-of-view checks are made. The preliminary spectral radiometric calibration is done just prior to thermal-vacuum testing, on the Primary Test Fixture (PTF), in air. During thermal vacuum, the spectral radiometric calibration is measured at the required temperature plateaus down to 160nm using the Vacuum Test Fixture (VTF). The calibration transfer standard sources are returned to NBS for recalibration as necessary to allow the closest possible interpolation between standardizations. During thermal vacuum testing, the wavelength calibration is monitored for changes. A final radiometric calibration in air completes the instrument calibration.

4.2.1 Deleted

4.2.2 FIXTURING FOR SYSTEM CALIBRATION

The arrangement for full system radiometric calibration is shown in Figure 5-6, Section 5. Since radiometric calibrations and response verifications are done in both air and during the thermal vacuum test, there are two fixtures. The Primary Test Fixture is located in a clean room and has no vacuum chamber. The Vacuum Test Fixture shown in Figure 5-5 is used during vacuum procedures.

The two fixtures are essentially identical except for the vacuum chamber. The fixtures locate the instrument, a collimating mirror and the light sources relative to each other accurately and repeatably. Light from the source is collimated by the mirror and illuminates the instrument diffuser at the proper angle. When the instrument diffuser is stowed for Earth Viewing Mode, a test diffuser swings into place to provide a source of radiance. The PTF is inherently more acurate than the VTF because it has no window transmission errors, it allows better control of scattered light, and there are no dimensional changes due to pressure differentials.

Quartz windows are used with the VTF to transmit light into the chamber. One window is kept protected from contamination and radiation except for momentary use to check the transmission of the working windows by comparison. The argon mini-arc lamp has a MgF_2 window and attaches directly to the chamber wall.

To select different radiometric standards, a carousel carries the light sources. On the VTF, this assembly is located accurately relative to the chamber wall and thus to the calibration test fixture inside the chamber.

An additional radiance calibration fixture allows the instrument to view a large (one foot square) test diffuser illuminated at normal incidence by a calibrated lamp 50 cm away. The simple geometry of this Normal Incidence Fixture eliminates the uncertainties of the PTF arrangement.

4.2.3 RADIANCE AND IRRADIANCE CALIBRATION

In calibrating the Earth Viewing (radiance) mode of operation with the PTF or VTF, the target seen by the instrument is a NIST-calibrated reflective diffuser illuminated by collimated light from an NIST-calibrated source of spectral irradiance. The absolute value of the radiance of the test diffuser is a function of the source irradiance, the efficiencies of the intervening components and their geometries.

In calibrating the Sun Viewing (irradiance) mode of operation, the source is the same collimating mirror illuminated by the same NIST-calibrated source. In this case, the absolute value of the irradiance at the instrument's diffuser is a function of the source irradiance and the intervening components and their geometries.

In calibrating the radiance to irradiance ratio, the set-up is fixed and the test diffuser and the instrument diffuser are alternately put into the light path.

Three types of calibrated standard lamps are used for stability cross-checking. The Quartz Iodine 1,000W FEL lamp is used for calibration in the 250 to 400nm range. The argon mini-arc is used for calibration in the 160 to 280nm range allowing some overlap with the FEL lamp. The Deuterium (D_2) lamp is not as stable in its overall output as the other two lamps because the arc does not attach itself to the same locations on the electrodes each time. This results in a ± 5 percent uncertainty in output. But the relative spectral irradiance (that is, the spectral irradiance curve shape) of the D_2 lamp is reproducible to within one percent and thus can be used to compare the output of the mini-arc at short wavelengths to the very stable output of the FEL lamp at long wavelengths. Thus, the intercomparison of the instruments response to the lamps serve to verify the stability of the radiance and irradiance target during the calibration sequence. See Figure 4-2 for typical source spectral irradiance.

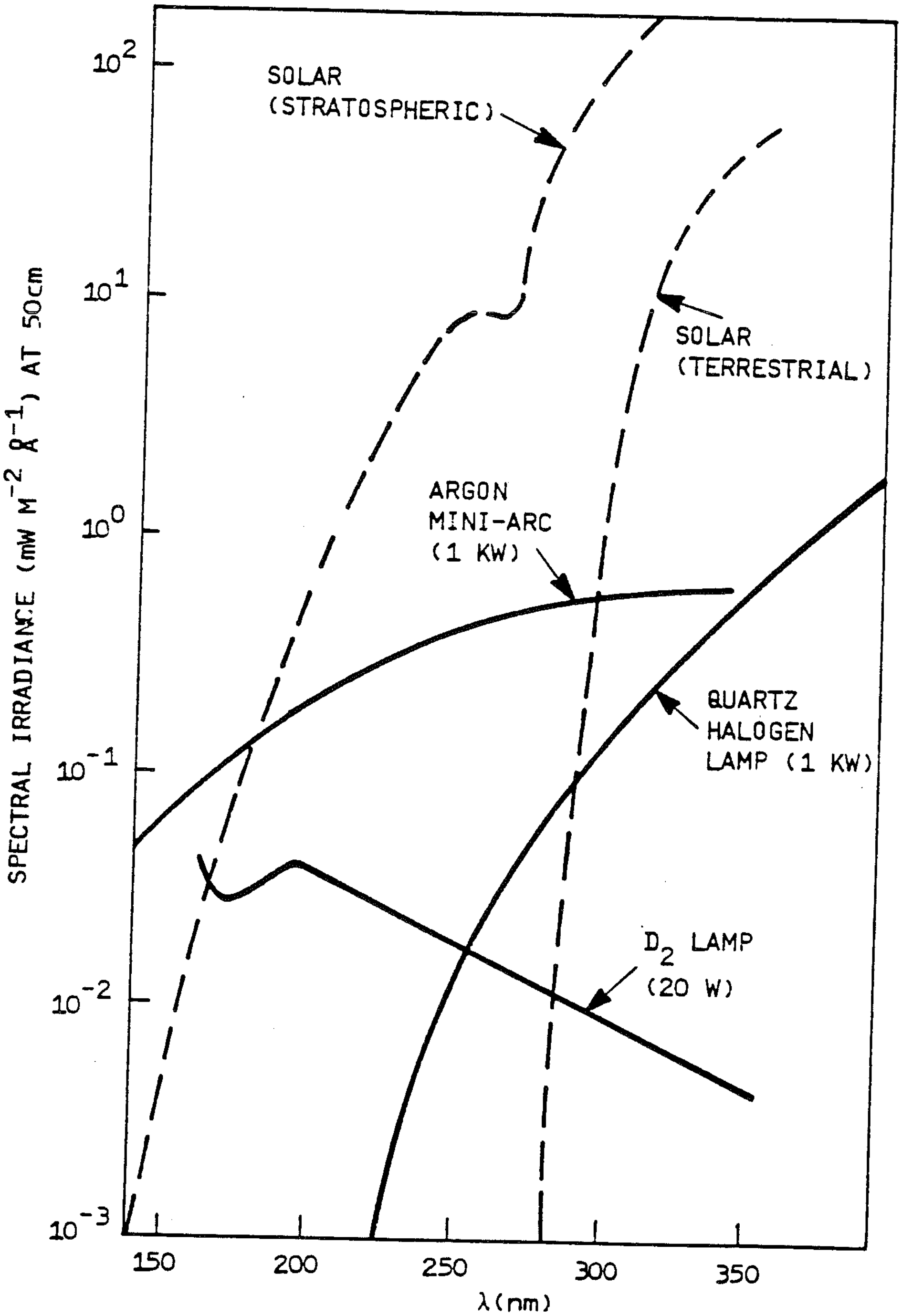

*NBS (NIST), Fifth Workshop on the VUW Radiometric Calibration of Space Experiments

Figure 4-2
Comparison of Spectral Irradiance from the Sun and from NBS (NIST) Transfer Standard Sources

4.2.4 RADIOMETRIC CALIBRATION TRANSFER

The instrument is designed to respond in proportion to the spectral radiance, ($mW\text{-}m^{-2}\text{-}sr^{-1}\text{-}\AA^{-1}$) incident upon its entrance slit. The area of the entrance slit, the field-of-view defined by the field stop, and the bandpass of the monochromator determines the radiant flux ϕ (W) which enters the system. The system transmission efficiency determines the radiant flux at the photocathode. The quantum efficiency and gain of the detector system determines the final response to a given input. To calibrate this system, standard sources of spectral irradiance that produce a certain spectral irradiance ($mW\text{-}m^{-2}\text{-}\AA^{-1}$) at a given distance under carefully controlled conditions are available.

The approach taken is to use a standard of spectral irradiance to illuminate a diffuser of known spectral goniometric efficiency. A collimating mirror is used to achieve uniformity of irradiance and of angle of illumination at the diffuser. Thus, at given angles of view, the spectral radiance of the diffuser is known and the instrument response to this radiance is measured. The problem is that three elements (window, collimating mirror, and diffuser) have been interposed between the standard source and SBUV and each introduces an error into the transfer process. The window and collimating mirror can be measured for spectral transmission and reflectance to within three percent to one percent errors. This is done before and after each major calibration sequence.

The test diffuser efficiency and BRDF are measured directly by NIST.

With the standards of irradiance, the collimator and the test diffuser, the instrument is presented with a diffuse source of known radiance against which its response can be calibrated. To calibrate the irradiance mode of operation, the test diffuser is moved out of the way as the instrument diffuser is deployed. In effect, what this does is to compare the efficiencies of the two diffusers since their interchange is the only difference in the two measurements.

4.2.5 ACCURACY OF CALIBRATION

The inaccuracy of the radiometric calibration is the combination in quadrature of the uncertainties in the standards of spectral irradiance with the errors of the transfer process. These latter errors are due to source control and drift, error in transfer optics efficiency measurements, fixture dimensional errors, and noise-induced errors in the instrument. The specified maximum errors are listed in Table 4-1. Calibration is performed below 200nm down to 160nm but with larger errors.

The specified maximum errors in the ratios of measured radiance to irradiance are listed in Table 4-2. These errors arise from the test diffuser efficiency error, instrument noise, and instrument nonlinearity over the range spanned by the ratio.

Table 4-1
ABSOLUTE RADIOMETRIC ACCURACY

Wavelength (nm)	Source	Maximum Error of Source	Calibration Transfer	Test Diffuser	Other	Total Absolute Error (RSS)
Spectral Irradiance Calibration (Instrument Diffuser)						
200-250	Mini-Arc	6.0	3.5	----	1.0	7.02
250	FEL	2.6	2.0	----	1.0	3.43
300	FEL	2.1	2.0	----	1.0	3.07
350	FEL	1.7	2.0	----	1.0	2.81
400	FEL	1.5	2.0	----	1.0	2.69
Spectral Radiance Calibration (Test Diffuser)						
200-250	Mini-Arc	6.0	3.5	2.0	1.0	7.30
250	FEL	2.6	2.0	1.0	1.0	3.57
300	FEL	2.1	2.0	1.0	1.0	3.23
350	FEL	1.7	2.0	1.0	1.0	3.98
400	FEL	1.5	2.0	1.0	1.0	2.87

Table 4-2
RATIO ERRORS (Radiance/Irradiance)

Wavelength	Error (Percent)
200-250	2.35
250	1.53
300	1.57
340-400	1.82

Section 5
GROUND SUPPORT EQUIPMENT

5.1 SCOPE

This section contains a functional and physical description of the test equipment and fixtures which comprise the Ground Support Equipment (GSE) for the SBUV/2 instrument. The GSE includes:

- System Test Equipment (STE)
- Bench Checkout Unit (BCU)
- Vacuum Test Fixture (VTF)
- Primary Test Fixture (PTF)
- Miscellaneous Test Fixtures
- Mechanical Fixtures and Shipping Containers

The electrical ground support equipment consists of the System Test Equipment and the Bench Checkout Unit. The system test fixtures consist of the Vacuum Test Fixture and the Primary Test Fixture. Both fixtures contain calibration sources or targets, and a target control console.

The miscellaneous test fixtures are those special items of equipment which are required to support field-of-view, alignment, linearity checks, calibration and vibration testing of the instrument at BACG. Thus, these items are not required for post-delivery support of the instrument.

The mechanical fixtures and shipping containers include the instrument shipping containers and those special items of equipment required for post-delivery support of the instrument.

Figure 5-1 shows a complete breakdown of the GSE hardware items and the major components which comprise the end items. This figure also depicts the categorical grouping of the GSE.

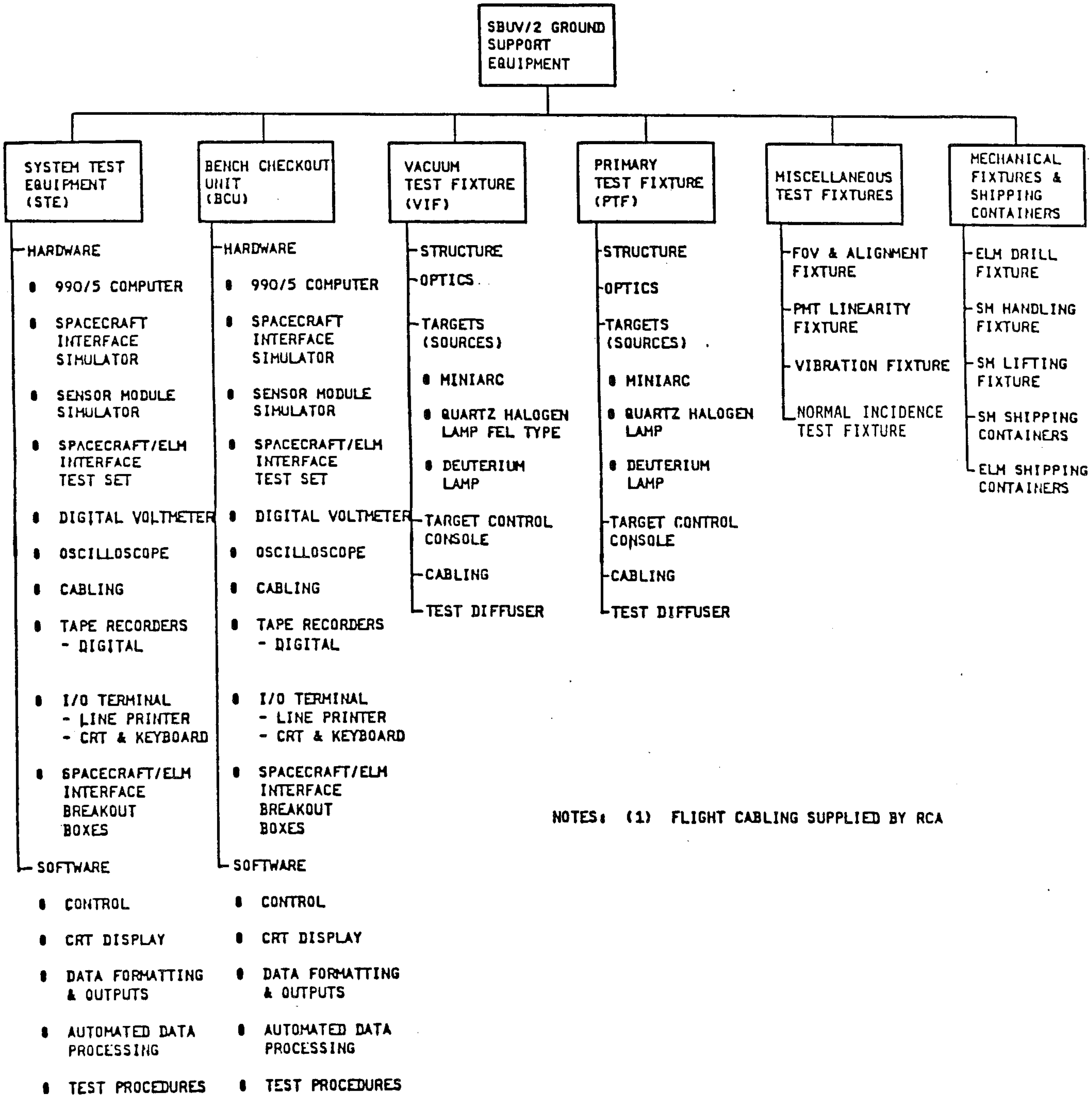

Figure 5-1
SBUV/2 Ground Support Equipment

5.2 SYSTEM TEST EQUIPMENT (STE)

5.2.1 PURPOSE

The System Test Equipment supplies and controls all of the electrical interfaces to the instrument and is used to test each instrument (engineering model and flight units) at BACG. The STE is the nucleus of the equipment necessary for performance, calibration, and functional testing of the SBUV/2 instrument.

The STE interfaces with the complete instrument to provide power, commands, timing, data collection, instrument control, data storage, data reduction, and data display functions. It also monitors data from calibration sources, and has the capability of separately testing the Electronics and Logic Module.

The STE performs the following specific functions:

- Simulate all interfaces normally supplied by the spacecraft.
- Provide automatic data processing equipment for data analysis and control of the instrument.
- Provide specially formatted digital data tape recordings.
- Provide hard copy of instrument raw data and specially-formatted data.
- Provide real-time display of instrument telemetry including status bits, subcommutated analogs, and radiometer data.
- Provide for automatic monitoring and recording of data from the calibration sources.
- Provide the capability for separate testing of the Electronics and Logic Module.

- Provide isolated test jacks for all spacecraft related signals, instrument test points, and other significant STE and instrument voltages.

5.2.2 HARDWARE DESCRIPTION

The physical layout of the STE is shown in Figure 5-2. Figure 5-3 is a block diagram of the STE.

The STE includes features providing instrument safeguards, such as over-voltage protection, current-limiting, warning indicators, and isolated test jacks. The STE is designed to use its Automatic Data Processing Equipment (ADPE) facilities for additional automated functions in the areas of instrument control, test fixture monitoring, status display, and test procedure generation and control. The automation of STE tasks and functions assures a high degree of confidence in test repeatability and configuration control.

The following subparagraphs describe the major components of the STE.

5.2.2.1 Control Assembly

Texas Instrument (TI) Model 990/5 CPU with 32K (16-bit) MOS Memory.

This is the Central Processing Unit (CPU) for the STE Automatic Data Processing Equipment and is the controller for all STE interfaces. It is used for operating the system resident modules, data reduction programs, control programs, data buffers, tables, and algorithms.

Spacecraft Interface Simulator.

This is a program-controlled peripheral that simulates all spacecraft interfaces. It mounts in the STE rack and interfaces to the instrument through spacecraft equivalent connectors and cables exiting from the rear of the rack. The simulator meets all of the electrical and timing requirements of the TIROS-N General Instrument Interface Specification IS-2280259. The simulator uses program control to acquire data from Digital A, Digital B, and analog interfaces. Commands are under software control.

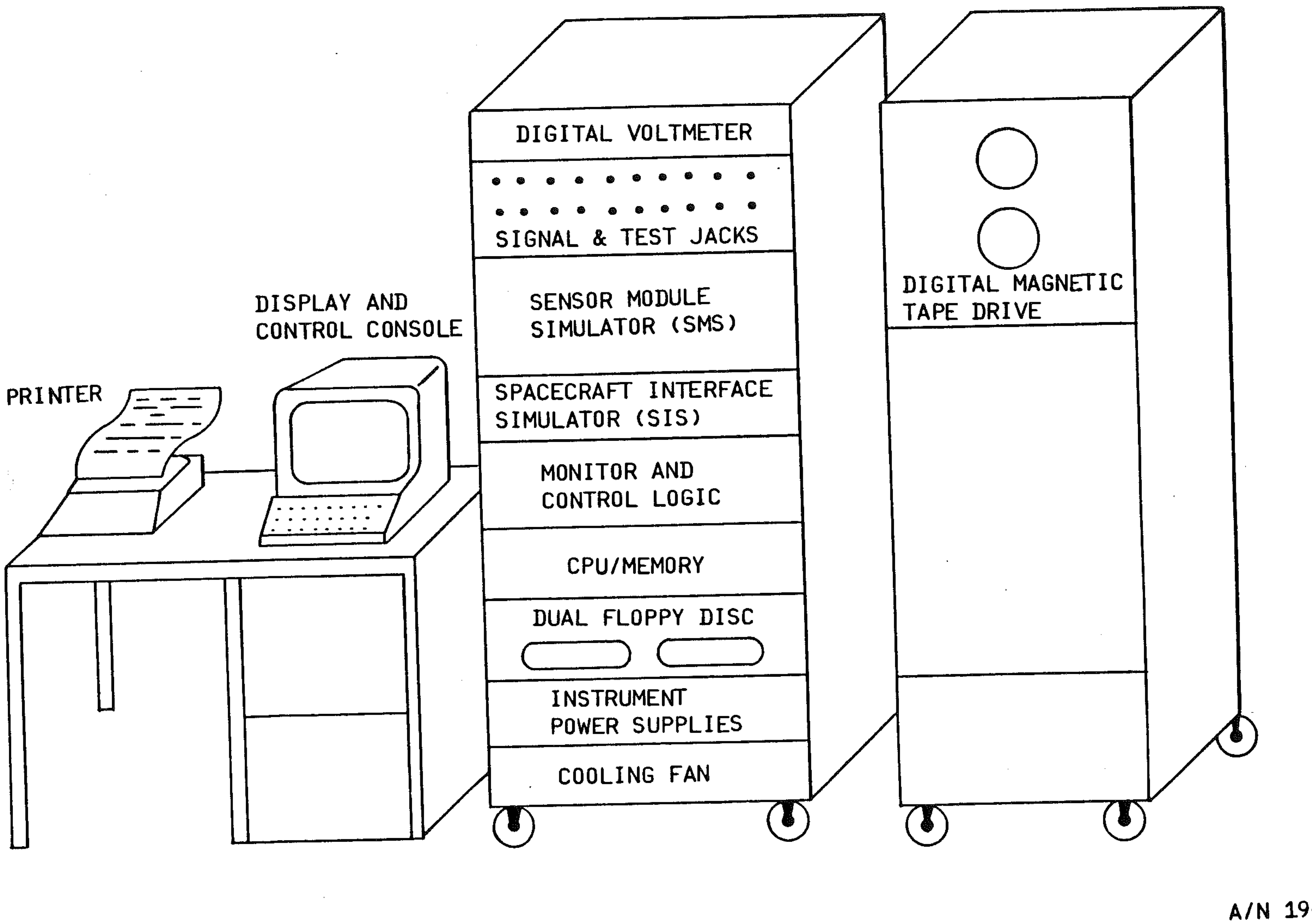

Figure 5-2
STE Physical Layout

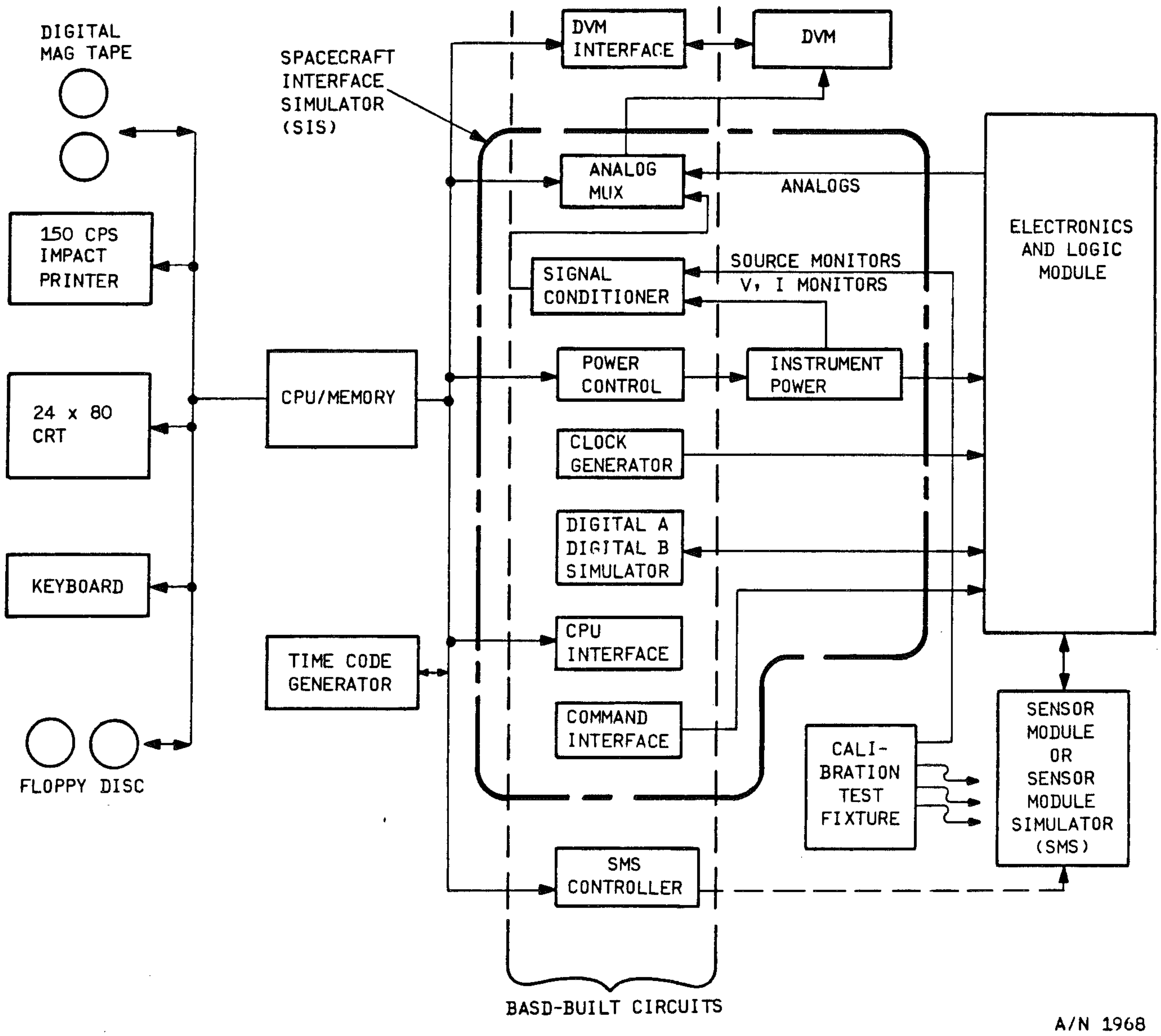

Figure 5-3
Integrated STE Block Diagram

Sensor Module Simulator.

This simulator permits separate checkout and testing of the Electronics and Logic Module. Its circuitry is built on wire wrap boards located in the STE rack and has connectors identical to the Sensor Module. It provides simulated radiometric data and digital housekeeping bits. It also simulates power loads and provides test jacks to verify proper stepper motor drive signals from the Electronic and Logic Module.

Digital Voltmeter (DVM).

The DVM is computer-controlled and converts instrument analog telemetry, test point voltages, and pertinent STE voltages to digital. Digital readings are transformed, as necessary, using look-up tables to yield engineering units and displayed on the CRT. A program-controlled analog multiplexer sends voltages to the DVM.

Remote DVM.

The external DVM is also computer controlled, but is located in the Target Control Console, where it monitors calibration source current or voltage.

5.2.2.2 Input/Output Devices

Dual 256K Byte Flexible Disc Drive.

The flexible (floppy) discs are the primary system storage media. The manufacturer (Texas Instruments) provides comprehensive multi-tasking, operating system software, and system utilities on this media. The custom operating systems are derived from these building blocks. The disc is used for assembly and Fortran source and object files, system utilities, test procedure file generation, and is the residence for automatic test procedures.

Texas Instrument (TI) Model 911 Video Display Terminal with 1,920-Character (24 lines x 80) Display (Including Full Alpha-Numeric Keyboard).

This terminal is the STE system control and display console. It serves many functions including the following:

- Software development by the programmer
- Display console for real-time status, science, and analog telemetry during test
- Input terminal for control

Texas Instrument (TI) Model 810 Printer.

This is a 120 character-per-second impact printer using standard 14-inch fanfold paper used to make hard copy of instrument raw data, specially-formatted data, program listings, and as-run test procedure listings.

5.2.2.3 Tape Recorder

The tape recorder is a Texas Instrument Model 979A digital magnetic tape recorder. It records nine tracks at 800 bits per inch. The primary purpose is to record test data to be delivered to NOAA or GSFC. Test data is recorded in the standard decommutated TIROS information processor format. Each file has a header containing pertinent test conditions, time of day, operator ID, etc. Each data field within a record is identified by a major frame number.

Target information and other data pertinent to the test is recorded in special data fields. The end of a test or test condition is noted by an "end of file" statement. A chronological test log is maintained of each special delivered tape and is properly annotated with the date, test data contained thereon, etc., to facilitate use.

5.2.3 SOFTWARE DESCRIPTION

The software runs under a multi-tasking, real-time operating system in which multiple tasks may run using time slices in accordance with their priority level. There are event-driven tasks executed from hardware interrupts derived from the STE system timing logic.

Software is divided into automated data processing, control/display tasks, and test procedure run time tasks. All STE functions are software-controlled from the CRT console using the keyboard or run automatically from test procedures stored on disc files.

The only exception to total automation of STE tasks and functions is that test fixture positional control (such as is needed in field-of-view tests) is not directly computer-controlled. However, procedural confidence is maintained through the use of manual positioning directives, to be displayed as operator prompts, during test sequences. These prompts appear on the console and line printer and the test sequence pauses until the operator signals, via keyboard, that the directive has been accomplished.

5.2.3.1 Software Control Functions

The following spacecraft interfaces are controlled by software:

- Instrument commands
- Digital A Interfaces
- Digital B Interfaces
- Analog Interfaces

5.2.3.2 Software Display Functions

The software controls the decommutation and display of the following:

- Digital A and B status bits on CRT
- Digital B telemetry words in real time
- Pertinent instrument and STE voltages
- Digital A subcommutated analog on CRT in engineering units
- Time of day
- Last test procedure directive issued

5.2.3.3 Data Formatting and Output Software

This software is used to:

- Format CRT screen to display in real-time all required instrument and STE data necessary to determine quick look operating status

- Format hard copy outputs of raw data, formatted data, and data reduction products

- Format files and records on magnetic tape

5.2.3.4 Automated Data Processing Software

This software performs processing of instrument radiometric data, other telemetry data, and source or target data to arrive at final data products which are used for verification of instrument performance. The software also provides a real-time out-of-limits program that will sound an alarm and print any out-of-limit items as they occur. Self-check programs for verification of STE are also provided.

5.2.3.5 Test Procedures

Figure 5-4 is a flow chart of software development and test procedure generation. The test procedures provide the facility for functional, calibration, and performance level testing. Software development proceeds in two distinct phases in order to provide test procedures which are easily written, executed, and interpreted by people that are not professional programmers.

During Phase I, the programmer wrote assembly and Fortran program modules to control all system peripherals and to implement all required STE tasks with task definition inputs coming from design personnel. Each task required by the STE was assigned a unique descriptive name called a Test Control Directive (TCD). The programmer then created a TCD interpreter which allows each task to be executed upon receipt of the associated TCD.

During Phase II, TCD's are filed on disc in various sequences using the text editor. These lists of TCD's then become the stored test procedures for functional, calibration, and performance testing. TCD's are usually input as stored sequences retrieved automatically from the disk; however, they can also be input individually from the keyboard. The currently-executing TCD is always displayed on the system CRT console and all TCD's are output to the printer and tape files as they are received. The result is an as-run record of the TCD's interlaced with the resulting data including time tagging. Phase II is characterized by visibility and familiarity in test procedure definition and operation by those actually involved in interpreting the data.

Test procedures generated in this manner provide completely annotated and totally repeatable test sequences to the hard copy device and magnetic tape files.

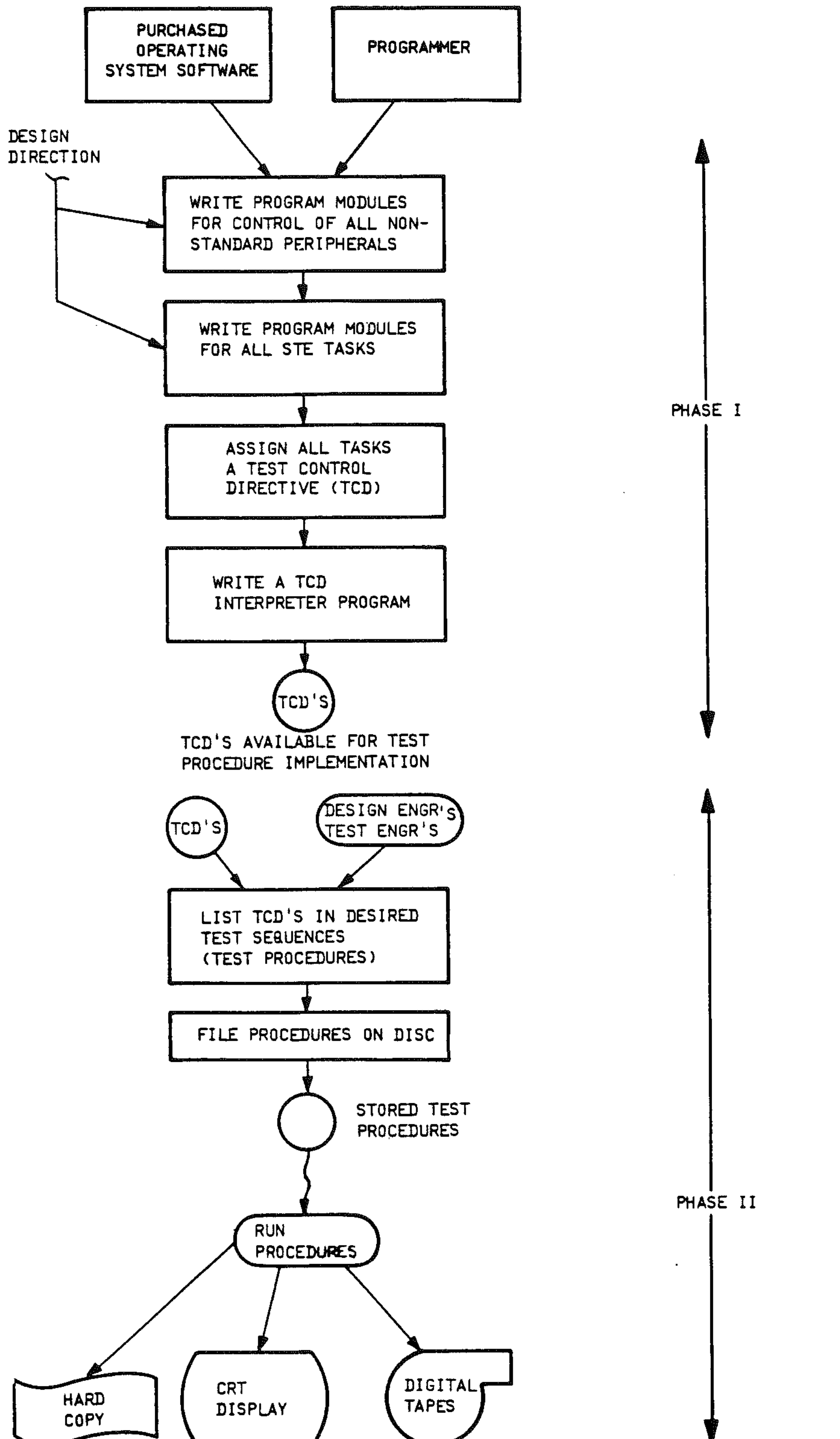

Figure 5-4
Flow Chart of Software Development and Test Procedure Generation

5.3 BENCH CHECKOUT UNIT (BCU)

5.3.1 PURPOSE

The Bench Checkout Unit was originally specified to be a smaller version, both physically and in capabilities, of the System Test Equipment. It was planned to be used at the spacecraft contractor's facility to verify the post-delivery operation of each instrument. However, the need for two STE's developed so that two instruments could be tested simultaneously at BACG. Therefore, the BCU was modified to be functionally identical to the STE.

5.3.2 DESCRIPTION

The description of the STE in paragraph 5.2 applies in its entirety to the BCU.

5.4 VACUUM TEST FIXTURE (VTF)

5.4.1 PURPOSE

The purpose of this fixture is to provide a calibrated source of illumination to extend the instrument's calibration below the air cut-off to the 160nm during thermal vacuum testing.

5.4.2 DESCRIPTION

The Vacuum Test Fixture (VTF) (see Figure 5-5) consists of a bench or structure that provides a stable instrument mounting interface. Three light sources are mounted on a table which locates each source at the focal plane of the collimator and provides repeatable location of each source . The light beam is collimated by a concave mirror located on the fixture. This light beam illuminates either the instrument diffuser or a Lambertian-type test diffuser which provides illumination to the instrument.

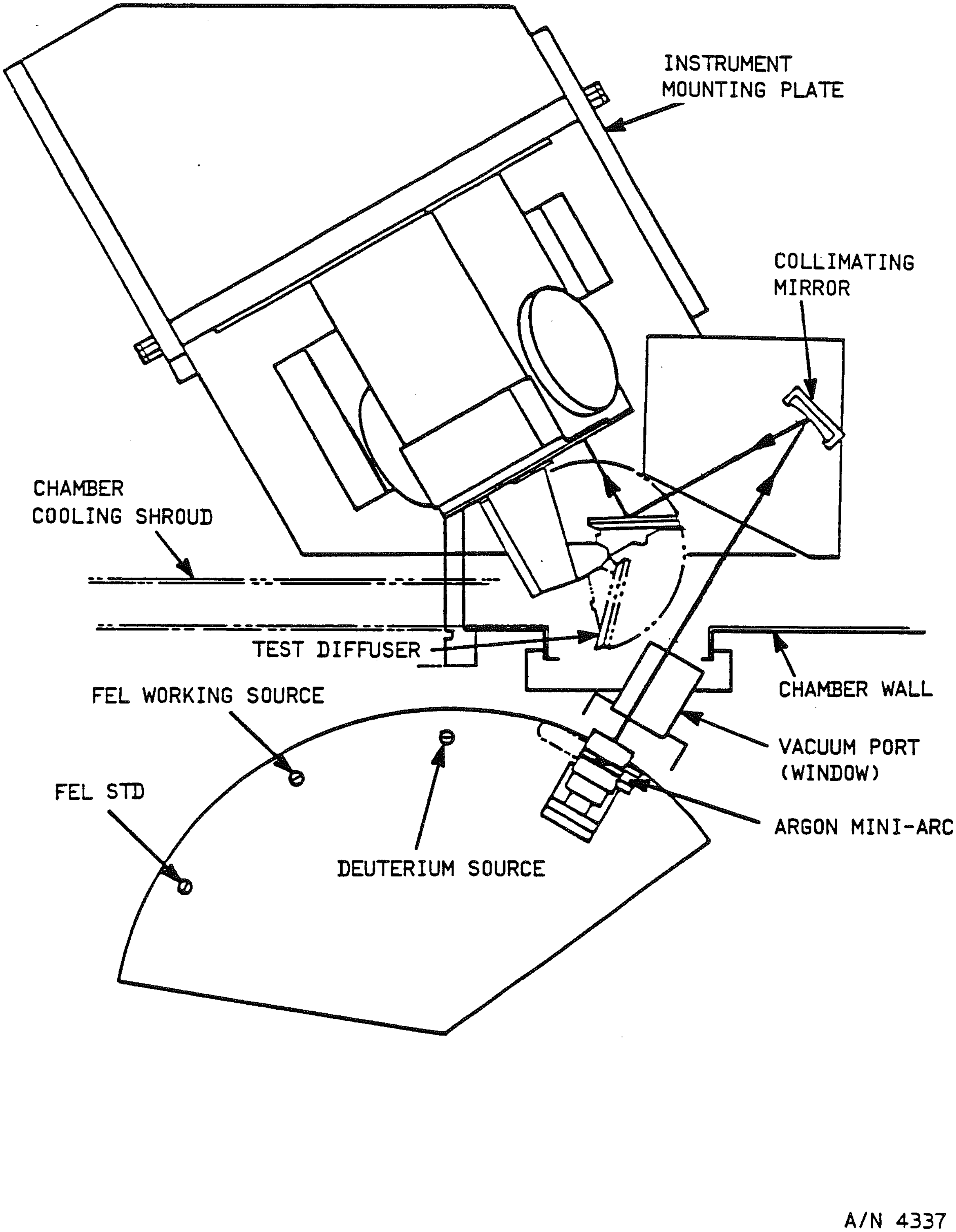

Figure 5-5
Vacuum Test Fixture

The fixture is vacuum-compatible as it will be most often used in a vacuum chamber. However, it can also be used outside the chamber. In these instances, the light source table is attached to the fixture in the same location as it is in the vacuum chamber.

A Target Control Console provides the power, control, regulation, and monitoring of the VTF calibration sources. The console provides a display of the monitors as well as interfaces for the System Test Equipment (STE).

5.4.2.1 Structure

The VTF structure is a bench to which the collimator mirror and instrument are mounted. The structure provides a rigid and highly repeatable location of the instrument and other sub-assemblies mounted on the fixture.

5.4.2.2 Targets

Three targets or sources of radiation are used: (1) Quartz Iodide Lamp, FEL type; (2) Deuterium Lamp, and (3) Argon Mini-Arc. These targets are NIST calibrated sources of radiation and thus the primary standard for calibration of the SBUV/2 instrument.

5.4.2.3 Target Control Console

The Target Control Console is a separate unit that provides power, control, data collection and panel readout for the VTF. It also interfaces to the STE for monitoring of the ultraviolet sources. It interfaces directly to the STE and BCU, and provides an output for the DVM. Discrete outputs for monitoring each target source and a test point selector switch provide manual monitoring of any output.

5.4.2.4 Collimator

The collimator consists of a mirror and its mount, an aperture and light baffle. It is mounted directly onto the structure of the VTF. The collimator mirror parameters area:

- Size: 6 inch diameter, spherical
- Focal Length: 50 cm
- Coating: Al-MgF_2
- Reflectivity: 88 percent at 200nm

The aperture size is fixed.

5.4.2.5 Window

A cultured quartz window is used at the vacuum chamber interface.

5.4.2.6 Test Diffuser

The test diffuser is used to convert the collimated light from the collimating mirror to a calibrated diffuse radiant source for the radiance calibration. The test diffuser is mounted onto the back of the SBUV/2 instrument's diffuser mechanism which positions it either in the radiance test position or in the unused position. The test diffuser size is 3.250 inches x 4.500 inches and is a ground aluminum surface coated with aluminum.

5.4.2.7 Deleted

5.4.2.8 VTF Cables

The following is a list of the cables for the VTF:

- Target Control Console to STE
- Target Control Console to targets
- Vacuum chamber feed through cables, STE to ELM
- Vacuum compatible cables, ELM to SM

5.5 PRIMARY TEST FIXTURE

5.5.1 PURPOSE

The purpose of this fixture is to provide a calibrated source of illumination for the absolute calibration of the instrument above the air cut-off. Primary radiometric checks of the instrument are made with this fixture. It is also to be used to demonstrate instrument stability and repeatability during system functionals, electrical checks, optical checks, and performance verification.

5.5.2 DESCRIPTION

The Primary Test Fixture is identical to the Vacuum Test Fixture with two exceptions: (1) It is not used in the vacuum chamber and therefore does not have a vacuum window in the light path, and (2) it is a bench unit with a rigid structure. A Target Control Console for the Primary Test Fixture is also provided. The collimator, targets, and structure are the same as the Vacuum Test Fixture. The diffuser used with the PTF is an aluminum plate coated with $BaSo_4$ (Kodak white) paint. The fixture is shown in Figure 5-6.

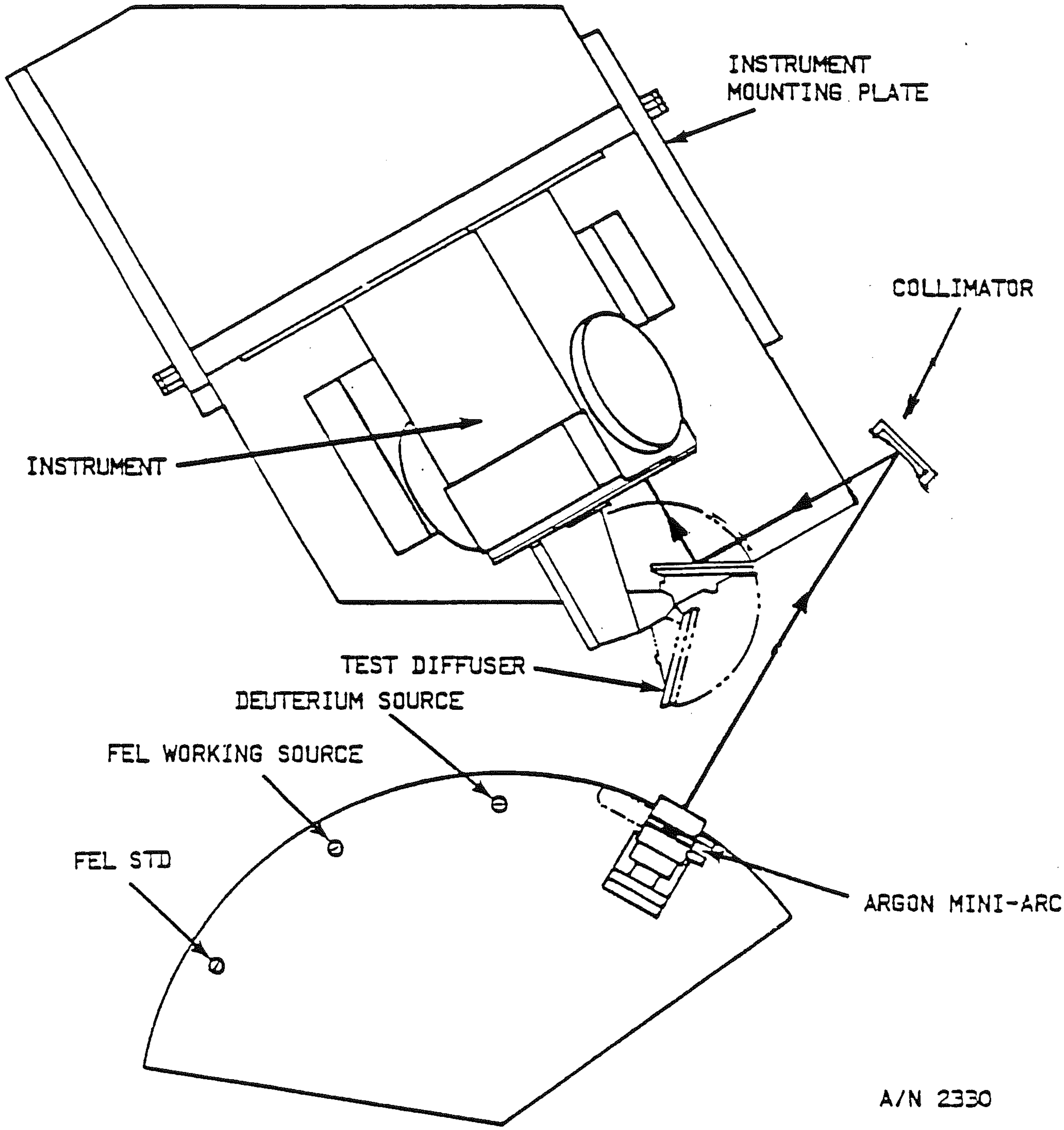

Figure 5-6
Primary Test Fixture

5.6 MISCELLANEOUS TEST FIXTURES

5.6.1 FIELD-OF-VIEW AND ALIGNMENT FIXTURE

5.6.1.1 Purpose

The Field-of-View and Alignment Fixture will be used to determine the field-of-view size, field uniformity, field registration of the CCR to monochromator, and the alignment of the instrument.

5.6.1.2 Description

Figure 5-7 illustrates the fixture and set-up for alignment and field-of-view tests. The instrument is mounted on rotary tables whose axes of rotation intersect at the center of the instrument entrance slit. The table has readouts of 0.05° increments. The target is placed at a fixed distance of 1.5 meters from the instrument. The target shown in Figure 5-7 is a slot-shaped diffuser of 11.33° x 1.13° angular size. The light source, (two 500W Quartz Iodide Lamps) illuminates the transmissive diffuser from behind. A thin Quartz test lens of focal length equal to the instrument slit-to-target distance is fitted in front of the instrument slit for these tests so that the target is focused at the proper conjugates within the instrument.

A partially-aluminized transfer flat is located between the instrument and the target. Prior to the test, it is set parallel to the optical reference cube using an alignment telescope. The axis of the target and the instrument is set normal to the transfer flat.

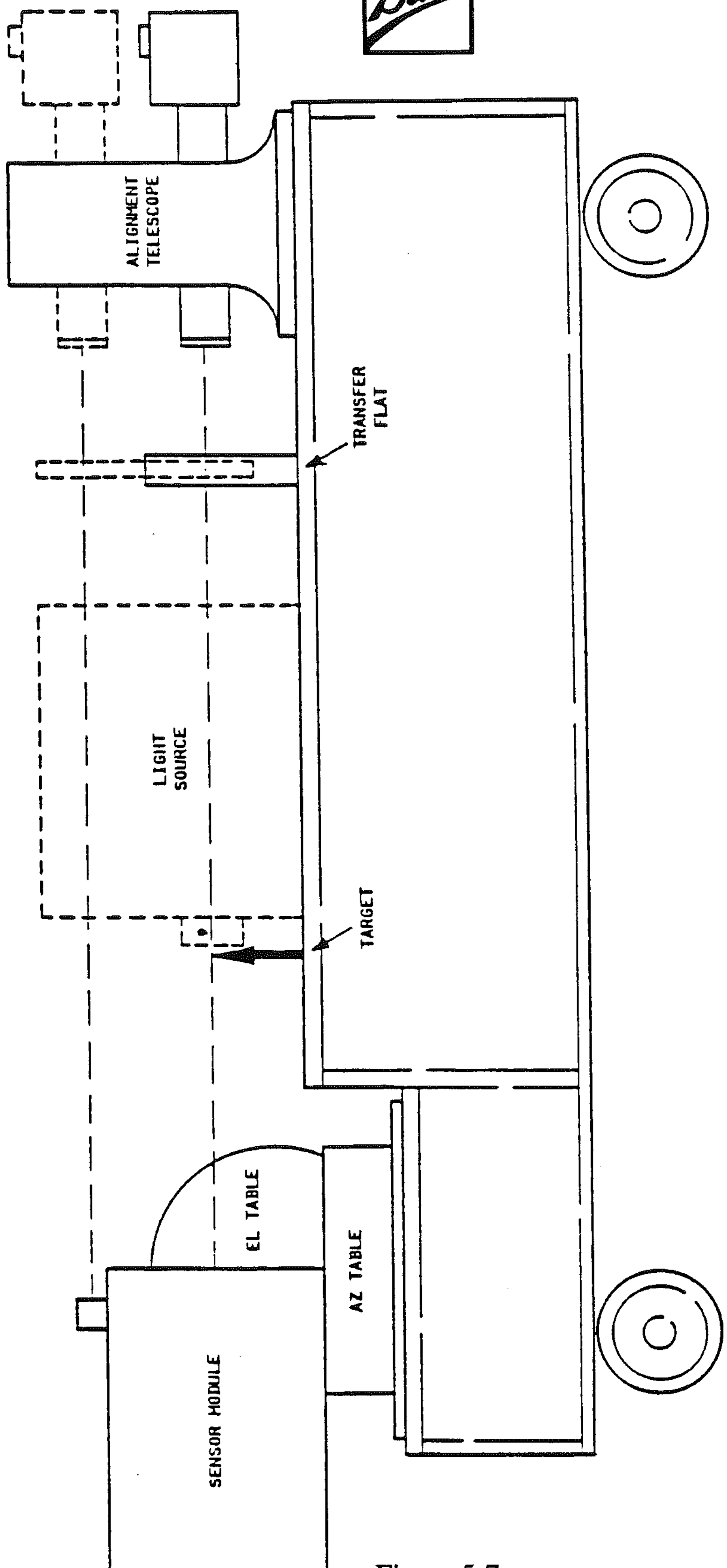

Figure 5-7
Field-of-View and Alignment Fixture

By means of the rotary tables, the half-power points of the field of view are located and their angular separation measured with the rotary tables. A target having a diffuser of 11.33° x 1.13° angular size is used to determine the field uniformity of the instrument. This target is illuminated by the Quartz Iodide Lamp which is controlled and monitored to provide one to two percent uniformity output from the diffuser. The instrument is rotated about its entrance slit with the rotary tables to provide the response versus angle.

The fields-of-view of the monochromator and CCR must coincide to within 0.1°. The thin Quartz lens spans the entrance apertures of both the monochromator and CCR. The focal length of the lens is such that rays entering either aperture from a single point on the target are rendered parallel. In this way, the field-of-view edges of the CCR and monochromator can be measured simultaneously without need to translate the instrument or target to compensate for aperture separation.

5.6.2 LINEARITY FIXTURE

5.6.2.1 Purpose

The Linearity Fixture is used to test for instrument nonlinearity. Tests will be made over a range of approximately 10^8.

5.6.3.2 Description

The fixture for making these measurements is shown in Figure 5-9. The photocathode of the PMT will be illuminated by using the instrument monochromator with its gratings positioned to send zero order through the exit slits. This allows a complete linearity verification of the entire system up to the maximum stimulus.

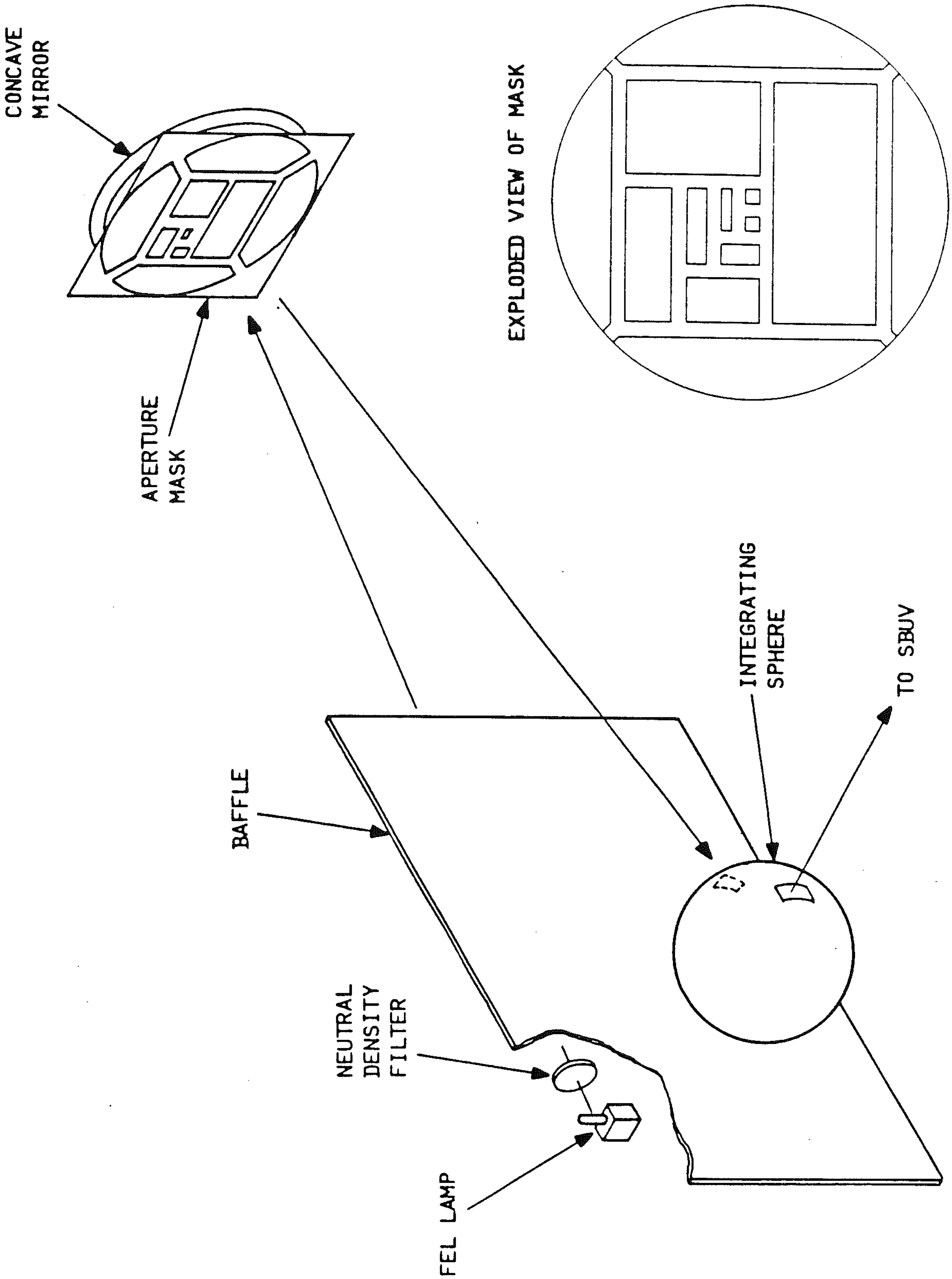

Figure 5-9
Linearity Fixture

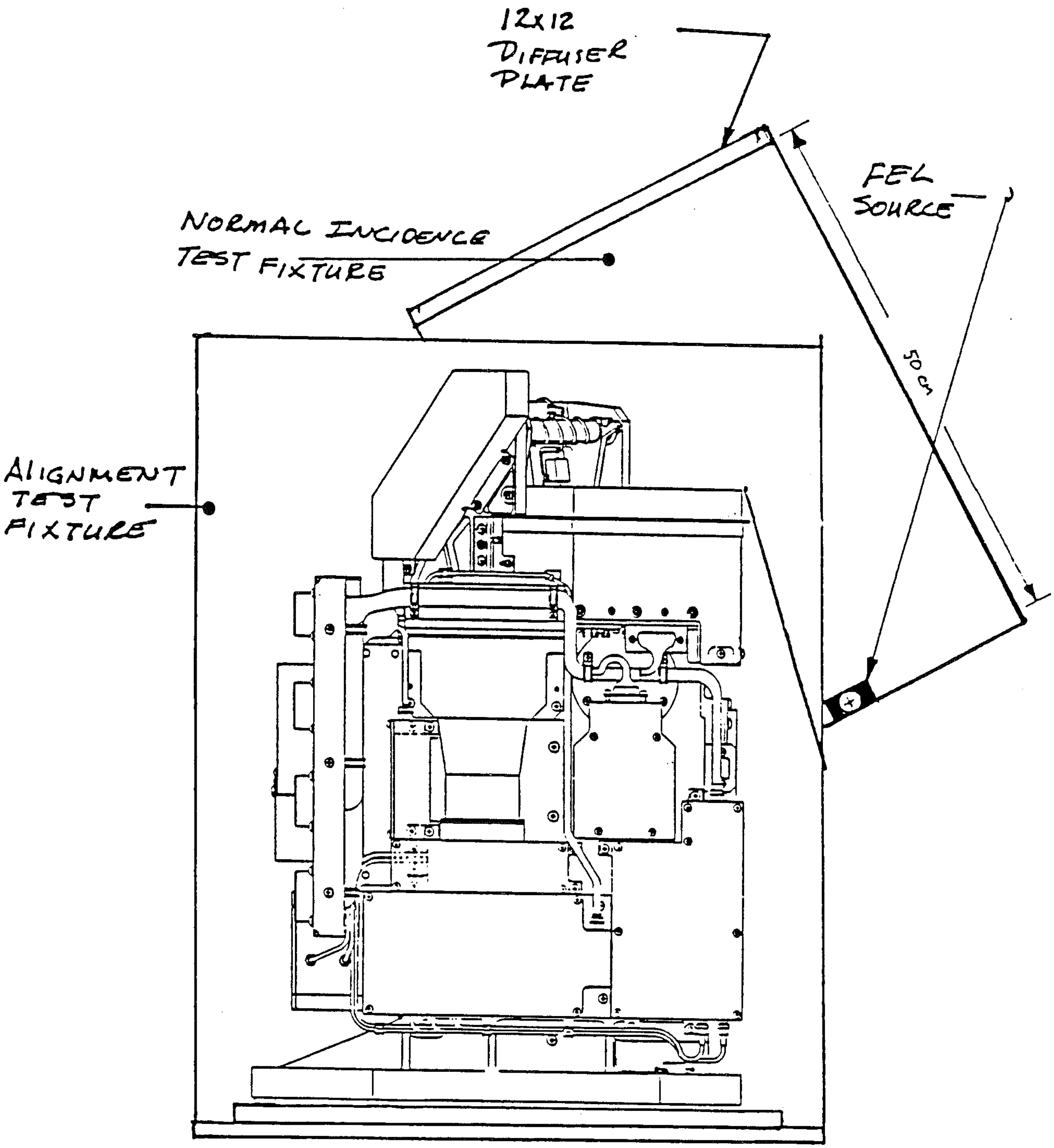

Figure 5-10
Normal Incidence Test Set Up

The monochromator is illuminated by the test fixture as shown in Figure 5-9. The nonlinearity of the instrument is measured directly over each range by the two aperture method. This method employs an aperture plate which is the essential part of the fixture. It provides illumination to the instrument in a fashion that is successively doubled by uncovering apertures in the fixture. A range of about 500 to 1 can be covered by changing apertures. By using neutral density filters at the light source, the range of illumination is extended to cover the instrument's dynamic range of 10^8.

5.6.3 NORMAL INCIDENCE FIXTURE

5.6.4.1 Purpose

This fixture provides an alternate means of calibrating the instrument in radiance (earth-viewing) mode. It compliments the PTF by having a simpler geometry and higher light levels.

5.6.3.2 Description

A calibrated lamp is positioned 50 cm from a 12 x 12 inch diffuser plate, normal to the center of the plate. See Figure 5-10. The plate is positioned so that the optical axis of the monochromator intersects the center of the diffuser plate at an angle of 28° from the normal. The diffuser plate is painted with $BaSo_4$ (Kodak White), and is calibrated by NIST.

5.6.4 GONIOMETRIC CALIBRATION FIXTURE

5.6.4.1 Purpose

The purpose of this fixture is to characterize the radiometric response of the instrument, including its diffuser, over the expected range of solar incident angles. This fixture allows the direct measurement of the instrument response as a function of illuminating angle to the diffuser. See Figure 5-11.

A fixture with an axis of rotation which is coincident with the center of the diffuser plate is used on the horizontal rotary table from the field-of-view test fixture. A FEL lamp is set up at the end of the field-of-view fixture along with a series of baffles to minimize stray light.

Both axis of rotation pass through the center of the diffuser. The instrument and light source are aligned with the reference cube. The instrument then scans over the range of angles of incidence of solar illumination expected in orbit.

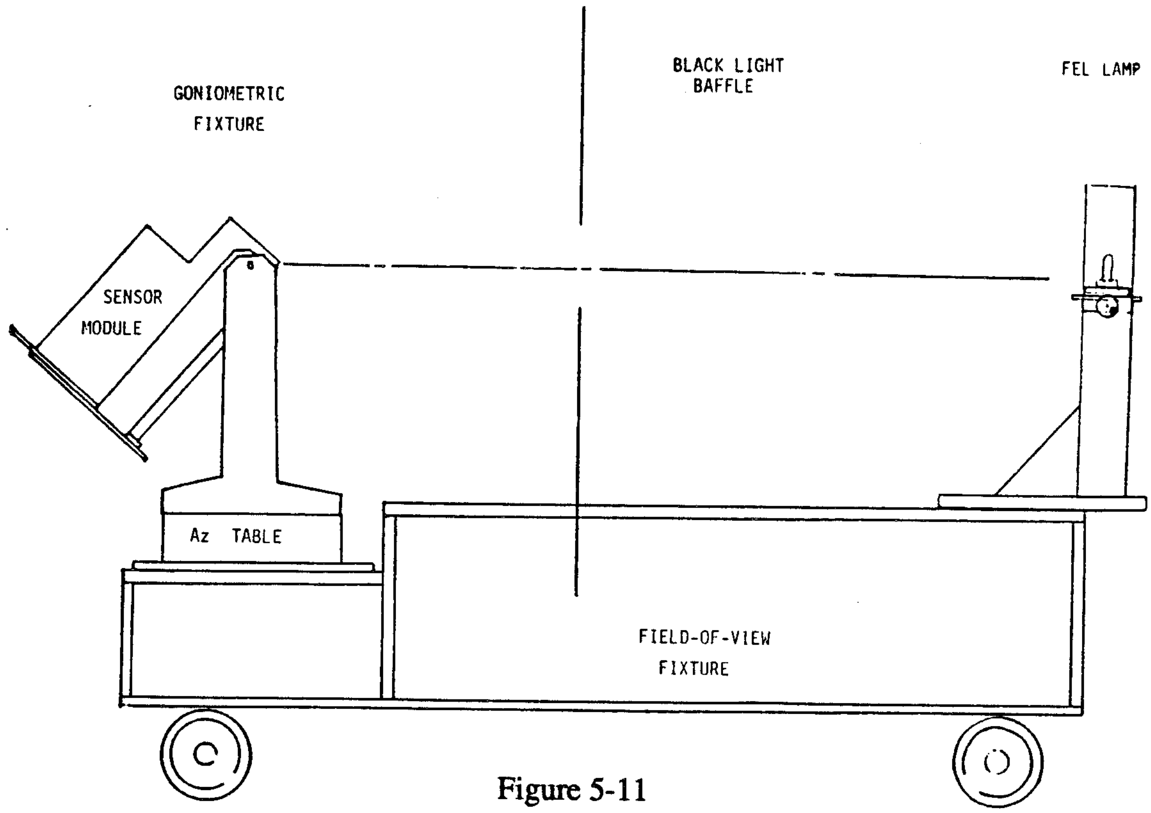

Figure 5-11
Setup For Performing Relative Goniometric Calibration

5.6.5 VIBRATION FIXTURE

5.6.5.1 Purpose

The vibration test fixture is used to attach either the Sensor Module or the Electronics and Logic Module to the shaker table at BACG for the purpose of performing the vibration tests.

5.6.5.2 Description

The vibration fixture is fabricated from aluminum plate approximately 30 x 30 x 2 inches thick.

5.7 MECHANICAL FIXTURES AND SHIPPING CONTAINERS

5.7.1 ELM DRILL FIXTURE

5.7.1.1 Purpose

To assure matching hole patterns between the Electronics and Logic Module (ELM) and spacecraft, two drill fixtures have been fabricated and drilled simultaneously. One drill fixture has been delivered to the spacecraft contractor for drilling each spacecraft. The other remains at BACG for drilling each ELM.

5.7.1.2 Description

The fixtures are fabricated from BACG Drawing No. 67768 using aluminum tooling plate and fitted with press fit liners and replaceable slip fit drill bushings. The fixtures have spacecraft coordinate markings.

5.7.2 SENSOR MODULE HANDLING FIXTURE

5.7.2.1 Purpose

This fixture is used to hold and protect the Sensor Module and to allow handling of the Sensor Module without contacting critical surfaces or subassemblies. The fixture is used for:

- Handling during instrument assembly, test, and calibration
- Mounting interface with the shipping container

5.7.2.2 Description

5.7.3 SENSOR MODULE LIFTING FIXTURE

5.7.3.1 Purpose

The lifting fixture is designed to allow installation of the Sensor Module to the spacecraft in a horizontal manner.

5.7.3.2 Description

The lifting fixture attaches to three points provided on the Sensor Module structure. It is counter-balanced and has provisions to attach to an overhead crane. The fixture will be capable of a 6g loading without yield.

5.7.4 SENSOR MODULE SHIPPING CONTAINERS

5.7.4.1 Purpose

The shipping containers provide a clean, protective environment for the Sensor Module during air or ground transportation and during periods of ground storage.

5.7.4.2 Description

The container is a standard, sealed commercial container fitted with shock mounts. The Sensor Module handling fixture attaches to the shock mounts. Purge fittings and two-way pressure relief and two-way pressure relief valves are used to allow initial N_2 purge and breathing to accommodate pressure changes in excess of container capabilities. The Sensor Module will be bagged and purged to protect it from contamination which may be introduced by case relief valve inward flow.

5.7.5 ELM SHIPPING CONTAINER

5.7.5.1 Purpose

The shipping containers will provide a clean, protective environment for the ELM during air or ground transportation and during periods of ground storage.

5.7.5.2 Description

These are standard shipping containers furnished by GSFC. They have been fitted with special foam liners to hold the ELM.

Section 6
NOTES

6.1 SCOPE

This section contains a listing of acronyms and abbreviations used herein. Also, definitions of some terms used herein are included for clarity.

6.2 ACRONYMS AND ABBREVIATIONS

TERM	DESCRIPTION
A	Amps
Å	Angstrom (0.1 nm)
A/D	Analog-to-digital converter
ADPE	Automated Data Processing Equipment
ATN	Advanced TIROS-N
BAK	Backup
BACG	Ball Aerospace and Communications Group
BASG	Ball Aerospace Systems Group
BASD	Ball Aerospace Systems Division
BECD	Ball Electro-Optics and Cryogenics Division
BCU	Bench Checkout Unit
CAL	Calibration
°C	Degree Centigrade
CCR	Cloud Cover Radiometer
CCW	Counterclockwise
CLPS	Calibration Lamp Power Supply
cm	Centimeter
CMD	Instrument Command
CRT	Cathode Ray Tube
CTF	Calibration Test Fixture
CW	Clockwise
DC	Direct Current
DVM	Digital Voltmeter
ELM	Electronics and Logic Module

TERM	DESCRIPTION
ESM	Equipment Service Module
eV	Electron Volts
FEL	ANSI Designation for 1000W Lamp
FET	Field-effect Transistor
FOV	Field of View
GSE	Ground Support Equipment
GSFC	Goddard Space Flight Center
HVPS	High-Voltage Power Supply
Hz	Hertz
I/F	Interface
k	Kilo (10^3)
°K	Degrees Kelvin
LED	Light-Emitting Diode
LSB	Least Significant Bit
LVPS	Low-Voltage Power Supply
MgF_2	Magnesium Fluoride
mm	Millimeter
MOS	Metal Oxide Semiconductor
MSB	Most Significant Bit
MUX	Multiplexer
NIST	National Institute of Standards and Technology [formerly National Bureau of Standards (NBS)]
NOAA	National Oceanic and Atmospheric Administration
nm	Nanometer
OG	Outgas
PCB	Printed Circuit Board
PED	Photoemissive Diode
PMT	Photomultiplier Tube
POR	Power-on Reset
PRI	Primary
PROM	Programmable Read-only Memory
PTF	Primary Test Fixture
PWA	Printed Wiring Assembly
PWB	Printed Wiring Board
R1	Range 1 (PMT)
R2	Range 2 (PMT)

TERM	DESCRIPTION
R3	Range 3 (PMT)
RAM	Random Access Memory
RDCL	Radiometric DC Level
RSS	Root-sum-square
SBUV/2	Solar Backscatter Ultraviolet Radiometer (Mod 2)
SER	System Engineering Report
SIS	Spacecraft Interface Simulator
SM	Sensor Module
SMS	Sensor Module Simulator
SNR	Signal-to-noise Ratio
sr	Steradian
STE	System Test Equipment
TBD	To Be Determined
TBS	To Be Supplied
TCC	Target Control Console
TCD	Test Control Directive
TI	Texas Instruments
TIP	TIROS Information Processor
TIROS-N	Television Infrared Operational Satellite, "N" Series
TM, TLM	Telemetry
VFC, V/F	Voltage-to-frequency Converter
VTF	Vacuum Test Fixture
W	Watt

6.3 DEFINITIONS

FIXed Memory	Non-volatile PROM, programmed at BASG with grating positions for each mode of operation.
FLEX Memory	Volatile RAM programmable by command.
E-CAL	(Electronic Calibration) Preset voltage levels switched into the amplifiers at the end of each data sampling sequence to verify the calibration of the electronics.

WAVEL... (r	...IN	G_a PREAMPLIFIER GAIN (Volts/Amp)	G_E ELECTRONIC GAIN	V_f VOLTS TO FREQUENCY RATIO (Hz/Volt)	SNR (Includes N_s)		SNR (Excludes N_s)		SPECIFIED SNR	
					...SCRETE ...F = 0.4	SWEEP ΔF = 5	DISCRETE ΔF = 0.4	SWEEP ΔF = 5	DISCRETE ΔF = 0.4	SWEEP ΔF = 5
	5	432 x 10^6	100	12,136	22 50	6 14	24 60	7 17		2
16(	5	432 x 10^6	100	12,136	130	37	200	57		50
17(	5	432 x 10^6	100	12,136	350	99	980	280		250
18(	5	432 x 10^6	100	12,136	640	180	3,000	850		400
19(	5	432 x 10^6	100	12,136	1,100	320	9,000	2,600		400
20(	5	432 x 10^6	100	12,136	70	20	90	26	35[2]	10[2]
25	±5	432 x 10^6	100	12,136	220	63	450	130	100	30
27	±5	432 x 10^6	100 1	12,136	350	99	980	280	200	60
28	±5	432 x 10^6	100 1	12,136	390	110	1,200	340	260	80
28	±5	432 x 10^6	100 1	12,136	530	150	2,100	600	400	145
29	±5	432 x 10^6	100 1	12,136	670	190	3,200	920	400	210
29	±5	432 x 10^6	100 1	12,136	700	200	3,500	1,000	400	230
30	±5	432 x 10^6	100 5	12,136	920	260	6,000	1,700	400	400
30	±5	432 x 10^6	1 5	12,136	1,360	400	4,100	3,000	400	400
31	±5	432 x 10^6	1 5	12,136	2,000	570	8,200	5,900	400	400
31	±5	432 x 10^6	1 5	12,136	5,100	1,400	52,000	37,200	400	400
33	±5	432 x 10^6	1 5	12,136	7,200	2,000	104,000	74,400	400	400
33		432 x 10^6	5	12,136					---	---
4		432 x 10^6	4.31	11,650	590		590		100	
3 (C		432 x 10^6	5	12,136	200 107,000		110 34,000		200	
CAT CUR MON	NE- 0	SBUV-NE-80-100	SBUV-NE-80-100	SBUV-NE-80-100	Calculated	Calculated	Calculated	Calculated	Specification	Specification
RAW SOU										

A/N 1961

Table 2-1

SUMMARY OF PERTINENT SYSTEM PERFORMANCE PARAMETERS

NOTES:

[1]

[2]

[3]

[4]

[5]